Developing quantitative approaches to determine microbial colonisation and activity in mineral bioleaching and characterisation of acid rock drainage

Didi Xhanti Makaula

In fulfilment of the requirements for the degree of
Doctor of Philosophy

Department of Chemical Engineering
Faculty of Engineering and the Built Environment
University of Cape Town

31 October 2019

Supervisor: **Susan Harrison**

Co-supervisors: **Marijke Fagan-Endres and Robert Huddy**

Plagiarism Declaration

1. I know that plagiarism is wrong. Plagiarism is to use another's work and to pretend that it is one's own.
2. I have used the Minerals Engineering journal system for citation and referencing. Each significant contribution to, and quotation in, this report from the work, or works, of other people has been attributed, and has been cited and referenced.
3. This report is my own unaided work, except for assistance received from the teaching staff.
4. I have not allowed, and will not allow, anyone to copy my work with the intention of passing it off as his or her own work.

Signed by candidate

Signature

Inclusion of publications

I confirm that I have been granted permission by the University of Cape Town's Doctoral Degrees Board to include the following publication(s) in my PhD thesis, and where co-authorships are involved, my co-authors have agreed that I may include the publication(s):

1. Didi X. Makaula, Robert J. Huddy, Marijke A. Fagan-Endres, Susan T.L. Harrison. Using isothermal microcalorimetry to measure the metabolic activity of the mineral-associated microbial community in bioleaching. Minerals Engineering, 106, (2017) 33 – 38

2. Didi X. Makaula, Robert J. Huddy, Marijke A. Fagan-Endres, Susan T.L. Harrison. Developing a Flow-Through Biokinetic Test to Characterize ARD Potential: Investigating the Microbial Metabolic Activity on Pyrite-bearing Waste Rock Surfaces in an Unsaturated Ore Bed. Proceedings 11th ICARD | IMWA, Wolkersdorfer, Ch.; Sartz, L.; Weber, A.; Burgess, J.; Tremblay, G. (eds.) | MWD Conference – "Risk to Opportunity"

3. Didi X. Makaula, Susan T.L. Harrison. Establishing the flow-through biokinetic test to characterise sulfidic waste rock mineral for its potential to form ARD. Minerals Engineering (under revision)

Signature: Signed by candidate Date: 31 October 2019

Student Name: Didi Xhanti Makaula Student Number: MKLDID003

Abstract

Colonisation of mineral surfaces by acidophilic microorganisms during bioleaching is important for accelerating the extraction of valuable metals from mineral sulfide ores of varying grades through biohydrometallurgy. It also influences acid formation and mineral deportment from sulfidic waste rock generated in mining processes and is key to its comprehensive waste rock characterisation for acid forming potential. This study assesses mixed mesophilic microbial interactions with, and colonisation of, pyrite concentrates and pyrite bearing waste rocks. The assessment of these interactions was carried out in this study in a synergistic qualitative as well as quantitative manner, with a particular focus on heap bioleaching for metal extraction and on disposal of waste rock, the latter through the case of characterisation of ARD generation potential. Using the tools developed, both the course of colonisation and development of metabolic activity with time of colonisation, as well as their correlation with leaching performance were studied. Furthermore, specific operating parameters such as ore grade and irrigation rates were explored. Finally, the application of this knowledge in a characterisation study was explored.

To achieve the set of tools required for this study, two quantitative techniques were refined to characterise these microbial-mineral interactions. In the first, an isothermal microcalorimetric (IMC) method was developed and optimised to determine microbial colonisation of mineral surfaces quantitatively as a function of surface area (m^{-2}). Three IMC configurations were considered: colonised pyrite-coated beads submerged in fresh media; beads submerged in cell free leachate; and beads in an unsaturated bed, each in the IMC vial. The highest heat output was measured in the unsaturated bed (263.3 mW m^{-2}). The consistency of heat produced by the colonising microorganisms was determined through reproducibility studies. Using IMC, chemically and microbially facilitated pyrite oxidation rate studies were performed on unsaturated beds with varying surface area loadings, correlating to varying bead number. Results obtained showed similar normalised oxidation rates per surface area across the surface loadings. However, with more microbially colonised surface area loaded, the maximum heat generated was reached more quickly. This suggested that there was reagent (possibly O_2) limitation in the system, which restricted microbial activity and its associated heat generation. Reagent limitation in the system was tested and validated through varying the O_2 availability in the IMC vial by air displacement with CO_2 and N_2 gas, with the systems containing less O_2 showing limited activity. Collectively the data showed that high activity, facilitated microbially, was achieved in unsaturated systems in a reproducible manner. Secondly, oxidation rates were determined and O_2 limitation in the system was overcome.

This then fundamentally informed the determination of activity from microbial-mineral interaction, using IMC, as a function of surface area.

Secondly, a detachment protocol developed at UCT to recover microbial cells from surfaces of crushed and agglomerated ore to assess microbial growth rates and distribution in the ore bed, including cells in the interstitial phase and those weakly and strongly attached to the ore surface, was refined to assess colonisation of the finely milled pyrite-bearing concentrate or waste rock coated onto glass beads in continuous flow assays. The detachment protocol was assessed quantitatively by measuring initial and residual microbial activity, as a function of wash number, using IMC, thus providing a new level of confidence in the method. Mineral surfaces were visualised using scanning electron microscopy (SEM) following detachment for qualitative assessment. These data, together with microscopic enumeration of detached cells with increased number of washes, allow refinement of the assay and showed that six washes provided reliable estimation of mineral associated microbial cells. Extracellular polymeric substances (EPS) produced in this process were extracted using crown ether and the capsular bound components analysed. The analysed components included lipids (4.2 %), iron (16.4 %), DNA (26.8 %), and total carbohydrates (28.5 %), which are typical components of EPS. The carbohydrate fraction was further resolved to trehalose (26.2 %), fructose (36.5 %) and galactose (37.3 %) sugar monomers. The analysed EPS components confirmed presence of the EPS secreted by cells colonising the mineral ore or waste rock surface in a flow-through system, and visualised via SEM.

The microcalorimetric approach developed together with the refined detachment method were applied to samples from a flow-through mini-column system, used to simulate microbe-mineral contacting in a heap. Here, the colonisation of pyrite concentrate by a mixed mesophilic culture of iron and sulfur oxidising microorganisms was assessed progressively over 30 days. The progression of mineral colonisation in the mini-column system was monitored using a combination of IMC, scanning electron microscopy, detachment method and conventional wet chemistry measurements. We observed an increase in the heat output from the colonised surfaces of pyrite mineral concentrate caused by oxidative reactions facilitated by mineral-microbial biofilm. This confirmed that the attached microorganisms were metabolically active and facilitated ongoing mineral leaching through regeneration of lixiviants. Correlation was shown between number of cells detached from the mineral surface and the heat generated, with a constant heat output per cell observed until day 15 of operation. Thereafter, the measured heat generated per cell increased, suggesting reduced efficiency of cell detachment owing to increasing firm attachment, or the lack in separation of single cells embedded within EPS matrix (clumps observed under light microscope after detachment). Using IMC to quantify the activity of the residual microorganisms on the mineral surface

following detachment, it was confirmed that >95% of activity was detached through this protocol, hence the lower detached cell numbers determined following EPS formation were attributed to clumping of the detached cells. This correlated to an increased presence of EPS and was supported by SEM observation.

Following the study of pyrite concentrate, colonisation of two pyrite bearing waste rock samples was assessed, with simultaneous establishment of the flow-through mini column biokinetic test configuration that resembles open flow in the waste rock dump. The flow-through configuration was run alongside the refined UCT-developed batch biokinetic test using suspended mineral. In this study, two pyritic waste rock samples, liberated by milling, were characterised using three biokinetic test approaches: the slurry batch test (BT), the batch test using mineral-coated beads (BT-CB) and flow-through column test with mineral-coated beads (FT-CB). Our results have shown through static tests, solution redox potential and pH analysis that both waste rocks were acid forming. Furthermore, it was demonstrated in the FT-CB system that microbial proliferation on the waste rock surfaces progressed with time such that oxidative exothermic reactions facilitated by the increasing microbial presence on the surfaces were demonstrated using Isothermal microcalorimetry. This study presents and informs the on-going refinement of the biokinetic test through establishment of a flow-through test for ARD characterisation while providing insight into the role of the microbial phase in ARD generation.

Microbial-mineral association was assessed under various operating conditions, including two solution flow rates (60 and 4 ml h^{-1}) and minerals of varying sulfide content, including a pyrite concentrate (96 % pyrite), a high sulfide waste rock (33 % pyrite) and a low sulfide waste rock (14 % pyrite). Mineral grade impacted the activity of mineral associated microorganisms with higher activities observed on a mineral surface with high sulfide content. The activity measured from microorganisms that were associated with the pyrite concentrate was 827 mW m^{-2} at a 60 ml h^{-1} flow rate, whereas activity measured on low and high sulfide waste rock (PEL-LS and PEL-HS) were 293 mW m^{-2} and 157 mW m^{-2} respectively operated on the same flow rate. On decreasing the flow rate to 4 ml h^{-1}, the activity of microbial cells on PEL-LS and PEL-HS were 153 mW m^{-2} and 146 mW m^{-2} respectively.

This study showed that the growth of microbial cell numbers coupled with metabolic activity is important to facilitate accelerated dissolution of sulfidic mineral surfaces. The rate of oxidation increased in the presence of EPS and thus EPS was further analysed, and its composition was confirmed. Overall, this study contributed to the understanding of microbial colonisation of mineral surfaces in a non-destructive quantitative manner. This study thus demonstrates the ability to measure and track both the growth and activity of microorganisms that are associated with mineral surfaces. This is important as it provides an approach to

understanding microbe mineral surface interactions and, therefore, potential strategies to increase microbial colonisation of low-grade minerals that house valuable metals, during commercial heap bioleach processes. Furthermore, the ability to monitor progressive growth and activity of mineral associated microbial communities within a flow-through biokinetic test, as successfully demonstrated in this study, has the potential to significantly enhance current management of mine waste materials and ARD mitigation strategies. Therefore, on-going investigations of progressive microbe-mineral interactions will continue to be valuable both in terms of bioleaching for metal recovery and the mitigation of ARD through effective characterisation of mine waste material.

Acknowledgements

I would like to thank my principal supervisor Prof. Sue Harrison for her guidance, confidence, and patience throughout my PhD. I am very grateful for the opportunity that you gave me.

Thanks to my co-supervisors, Dr Rob Huddy and Dr Marijke Fagan-Endres for their valuable contributions in shaping up the discussions around this project and for their constructive critique when editing manuscripts and this thesis document. I'm also grateful that I could pop in your offices anytime I needed assistance.

Financial support from NRF South Africa Research Chair Initiative in Bioprocess Engineering (UID 64778) and Council for Scientific and Industrial Research (CSIR) interbursary is appreciated.

Thanks to the biomineral discussion group for the candidness during progress presentations. A heartfelt thank you to the Centre for Bioprocess Engineering Research (CeBER) students. Thanks to Emmanuel Ngoma (Baba) who managed the Fe/S lab and was always ready to assist both academically and technically. Thanks to Tich who managed the CeBER labs and who contributed in designing the reactor incubator. Thank you to Mhlangabezi Golela for assisting with static tests and good chats in the lab.

The technical support of Miranda Waldron of the Electron Microscope Unit, UCT and Gaynor Yorath (QEMSCAN analysis) of CMR, UCT is greatly appreciated.

I would like to extend my appreciation to the administrative staff CeBER. Sue Jobson, Candice, Lesley, Sandra and Ruegshana, I am grateful for your support and assistance.

To Unathi who continues to help tremendously and effortlessly in the bringing up of our son, thank you.

My brothers and sister who constantly call to check up on me and support me in everything, thank you guys.

To Hlomani, thank you for not giving me any option but to see this PhD through.

To my mother (Ma'am), I have always been absolutely nothing without you, and I will continue to be nothing without you. Your unwavering and unconditional love, support and presence continues to be everything I ever needed. Ndibulela ngento yonke *MABHAYI*.

*To **Phozisa Sithule Makaula***

Your departure inflicted the maximum pain possible

to the Makaula family, and we still carry that pain with us, daily.

Rest well MAZULU

Table of Contents

List of Figures

List of Tables

Acronyms and Abbreviations

AMD	Acid mine drainage
ARD	Acid rock drainage
ABA	Acid base accounting
AF	Acid forming
AFM	Atomic force microscopy
AHL	N-Acyl homoserine lactones
ANC	Acid neutralizing capacity
CAF	Central analytical facility
CE	Crown ether
CeBER	Centre for Bioprocess Engineering Research
CIA	Centre of Imaging and Analysis
CLSM	Confocal laser scanning microscopy
CSIR	Council for Scientific and Industrial Research
CSTR	Continuous stirred tank reactor
DAPI	4', 6-diamidino-2-phenylindole
DNA	Deoxyribonucleic acid
eDNA	Extracellular deoxyribonucleic acid
EDS	Energy-dispersive X-ray spectroscopy
EDTA	Ethylenediaminetetraacetic acid
EFM	Epifluorescent microscopy
EPS	Extracellular polymeric substance
GC	Gas chromatography
GC-MS	Gas chromatography–mass spectrometry
ICP-OES	Inductively coupled plasma atomic emission spectroscopy
IMC	Isothermal microcalorimetry
MPA	Maximum potential acidity
MPN	Most probable number
NAG	Net acid generation
NAPP	Net acid neutralizing potential
PAF	Potentially acid forming
PEL-HS	Pelitic high sulfur
PEL-LS	Pelitic low sulfur
PLS	Pregnant leach solution
PSD	Particle size distribution
QEMSCAN	Quantitative evaluation of minerals by scanning electron microscopy
qPCR	Quantitative real-time polymerase chain reaction
ROM	Run-off mine

SDS	Sodium dodecyl sulfate
SEM	Scanning electron microscopy
TAM	Thermal activity monitor
TEM	Transmission electron microscope
UCT	University of Cape Town
USA	United States of America
WRD	Waste rock dump
XRD	X-ray diffraction

Chapter 1: Introduction

1.1 Background and motivation of the study

The readily accessible high-grade ores found on the earth's surface have been depleting rapidly over the past few decades (Watling, 2006). In many of the remaining ores, mineralogical complexity or low-grade or both imply that conventional mining technologies are less appropriate or less economically feasible for their exploitation. This has motivated the pursuit of alternative extraction methods such as mineral bioleaching (Rawlings et al., 2003). Bioleaching is a biotechnological application used in the mining industry to recover metals; to date, it has been used primarily for low-grade ores. Specialized iron- and/or sulfur- oxidizing microorganisms facilitate the dissolution of metals from minerals (Colmer and Hinkle, 1947; Schippers et al., 1999; Kelly and Wood, 2000). These typically occur naturally in the soil or mineral environment.

The role of microorganisms in metal extraction can be traced back as far as 23-79 A.D. as described by König and Winkler (1989). The first report of the role of microorganisms was in the 1920s when Waksman and Joffe (1922) reported microbial involvement in the leaching of zinc and iron sulfides. Colmer and Hinkle (1947) discovered two unidentified microorganisms and their role in leaching processes. The two microorganisms were found in an acid rock drainage (ARD) environment with one being an iron oxidiser and the other a sulfur oxidiser that resembled *Acidithiobacillus thiooxidans*. Mineral bioleaching is successfully applied for industrial scale metal extraction (Brandl, 2001). There are two broad categories of this bio-based technology applied in biohydrometallurgical processes, namely tank and heap processes. These can be used for both bioleaching (the dissolution of mineral ores containing metals of interest) or biooxidation (the dissolution of pyrite as a pretreatment to make available precious group metals for subsequent recovery). The application of these processes is mostly dictated by the grade of the mineral to be processed as well as the presence of complex ores or penalty metals.

Tank biooxidation or bioleaching processes may be a technology of choice for complex polymetallic mineral concentrates (above 0.5 wt.% for copper) or concentrates containing penalty metals such as arsenic or antimony. Tank biooxidation is most common for refractory gold ore deposits. However, tank bioleaching has also been demonstrated and has potential for concentrates not well suited to smelting. In cases where the initial ore grade is low or the metal value limited (e.g. zinc), tank leaching is unlikely to be economically feasible and heap bioleaching has potential as an attractive alternative technology.

In the heap bioleaching process, most commonly used to extract metals from low-grade base metal sulfide ores (e.g. 0.1-0.5 wt.% in the case of copper), the ore is crushed and stacked onto constructed leaching pads. A downward flow of leach solution and the upward flow of air or enriched air is maintained through the ore bed and the leachate or 'pregnant leach solution' (PLS) is collected for metal recovery. Owing to the nature of the ore bed, heap bioleaching is a complex, heterogeneous system that involves several sub-processes and is affected by many parameters, some of which are yet to be fully understood. Factors affecting heap bioleaching processes include, but are not limited to: irrigation (Chiume et al., 2012; Fagan et al., 2014), aeration (Pradhan et al., 2008; Petersen et al., 2010), solution flow and distribution (Pradhan et al., 2008; Fagan et al., 2014), mineral ore type (Munoz et al., 1995; Watling, 2006), crush size and packing method, solution chemistry and pH (Tupikina et al., 2011; Ngoma et al., 2015), temperature (Franzmann et al., 2005; Watling et al., 2016), microbial consortium and microbial-mineral association and succession (Gehrke et al., 1998; Gehrke et al., 2001; Kinzler et al., 2003; Noël et al., 2010; Africa et al., 2013a; Tupikina et al., 2014).

Microbial-mineral association and subsequent colonisation form one of the critical components when optimising the performance of a bioheap and the very same association is important to understand when trying to abate ARD formation. Heap bioleaching operations are typically subjected to long start-up periods during which microbial activity is low. This is because of lower temperatures at the start of the process, lack of established colonisation, hence insufficient microbial activity, lack of high Fe^{3+} concentrations and limited microbial species distribution across the ore bed via the flowing solution and those associated with ore surfaces (Demergasso et al., 2010). These result directly in slow oxidative reactions and therefore low mineral dissolution rates (Kinzler et al., 2003). The exothermic sulfide mineral dissolution reactions that generate heat within the heap are primarily dependent on both chemical and microbial species, distributed within the heap by the flow-through irrigation solution and microorganisms associated with the ore surface (Bartlett, 1997; Kinzler et al., 2003). Mechanisms for the generation of chemical lixiviants such as Fe^{3+} and H^{+} and their subsequent regeneration applicable in commercial bioleaching processes, also apply in the formation of undesired ARD from sulfide-bearing wastes. Knowledge of the bioleaching mechanism may therefore be exploited both for recovery of metal values from low-grade mineral ores and for appropriate processing and disposal of mine tailings and waste rock or ore to prevent pollution that results from the uncontrolled leaching of the material that occurs from liberated mineral sulfides (Watling, 2006; Brierley and Brierley, 2013).

Encouraging microbial ore colonisation in the early stages of a bioheap would potentially fast track the onset of metal dissolution and thus leverage pay-back on capital expenditure (Figure 1.1). Low-grade chalcopyrite mineral ores leach well at temperatures around and above

moderate thermophilic conditions; therefore, it is of utmost importance to have a well-colonised heap at mesophilic conditions (Demergasso et al., 2010) to establish higher exothermic oxidative reactions used to heat the heap and allow the heap to reach optimum leaching temperatures faster (Chen and Wen, 2013). On the other hand, discouraging colonisation in waste rock dumps would delay the accelerated generation of chemical lixiviants responsible for acid-laden effluents typical of ARD and containing high amounts of heavy metals.

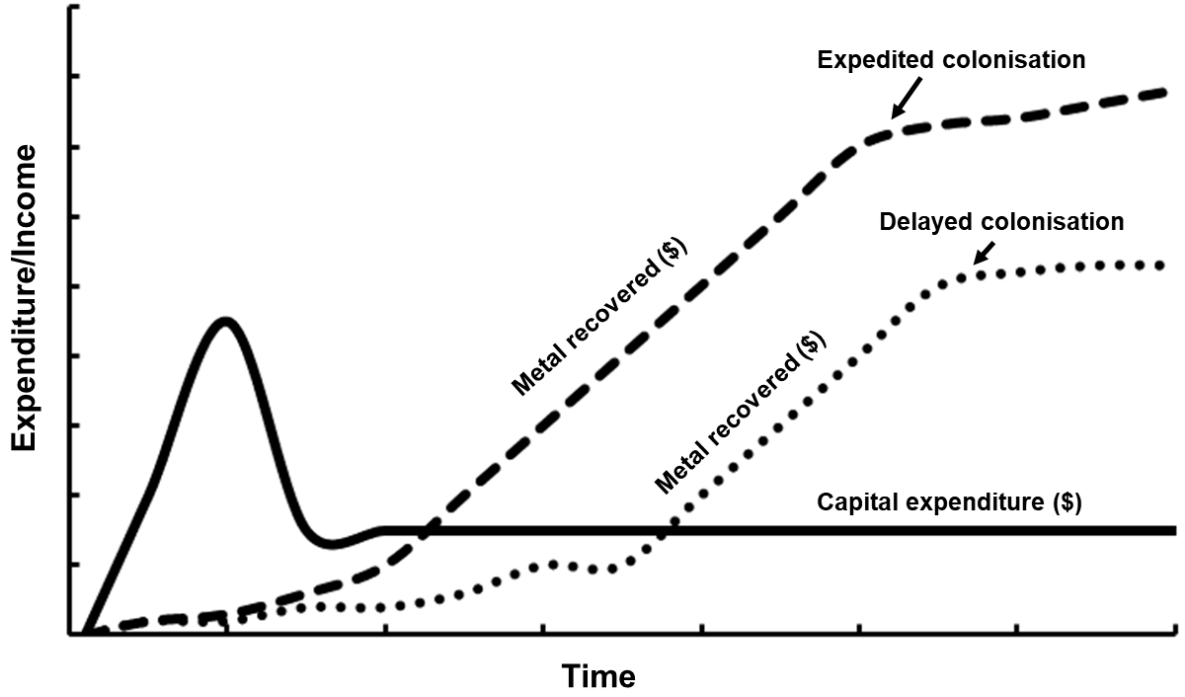

Figure 1.1: An idealised heap process where colonisation of mineral ore surfaces would be expedited, leading to early onset of metal recovery and therefore more rapid pay-back on capital expenditure and ensuing profit

1.2 Problem statement

Heap bioleaching has potential for the recovery of metals from low-grade mineral ores, mostly due to its potential economic feasibility that allows reasonable metal recovery for low capital input. Owing to the nature of ore packing in constructed heaps, which promotes heterogeneity, it is critical to have an effective early mesophilic microbial inoculation strategy that encourages appropriate distribution of microorganisms throughout the heap and subsequent colonisation. In heap bioleaching processes, microorganisms facilitate the dissolution of sulfide metals by oxidising Fe^{2+} and reduced sulfur species to Fe^{3+} and H^{+} which in turn serve as lixiviants for dissolution of sulfide mineral grains exposed to the mineral ore surface. A well-colonised heap with a metabolically active microbial population is essential for providing a continuous and potentially well-distributed source of leach agents that ultimately promote optimal recovery of the metal of choice. A heap that is well colonised with a mesophilic microbial community results in accelerated oxidative reactions and generation of leach agents. The oxidative

reactions are heat producing (exothermic), enhancing the leach rate. Further, the heat significantly dictates the microbial community structure within the heap, progressing from mesophilic, through moderate thermophilic to thermophilic species to match temperature conditions. Conversely, well-colonised sulfide-bearing mine waste dumps have the potential to expel acidic effluents that are heavily burdened with a cocktail of heavy metals that could be detrimental to the ecosystem if unabated.

Literature shows that microbial populations associated with mineral ore surfaces are critical and contribute to increased oxidation rates when compared to the populations in the flowing solution, across different scales (Bhappu et al., 1969; Murr and Brierley, 1978; Chiume et al., 2012; Govender et al., 2013). Studies have investigated colonisation, including investigating parameters that encourage optimum colonisation in heaps. These studies were performed using laboratory tests to simulate heap bioleaching environments and ranged from the addition of sulfur content (e.g. FeS_2), to increase temperature via colonisation and subsequent exothermic reaction (Dew et al., 2011; Chen and Wen, 2013), controlling aeration which influences CO_2 and O_2 concentrations within the heaps (Lizama, 2001; Dew et al., 2011; Chen and Wen, 2013), addition of yeast extract in the presence of thermophiles (Chen and Wen, 2013), an efficient sequential inoculation strategy and irrigation rates (Munoz et al., 1995; Petersen and Dixon, 2006; Watling et al., 2009; Dew et al., 2011; Chiume et al., 2012; Gericke, 2012; Panda et al., 2012), and increased permeability within the ore bed to allow unhindered flow of leach agents (Bartlett, 1992; Munoz et al., 1995; Petersen and Dixon, 2007a). Microbial population distribution and activity in the whole ore, as well as the effects of physicochemical parameters on colonisation have been investigated (Chiume et al., 2012; Govender et al., 2013, 2015). Formation of extracellular polymeric substances (EPS) on mineral surfaces has been shown previously to contribute significantly to firm attachment and colonisation of ore surfaces (Gehrke et al., 1998; Harneit et al., 2006; Sand and Gehrke, 2006; Ghauri et al., 2007). Gehrke et al. (1998) showed high amounts of iron were complexed within EPS of *At.ferrooxidans* grown on pyrite surface. Kinzler et al. (2003) showed that, in the presence of high amounts of iron, *At. ferrooxidans* cultures associated with pyrite possessed higher oxidation activity compared to strains with lower iron.

The link between the metabolic activity and performance of mineral associated microorganisms in systems is yet to be firmly established in bioleach processes. Secondly, visualisation of EPS together with biochemical composition analysis have been investigated across various microbial populations and various mineral substrates in bioleach environments (Harneit et al., 2006; Africa, 2017). EPS cultivation, extraction, and biochemical characterisation is yet to be demonstrated in a complete flow-through bioleach ore bed system. Using the biokinetic test that is under development, investigations that assessed

parameters such as the impact that solid loading and particle size (Hlongwane, 2015), and inoculum size (Opitz and Harrison, 2016) have on the ability of specific waste materials to form acid have been shown and this has contributed to the continuing refinement of the test. A mine waste characterising system that resembles a waste dump whilst accounting for microbial-mineral interaction has not yet been shown extensively during the characterisation of mine waste processes.

This study seeks to investigate the interactions between microbe and mineral in systems in which mixed mesophilic cultures and pyrite minerals, or other base mineral sulfides, of various sulfide content are contacted during initial colonisation stages of heap bioleaching or during the onset of ARD formation environments. A microcalorimetric method to measure microbial metabolic activity under unsaturated conditions in a quantitative manner was refined for this study. This method was then applied to a flow-through mini-column in which microbe-mineral contacting was simulated to quantify microbial-mineral interaction over a defined surface area and period of operation. These microbial activity data were integrated with the data on solution chemistry generated by the leach reactions and with microscopic measurements. Flow rates typically used in heap processes were applied in this study, as were high flow rates. Studies investigating progressive microbial abundance in different locations of the ore bed (free-flowing liquid, interstitial mineral-associated zone and mineral attached zone) to allow description of microbial colonisation by utilising a detachment method were previously developed in the Centre for Bioprocess Engineering at the University of Cape Town (UCT) and applied across a range of studies (Chiume et al., 2012; Govender et al., 2013, 2015; Cox and Bryan, 2017). In this study, the detachment method was further refined both for use with mineral-coated particles and to validate the degree of detachment of microorganisms. It was integrated with isothermal microcalorimery (IMC) to account for the metabolic activity of detached and residual populations on the surface, thereby enabling the tracking of degree of microbial colonisation of the ore over time. Cultivation and extraction of extracellular polymeric substances (EPS) from the complete flow-through system coupled with analysis of its biochemical composition was performed in this study. This builds on previous work on the formation and proliferation of EPS and biofilm on various mineral surfaces, which have been studied mostly in batch reactors with very limited studies on flow-through systems (Gehrke et al., 1998; Africa et al., 2010; Florian et al., 2011; Africa et al., 2013a; Africa, 2017).

This study also investigates microbial-mineral interaction in the context of ARD, where the characterisation of the potential of waste rocks to form acid is assessed. The current UCT developed batch biokinetic test successfully demonstrates the combined impact of biologically leachable material with the inhibiting or neutralising environments or both and allows assessment of their relative rates (Hesketh et al., 2010; Broadhurst et al., 2013; Harrison et

al., 2013; Opitz et al., 2016; Opitz and Harrison, 2016). However, it does not account for the washout of neutralising minerals that would be observed in the open waste dump environments. Golela (2018) improved this method by developing a draw and fill semi-continuous biokinetic test to provide relative kinetics of acid neutralising and acid forming reactions that closely represent a waste dump. However, this still does not represent a waste dump that is characterised by a complete flow-through process nor does it represent the mineral-microbe-solution contacting typical in an unsaturated ore or waste rock bed. In this study, a complete flow-through column system was proposed to better represent the unsaturated open system found in the waste rock dump. Its relevance to characterising the potential of waste rock samples to form ARD through considering their ability to form acid was assessed. Further, the progressive microbial-mineral interaction over a period of time was investigated using lower grade ores and across two irrigation rates.

1.3 Thesis layout

Chapter 2 delivers a synthesis of the relevant body of knowledge available on microbial-mineral interaction in bioleaching and ARD and clearly demonstrates the gaps in the existing knowledge base. The fundamental reactions implicated in both bioleaching and ARD formation are described and the role of microorganisms indicated. The operating environments found in heap bioleaching for recovery of metals of value and in waste dumps of sulfidic minerals likely to cause ARD are covered. The various acidophilic microorganisms implicated in these processes are introduced, with emphasis placed on the relevant mesophilic microorganisms. Factors that influence bioleaching rates in a heap are explored, with emphasis placed on the role of microbial-mineral interaction. The mechanisms manifested by the microbial-mineral interaction process and their influence on leaching rates, localisation, activity and overall colonisation of sulfide minerals are interrogated. The application of isothermal (micro)calorimetry (IMC) on biomineral and ARD studies is explored. This chapter is concluded by a brief overview of the reviewed literature, analysis of gaps in the literature pertaining to the scope of this thesis, followed by the objectives, hypotheses, and key questions addressed in the thesis.

Chapter 3 describes the overall experimental design in this study and common methods applied across the research chapters including: (1) reactor design, set-up and operating conditions, (2) microbial culture and growth conditions, (3) wet chemistry analysis as well as microscopic microbial analysis, (4) mineralogical analysis, (5) detachment studies, (6) scanning electron microscope (SEM) analysis, (7) IMC measurements, and (8) EPS extraction methods.

Chapter 4 focuses on configuring and optimising an IMC method to measure activity of mineral associated microorganisms as a function of the surface area of the mineral ore. This chapter demonstrates the best possible heat-flow measuring method that is reproducible using materials from in batch and flow-through systems. It uses an unsaturated reaction system and takes into consideration reagent limitations experienced when measuring heat-flow output.

Chapter 5 focuses on the refinement of the detachment method (Chiume et al., 2012; Govender et al., 2013; Tupikina et al., 2014; Cox and Bryan, 2017) for assessment of colonisation of pyrite-bearing waste rock in a continuous flow-through system. SEM is used as a qualitative tool to visualise any residual cells on the surface after detachment. IMC is used as a quantitative tool to measure metabolic activity of residual cells after wash steps to enable the tracking of progressive microbe-mineral association. Furthermore, biochemical composition of EPS secreted on the waste rock surface is analysed to gain more insight on the structural make-up of the biofilm in a complete flow-through system using low-grade waste rock.

In **Chapter 6,** the application of the IMC method developed and the refined detachment method to a flow-through column system is undertaken using a surface coating of finely milled high grade mineral concentrate. In this chapter, IMC is also used in conjunction with traditional methods to present the progression of microbial-mineral interaction. The integration of IMC with traditional solution analysis by wet chemistry analytical methods is used to establish a relationship between (1) metabolic activity on the ore surface and number of colonising cells; (2) metabolic activity and the mineral surface coverage by colonising cells i.e. on the basis of mineral surface area; and (3) metabolic activity and leaching performance of the flow-through mini column leaching system to be established.

In **Chapter 7** the approach is applied to an unsaturated bed using a surface coating of finely milled low-grade ore. Through this, the research seeks to develop and test the viability of a flow-through biokinetic test configuration for assessment of ARD potential through the characterisation of two pyrite-bearing waste rock materials with potential to form ARD. The configuration seeks to account for the limitations that are encountered in the batch and semi-batch biokinetic configuration and that under submerged reaction conditions. This study informs the on-going refinement of the biokinetic test through establishment of a flow-through test for ARD characterisation.

The thesis finishes with **Chapter 8**, which provides conclusions from this investigation and, based on the findings from this study, provides a series of recommendations for future studies.

Chapter 2: Literature Review

2.1 Mineral bioleaching

The bioleaching of sulfide minerals such as pyrite and chalcopyrite is a chemical-biological synergistic process that involves a chemical oxidant, such as ferric iron ions (Fe^{3+}), which attacks the mineral surface, liberating metal ions. This oxidative process results in the reduction of the ferric oxidant to ferrous iron ions (Fe^{2+}) and, where pyrite is the mineral leached, the liberation of further Fe^{2+} (Equation 2.1 and Equation 2.3). Fe^{3+} forms, or is re-generated, when oxygen oxidizes the Fe^{2+}, according to Equation 2.2. This takes place at low pH; further, the rate of oxidation of Fe^{2+} by oxygen is slow, particularly at ambient or mesophilic temperature. The leaching of sulfide minerals is accelerated by the metabolic activity of naturally occurring chemolithotrophic microorganisms, which accelerate the regeneration of lixiviants (Fe^{3+} from Fe^{2+}) and H^+ acidity as shown in Equation 2.2 and Equation 2.4.

$$FeS_2 + {}^7/_2\, O_2 + H_2O \rightarrow Fe^{2+} + 2SO_4^{2-} + 2H^+ \qquad \text{Equation 2.1}$$

$$Fe^{2+} + {}^1/_4\, O_2 + H^+ \rightarrow Fe^{3+} + {}^1/_2\, H_2O \qquad \text{Equation 2.2}$$

$$FeS_2 + 14Fe^{3+} + 8H_2O \rightarrow 15Fe^{2+} + 2SO_4^{2-} + 16H^+ \qquad \text{Equation 2.3}$$

$$2S + 3O_2 + 2H_2O \rightarrow 2H_2SO_4 \qquad \text{Equation 2.4}$$

Two different reaction mechanisms for the dissolution of sulfide minerals are proposed: the thiosulfate mechanism for acid non-soluble metal sulfides such as pyrite and the polysulfide mechanism for acid-soluble metal sulfides such as chalcopyrite (Schippers, 1998; Schippers and Sand, 1999; Sand et al., 2001; Rohwerder et al., 2003). In the acid-insoluble thiosulfate pathway, iron oxidising microorganisms oxidise Fe^{2+} in acidic conditions thereby regenerating Fe^{3+} that is responsible for leaching of the metal sulfide mineral grain. Sulfur-oxidising microorganisms oxidise the thiosulfate to tetrathionate and polythionates and ultimately to sulfates. In the acid-soluble polysulfide pathway, in addition to the Fe^{3+} attack, acid also attacks the surface of metal sulfides resulting in the formation of Fe^{2+}, metal (e.g. Cu), and sulfide cations (HS^-). The role of iron oxidising microorganisms in both pathways is the regeneration of Fe^{3+}, whilst sulfur oxidisers transform the intermediary reduced or partially oxidised sulfur compounds to sulfuric acid (H_2SO_4), which contributes to the acidic environment (Rohwerder et al., 1998; Schippers and Sand, 1999). The presence, and the role of active microorganisms responsible for the regeneration of the lixiviants required for mineral dissolution to continue is explained through the indirect mechanism in Section 2.2.

Bioleaching technology has realised considerable growth in scale and application for recovery of valuable metals over the last six decades (Rawlings and Johnson, 2007) with noticeable

economic impact in the mining industry. The technology can be carried out in highly aerated, continuous flow, stirred tank reactor trains containing finely ground mineral concentrates, such as the BIOX™ process (Van Aswegen et al., 2007; Gericke et al., 2009). Tank processes are, however, typically limited to use in extracting high value mineral concentrates (Rawlings et al., 2003). The bioleaching technology is also carried out in a heap process in which an ore bed of crushed whole or run off mine (ROM) ore is irrigated and aerated to facilitate microbial regeneration of lixiviants within the bed and subsequent metal dissolution and transport from the ore bed (Suzuki, 2001; Watling, 2006; Pradhan et al., 2008). Utilising the same reactions, microbially facilitated leaching of mine waste material can also occur as an unwanted natural ARD process that is accompanied with acidification and metal pollution of water bodies resulting in a significant long-term environmental problem worldwide (Barnes and Romberger, 1968; Gray, 1996).

The understanding of the microorganisms (Section 2.3) that are involved in these bioleaching processes, the mechanism (Section 2.2) that they employ during microbial-mineral interaction (Section 2.4), and microbial colonisation of the mineral surfaces (Section 2.4.1), is critical to promote high metal recovery or to prevent the formation of ARD. These microbiological phenomena are observed in both heap bioleaching (Section 2.5.1) and ARD (Section 2.5.4).

2.2 Contact and non-contact mechanisms of mineral leaching

Sub-mechanisms, namely “contact” and “non-contact” mechanisms, have been proposed for the biological dissolution of metal sulfides (Tributsch and Bennett, 1981; Sand et al., 2001; Rawlings, 2002). The involvement of microorganisms in mineral degradation has been explained in three ways: i) the non-contact, ii) the indirect contact and iii) the direct contact mechanism (Figure 2.1) (Sand et al., 1995). In the non-contact mechanism, the planktonic cells oxidise Fe^{2+} available in the bulk solution to Fe^{3+}, which is the oxidizing agent that reacts with metal sulfides chemically (Figure 2.1 A). This is consistent with the indirect mechanism (Sand et al., 1995).

The indirect contact mechanism (Figure 2.1 B) describes the dissolution of metal sulfides as an electrochemical reaction between Fe^{3+} and metal sulfides. It takes place at the interface between the microbial cells and the mineral surface “reaction space”, hence accounts for the many cells attached to the surface of sulfide minerals. The reaction space is normally occupied with microbial extracellular polymeric substances (EPS) (see Section 2.4.2 for description). The microbial-mineral surface association have been shown in previous studies to play a key role in the leaching process and has also been shown to increase leach rates (Gehrke et al., 1998; Fowler et al., 1999; Kinzler et al., 2003). Sand et al. (2001) presented evidence that disputed the existence of the direct contact method (Figure 2.1 C) of leaching by showing that

without Fe, *At. ferrooxidans* does not oxidise the acid non-soluble metals, such as FeS_2, MoS_2 and WS_2, whereas the leaching of acid soluble sulfides, such as ZnS, CdS, NiS, CoS, CuS, or Cu_2S, continued via proton attack in the absence of Fe. The addition of Fe^{3+} to the microbial cultures enhanced leaching rates.

Based on the mechanisms presented, the direct contact method, i.e. enzymatic attack, has been shown to be non-existent or very unlikely (Sand et al., 2001), however, the indirect contact mechanism governed by microbial attachment and biofilm formation plays an important role in bringing the microbial catalysts, the reactants and the mineral surface into close proximity with each other in order to facilitate mineral degradation. Microbial communities present in heap bioleaching processes are largely found on the mineral surface (mineral associated state), and this is shown in the indirect contact mechanism (Figure 2.1 B). This is described by Govender et al. (2013, 2015) and Cox and Bryan (2017) who present data supporting the importance of the indirect contact mechanism.

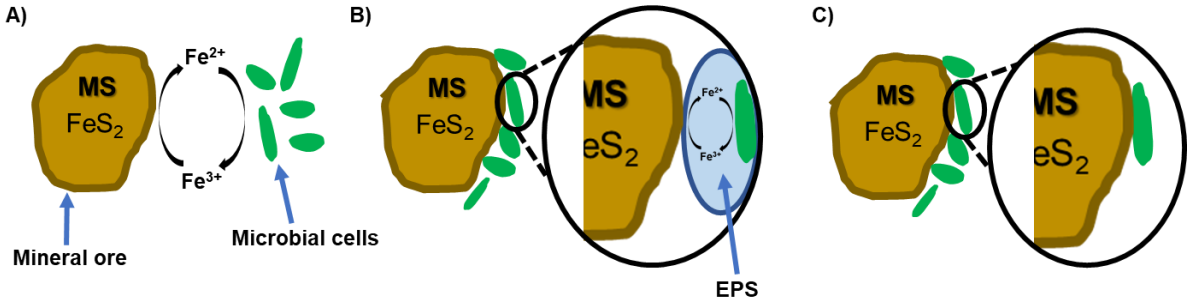

Figure 2.1: The role of microbial-mineral interaction is explained through the indirect mechanism (A), in which microorganisms oxidise Fe^{2+} in the bulk solution to Fe^{3+} and Fe^{3+} leach the mineral. The indirect contact mechanism (B), in which attached microorganisms (shown in green) oxidise Fe^{2+} to Fe^{3+} within layer of microorganisms and EPS, and the Fe^{3+} within this layer leach the mineral. The direct contact mechanism (C), in which the microorganisms directly oxidise the mineral by biological means, without any requirement for Fe^{3+} or Fe^{2+} (adapted from Crundwell, 2003).

2.3 Microbiology of metal sulfide oxidation

Bioleaching and biooxidation require acidophilic metal sulfide oxidizing microorganisms that oxidize Fe^{2+} to generate Fe^{3+} which catalyses the chemical oxidation of the metal sulfide bond. Sulfur is also oxidised to generate H^+ and SO_4^{2-}, maintaining the acid environment. These microorganisms are typically isolated and characterised from tank, heap and mine waste environments or from natural hot and sulfurous regions including hot sulfurous springs and volcanic regions. They have an optimal pH for growth below pH 3 (Watling, 2006). These acidophiles are classified based on the type of substrate they require for growth and maintenance. Chemotrophic microorganisms derive their energy from external chemical substrates and may oxidise inorganic chemical species such as Fe^{2+} or sulfur species (lithotrophic) or organic compounds (organotrophic). Autotrophic, heterotrophic and mixotrophic micro-organisms synthesise carbon from carbon dioxide, organic compounds or

both, respectively. These microorganisms can also be classified based on their temperature growth range, as mesophiles (25-40 °C), moderate thermophiles (40-55 °C) and extreme thermophiles (above 65 °C) (Johnson, 2009).

Mesophilic chemolithoautotrophs found in these environments may include *At*. *ferrooxidans* (oxidising both Fe^{2+} and reduced sulfur species), *L. ferrooxidans* (oxidising only Fe^{2+}) and *At. thiooxidans* (oxidising only reduced sulfur species). *At. caldus*, *L. ferriphilum* and *Acidimicrobium ferrooxidans* are examples of moderate thermophiles. Am. *ferrooxidans* grows autotrophically on iron, or mixotrophically on yeast extract, whilst *At. caldus* oxidises reduced sulfur species only. *L. ferriphilum* is chemolithoautotrophic and oxidises Fe^{2+} for metabolic energy (Shiers et al., 2016; Watling, 2016). *Ferroplasma acidiphillum* (Fe^{2+} oxidiser) and *Thermoplasma* archaeon are typically prevalent in pilot and commercial stirred tank bioreactors (van Hille et al., 2013; Smart et al., 2017) and a moderate thermophilic Fe^{2+} oxidiser, *Acidiplasma cupricumulans*, originally isolated from a heap copper bioleaching environments (Golyshina et al., 2009; Hawkes et al., 2006) is also found in tank bioreactors to play a role in the facilitation of mineral dissolution (Hawkes et al., 2006; Golyshina et al., 2009; Smart et al., 2017). Thermophilic chemolithoautotrophs such as *Sulfolobus metallicus*, *Acidianus brierleyi* and *Metallosphaera* (*M.*) *hakonensis* have been reported to be both iron and sulfur oxidisers (Plumb et al., 2007; Brierley, 2008b; Africa et al., 2013a; Shiers et al., 2013). These microorganisms, and their operation across the temperature ranges and energy sources, are described in Table 2.1.

Table 2.1: Selection of Fe and sulfur microorganisms commonly found in bioleaching environments (Watling, 2006; Schippers, 2007; Schippers et al., 2014).

Microorganism	Temperature opt (°C)	Growth substrate	Energy	pH opt	G+C (mol %)
Mesophiles					
Acidithiobacillus ferrooxidans	30-35	Fe and Sulfur	Autotroph	2.5	58-59
Acidithiobacillus albertensis	25-30	Sulfur	Autotroph	3.5-4	61.5
Acidithiobacillus thiooxidans	28-30	Sulfur	Autotroph	2-3	52
Leptospirillum ferriphilum	30-37	Fe	Autotroph	1.3-1.8	55-58
Leptospirillum ferrooxidans	28-30	Fe	Autotroph	1.5-3	52
Sulfobacillus benefaciens	38.5	Fe and Sulfur	Facultative	1.5	50
Moderate thermophiles					
Acidiplasma cupricumulans	54	Fe and Sulfur	Facultative	1-1.2	34
Ferroplasma acidiphilum	35	Fe	Facultative	1.7	36.5
Acidithiobacillus caldus	45	Sulfur	Facultative	2-2.5	63-64
Sulfobacillus acidophilus	45-50	Fe and Sulfur	Facultative	~2	55-57
Sulfobacillus thermosulfidooxidans	45-48	Fe and Sulfur	Facultative	~2	48-50
Ferroplasma thermophilum	45	Fe	Heterotroph	1	34.1
Thermophiles					
Metallosphaera hakonensis	70	Fe and Sulfur	Facultative	3	46
Acidianus brierleyi	~70	Fe and Sulfur	Facultative	1.5-2	31
Metallosphaera prunae	~75	Fe and Sulfur	Facultative	2-3	46
Metallosphaera sedula	75	Fe and Sulfur	Facultative	2-3	45
Sulfolobus metallicus	65	Fe and Sulfur	Autotroph	2-3	38
Thermoplasma acidophilum	56	Sulfur	Heterotroph	1.8	46
Acidianus sulfidivorans	74	Fe and Sulfur	Autotroph	0.35-3	31
Sulfolobus acidocaldarius	75-80	Sulfur	Autotroph	2-3	36.7
Sulfurococcus yellowstonensis	60	Fe and Sulfur	Facultative	2-2.6	45

opt = optimum, Facultative = Facultative autotroph and/or mixotroph; G+C = mole % guanine + cytosine content of genomic DNA

The discovery and description of *At. ferrooxidans* (Colmer and Hinkle, 1947; Temple and Colmer, 1951) prompted a rapid increase in microbiological studies related to the oxidation of sulfide minerals. *At. ferrooxidans* is arguably the most studied acidophilic microorganism, with more than 9,000 journal articles published on it, far more than any other acidophile (Watling, 2016). The initial purported importance of *At. ferrooxidans* in bioleaching environments was largely due to its relative ease to enrich and isolate in pure culture, coupled with rapid growth in acidic Fe^{2+} media. Since then, many acidophiles have been isolated and described and many more are still expected to be discovered using modern techniques (Watling, 2016). Ward and Fraser (2005) demonstrated how the uncultured space of microbiology far outweighs the cultured one, and acidophilic microorganisms are no exception. This strengthens the expectation that there is still a substantial number iron and sulfur oxidising acidophilic microbes in heap, tank bioleaching reactors, ARD environments and hot springs that might play crucial roles under particular environments but be present in low numbers under other environments, and are yet to be identified (Rawlings, 2005; Watling, 2006; Norris, 2007; Johnson, 2008; Orell et al., 2010; Watling et al., 2010). Culture independent molecular based methods with the ability to analyse, characterise and identify role players within microbial communities in bioleach environments contribute greatly to this identification, supplementing the classic microbial culturing. These methods can be used independently or in concert with one another, and they include PCR based RAPD (Randomly Amplified Polymorphic DNA) (Novo et al., 1996), Terminal Restriction Fragment Length Polymorphism (T-RFLP) (Bryan et al., 2006; Mutch et al., 2010), denaturing gradient gel electrophoresis (DGGE) (González-Toril et al., 2003; Demergasso et al., 2005; Acosta et al., 2014) ARDREA (Amplified ribosomal DNA restriction enzyme analysis) (Coupland and Johnson, 2004; Johnson et al., 2005); and for quantification or semi-quantification of bioleaching microbes the use of real time PCR (RT-PCR) (Demergasso et al., 2005; Demergasso et al., 2010; van Hille et al., 2013; Tupikina et al., 2014; Smart et al., 2017), FISH (fluorescence in-situ hybridization) (Okibe and Johnson, 2004; Coram-Uliana et al., 2006) and metagenomics, which also make use of bioinformatics (Quatrini et al., 2007).

Microbial communities change in number and relative abundance with time in both heaps and tanks. This is influenced by parameters such as the content and availability of the carbon and energy sources, solution composition and acidity, solids loadings in tanks, gangue components and acid neutralisation in heaps, and temperature (Romero et al., 2003; Demergasso et al., 2010; van Hille et al., 2013; Tupikina et al., 2014; Wang et al., 2014; Yu et al., 2014). In the initial stages of heap bioleach processes, *Acidithiobacillus spp*. including *At. ferrooxidans* and sulfur-oxidising species *At. caldus*, *At. thiooxidans* and *At. albertensis* have been shown to be abundant due to the greater sulfur content in the beginning of these

processes (Remonsellez et al., 2009; Demergasso et al., 2010). Later on, when Fe^{3+} concentration increases and become inhibitory to *Acidithiobacillus spp*. and other species, more Fe^{3+} tolerant *Leptospirillum* and *Ferroplasma spp*. become more abundant in the tank and heap leaching systems (Rawlings et al., 1999; Kawabe et al., 2003; Okibe et al., 2003). In previous studies performed under mesophilic conditions as well as temperature progression studies (mesophilic through moderate thermophilic), *L. ferriphilum*, *L. ferrooxidans*, *At. thiooxidans* or *Acidithiobacillus caldus* and *At. ferrooxidans* were demonstrated as the dominating microbial species (Dew et al., 2011; Acosta et al., 2014; Tupikina et al., 2014; Watling et al., 2016).

In ARD environments, microorganisms with the same functions are found. Druschel et al. (2004) used culture independent 16S rRNA gene clone libraries and rRNA probe-based molecular techniques to study microbial community structure in an active pyritic oxidising mine environment. A range of communities were identified at various regions of the mine, including Fe oxidisers *Ferroplasma* and *Leptospirillum spp*., *Acidithiobacillus spp*. and relatively small populations of *Sulfobacillus spp*. and *At*. *caldus*.

For the longest time, the presence and function of the microbial component on the rate of ARD generation was not taken into account and the chemical-based methods for the characterisation of ARD provided limited insight into the process. Inclusion of microorganisms in ARD characterisation tests have been proposed through experimental tests utilising shake flasks experiments on finely ground waste samples inoculated with microorganisms typically found in the bioleaching of mineral sulfides (Bruynesteyn and Hackl, 1982). Several studies (Hesketh et al., 2010; Broadhurst et al., 2013; Harrison et al., 2013; Opitz, 2013; Dyantyi, 2014; Becker et al., 2015; Opitz et al., 2016; Opitz and Harrison, 2016; Golela, 2018) have investigated the presence and influence of microorganisms on the rate of ARD formation. In all these studies, mesophilic and/or moderate thermophilic iron and sulfur oxidising microorganisms played a critical role in the characterisation of mine waste.

Abundant attachment and colonisation of the mesophilic microbial community at the beginning of a heap bioleaching process is crucial for their proliferation on the mineral surface, leading to, extensive oxidation and accelerated metal recovery. Similarly, understanding the extent to which microorganisms adhere to and colonise waste rocks on their disposal would provide insight into solutions on how to deter those interactions and consequently prevent the ARD formation.

2.4 Microbial-mineral interactions

It is well established that certain microorganisms possess the ability to attach to solid surfaces (Watling, 2006) with these surfaces being the major site of microbial activity (van Loosdrecht et al., 1990). van Loosdrecht et al. (1990) postulated that microbial attachment progressed through a series of steps, starting with microbial transport to the vicinity of the mineral surface by diffusion, convection and chemotaxis, moving through initial adhesion and attachment to biofilm formation, resulting in colonisation of the mineral surface (Gehrke et al., 1998; Rohwerder et al., 2003; Sand and Gehrke, 2006; Africa et al., 2010; Africa et al., 2013a; Govender et al., 2013; Tupikina et al., 2013) (Figure 2.2).

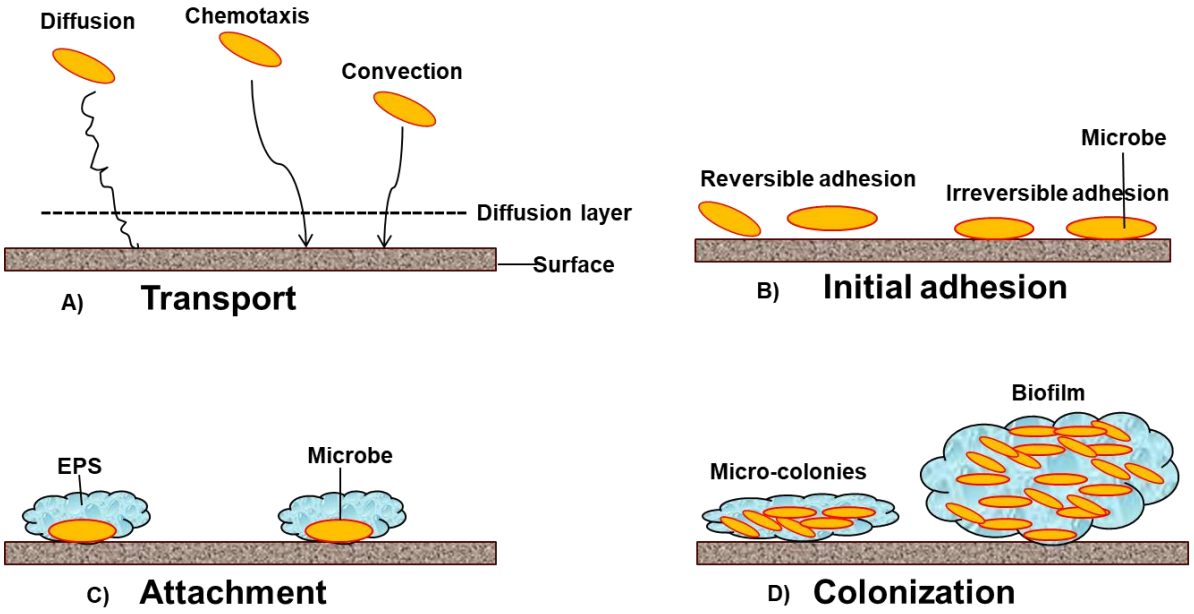

Figure 2.2: Schematic representation of the sequence of steps (A-D) involved in the colonization of surfaces by microorganisms. (A) Shows the routes involved in delivering microbial cells to the mineral surface vicinity. (B) Once there, the cells attach to the surface in two ways: reversible adhesion that is susceptible to removal by shear liquid flow and irreversible adhesion that remains. (C) The irreversibly attached cells consolidate their attachment through the production of extra-polymeric substance (EPS). (D) EPS allows cells to grow and multiply leading to a biofilm (adapted from van Loosdrecht et al., 1990).

Initial attachment is described as either reversible or irreversible. In reversible attachment, the microorganisms are transported to, and attach to the mineral surface either through chemotactic, electrostatic, hydrophobic attraction but do not firmly attach. In irreversible attachment, the microorganisms are transported in a similar manner, however, their interaction with the mineral surface becomes established through polymeric substances or irreversible bonding, unlike the reversible forces of attraction (Rodríguez et al., 2003). Microorganisms that are reversibly associated with the mineral surface are proposed to retain their ability to transport away from the mineral surface through convection or chemotaxis, whilst irreversible

attachment may be facilitated by the production of EPS, which enclose the attached microorganisms or through the assistance of microbial appendages or both (Zobell, 1943; van Loosdrecht et al., 1990; Gehrke et al., 1998). It is further postulated that subsequent microbial proliferation and colonisation occurs within the EPS layer, with new microorganisms remaining within a biofilm layer (van Loosdrecht et al., 1990).

The Zobell's model (Equation 2.5) that describes the initial interaction between microorganisms and surface sites, requires the formation of a metastable complex between the two that is brought about by the balance of repulsive and attractive forces (Echeverría-Vega and Demergasso, 2015). B is the microorganism(s), S is the surface site involved, [BS]* is the reversible attachment and formation of the metastable complex and BS represents irreversible attachment (Rodríguez et al., 2003).

$$\boldsymbol{B + S \underset{K2}{\overset{K1}{\leftrightarrow}} [BS]^* \overset{K3}{\rightarrow} BS} \qquad \text{Equation 2.5}$$

The repulsive and attractive forces that facilitate the initial adhesion of microorganisms to surfaces are primarily due to physicochemical processes explained by non-specific hydrophobic and electrostatic interactions between the cell surface and minerals (van Loosdrecht et al., 1990; Devasia et al., 1993; Harneit et al., 2006).

Chemotaxis is when a microorganism responds to a stimulus. The stimulus may be a nutrient concentration gradient; where a motile microorganism moves towards higher concentrations of the stimulant. On the other hand, the stimulus may be a repellent with the motile microorganism moving away from its higher concentrations. The process utilises signal transduction proteins that contain two functional domains, a sensory domain that interacts with the stimulant at the cell surface and a signalling domain that modulates effector activities within the cell causing movement toward or away from the stimulus (Surette and Stock, 1994; Delgado et al., 1995; Rojas-Chapana et al., 1998). Rojas-Chapana et al. (1998) suggested that the attachment of *At. thiooxidans* and *At. ferrooxidans* to sulfur/sulfide substrates and pyrite was as a result of chemotactic behaviour. This was confirmed by the addition of the non-ionic detergent Tween® 80, which affected the surface behaviour of microorganisms and neutralised that phenomenon (Rojas-Chapana et al., 1998). Ghauri et al. (2007) and Kinzler et al. (2003) also established the role of chemotactic and electrostatic forces during initial attachment. Ghauri et al. (2007) screened sixteen acidophilic microorganisms for their abilities to adhere to pyrite ore, glass beads and Fe^{3+} hydroxysulfates. Variations were found between the rates and extents to which acidophilic bacteria attached to the three different solid materials tested. In most cases, the acidophiles attached more readily to pyrite than to glass

or Fe^{3+} hydroxysulfates. Gehrke et al. (1995) demonstrated that Fe^{3+} ions within the EPS influence the surface charge of *At. ferrooxidans*, thereby enabling an electrostatic interaction with pyrite and Kinzler et al. (2003) also demonstrated that *At. ferrooxidans* strains with more EPS-complexed Fe^{3+} adhered more rapidly and in greater numbers than strains with less iron, which adhere more slowly or not at all. Echeverría-Vega and Demergasso (2015) investigated the behaviour of bioleaching microorganisms and their interaction with pyrite and chalcopyrite minerals. The authors demonstrated that hydrophobicity was an important factor in the early stages of the microbial-mineral interaction as it determines the free energy of the adhesion process. Whereas from a microbial point of view, microbial properties such as chemotaxis, motility and copper resistance, where shown to determine the grade and the stability of the attachment. Jerez (2001) isolated and characterised a gene from *L. ferrooxidans*, encoding a putative chemotactic receptor (LcrI). The LcrI protein structure was similar to that of methyl-accepting chemotaxis proteins, which suggested that *L. ferrooxidans* possessed a chemotactic signal transduction mechanism similar to that of other microorganisms. The association of bioleach microbes with the surface for the onset of initial adhesion may therefore be a result of a chemotactic and electrostatic responses.

Ghauri et al. (2007) suggested that the availability of mineral surface area does not necessarily limit *At. ferrooxidans*. If the inoculum exceeds the available surface area, some cells may remain in the planktonic state. However, it has been reported that this occurs even if there is 5 % microbial coverage of the mineral surface area (Schippers et al., 2014). Africa et al. (2010) reported that microorganisms preferentially attach to regions on the ore surface that contain visible surface defects. In a subsequent study, Africa et al. (2013b) measured levels of attachment across different minerals (pyrite concentrate, chalcopyrite concentrate and low-grade chalcopyrite ore) with pyrite adapted and Fe^{2+} grown microorganisms (*A. ferrooxidans* and *L. ferriphilum*). Mineral adapted microorganisms were shown to generally have higher surface coverage when compared to the Fe^{2+} grown microbes, however, a substantial part of the surface area was not covered. This shows that the space on the surface of a metal sulfide is non-limiting for attachment.

This, and many of the studies on mesophilic microbial attachment to pyrite and chalcopyrite mineral surfaces, focused on single species or a limited number of species and were performed on mineral samples submerged in batch shake flasks (Rodríguez et al., 2003; Harneit et al., 2006; Ghauri et al., 2007). These studies provided insights into the fundamental understanding of mineral-microbe interactions, however, as aforementioned, the future of metal recovery lies in low-grade ores. Secondly, the mine waste material from which ARD is formed is mostly lower in sulfide content (%), thus it is of essence to focus on flow-through systems and variable sulfide grade. Thirdly, in mine waste dumps as well as in bioleach

conditions, complex microbial populations are found working synergistically to exert maximum mineral surface degradation. Fourthly, large-scale commercial low-grade ore leaching operations are operated as packed-bed heaps, and mine wastes are also mostly packed in dumps. Thus, to provide practical and readily applicable knowledge on colonisation, an open, flow-through unsaturated bioleach environment that is representative of a heap or dump is essential in providing further understanding of microbial-mineral interactions.

2.4.1 Microbial colonisation of mineral surfaces

The final stage of microbial adhesion is colonisation and biofilm formation (Figure 2.3 D) (van Loosdrecht et al., 1990). To date, the majority of studies on colonisation have focused largely on mesophilic and moderately thermophilic microorganisms in submerged, batch culture (Gehrke et al., 1998; Sanhueza et al., 1999; Gehrke et al., 2001; Kinzler et al., 2003; Harneit et al., 2006; Mangold et al., 2008b; Pradhan et al., 2008; Lei et al., 2009; Noël et al., 2010; Florian et al., 2011; Bellenberg et al., 2012; González et al., 2012; Bellenberg et al., 2014; Zhang et al., 2014; Bellenberg et al., 2015; Ramirez-Aldaba et al., 2017). A select number of studies have also focused on colonisation by thermophiles (Africa et al., 2013a; Castro et al., 2016; Li et al., 2016; Li et al., 2017; Zhang et al., 2019a; Zhang et al., 2019b). Although these studies were conducted in well mixed batch systems, they provided insights into the visualisation and qualitative aspects of colonisation and reported further on the subsequent formation of monolayer biofilms.

The above-mentioned investigations into microbial colonisation of sulfidic mineral surfaces were performed under conditions that were not representative of heap bioleach environments. Studies focusing on the investigation of microbial-mineral interactions and colonisation under heterogeneous heap simulating conditions are not as prevalent as those conducted in well mixed batch systems. Colonisation in heap simulating conditions require a consideration of additional parameters such as the unsaturated environment and fluid-flow dynamics, including liquid contacting and flow rates (Chiume et al., 2012; Fagan et al., 2014) . Africa et al. (2013a) used a novel biofilm reactor, mounted with thin mineral sections, with operating conditions simulating those of a bioheap in terms of fluid-flow and mineralogy. Preferential attachment and biofilm formation to sulfide minerals was observed, with increased surface coverage of pyrite mineral surfaces relative to chalcopyrite and low-grade ore. The atomic force and epifluorescence microscopy (AFM-EFM) technique enhanced the level of detail at which site-specific associations of microorganisms with mineral surfaces could be assessed. Spatial orientation and density of attached micro-colonies were evident. When studying microbial colonisation and performance of a bioheap or a waste dump, it is important to account for the microbial communities within the PLS as well as those associated with the mineral surface. In

bioheap systems, microorganisms are observed within three discrete phases: 1) directly associated with the mineral surface; 2) in stagnant interstitial liquid trapped in between ore/waste rocks; and 3) within the bulk flowing PLS (Figure 2.3) (Govender et al., 2013).

Govender et al. (2013) quantified the microbial colonisation, growth and propagation of *At. ferrooxidans* in an unsaturated bed of crushed and agglomerated low-grade chalcopyrite ore. Microbial populations distributed across the PLS, the stagnant interstitial liquid and weakly and strongly attached to the mineral surfaces were determined at various time points, through progressive column sacrifice, during the leach period. Distinct differences in population dynamics in each of these discrete phases were observed (Govender et al., 2013). The microbial cells in the interstitial phase were 2-3 orders of magnitude higher than those in the free flowing PLS, and they also dominated the microbial population in the ore bed. Microbial concentration in the free flowing PLS, which was previously used as the standard measure for representation, was found to be a poor representation of the ore-associated microbial populations. In a subsequent study, Govender et al. (2015) investigated the effect of a selection of physico-chemical and operating conditions on microbial growth, colonisation and substrate utilisation kinetics, where both planktonic and mineral associated populations of *At. ferrooxidans* were considered. The factors studied included inoculum size, inoculum cultivation conditions, availability of Fe^{2+} in the bulk flowing solution and copper concentration in the bulk flowing solution. Microbial populations in the stagnant interstitial phase were also observed to be more represented when compared to other various phases.

A model was further developed to describe microbial growth and transport in the flowing bulk solution and ore-associated phases within a mineral bioleaching heap with the populations retained in the interstitial phase assumed to be a function of microbial transport between the ore surface and the bulk solution, as well as growth in each of these phases (Govender et al., 2014). Cox and Bryan (2017) conducted a similar experiment using low-grade copper ore, in which the ore bed was not sterilised, and the system was inoculated with a mixed mesophilic culture. They observed a significantly lower microbial concentration in the PLS compared to the ore associated phases throughout a 6-month experimental period. This was consistent with previous observations of microbial population distributions within the various ore phases (Govender et al., 2013, 2015). Chiume et al. (2012) studied the prevalence of microbial populations in these phases, as a function of irrigation rates ranging from 2, 6 and 18 (L m^{-2} h^{-1}). It was shown that microbial colonisation was higher at lower irrigation rates, and that there was increasing microbial detachment from the ore surface to the PLS when irrigation rates were increased (Chiume et al., 2012). The above collective studies used the UCT developed detachment method to highlight the significant difference in microbial diversity and abundance between the PLS and ore-associated phases. The method was developed to differentiate

between the interstitial, weakly-attached and strongly attached microorganisms present within the bed of crushed ore. A surfactant (0.4 % Tween® 20) together with vortexing of firm ore-associated populations is used to remove the strongly attached cells. Post the removal and recovery of cells from mineral ore surfaces, they are enumerated using light microscopy. This standardised detachment method relies on enumeration of the detached cells and assumes their complete detachment.

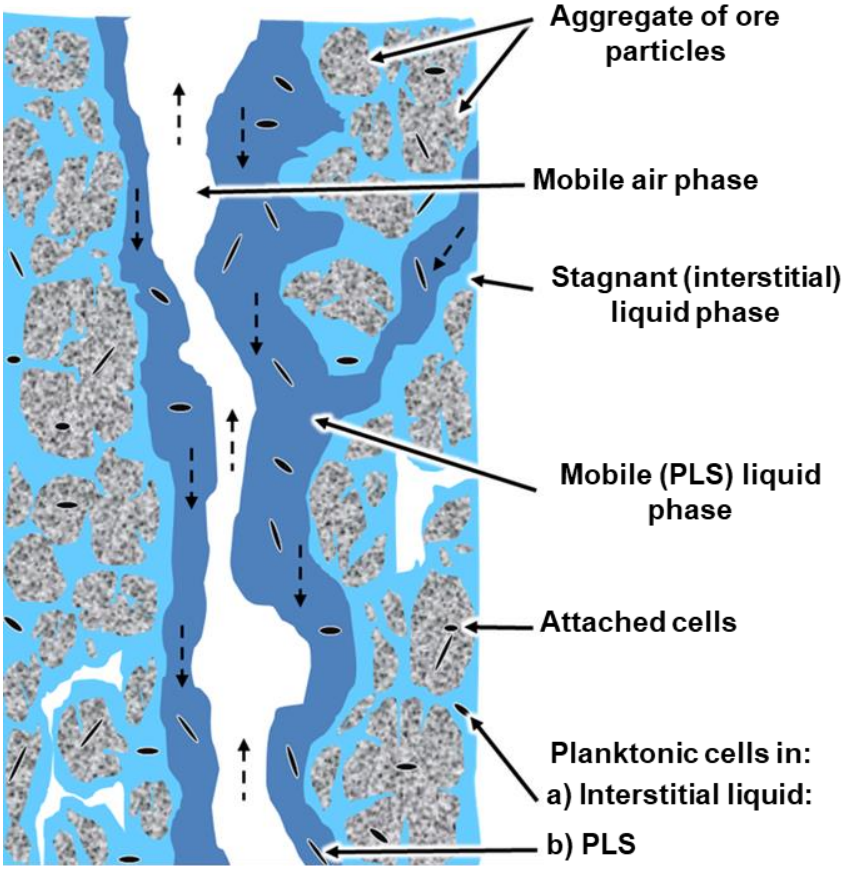

Figure 2.3: Diagram illustrating the inside of the heap, showing planktonic cells in the flowing mobile liquid phase, microorganisms weakly and strongly associated with the ore surfaces, and microorganisms accumulating within the stagnant regions of the porous rocks (interstitial cells) (Govender et al., 2013).

2.4.2 EPS and biofilm formation

In nature, microorganisms predominantly exist as aggregates in the form of biofilms, which are defined as communities of immobilised microorganisms that form at air-liquid and/or liquid-surface interfaces (Wingender et al., 1999; Flemming and Wingender, 2010). Investigations of microbial communities found in ARD environments have shown that biofilms are not composed of a single microbial species, but are rather made-up of complex mixed consortia of bacteria and archaea (Bond et al., 2000; Tyson et al., 2004). In most biofilms, EPS accounts for over 90 % of the dry mass (microorganisms account for less than 10 %) (Flemming and Wingender, 2010). EPS are described by Wingender et al. (1999) as the “building-blocks” of

a microbial biofilm, conveying and maintaining structural integrity and stability to the biofilm. EPS play a crucial role in the attachment of cells to a solid substrate as well as in the attachment of cells with other cells or particulate matter. As such, EPS also mediates microbial attachment and biofilm formation on mineral surfaces (Rohwerder and Sand, 2007). EPS provide a “safe haven” microenvironment for microorganisms within the biofilm, which allows for the proliferation of microorganisms and their protection from environmental stress such as UV radiation, pH shifts, osmotic shock, hunger and desiccation (Flemming, 1993). Production of EPS occurs both in prokaryotic and in eukaryotic microorganisms.

Biofilms have been shown to provide protection against hydrodynamic shear. Purevdorj-Gage and Stoodley (2004) studied the effect of hydrodynamic shear on the biofilm architectural development and structure of *Pseudomonas aeruginosa*. It was demonstrated that biofilms grown in high shear conditions had a stronger EPS matrix and had more strongly adhered cells than those grown under low shear. This phenomenon was attributed to the stretching of biofilm in response to higher shear, causing the individual polymer strands to become physically aligned allowing additional electrostatic as well as hydrogen bonding to occur between the closely pulled neighbouring polymers (Flemming et al., 2000). Given the occurrence of channelling in bioheap environments, that lead to varying degrees of hydrodynamic shear (O’Kane et al., 1999), biofilm and the production of EPS may be valuable. EPS within has also been shown to provide significant protection against reactive oxygen species and heavy metals (Starkey et al., 2004). This would be beneficial in a bioleach environment where reactive oxygen species have been shown to form in association with pyrite (Jones et al., 2013). The highly permeable water channels within the biofilm allow the exchange of nutrients and metabolites with the environment, thereby enhancing nutrient availability and removal of metabolites (Costerton et al., 1995). Once formed, the microorganisms within a biofilm have increased opportunities, due to close proximity, for horizontal gene transfer (Dahlberg et al., 1997). Microorganisms derive benefits from the production of EPS through its modification of their macro-and microenvironments. Some of the proposed functional benefits of EPS production are presented in Table 2.2.

The biochemical composition of the EPS is considered to be important for the activity of the microorganisms encased by it (Nielsen and Jahn, 1999). EPS are mainly composed of polysaccharides, proteins, nucleic acids and lipids (Flemming and Wingender, 2010). In acidic environments, uronic acids, humic substances and heavy metals have been reported (Gehrke et al., 1998; Gehrke et al., 2001; Aguilera et al., 2008; Michel et al., 2009; Tapia et al., 2009; Africa, 2017). Costerton et al. (1981) reported polysaccharides as the major composition of the EPS whereas Dignac et al. (1998) showed that protein was prominent in activated sludge biofilm. However, Harneit et al. (2006) showed that the exact nature of this matrix may vary

depending on the surrounding environment and the microorganisms involved. Gehrke et al. (2001) analysed the chemical composition of partially purified EPS and reported that EPS excreted from *At. ferrooxidans* was comprised predominantly of neutral sugars and lipids with the composition dependent on growth medium. Similar findings were observed by Kinzler et al. (2003) and Harneit et al. (2006) assessing *At. ferrooxidans*. Gehrke et al. (2001) reported that growth of *At. ferrooxidans* on different substrata influenced the yield of EPS produced. Kinzler et al. (2003) using similar growth substrates, measured neutral sugars, fatty acids and uronic acids from EPS of *At. ferrooxidans*, *At. thiooxidans* and *L. ferrooxidans* respectively. The composition varied with the strain and the growth substrate.

Table 2.2: Selection of functions of EPS that determine the mode of life in a given microbial biofilm (adapted from Wingender et al., 1999; Flemming and Wingender, 2010).

Function	Relevance for biofilms
Adhesion to surfaces	Mediates firm adhesion and colonisation of surfaces, microbial growth on nutrient rich surfaces in oligotrophic environments
Cohesion (aggregation of microbial cells, formation of flocs and biofilm)	Connecting cells, inorganic particles and mineral surface-active sites, immobilise microbial populations. Encourage development of high cell densities, generation of a medium for communication processes, provide a reactive space for mineral dissolution reactions, aid sediment stability, and alter the micro and macro-environment
Cell-cell recognition and associations	EPS concentrate cells and or signalling molecules enabling these associations
Structural elements of biofilm	Mediation of mechanical stability of biofilms, often in conjunction with multivalent cations, governs EPS architecture
Protective barrier	Resistance to extreme pH, elevated temperature, dehydration, freezing, biocides and heavy metals and detergents
Retention of water	Hydrodynamic stability (cell walls need to remain hydrated to maintain selective permeability; exo-enzymes need hydrated environments in which to be active (Wolfaardt et al., 1999), prevention of desiccation
Sorption of exogenous organic compounds	Scavenging and accumulation of nutrients from the environment, sorption of xenobiotics (detoxification) terraforming macro-environment
Sorption of inorganic compounds	Accumulation of toxic metal ions (detoxification), promotion of polysaccharide gel formation, mineral formation, terraforming macro-environment
Enzymatic activities	Digestion of exogenous macromolecules for nutrient acquisition, release of biofilm cells by degradation of structural EPS of the biofilm. Excretion of bacteriolytic enzymes (Wolfaardt et al., 1999)
Interaction of polysaccharides with enzymes	Accumulation, retention and stabilization of secreted enzymes

Jiao et al. (2010) analysed EPS compounds from two natural microbial pellicle biofilms, grown in acid mine drainage solution from Iron Mountain in California. Both samples were composed of carbohydrates, and metals as second major constituents, small amounts of proteins and low amounts of DNA and lipids. Govender and Gericke (2011) extracted EPS from bioleaching consortia grown on various mineral substrates including sphalerite, pyrite and chalcopyrite-pyrite and at various temperature profiles (37-70 °C). The extracted EPS consisted mainly of carbohydrates, proteins and uronic acids across the growth substrates. In more recent studies, Africa (2017) cultivated *M. hakonensis* EPS on chalcopyrite, sulfur and ferrous sulfate and

used EDTA and crown ether (CE) to extract EPS. Major biochemical components observed from the growth substrates were proteins, sugars, uronic acids and inconsistent minor amounts of nucleic material and iron for both extraction methods. Li and Sand (2017) used ion exchange resin to extract EPS from *S. thermosulfidooxidan* that was grown on pyrite and humic substance was the component identified, followed by proteins, polysaccharides and uronic acids. In a subsequent study, using the same extraction method, Li et al. (2019), reported similar biochemical components on EPS of the same species grown on pyrite and sulfur. Zhang et al. (2019b) used EDTA to extract EPS from *Acidianus spp* and *S. metallicus* that were grown on sulfur prills. Sugars, uronic acids, proteins and lipids were reported on both EPS (Table 2.3).

Table 2.3: Summary of key investigations in which EPS were extracted and characterised from bioleaching environments.

Growth medium(s)	**Microrganism(s)**	**Extraction method**	**EPS composition**	**Author**
Pyrite, Fe^{2+} and Sulfur	*At. ferrooxidans*	Homogenization and centrifugation	Sugars and lipids	Gehrke et al. (1998); Gehrke et al. (2001)
Pyrite	various strains of *At. ferrooxidans*	Homogenization, filtration and centrifugation	Sugars and lipids	Kinzler et al. (2003)
Pyrite, Fe^{2+} and Sulfur	*At. ferrooxidans, At. thiooxidans and L. ferrooxidans*	Cross-filtration and centrifugation	Sugars, lipids and Fe	Harneit et al. (2006)
AMD solution	*Leptospirillum* group II (43 %) and III (28 %) as well as archaea (29 %)	Sulfuric acid and centrifugation to extract EPS	Carbohydrates, metals, protein, DNA	Jiao et al. (2010)
Sphalerite, pyrite, chalcopyrite-pyrite	Mesophiles (*At. caldus, Leptosprillium spp, Sulfobacillus spp*) Moderate thermophiles (*At. caldus, Leptosprillium spp, Sulfobacillus spp, Ferroplasma spp*) Thermophiles (*Acidianus spp, Metallosphaera spp, Sulfolobus spp*)	Ethanol	Carbohydrates, proteins, uronic acids and humic acids	Govender and Gericke (2011)
Chalcopyrite, Fe^{2+} and sulfur	*M. hakonensis*	EDTA and Crown ether	DNA, sugars, uronic acids, proteins and iron	Africa (2017)
Pyrite and sulfur	*S. thermosulfidooxidans*	Ion exchange	Polysaccharides, proteins, uronic acids and humic substances	Li and Sand (2017) Li et al. (2019)
Sulfur	*Acidianus spp* and *S. metallicus*	EDTA	Sugars, uronic acids, proteins and lipids	Zhang et al. (2019b)

2.5 Applications of mineral bioleaching

Mineral bioleaching is applicable across tank, heap and ARD processes. These are highly dependent on a number of parameters including, but not limited to, the grade of the metal of choice, the type of metal and the economics around that metal as well as the associated gangue materials, degree of liberation and the physicochemical conditions and microbial activity within the heap or dump.

2.5.1 Heap bioleaching

Heap bioleaching and biooxidation are biotechnological processes that potentially enable the recovery of predominantly semi-precious (e.g. titanium, nickel), precious (e.g. gold, platinum) and base metals (e.g. copper) from low-grade mineral ore with the assistance of microorganisms. To date, copper and gold heap processes have been commercially exploited most commonly (Ghorbani et al., 2015). Heap bioleaching is attractive as an industrial process as it is technologically extremely simple and involves relatively low capital and operating expenses (Figure 1.1). Challenges to its feasibility include the long operating times and, depending on the ore, the ability to achieve complete extraction.

Heaps are constructed in a manner that makes them highly heterogeneous, unsaturated systems with gas occupying the spaces not taken up by solids or liquid solution. Heaps are aerated from the base by blowing in air to provide O_2 to assist with microbial oxidation reactions and CO_2 for assimilation into microbial biomass. A leach solution is distributed across the top of the heap by sprinklers or, most typically, drip irrigation. This solution permeates the packed ore and is collected from the bottom as a pregnant leach solution (PLS) that contains the metal of interest. The PLS is further processed by solvent extraction and electrowinning to recover the metal. The leach solution that is recovered from the solvent extraction stage is known as the raffinate. It is supplemented with nutrients, microorganisms and acid if necessary, before being recycled back to the heap (Figure 2.4) (Rohwerder et al., 2003; Watling, 2006; Petersen and Dixon, 2007a; Pradhan et al., 2008). A typical heap is packed with the low-grade mineral sulfide ore of choice. This is typically crushed to a particle size distribution (PSD) of 25 mm and less (Petersen and Dixon, 2007a; Brierley, 2008a). The smaller crush size results in increased liberation and accelerated extraction within a reasonable timeframe (Bartlett, 1992; Miller et al., 2003); however, too small a crush size impacts the bed permeability and hence distribution of irrigant and gases. In some cases, run-of-mine (ROM) ore is used directly to reduce processing costs, but at the cost of further expanding time of operation and reducing maximum extraction efficiency.

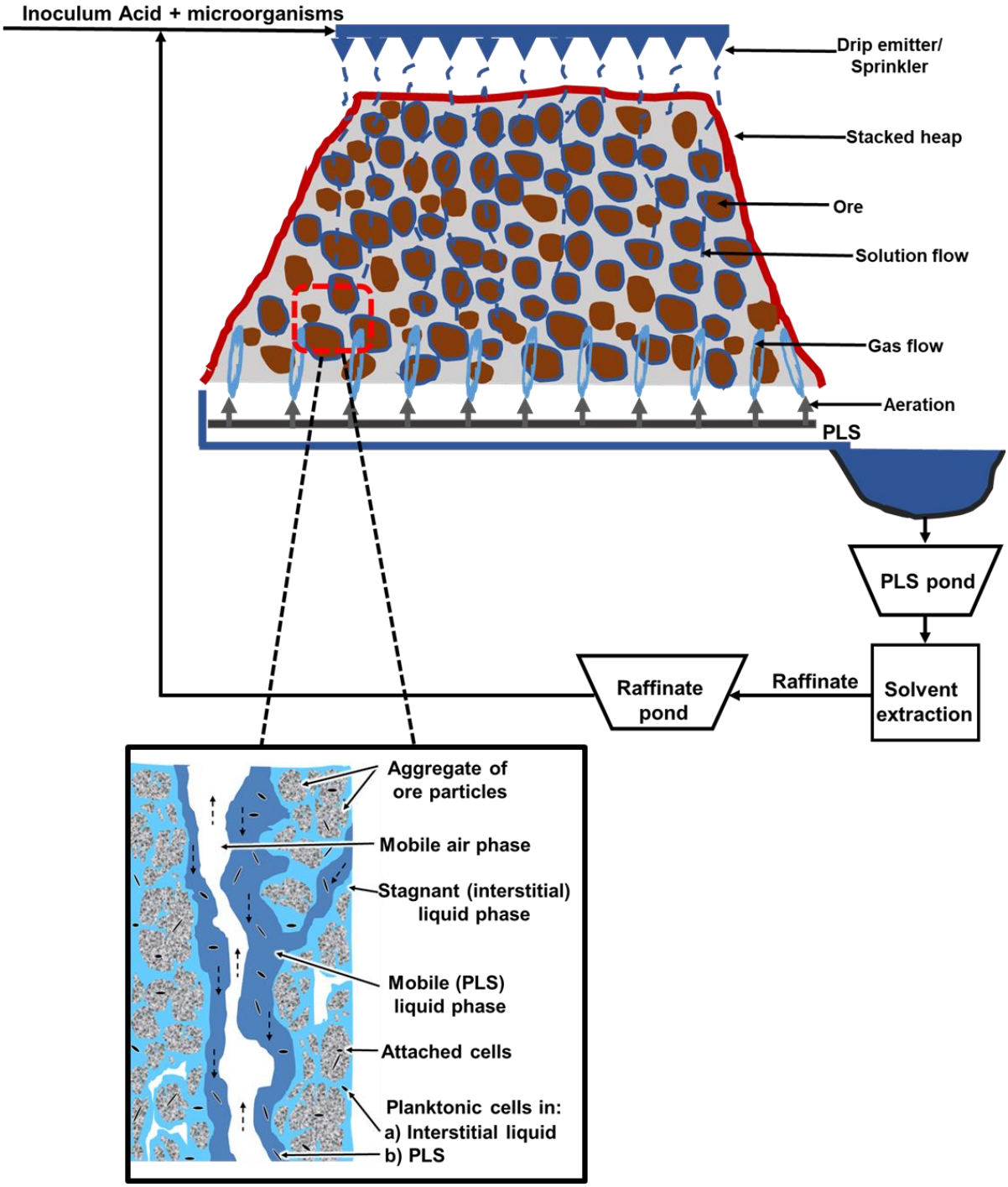

Figure 2.4: A schematic of the heap (bio)leaching process (adapted from Petersen and Dixon, 2007a). The insert shows the interactions of microorganisms with liquid, gas (air) and solid phases and their positioning within the heap (Govender et al., 2013).

The crushed or run-of-mine (ROM) ore is then either loaded onto a heap directly (ROM or crushed) or agglomerated with acidic solution (crushed only), using either a rotary drum or belt agglomeration depending on the physical properties of the ore, prior to being loaded onto a heap (Kappes, 2002). The agglomeration process helps to minimise the presence of finer particles and clays that could result in restricted solution and gas flow leading to sections of the heap remaining unleached. Furthermore, good fluid flow is imperative to ensure that the

microorganisms do not become oxygen and carbon dioxide deprived, rendering them ineffective and that good mineral-irrigant contacting is maintained.

The heap is stacked on an impermeable layer (polyethylene or plastic sheet) connected to a drainage system (Petersen and Dixon, 2007a). This is to prevent the loss of PLS through seepage to the ground and water table, which would lead to both production loss and an environmental risk (Rawlings, 2002; Rawlings et al., 2003). Aeration pipes are placed at the base of the heap and provide aeration at rates ranging from 0.08 to 2 $m^3 m^{-2} h^{-1}$. Aeration from underneath the ore bed allows for the distribution of air throughout the heap in a reasonably homogeneous manner in a well-stacked heap, creating complex patterns that promote heat generation in the heap and its transfer through the heap (Petersen and Dixon, 2007a).

The leach solution or raffinate is distributed across the top of the heap by either sprinklers or drip emitters at a rate between 4 to 18 L $m^{-2} h^{-1}$ (Dixon, 2000; du Plessis et al., 2007). This flows downwards through the heap under gravity. As the solution flows through the ore bed, it, together with the microorganisms it carries, interact with the ore surfaces with a significant portion of solution trapped in pores and crevices between ore particles. This distribution of fluid and associated microorganisms and their retention or hold-up in the interstitial spaces helps to facilitate the dissolution of mineral-entrained metals into solution. Depending on the solution flow distribution patterns and sizes of the stagnant zones, the flowing solution interacts with the largely stagnant moisture in the interstices and exchanges dissolved components with it. A typical leach solution is supplemented with essential nutrients for microbial growth and metabolism as well as acid. Iron and sulfate concentrations typically are allowed to build up to a pre-set, non-inhibitory level in heaps.

Microorganisms are introduced to the heap system during the agglomeration process or are inoculated and transported via the feed irrigation system. This takes place at the inception and in some cases at periodic intervals during the heap leach life (Gericke, 2012; Tupikina et al., 2014). Heaps are inoculated, mostly with mixed microbial cultures, to promote colonisation of the ore surfaces by providing substantial microbial diversity that is suitable for and will thrive across the various conditions experienced throughout the lifespan of the heap. Proportional distribution of microbial cultures ensures that adequate numbers of active leaching microorganisms are present throughout the life of a heap so that optimum heap performance is achieved (Rawlings and Johnson, 2007). In order to achieve a relatively high performing heap, an intermittent inoculation strategy may be adopted, where initial irrigation of inoculum that consists of mesophilic microbial communities, possibly followed by a secondary inoculation with moderately thermophilic and thermophilic communities, or various combinations thereof, whenever the appropriate temperature is reached (Dew et al., 2011;

Gericke, 2012). Microbial diversity and activity are normally monitored by analysing the PLS that is expelled from the heap. This analysis is largely used as an indicator of the performance of an entire heap, including representation of the diversity as well as activity of microbial populations interacting with ore surfaces (Demergasso et al., 2005; Demergasso et al., 2010).

To operate optimally, a bioheap relies on numerous aspects including engineering that involves the construction of carefully designed heaps, appropriate and balanced aeration for the availability of oxygen and carbon dioxide to microbes and hydrology to ensure that sufficient nutrients are supplied to the microbial population, without saturating the heap. Ultimately, bioheaps are typically designed with the optimisation of microbial activity in mind, thus leaching efficiency and metal recovery are therefore paramount to any bioheap operation (Gahan et al., 2012).

2.5.2 Heap simulating reactor application in bioleaching studies

Table 2.4 provides a summary of selected studies conducted in heap simulating systems that focused on microbial-mineral interaction in bioleach environment. The reactors used in these studies were tailored to act as structures that allowed for the extraction of the information presented in these studies. At a demonstrational level, Dew et al. (2011) used large 6m column reactors to investigate different inoculation strategies as well as microbial succession. In this column reactor, heat generation resulted only from mineral sulfide oxidation and not from applied external heating, which allowed the simulation of the temperature profile of a section of ore in a commercial heap. The authors showed that self-generation of heat from microbial facilitated leaching of pyrite contained in the ore may be managed to sustain high operating temperatures, with average temperatures of 70 °C being achieved. The authors also showed that the success of bioleaching was attributed to the inoculation strategy and the ability to achieve microbial succession as the ore temperature increased.

On medium lab scale column reactors, Tupikina et al. (2013), using multiple heat jacketed glass columns packed with 5kg chalcopyrite ore, investigated the effect of pH and inoculum size and succession subsequent to that (Tupikina et al., 2014). Ngulube (2013) used the same reactor to study microbial colonisation and growth of moderate thermophiles at 50 °C. These collective studies were informed by microbial growth and colonisation as a function of various physicochemical parameters. Chiume et al. (2012) used the PVC column reactor, loaded with 4 kg, with a tailored in bed sampling technique to investigate colonisation as a function of solution flow rates. In a subsequent study, Fagan et al. (2014) used a box reactor loaded with 135 kg of ore to study microbial colonisation as a function of solution flow dynamics. These studies of microbial colonisation in bioheap simulating reactors have highlighted the significant difference in microbial diversity and population abundance between the PLS and ore-

associated phases, the importance of the interstitial phase where microbial population and growth appear to be highest and the impact of fluid flow dynamics on the rate and extent of colonisation of a heap.

To further understand these microbial population dynamics, multiple polyethylene columns packed with 150 g ore and microbial growth and colonisation of ore surfaces were studied with microbial population behaviour modelled (Govender et al., 2013; Govender et al., 2014; Govender et al., 2015; Cox and Bryan, 2017). At a particulate level, glass column reactors packed with glass beads that are coated with varying mineral particles to mimic an ore surface were investigated. Initial attachment (Bromfield et al., 2011; Africa et al., 2013b) in mini glass columns and EPS formation (Africa et al., 2010; Africa et al., 2013a) in a biofilm reactor by various microorganisms as a function of different physicochemical parameters were assessed. Ghadiri et al. (2018) using a similar system, however at a smaller scale, determined colonisation of ore surface as a function of X-ray energy impact on microbial activity. Based on the insights gathered from using these reactors, it is desirable to have a reactor system that would make it possible to collectively study the impact of flow rates, colonisation and EPS formation in a quantitative manner

Table 2.4: Selected reactor studies conducted on microbial-mineral interactions

Reactor description	Focus of the study	Mineral type	Test parameter	Authors
Mini glass column 190 × 250 mm	Study of microbe-mineral contacting for microbial initial attachment. Representative of submerged culture conditions over unsaturated heap bioleach conditions.	Pyrite and chalcopyrite concentrate, low-grade chalcopyrite and quartz particles coated onto 6mm glass beads	Mineral, microbial growth history, and temperature	Bromfield et al. (2011); Africa et al. (2013b)
Biofilm reactor	*In situ* fluorescent visualisation of microbe-mineral interaction and colonisation in heap bioleaching simulating environments	Thin chalcopyrite mineral sections mounted onto glass slides	Microbial cultures, temperature	Africa et al. (2010); Africa et al. (2013a)
PVC column 360 × 100 mm, insulated with element	Investigating colonisation of ore surfaces by mixed mesophilic cultures as a function of flow rate	Low-grade chalcopyrite ore (4 kg)	Flow rate	Chiume et al. (2012)
Jacketed glass column 500 × 100 mm	Colonisation and microbial persistence as a function of pH, microbial succession, inoculum size and temperature	Low-grade chalcopyrite ore (5 kg)	Acid stress, inoculum size, microbial succession and temperature	Ngulube (2013); Tupikina et al. (2013); Tupikina et al. (2014)
Perspex box	Liquid distribution and subsequent microbial propagation in agglomerated chalcopyrite ore beds	Low-grade chalcopyrite ore (132 kg)	Flow rate and irrigation scheme	Fagan et al. (2014)
Pilot scale simulation columns 6 × 1 m column	Bioleaching of a primary copper ore in a 6m Simulation Column, which demonstrates the process of microbial succession	Low-grade chalcopyrite ore (5,660 kg)	Inoculation strategy, microbial succession and temperature	Dew et al. (2011)
Disposable syringe 10 ml	Effect of X-ray energy exposure on the activity of mixed mesophilic leaching microorganisms	Pyrite concentrate coated onto 5 mm glass beads	Effect of X-ray µCT energy exposure	Ghadiri et al. (2018)
Jacketed stainless-steel column	Investigate the impact of temperature on the survival of inoculant strains	Low-grade chalcopyrite ore (36 kg)	Temperature	Mutch et al. (2010)
High density polyethylene column 100 × 80 mm	Investigate microbial population dynamics at an agglomerate scale	Low-grade chalcopyrite ore (150 g)	Colonisation and microbial population / community growth	Govender et al. (2013); Govender et al. (2014); Govender et al. (2015); Cox and Bryan (2017)
Petri dish reactor	Bacterial adhesion in bioleaching	Chalcocite and pyrite concentrate	Attachment preference, Microbial and mineral hydrophobicity	Echeverría-Vega and Demergasso (2015)

2.5.3 Industrial application and viability of heap bioleaching

The majority of commercial heap bioleaching operations have focused on the recovery of copper from ores with 0.1-0.5 wt.% total copper. Copper is one of the most important raw materials in the world (Dimitrijević et al., 2009) and is ranked after iron and aluminium in importance for infrastructure and technology (Sverdrup et al., 2014). According to the United States Geological Survey, copper in the US was mainly consumed in the sectors shown in Figure 2.5 in 2017. Heap bioleaching contributes approximately 7 % of the world's 17 million tonnes of copper (Brierley, 2008a).

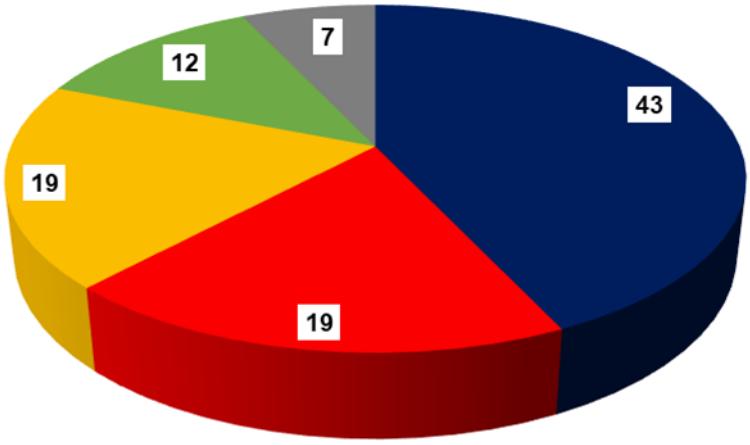

Figure 2.5: This pie chart shows how copper was used in the United States during 2017 by industry sector including building construction ■, electrical and electronics ■, transportation equipment ■, consumer products ■, machinery ■. Data sourced from the United States Geological Survey Mineral Commodity Summary for 2018 (https://geology.com/usgs/uses-of-copper/).

The first fully commissioned commercial application of heap bioleaching was established in 1980 for copper leaching. The Lo Aguirre mine in Chile processed about 16,000 tonnes of ore per day between 1980 and 1996 using bioleaching (Bustos et al., 1993). Several copper oxide heap leaching coupled with dump leaching and bioheap operations have been commissioned since then (Brierley and Brierley, 2001; Gericke, 2012). Chile produced about 400,000 tonnes of cathode copper by the heap bioleaching process, representing 5 % of the total copper production by the year 2003 (Cuevas and Valenzuela, 2004). Table 2.5 shows a select of various commercial heap bioleaching operations that are operating globally. The El Abra heap and Radimiro Tomic heaps near Calama, Chile process oxide-sulfide ore deposits including porphyry chalcopyrite- and bornite-containing primary sulfides and some chalcocite secondary sulfide at El Abra and secondary sulfides including chalcocite and covellite at Radimiro Tomic. They are the two of the largest copper producing operations in Chile (Pradhan et al., 2008). The Escondida heap operation that processes the secondary sulfide-rich chalcocite and covellite materials from a copper-bearing oxide-sulfide ore deposit have similar copper production rates to the El Abra and Radimiro Tomic heaps and is also the largest heap leaching operation globally (Chen and Wen, 2013). Chile remains a pioneer when it comes to

the recovery of copper through heap biohydrometallurgical technology from low-grade ores. In 2002, the Chilean government, through Codelco, took the initiative to become a leader in the application of biotechnology in the processing of copper sulfide ores. A particular target was the establishment of a technology for the direct leaching of chalcopyrite ores to enable the hydrometallurgical treatment of the massive reserve of otherwise sub-economical ores of this type that exist in this country (Domic, 2007).

Table 2.5: A selection of commercial heap bioleaching plants across the world. The list is not exhaustive

Mine	Country	Metal type	Production rate (t/a)	Reference
El Abra	Chile	Copper	225,000	Chen and Wen (2013)
Radimiro Tomic	Chile	Copper	180,000	Chen and Wen (2013)
Escondida	Chile	Copper	200,000	Panda et al. (2015)
Zijinshan	China	Copper	20,000	Renman et al. (2006)
Dexing*	China	Copper	1,500	Wu et al. (2009)
Ahtium	Finland	Nickel	15,000	www.talvivaara.com (2012)
Quebrada Blanca	Chile	Copper	75,000	Schippers et al. (2014)
Cerro Colorado	Chile	Copper	85,000	Schippers et al. (2014)
Whim Creek and Mons Cupri	Australia	Copper	17,000	Watling (2006)
Girilambone	Australia	Copper	14,100	Ghorbani et al. (2015)
Zaldivar	Chile	Copper	140,000	Schippers et al. (2014)
Carmen de Andacollo	Chile	Copper	21,000	Watling (2006)
Nifty Copper	Australia	Copper	16,000	Watling (2006)
Lady Annie	Australia	Copper	20,000	Panda et al. (2015)
Morenci	USA	Copper	230,000	Panda et al. (2015)
Ivan Zar	Chile	Copper	10,000	Schippers et al. (2014)
Punta del Cobre	Chile	Copper	7,000-8,000	Watling (2006)
S&K Copper, Monywa	Myanmar	Copper	40,000	Watling (2006)
Huogeqi	China	Copper	20,000	Schippers et al. (2014)
Cerro Verde	Peru	Copper	66,000	Schippers et al. (2014)
Tres Valles	Chile	Copper	18,500	Schippers et al. (2014)
Lomas Bayas	Chile	Copper	60,000	Watling (2006)
Morenci	USA	Copper	230,000	Schippers et al. (2014)

*Dump leaching

China has embraced heap leaching technology and Zijinshan and Dexing Copper Mines are some of the more advanced operations. The Zijinshan copper mine has been extracting copper via bioleaching since 1979 with a bioleaching factory built in 1997 (Yin et al., 2018) and has the largest chalcocite deposit with approximately 13.9 million tonnes of low-grade copper sulfide ore (Cu 0.38 wt.%) (Yuan et al., 2000; Ruan et al., 2011; Ruan et al., 2013). Talvivaara Mining Company Plc. (later Ahtium) in Finland commenced their bioheap process, reaching full production of nickel in 2010 with the potential to provide 2.3 % of the world's current annual production of primary nickel and making it the first nickel bioheap producers in the world (https://www.terrafame.com/front-page.html, 2019), alongside cobalt, copper and zinc.

In Africa, GeoBiotics successfully commercialised the GEOCOAT® process for the treatment of refractory gold concentrates at African Pioneer Mining Agnes Mine near Barberton, Mpumalanga, South Africa (S.A.) (Harvey and Bath, 2007). Mintek is a research and development institute in S.A that amongst other processes, focuses on the development and application of bioheap technology for primary copper ore deposits containing chalcopyrite over the past decade (Gericke et al., 2009). The bioheap process focuses on promoting the preservation of heat within the heap, in order to achieve a high internal heap temperature, thereby overcoming the passivation of chalcopyrite and an example of this is the BHP hot heap at Escondida (Dew et al., 2011) . This high-temperature heap bioleach technology for chalcopyrite has been successfully demonstrated in partnership with the National Iranian Copper Industries Company (NICICO) in Iran, treating low-grade chalcopyrite ore. The pilot plant has been in operation since 2005 and by 2009 fourteen 20,000 tonne heaps have been put into operation (Van Staden et al., 2005; Robertson et al., 2007; Van Staden et al., 2008). The test heap material contained 0.6 % copper, of which about 50 % is in the form of chalcopyrite, and the balance occurs essentially as chalcocite. Temperatures of around 40 °C were maintained in the heaps, with maximum of around 45 °C being observed. An acceptable rate of copper extraction could be maintained, while the formation of jarosite remained under control (Gericke et al., 2009).

Heap bioleaching has experienced limited application at an industrial scale in Africa. This could be because of the abundance of high-grade ores in the continent. According to Yager et al. (2015), Africa hosts ~ 30 % of the world's mineral reserves and the outlook on the mining of strategic minerals was expected to increase yearly between 2012 and 2019. Cobalt mine production is expected to increase by an average of 6 %, copper (>9 %), gold (3 %), nickel (15 %) and platinum group metals (PGM's) (4 %) per annum. However, despite these projections and mineral abundance in Africa and South Africa to be specific, there has been a growth in research outputs from continental research institutions. These outputs use various lab-scale methods to interrogate various aspects of, and factors that influence, heap bioleaching (Rawlings et al., 2003; Gericke et al., 2005; Dew et al., 2011; Tupikina et al., 2014). This puts Africa in an advantageous position in the long term to provide advanced processes for extraction of low-grade ores upon the depletion of higher-grade ores.

2.5.4 Acid rock drainage

ARD occurs when sulfide bearing minerals, mostly in the form of pyrite present in waste rock, tailings and coal discards, are exposed to both water and oxygen (Dold et al., 2009). The effluent resulting from this exposure is laden with low pH and high metal concentrations such as iron, copper and silver, and poses a significant environmental problem that can be

potentially harmful to humans and other life forms (Ma and Banfield, 2011). This chemical reaction is exacerbated by the presence and activity of naturally occurring iron and sulfur oxidising microorganisms (described in Section 2.1) (Egiebor and Oni, 2007). Sulfide bearing minerals that are susceptible to uncontrolled oxidation include pyrite, pyrrhotite, marcasite, chalcopyrite, galena, and sphalerite. However, the most widely occurring sulfide bearing mineral in gold and copper deposits, and in coal discards, is pyrite (FeS_2).

The general oxidation reactions of pyrite are shown in Section 2.1. These reactions are undesirable in the context of uncontrolled leaching emanating from mine wastes and their products are toxic to aquatic organisms, destroy ecosystems, corrode infrastructure, and pollute water in regions where freshwater is already in short supply (Singh, 1987; Ruihua et al., 2011). Under abiotic conditions, in the presence of O_2 and water, the oxidation rate of pyrite occurs at close to neutral pH (>4.5) and yields Fe^{2+}, SO_4^{2-} and H^+. The dissolution of these components lowers the solution pH and at below ~pH 3 (taking factors such as temperature and surface area of exposed mineral into consideration) the oxidation of pyrite by Fe^{3+}, which is regenerated by Fe^{2+} is about ten to a hundred times faster than by O_2 (Ritchie, 1994; Akcil and Koldas, 2006). Acidophilic microorganisms such as *At. ferrooxidans* and *L. ferriphilum*, which are also found in bioleaching processes for metal recovery, that obtain energy by oxidizing Fe^{2+} to Fe^{3+}, thereby catalysing this reaction (Bryner et al., 1967) may increase the rate of reaction up to the factor of about 10^6 (Singer and Stumm, 1970). ARD is globally prevalent and has adverse effects. The primary factors that are known to influence the rate of acid generation include pH, temperature, O_2, chemical activity of Fe^{3+}, surface area of exposed mineral sulfide and its sulfide content, and microbial activity (Akcil and Koldas, 2006).

2.5.5 Factors affecting bioleaching in heaps and waste rock dumps

2.5.5.1 Determining key factors affecting bioleaching of unsaturated ore beds

Bioleaching performance in an unsaturated ore bed is typically dependent on several factors, ranging from engineering and design to environmental, biological and physicochemical factors. Operating temperature, acidity, aeration and heap hydrodynamics are the most important factors, which have the potential to dictate to the efficacy of bioleaching microorganisms and therefore influence the leaching operation. A body of literature that studies the various factors at different scales is available (Watling, 2006; Petersen and Dixon, 2007b; Tupikina et al., 2011; Chiume et al., 2012; Govender et al., 2013; Ngoma et al., 2015). This is relevant to both enhancing metal extraction and recovery in bioheaps and in its prevention in waste rock dumps to prevent ARD generation.

Construction of heaps normally follows successive stages of feasibility assessment, design and testing; from column tests, through pilot demonstration heaps to full-scale commercial heaps. The design and construction process considers crush size, heap stability, permeability, heap height, the need for agglomeration, leach time, chemical consumption and maximum possible recovery (Kappes, 2002; de Andrade Lima, 2006). Test heaps are normally performed as the final stage of heap development and are monitored for factors such as fluid distribution, metal extraction and microbial abundance and activity. Parameters such as irrigation and aeration rates for optimum heat generation and microbial colonisation of the heap as well as validating the characteristics of the ore bed selected are set from the test heap study before moving to commercial heaps (Lizama, 2001; Demergasso et al., 2005; Watling et al., 2009; Panda et al., 2012). Key factors in flow-through systems (heap bioleach and waste rock dumps) are summarised in Table 2.6 and a selected sub-set discussed in the sections that follow.

Table 2.6: Summary of factors that affect heap bioleaching and ARD from waste rock dumps (adapted from Brandl, 2001; Pradhan et al., 2008)

Factor	Parameters affecting performance
Ore mineralogy:	Composition, mineral type, acid consumption, grain size, mineral dissemination, surface area, porosity, hydrophobic galvanic interactions, and formation of secondary minerals (Munoz et al., 1995)
Aeration:	Availability of O_2 and CO_2 for microbial growth and Fe^{2+} oxidation (Petersen and Dixon, 2007a).
Irrigation:	Supplies reactant solutes e.g. H_2SO_4 and controls precipitation of salts that might block the percolation channels, pH and, temperature via heat transfer within the heap. Acid consumption is a major contributor to processing costs in metal recovery (Watling, 2006) and assists with acid neutralisation in waste rock dumps.
Temperature:	Temperature of the heap determines which microorganisms govern the heap during bioleaching process. Microbial communities are dynamic, adapting to the changing heap leaching environment (Watling et al., 2016).
Microbiology	Microbial diversity, population density, microbial activities, metal tolerance, spatial distribution of microorganisms, attachment to ore particles, adaptation abilities of microorganisms, and inoculum (Watling, 2006)
pH:	Control of the leaching environment for optimal microbial activity (Shiers et al., 2016). Effect of pH resulting from H_2SO_4 agglomerated ore (Ngoma et al., 2015). Impact of acid stress on thermophilic cultures (Tupikina et al., 2011) as well as microbial succession (Tupikina et al., 2013).
Redox potential:	The rate of mineral dissolution is a function of the ferric to ferrous iron ratio (Fe^{3+}/Fe^{2+}). High redox potentials tend to inhibit the bioleaching of chalcopyrite in metal recovery (Córdoba et al., 2008).

2.5.5.2 Mineralogy

The mineralogy of an ore used in heap bioleach processes has a direct impact on the efficiency of bioleaching and on the nature of the reaction products (Watling, 2006). Low-grade copper mineral ores (with copper content of 0.5 % and less) are typically subjected to heap bioleaching technology (Clark et al., 2006; Watling, 2006). Copper sulfide minerals generally

categorise in two main categories: secondary sulfides (e.g. chalcocite, bornite, digenite and covelite) and primary sulfide minerals (e.g. chalcopyrite, bornite) (Schlesinger et al., 2011). Secondary sulfide minerals can be leached under biological oxidising conditions (Schlesinger et al., 2011) whereas primary sulfide minerals like chalcopyrite are less easily leached in heap bioleaching, requiring hot heaps for increased recovery rates. Chalcopyrite is the most abundant form of copper mineral accounting for ~70 % of global copper reserves (Koleini et al., 2011). Heap (bio)leaching of oxide and secondary sulfiide copper minerals has been developed over the years and it has been widely applied in the mineral processing industry. However, it is still a challenge to process refractory primary sulfide copper minerals like chalcopyrite using (bio)leaching at a commercial scale (Watling, 2006). Extensive research into the bioheap leaching of chalcopyrite across different scales is conducted globally (Watling, 2006; Córdoba et al., 2008; Pradhan et al., 2008; Córdoba et al., 2009).

Mineralogy and texture are also important factors that affect sulfide oxidation in both metal recovery and ARD processes. These include crystal structure, morphology, mineral liberation and mineral association (Parbhakar-Fox, 2012). These mineralogical factors affect how accessible the sulfide mineral is for oxidation. Sulfide alterations could determine the extent of weathering of sulfide mineral, thus determining solubilisation and acid generating potential. A mineralogical sample can contain various proportions of different minerals or mineral groups, including silicates, carbonates, sulfides, sulfates, oxides. Within these, there are minerals, which can produce acidity (e.g. sulfides through oxidation or Fe(III) hydroxides and/or sulfates through equilibrium reactions), liberating protons (H^+) into solution as well as elements, which can hydrolyse to complexes (e.g. Fe, Al, Mn) in solution and by doing so deprotonise water, also resulting in a liberation of protons into solution and causing further acidification (Dold, 2017).

The most prominent sulfides typical in mine wastes are pyrite and pyrrhotite. Sulfides such as pyrite often exist with copper minerals and, when copper metal has been recovered, the pyrite bearing waste rock is disposed. These sulfides are exposed to an oxygenated environment, which results in ARD generation that can cause long-term impairment to the biodiversity of surface and ground water bodies (Akcil and Koldas, 2006). Acid-consuming minerals present in the waste rock can neutralise protons (e.g. carbonates, hydroxides, and silicates) and act as buffers to control the pH at certain values (Stumm and Morgan, 1996; Langmuir, 1997). Brantley (2008) reported that minerals present in mine waste react at different rates. These neutralising minerals are classified on the basis of their reactivity into fast weathering (carbonates), intermediate weathering (hydroxides) and slow weathering minerals (silicate). The potential of neutralising acid relies on the reactivity and availability of acid-consuming minerals in significant quantities and these are shown in Table 2.7.

Table 2.7: Grouping of minerals according to their reactivity at pH 5, adapted from Lawrence and Wang (1996) and Kalinkin et al. (2004).

Mineral group	Typical minerals	Relative reactivity at pH 5
Dissolving	Calcite, dolomite, aragonite magnesite, brucite	1.0
Fast weathering	Wollastonite, leucite, nepheline jadeite, epidotes	0.6
Intermediate weathering	Chlorite, biotite, talc, epidote actinolite, zoisite, seperntine Kaolinite	0.4
Slow weathering	Feldspar (albite, oligoclase, labradorite), clay (kaolinite, vermiculite, montmorillinite)	0.02
Very slow weathering	Feldspar (K-feldspar), mica (muscovite)	0.01
Inert	Quartz, zircon rutile	0.004

Another important mineralogical factor with respect to low-grade heap bioleaching is the gangue mineral that is usually associated with mineral of interest. In the bioleaching process, achieving a solution pH that is less than 2 is key for microbial ability to facilitate leaching. This is dictated to by the acid used during agglomeration, the acid content of the raffinate, the irrigation flow rate, and the acid-generating/acid consumption properties of the sulfide and gangue minerals (du Plessis et al., 2007). The dominating gangue minerals are typically quartz, the silicate orthoclase, feldspars such as plagioclase and the mica biotite. The acid consumption of the gangue minerals is a key technical and economic factor (Dixon, 2004) and cannot be compensated for by increasing acid used (lower pH) during agglomeration, or in the raffinate solution as that would be detrimental to the microbial inoculum. In addition, the use of increased acid concentrations typically also increases the reactivity of the very same gangue minerals, resulting in an increase in gangue mineral dissolution. This, in turn, has two potential impacts. The first is that the concentration of total dissolved salts in solution is increased, which may result in detrimental ionic strength effects on microbial activity (Blight and Ralph, 2004; Shiers et al., 2005). Secondly, increased acid concentrations may compromise the structural integrity of the heap owing to the dissolution, particularly of clay minerals, possibly causing compromised hydraulic properties of the heap (du Plessis et al., 2007).

2.5.5.3 Temperature and microbial influence

The temperature of the bioheap and waste dump is mainly influenced by the sulfide mineral content of the ore body and hence the heat generated on its oxidative reaction, the microbial oxidation reactions as well as the air and liquid flow rates through the heap systems. Effective monitoring and control of temperature and other factors in industrial heap bioleach systems is challenging to achieve. These challenges are attributed to rate of reaction, aeration, fluid flow and distribution (Dixon, 2000; Petersen and Dixon, 2002; Olson et al., 2003; Dew et al., 2011)

with very few available control parameters. Heap operations typically start up at ambient temperature. The exothermic oxidation of sulfides is reported to increase internal heap temperatures, depending on heap design and operation. Fluid flow impacts both the distribution of the heat and its loss to the environment. Temperatures up to 81 °C have been reported for systems containing just 1.2-1.8 % sulfide-sulfur (Olson et al., 2003; Tempel, 2003). Bioleach rates are mostly influenced by temperature, with the microbiological processes operating within the physiological constraints of the microorganisms involved (Franzmann et al., 2005) and chemical oxidation reactions speeding up with increasing temperature. Franzmann et al. (2005) applied the Ratkowsky equation to describe the effect of temperature on the rate of Fe^{2+} oxidation or the time required to oxidise a specified amount of sulfur by a range of selected acidophilic bioleaching microorganisms. The application of the equation to iron oxidation data produced estimates of fundamental temperature range for activity (T_{MIN}, T_{OPT} and T_{MAX}) to a greater precision than previously presented. It was observed in this study that the oxidation rate of sulfur increased with increasing temperature above the T_{OPT} for growth until the increasing temperature affected the specific microbial activity to such an extent that it was reduced to below the threshold. The temperature progression that takes place inside the heap places selective pressures on the microorganisms in the system. In heap bioleaching, a succession of microorganisms occurs from mesophiles to moderate thermophiles, and finally extreme thermophiles (Figure 2.6) (Brierley and Brierley, 2001; Demergasso et al., 2005; Franzmann et al., 2005; Dew et al., 2011; Tupikina et al., 2014). Therefore, while heap operations may be inoculated with a consortium of microorganisms initially, the microbiology of the bioheap system changes in response to physicochemical conditions informed by the progression of the leach, with temperature being an important contributor. Bioleaching of chalcopyrite, specifically, has been demonstrated to be more effective at temperatures between 65 and 75 °C (Petersen and Dixon, 2002). It is difficult to use temperature controlling technologies in industrial heaps, therefore chemical methods are suggested as feasible for controlling temperatures within the heap to ensure maximum microbial colonisation and activity. Chen and Wen (2013) observed cases including Zijinshan, China and Talvivaara, Finland mines that had an increased sulfide content through the availability of pyrite. It was shown that higher sulfide content result in higher heap temperatures being quickly reached. Thermophilic microorganisms are key in regenerating Fe^{3+} in this operating window. Furthermore, an insightful understanding of microbial succession within heap environments is required with temperature being among the important driving forces (Acosta et al., 2014). Both the work of Dew et al. (2011) and Tupikina et al. (2014) has been key in building this. As much as higher temperatures are important in the dissolution of copper from chalcopyrite, the abundance and activity of mesophilic microorganisms such as *At. ferrooxidans*, *At. thiooxidans* and *L. ferriphilum* are a necessary

subclass of the microbial community essential for initial heat generation during the initial heap start-up phase (Demergasso et al., 2005; Dew et al., 2011; Gericke, 2012).

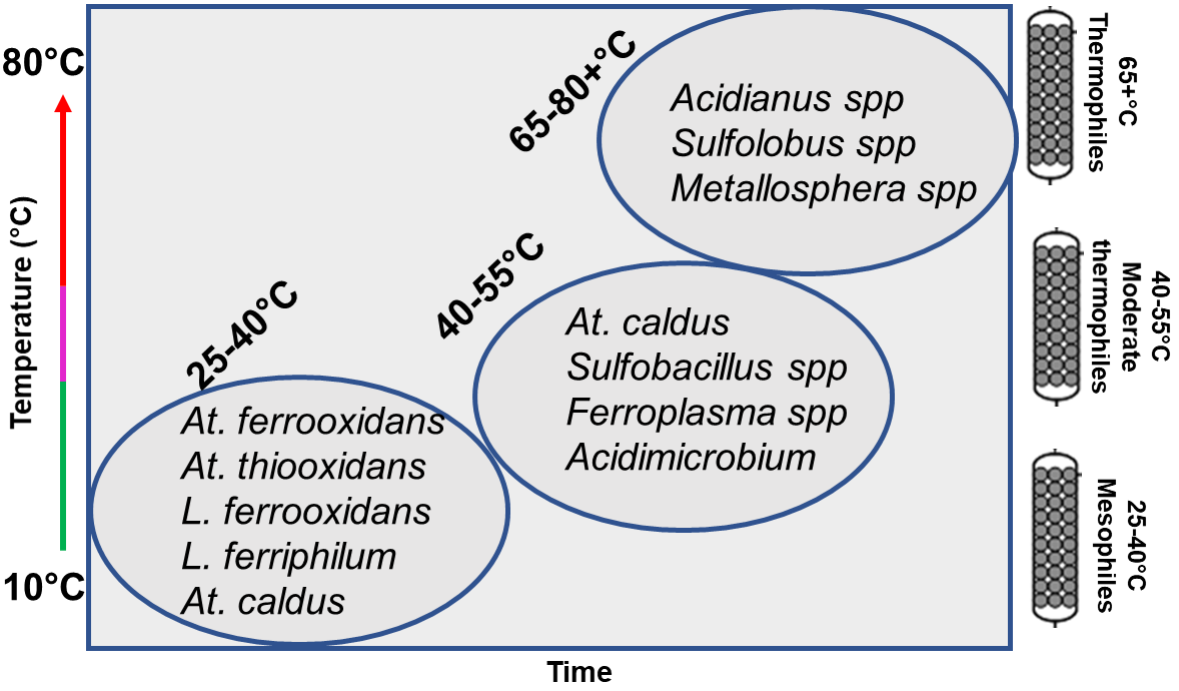

Figure 2.6: Illustration of the expected microbial succession and temperature progression in a typical low-grade chalcopyrite heap, inoculated from multiple stock reactors during either agglomeration or by irrigation (adapted from Dew et al., 2011).

In a study that assessed microbial communities over a range of temperatures (~15-32 °C), Demergasso et al. (2005) monitored temporal changes to the microbial community in the PLS solution coming from a field test heap that was loaded with approximately 200,000 tonnes of copper ore (50 % chalcopyrite, 40 % chalcocite and 10 % covellite) at the Escondida mine, Chile. A shift in microbial community dominance, from *Acidithiobacillus* sp. to *Leptospirillum* and *Ferroplasma* sp. and finally to a *Sulfobacillus*-like culture dominance was observed over the course of the 749 days of operation. The microbial community shift was largely attributed to the dynamics in the accessibility of the main substrates, such as Fe^{2+}, and increasing levels of inhibitory ions, such as sulfate. In a subsequent study conducted on a commercial scale, using the same mineral, microbial community dynamics, metal concentrations, temperature and pH of the PLS were assessed, and a model used to relate mineral leaching performance with microbial diversity and activity within the heap (Demergasso et al., 2010). The studies established a relationship between temperature progression, pH and microbial composition with mineral dissolution (Acosta et al., 2014; Marín et al., 2017). Watling et al. (2016) studied the effect of temperature and inoculation strategy on Cu recovery and microbial activity in column bioleaching. Mesophilic microorganisms, including a dominant temperature tolerant *Leptospirillum* strain, and moderately thermophilic strains were detected in the ore after a prolonged leach period at 60 °C. The inoculation and growth of thermophilic strains was less

successful. In the study of microbial colonisation and temperature progression in the pilot scale heap simulating 6 m columns packed with 5,660 kg chalcopyrite low-grade ore, Dew et al. (2011) presented the change in microbial abundance and diversity in the PLS with increasing temperatures within the ore bed. The relative dominance of species was similar to that previously found in heaps (Demergasso et al., 2005).

Whilst investigating the effect of acid stress on the persistence and growth of thermophilic microbial species after mesophilic colonisation of low-grade ore in a heap leach environment, Tupikina et al. (2013) demonstrated that there was a significant difference in microbial population found in the PLS and that associated with mineral ore surfaces. Furthermore, the authors also showed a shift in ore associated microbial community as a result of acid stress. In a subsequent study, Tupikina et al. (2014) reported similar findings. Govender et al. (2013, 2015); Cox and Bryan (2017) also showed that microbial populations associated with ore surfaces were significantly higher when compared to PLS populations, up to two orders of magnitude at some points. Roberto (2018) used sonic drilling to obtain samples and 16S rRNA gene targeted metagenomic sequencing to analyse microbial distribution in a 4-year running demonstration heap. The study showed substantial shift in planktonic microbial communities in the raffinate. The author further showed variations in microbial populations and communities in different sections (top, middle and bottom) within the heap. Dominant microbial communities identified in the raffinate (*Microbacterium*, *Achromobacter* and *Ferroplasma spp*) were different in cell abundance to those associated with ore (*Acidithiobacillus*, *Sulfobacillus*, *Leptospirillum*, *Ferroplasma* and *Acidiplasma spp*). These studies demonstrated that microbial colonisation, community representation and activity in the entire system could not be assumed to be represented by microbial communities detected in the PLS.

2.6 Available methods for microbial-mineral interaction analysis

The interaction of microorganisms with mineral surfaces, which leads to the production of EPS and biofilm as a consequence, can be analysed using various methods and techniques. These methodologies include both destructive and non-destructive approaches. Destructive methodologies include electron microscopy and scanning probe techniques as well as chemical extraction techniques. These techniques require preparation of the sample prior to visualisation (Woldringh et al., 1977; Neu and Lawrence, 1997), which typically involves a fixation step. Fixation of the sample can cause dehydration that may induce morphological changes or shrinkage of the sample or both, thus not providing an adequate representation of the biofilm structure being studied. Another destructive approach includes the isolation of the biochemical composition from a complex cell and EPS matrix, which results in disruption of

the original structure of the cells, aggregates, or biofilm matrix (Neu and Lawrence, 1997). The destructive chemical analysis of biochemical composition when analysing for sugars, proteins and lipids includes isolation from the culture supernatant by precipitation, release of the different constituents using various approaches such as hydrolysis before analysing the sugar or amino acid constituents by high pressure liquid chromatography (HPLC) or gas chromatography (GC) (Neu and Lawrence, 1997).

On the other hand, non-destructive, modern approaches allow for the *in-situ* investigation of a biofilm structure with minimal disruption. These approaches include the use of biomarkers, microelectrodes and gene probes that are compatible with microscopic techniques (Neu and Lawrence, 1999). The techniques also include atomic force microscopy (Gehrke et al., 1998; Africa et al., 2013a; Li et al., 2019) , confocal laser scanning microscopy (Neu and Lawrence, 1999; Africa et al., 2013a; Zhang et al., 2014; Zhang et al., 2019a) and other physico-chemical methods such the detachment method (Govender et al., 2013; Cox and Bryan, 2017) that require minimal sample preparation and are less disruptive. These are a few methods that could also be used in concert to achieve full analysis of a sample.

2.6.1 Atomic force microscopy

Atomic force microscopy (AFM) is a powerful imaging technique that, by scanning a sharp tip over a surface, can produce topographical images, which quantify surface morphology on an area scale comparable to that encountered by a colloid interacting with the surface. It has the ability to measure extremely small forces on an atomic scale (Binning et al., 1986). AFM is highly sensitive, able to detect in the pico-newton range (10^{-12} N). Except force measurement, AFM has other unique advantages in term of imaging. For instance, there are no special requirements for sample preparation and treatment, and it can produce atomic resolution images of both conductors and non-conductors either in air or in aqueous solutions. Over the years, the AFM technique has been used for imaging various biological samples, including biological molecules such as proteins, cells and biofilms, in their natural environment or under defined laboratory conditions (Drake et al., 1989; Müller et al., 1995; Schabert et al., 1995; Beech et al., 2002; Africa et al., 2013a; Zhang et al., 2013). The technique reveals structural surface information regarding the EPS coverage and spatial distribution around cells and over the surface. Use of a unique shuttle stage and coupling of the AFM with epi-fluorescent microscopy allows *in situ* visualisation of the attached biofilm and its speciation by FISH with high resolution (Gehrke et al., 1998; Mangold et al., 2008a; Mangold et al., 2008b; Noël et al., 2010; Florian et al., 2011; Africa et al., 2013a; Zhang et al., 2013).

In a study by Gehrke et al. (1998), AFM was used to investigate the attachment of *At. ferrooxidans* onto pyrite mineral surfaces. The AFM images obtained demonstrated that *At.*

ferrooxidans specifically attached to dislocation sites on pyrite, such as cracks and grain boundaries. A statistical evaluation indicated that 76 % of all cells adhered to (visible) surface imperfections. Mangold et al. (2008a) combined AFM and EFM to study the attachment areas of *At. ferrooxidans* on pyrite surfaces. AFM complemented the EFM results and the DAPI staining used in the study for visualisation of all cells, as using AFM did not to compromised the cell structure integrity. Florian et al. (2011) used the same combination to study attachment patterns pure *At. ferrooxidans* and *At. thiooxidans* and compared this to the mixed culture of the two on pyrite coupons. Applying both techniques, it was shown that the mixed cultures formed aggregates on the mineral surface when compared to the pure cultures. González et al. (2012) applied AFM and EFM to study the impact of quorum sensing signalling molecules such as the N-acylhomoserine lactone type (AHLs) on the ability of *At. ferrooxidans* to attach and form biofilm on sulfur and pyrite surfaces. Presence of AHL-signaling molecules with a long acyl chain (12 or 14 carbons) were shown to increase the adhesion of *At. ferrooxidans* cells to both sulfur and pyrite. The improvement of cell adhesion was also correlated with an increased production of extracellular polymeric substances. In recent studies, AFM has also been used to assess the attachment of thermophilic microorganisms. Li et al. (2019) investigated the adhesion of *Sulfobacillus thermosulfidooxidans*. AFM equipped with pyrite and chalcopyrite tips was used to measure the adhesion onto pyrite and sulfur grown cells. In the study, both pyrite and sulfur grown planktonic cells of *S. thermosulfidooxidans* had a high affinity to pyrite, but a low affinity to chalcopyrite. However, biofilm of *S. thermosulfidooxidans* grown on both sulfur and pyrite showed a low affinity to pyrite or chalcopyrite.

2.6.2 Scanning electron microscopy

Scanning electron microscopy (SEM) has a variety of applications in a number of scientific and industry-related fields, especially where characterization of solid materials is essential. In addition to topographical, morphological and compositional information, SEM can detect and analyse surface fractures, provide information in microstructures with great resolution, examine surface contaminations, reveal spatial variations in chemical compositions, provide qualitative chemical analyses and identify crystalline structures (Ratner et al., 2004). Sample preparation for analysis is relatively minimal and straightforward. The instrument also works relatively fast and, in the case of mineral analysis, it may be complemented by energy dispersive spectroscopy (EDS) and produce the elemental profile of a mineral. SEMs are typically limited to samples small enough to fit inside the vacuum chamber that can handle moderate vacuum pressure. In microbial-mineral interaction studies, Fowler and Crundwell (1999) used SEM to demonstrate that *At. ferrooxidans* attached to sphalerite mineral surfaces. SEM and energy dispersive spectroscopy of X-rays (EDS X-ray microanalysis) have been intensively used to investigate the attachment patterns of microorganisms on various mineral

surfaces (Jordan, 1993; Gómez et al., 1996; Sampson et al., 2000; Edwards et al., 2001; Liu et al., 2003; Lei et al., 2009; Liu et al., 2011; Ghadiri et al., 2018; Zhang et al., 2019b).

2.6.3 Confocal-Laser-Scanning-Microscopy

Confocal laser scanning microscopy (CLSM), unlike conventional fluorescence microscopy, collects light from a single focal plane. It scans the specimen point by point, line by line and assembles the pixel information into a single image (Brissova et al., 2005). The technique provides three dimensional structural information of the biofilm, as well as identification and distribution of various different components within the film (Vu et al., 2009), highlighting the structural complexity and heterogeneity within these interfacial environments. CLSM has been used routinely for the study of biofilms (Vu et al., 2009) and has been successfully utilised in combination with fluorescent labelled markers in numerous studies involving fully hydrated biofilms (Neu and Lawrence, 1997; Neu et al., 2001; Koerdt et al., 2010; Africa et al., 2013a). Moreover, information on the chemical composition can also be gained *in situ*. Fluorescent probes, or lectins, commonly used alongside the CLSM technique are specific for polysaccharides, proteins and nucleic acids (Neu and Lawrence, 1999). The CLSM technique is also regularly used in bioleach and ARD related studies to study microbial-mineral interactions (Florian et al., 2011; Bellenberg et al., 2012; Africa et al., 2013a; Bellenberg et al., 2014; Zhang et al., 2014; Echeverría-Vega and Demergasso, 2015; Li et al., 2016; Ramirez-Aldaba et al., 2017; Liu et al., 2019; Zhang et al., 2019a).

Africa et al. (2010) developed a novel biofilm reactor to investigate the interactions of mesophilic *At. ferrooxidans* and *L. ferriphilum* microorganisms *in situ* with sulfide minerals and low-grade chalcopyrite ore under conditions representative of a bioheap environment. CLSM was used in this study in conjunction with AFM and EFM to provide three dimensional topographical details of the association of the microbes with the mineral surface, as well as confirmation of the presence of EPS and cells (nucleic material) within the biofilm. In the case of both low-grade and massive sulfide mineral samples, attachment of mixed micro-colonies was observed in regions where surface defects were prevalent. In low-grade samples, preferential attachment was observed in regions where sulfide minerals were present. In a subsequent study, the same biofilm reactor, CLSM and AFM-EFM were used to investigate the attachment and subsequent biofilm formation by the thermophilic archaeon *M. hakonensis* on the surface of massive chalcopyrite and pyrite samples, as well as a low-grade chalcopyrite containing whole ore. Insights into biofilm structure and architecture as a function of the effect of varying temperature on the extent of attachment and biofilm development at room temperature (20 ± 1 °C), 45 °C and 65 °C were revealed. The extent of surface coverage and proliferation of the biofilm was shown to be dependent on the temperature, with surface

coverage being more extensive at 65 °C, near the optimal temperature for growth. Preferential attachment and biofilm formation to sulfide minerals was observed, with increased surface coverage of pyrite mineral surfaces relative to chalcopyrite and low-grade ore (Africa et al., 2013a).

Florian et al. (2011) used CLSM in combination with AFM to visualise initial colonization and biofilm formation on pyrite for mesophilic and moderately thermophilic species of the genera *Acidithiobacillus spp*., *Ferrimicrobium* and *Leptospirillum spp*. as well as a novel γ-proteobacterium with an aim to optimise bioleaching processes or to control unwanted natural leaching processes. The study showed that interaction of different species in mixed cultures resulted in increased attachment, increased production of EPS and leaching. Microorganisms like *Leptospirillum spp*. enhanced the attachment of other species in mixed biofilms and large areas of the surface of minerals remain uncolonised, whereas at some places, microorganisms attached in clusters. The authors concluded that attachment and microbially facilitated leaching can be improved by the production of EPS by several strains especially in combination with *Leptospirillum spp*. Bellenberg et al. (2012) used a combination of fluorescently-labeled lectin Concanavalin A (ConA) and (CLSM) to visualise capsular polysaccharides (CPS) of *At. ferrooxidans*. The authors suggested that the expression of CPS was inducible by several factors, including microbial contact with metal sulfide degradation products, while direct mineral contact seemed not to be a prerequisite.

Recent studies that used CLSM to visualise microbial-mineral interactions focused more on thermophiles (Echeverría-Vega and Demergasso, 2015) with Zhang et al. (2019a) characterising the initial cell attachment, biofilm development and EPS production of thermophilic *Acidianus spp*. on pyrite. Several microscopic techniques including AFM, EFM, CLSM, SEM and transmission electron microscopy (TEM) were used to study cell attachment and biofilm formation. CLSM combined with various fluorescent stains allowed for 3D multi-channel *in situ* visualization of biofilms. Liu et al. (2019) investigated the interspecies interaction and the early adsorption behaviour of moderately thermophilic consortia (*Ferroplasma thermophilum*, *L. ferriphilum* and *At. caldus*). Quantitative polymerase chain reaction (qPCR) and CLSM were adopted in this study and CLSM results showed the improved biofilm formation by bioaugmentation with adapted *Ferroplasma thermophilum*.

2.6.4 Isothermal microcalorimetry

All chemical, physical and biological processes are either producing or consuming heat (Russel et al., 2009). Isothermal microcalorimetry (IMC) is a highly sensitive non-invasive and non-destructive technique that measures the heat-flow of biological processes, which is directly proportional to the rate at which a given biochemical process takes place (Braissant

et al., 2010b). The technique requires no special sample preparation prior to measuring the heat produced by microorganisms in the microwatt range (Buchholz et al., 2010). The term isothermal means that the temperature of the calorimeter is constant or very nearly so within narrow tolerances (Wadsö and Goldberg, 2001). The sensitive nature of the instrument provides it with the ability to detect relatively low number of active cells (10^3 to 10^5 cells ml^{-1}). This is substantially lower than the detection limit required for spectrophotometers (threshold of ~0.75 x 10^8 CFU ml^{-1} at OD_{600}) (Braissant et al., 2010b) and light microscopy (> 10^5 cells ml^{-1}).

2.6.4.1 Application of IMC in biomineral studies

The IMC method is appropriate for the detection and quantification of microbial activity in bioleaching processes that would normally be not detected via traditional microscopic cell counting, since these microorganisms produce heat typically in the nano or microwatt range, especially during the start of leaching processes (Buchholz et al., 2010). In the main, IMC has been largely utilised in biomineral studies for:

- Thermodynamic investigations, which lead to values for different well-defined thermodynamic properties, such as enthalpy change, ΔH.
- Measuring of microbial activities of acidophilic microorganisms that facilitate dissolution of minerals for metal recovery.
- Measuring of microbial activities of acidophilic microorganisms that facilitate the degradation of mine wastes with the potential to form ARD.

Goodman and Ralph (1980) performed the first experiments with regards to mineral degradation when they studied the metabolic activity of various *Acidithiobacillus* strains. The authors developed a library of thermogram patterns in order for natural isolates to be identified more rapidly. Schröter and Sand (1988) introduced microcalorimetry as a technique for the fast evaluation of microbial activity associated with mineral degradation. The authors showed that thiosulfate oxidation proceeds via three steps and also could produce strain-specific thermograms. Schröter et al. (1989) published strain-specific thermograms for Leptospirilli and nitrifying microorganisms.

Various studies have incorporated IMC to study microbial metabolic activity in bioleaching processes, metal recovery and for ARD assessment. The influence of acidophilic chemoorganotrophic microorganisms on bioleaching by microcalorimetry was investigated by Hallmann (1991) who measured the activity of microorganisms in mineral ore samples and used in parallel the “most probable number“ technique for the quantification of viable cells. It was concluded that the heat output of an ore sample is proportional to the cell number. Schroeter and Sand (1993) demonstrated the application of microcalorimetry, using short term

experiments, on the estimation of the degradability of ores and microbial leaching activity through the direct measurement of microbial oxidation of pyrite and its correlation to the iron oxidation rate. In this study, microcalorimetric measurements allowed the best strains for a degradation of unknown substrates to be identified. Schroeter and Sand (1993) also performed microcalorimetric measurements on Fe^{2+} and thiosulfate oxidising chemolithotrophic microorganisms. It was shown that heat-flow can be directly correlated to the iron oxidation rate. Hedrich et al. (2016) assessed leaching of chalcopyrite concentrate catalysed by mixed moderate thermophilic culture in batch bioreactors. IMC was used in the study to measure the progression of microbial activity throughout the experimental run and it was shown that activity progressively increased. This was correlated with copper leaching rates. In a subsequent study, the authors performed temperature range studies between 42 and 50 °C and microbial activity was shown to be similar across the temperature ranges (Hedrich et al., 2018).

Microbial activity can directly be correlated with iron and sulfur oxidation, since the standard reaction enthalpy for the dissolution of mineral sulfides can be measured, e.g. the standard reaction enthalpy of pyrite oxidation has been determined to be -1546 kJ mol^{-1} (Schippers, 1998). Rohwerder (1995) correlated the heat output to the microbial leaching rate with defined cultures. It was calculated that 100 µW of heat production equals a pyrite oxidation rate of 6.0 µmol day^{-1} for *At. ferrooxidans* and a mixed culture of *At. thiooxidans* and *L. ferrooxidans*. For 100 µW of heat production, a leaching rate of 7.5 µmol day^{-1} was calculated for *L. ferrooxidans* (Rohwerder, 1995). Rohwerder et al. (1998) used microcalorimetry to investigate the thermodynamics of pyrite leaching. They determined the reaction energies of pyrite dissolution by acidophilic microorganisms, measuring reaction energies for pyrite dissolution ranging from -1100 to -1600 kJ mol^{-1} over 30 days. These values are similar to the calculated value of -1546 kJ mol^{-1}. In pure *At. ferrooxidans* cultures and mixed mesophilic cultures, the theoretical and measured values showed no significant differences. In contrast, *L. ferrooxidans* cultures showed reaction energies up to 200 kJ mol^{-1} lower than the theoretical ones. This effect was suggested to be due to the inability of *L. ferrooxidans* to oxidize reduced sulfur compounds (Rohwerder et al., 1998). In this study, the authors measured heat-flow output in a short space of time due to O_2 limitations observed in the sealed IMC ampoules when measuring microbially facilitated oxidation. Krok (2016) established a microcalorimetric determination method to assign chemical and biological degradation of copper sulfides (chalcopyrite, chalcocite and covellite). The microcalorimetric determinations were verified with the various ore types and bioleaching cultures growing at various temperatures. Thermodynamic calculations of the reaction energies $\Delta_r U$ were determined using the measured heat output from the microbially colonised mineral slurry, iron, copper and sulfate ions in the leachate. The different

chalcopyrite ores that were used in this study showed similar leaching characteristics and heat output values. This showed that microcalorimetry can be applied on various chalcopyrite ores.

An example of the application of IMC in assessing ARD potential is given by the work of Schippers et al. (2000). These researchers investigated the consequences of microbiological and chemical pyrite oxidation on the growth of vegetation on the slopes of a sulfidic mine tailings heap, located in Romania, to assist with the stabilisation of the slopes of the heap and to provide insight into approaches to prevent the migration of contamination to the surrounding agricultural land. Microcalorimetric activity measurements revealed microbial oxidation of pyrite and associated acid production. The microcalorimetric results were confirmed by the detection of high amounts of pyrite oxidation products, such as elemental sulfur and sulfate, as well as high amounts of water-soluble metals and arsenic in the samples from the eastern slope (Schippers et al., 2000). Schippers et al. (2001) used IMC to measure microbial activity with the aim to allow rapid evaluation of ARD countermeasures. The authors installed a large four-chamber percolator in a waste heap and filled each chamber with sulfidic waste material to test the effect of surfactant (sodium dodecyl sulfate) and alkaline layers (blend of limestone and burned lime) on the microorganisms catalysing the formation of ARD effluents. The effects on the bioleaching flora were evaluated over a period of 26 months and samples were taken from the different depths of the chambers and measured in the microcalorimeter. Sodium dodecyl sulfate was shown to inhibit microbial activity significantly and the heat output neared zero towards the end of the experimental run, whereas values of microbial activity in samples with alkaline layers were within the range of controls, signifying minimum to no impact on the microorganisms.

Kock and Schippers (2006) studied the impact of microbiological metal sulfide oxidation on ARD generation for two mine tailings, collected from a tailings dam in Botswana. IMC was used to measure potential oxidation rates of pyrite and pyrrhotite. The microcalorimetric data obtained showed that pyrite and pyrrhotite were biologically and chemically oxidized in the tailings. In a subsequent study, Schippers et al. (2007) measured potential pyrrhotite oxidation rates in pyrrhotite-containing tailings from a tailings storage facility (TSF). From these, they concluded that it would take between 80 and 140 years to oxidise the pyrrhotite tailings completely, assuming constant oxidation rates, providing an estimation of the time period of ARD formation, which was critical to inform safe mine closure. Sand et al. (2007) assessed ARD mitigation on several weathered rock samples over 3 years, including: 6-year-old waste rock material; sorted, freshly broken, low-grade ore; and unweathered tailings material, using the detergent sodium dodecyl sulfate as a deterrent for weathering in large lysimeters. In their study, sodium dodecyl sulfate was shown to reduce microbial activity only temporarily.

While use of microcalorimetry is not yet as widespread as other techniques, it possesses the potential for a rapid determination of microbial activity and oxidative leaching in both bioleaching and ARD formation. Furthermore, the heat production can be correlated with the iron and sulfur oxidation rates as well as other microscopic techniques to integrate heat production and microbial population size.

2.7 Brief overview of the literature reviewed

Metal recovery and ARD formation are both a consequence of microbially-facilitated leaching of sulfidic minerals, with the former being a structured process that leads to valuable metal recoveries such as gold (bio-oxidation) and copper (bioleaching), being ideal. The latter leads to environmental devastation and needs to be abated. Mechanisms of mineral bioleaching were explored, including the acid soluble polysulfide and acid insoluble thiosulfate pathways, as was the role that acidophilic microbial species plays during mineral dissolution. Relevant literature on the sub-mechanisms confirmed the indirect contact mechanism as the most likely mode of microbial-mineral interaction. The microbiology involved in both metal value extraction and ARD was discussed, together with the key mesophilic microbial species that play a role in mineral degradation. The implication of these species in both processes was also discussed, including species involved in bioleaching for metal recovery (Dew et al., 1997; Rawlings, 2002; Rawlings and Johnson, 2007; Dew et al., 2011) and species involved in the characterisation of mine waste (Hesketh et al., 2010; Broadhurst et al., 2013; Harrison et al., 2013; Opitz et al., 2016; Golela, 2018). Microbial-mineral interactions were discussed with the premise that microorganisms involved in bioleaching adhere to the mineral and form biofilm that results in colonisation (Gehrke et al., 1998; Rohwerder et al., 2003; Sand and Gehrke, 2006; Africa et al., 2010; Africa et al., 2013b; Govender et al., 2013; Tupikina et al., 2013). Various literature on the mode and process involved in microbial-mineral interactions was discussed as well as the role that EPS play. Colonisation of mineral surfaces by microorganisms was discussed with emphasis placed on heterogenous heap and waste dump simulating conditions. In these settings, a relationship between colonisation and other factors that affect heap performance such as temperature and the identified phases inside the heap were also described, supported by relevant literature.

Moreover, the general functions, properties and constituents of the EPS matrix that place biofilms as a key feature among some the most predominant forms of life on earth were described. Subsequent to that, EPS involvement in bioleaching studies was discussed including relevant literature attributed to those involvements. There are various methods that are available and are frequently used to analyse microbial-mineral interactions. The destructive and non-destructive nature of these methodologies was discussed as well as the

literature available on their application on the analysis of microbial-mineral interactions. Bioleaching in the context of value recovery was covered with an emphasis placed on heap bioleaching. The basic requirements for a successful operating bioheap including, but not limited to, mineral ore particle size and type, aeration, fluid flow and microbiology were addressed. Moreover, the global commercial successes of heap bioleaching across the minerals was covered. The uncontrolled leaching of sulfide waste material was also discussed. Lastly the techniques used to analyse and gain more insights into microbial interactions with mineral surfaces were discussed, leading to the introduction of IMC as an additional method with the capabilities to produce data on the activity of microorganisms interacting with mineral surfaces.

2.7.1 Summary of the limitations identified in the current literature

- The literature demonstrates colonisation of sulfide minerals by mixed cultures (especially mesophilic and moderate thermophilic cultures) as well as pure cultures across the temperature ranges. While dynamics of mixed mesophilic microbial communities have been studied in well mixed homogeneous reactors, very few studies have interrogated the colonisation of sulfide minerals and its impact at the early stages of a bioheap process.
- There is a fundamental necessity to study and understand colonisation of mineral sulfides (especially chalcopyrite) by mesophilic cultures during the initial stages of a bioheap process to accelerate the microbial community succession and thus reach optimum leaching conditions for chalcopyrite.
- Several techniques have been shown in the literature to assess colonisation of sulfide minerals by mesophilic cultures, however, the integration of qualitative and quantitative techniques to measure colonisation in the flow-through configuration is lacking.
- There are no studies on cultivation, extraction, and analysis of EPS reported on unsaturated ore bed systems that resemble fluid flow conditions of heaps and waste dumps.
- Solution flow rates as well as the type and grade of the mineral being leached are shown in the literature to play a fundamental role in the success of a heap bioleach process. However, the role that flow rate plays in influencing the interaction of microorganisms, including attachment, colonisation, growth and activity, with different minerals has not yet been explored.
- The presence and effect of microbial populations in the analyses used for characterisation of sulfidic waste rocks and coal waste for their potential to form acid have recently been interrogated, using the batch biokinetic or a draw-and-fill semi continuous biokinetic test. The presence and effect of these populations in flow-

through studies that resemble a waste dump, including their colonisation of waste rock sulfides, is yet to be fully interrogated.

2.8 Objectives of the study

The objective of this study is to design and apply a small diagnostic flow-through column system that would enable the quantitative investigation of colonisation of mineral surfaces, using pyrite-containing concentrates and ores in this instance. Colonisation is studied across varying sulfide mineral grade, by mixed mesophilic microbial cultures, with the aim of enhancing leaching for metal recovery and, on the other hand, characterising and understanding uncontrolled leaching, typical of ARD generation, with the aim of preventing it.

The objective is addressed through the following:

- Design a small-scale heap simulating system that has defined mineral surface area using mineral coated beads.
- Develop an IMC approach to measure quantitatively the activity of mineral associated microbial populations.
- Apply the developed IMC approach to the heap simulating flow-through system and progressively measure metabolic activity of microorganisms that colonise the surfaces of pyrite mineral with varying sulfide content under typical and high flow rates.
- Refine the detachment method and validate its efficacy through integration with IMC to account for total microbial populations that colonise mineral surfaces.
- Cultivate, extract and perform biochemical analysis of EPS produced by colonising populations, in a complete flow-through system.
- Integrate metabolic activity data of colonising populations with visualising tools and traditional analysing tools to better understand colonisation, particularly as a function of mineral surface area available.
- Develop insight into the impact of mineral grade and flow rate of irrigant on early stage microbial colonisation of the mineral.
- Demonstrate potential for application of the flow-through system in feasibility and characterisation studies through further refinement of the existing biokinetic method to characterise sulfide mineral-containing waste rock for their potential to form ARD.

2.8.1 Developed hypotheses and research questions

The following hypotheses and research questions were formulated to address the above objectives.

Hypothesis 1

Metabolic activity of mineral associated mixed mesophilic microbial communities that occupy available mineral surfaces, increases over time. The increase in metabolic activity is reflected by the growth in microbial cell numbers as well as activity per cell over the colonisation period on a basis of surface area. This is since microbial communities adapt well to the environment on the surface and become highly active over time until maximum activity is achieved, prior to limiting conditions occuring.

- Can isothermal microcalorimetry be used to investigate and assess the metabolic activity of microbial communities associated with pyrite mineral surface quantitatively as a function of surface area in a heap simulating system over time?
- Does microbial metabolic activity as well as microbial growth on the mineral surface and resultant surface coverage progress with time?
- Does growth in microbial numbers on the mineral surface result in increased microbial metabolic activity?
- Under what conditions is the highest microbial activity per unit surface area measured on mineral surfaces?
- Does an increased surface area load increase microbial activity (heat-flow)?
- Does reagent limitation affect microbial activity on the mineral surface?

Hypothesis 2

The current detachment method used to enable quantification of surface associated microbial populations is assumed to be completely efficient based on cell count limitations. IMC, as a more sensitive measure of microbial presence than cell counts, will account for, and reconcile for any population remaining on the surface post detachment, testing the complete efficiency assumption and providing an approach for its correction if not valid.

- Do detachment washes efficiently remove surface associated microbial populations and, if so, what number are required to achieve this?
- If not, what fraction of the surface associated population remains on the mineral surfaces?
- Using both IMC and the detachment protocol, can the residual population be accounted for? If yes, is it significant?

Hypothesis 3

Microorganisms typically attach and colonise mineral surfaces to exert enhanced facilitation of mineral leaching. The grade of the mineral and solution flow rate are key in influencing

microbial-mineral interaction including growth and activity in complete flow-through bioleach environments.

- What effect does mineral grade and flow rate have on the ability of microorganisms to attach to and colonise mineral surfaces?
- What effect does mineral grade and flow rate have on the growth of surface associated microorganisms as well as their activity?

Hypothesis 4

In the developed unsaturated complete flow-through system developed, mixed mesophilic cultures attach to available mineral surface and produce EPS. The EPS is characterised by varying biochemical properties and results in the facilitation of accelerated mineral surface degradation.

- Do mixed mesophilic microorganisms produce EPS in complete flow-through systems?
- If yes, what is the biochemical make-up of that EPS?

Hypothesis 5

The unsaturated flow-through mineral system with defined surface area provides a tool for use in feasibility and characterisation studies. For example, prior to their disposal, mine waste material needs to be characterised in terms of their potential to form ARD in the future. Development of a flow-through biokinetic configuration as a further refinement of the current batch biokinetic system, developed at UCT, allows for a truer representation of a waste rock dump and can account for the competing neutralising and acid forming reactions that take place, as well account for microbial-mineral interaction and mineral degradation.

- Are the initial neutralising reactions washed out in the flow-through configuration?
- Is microbial growth and activity progressive on the mineral surface of the waste rocks?
- Is the flow-through assay sensitive to the flow rate at which it is operated?

Chapter 3: General methodology

3.1 Research approach

This chapter seeks to describe the overall experimental design and protocols in this study as well as materials used, including: (1) Reactor design for development of the unsaturated flow-through ore bed presenting a defined surface area of ore, in which mini-columns are used to house mineral-coated beads irrigated under defined conditions to provide a defined surface area experiment and an incubator built and commissioned to provide a defined temperature environment. Microbial culture and growth condition (2) Mineralogical information of substrates used (3) Wet chemistry analytical methods (4) Detachment studies (5) SEM analysis (6) IMC measurements (7). Finally, the EPS compositional analysis methods are outlined in this chapter (8). The methods described in this chapter are common across the subsequent result chapters.

3.2 Microbial cultures and growth conditions

A mixed mesophilic culture was used in this study consisting of bacteria (including *L. ferriphilum* and *At. caldus*) and archaea (including *Ferroplasma acidiphilum* and *Acidiplasma cupricumulans*). The stock culture was maintained on a 3 % (w/v) pyrite concentrate in 0K basal salts medium made up of 3 g L^{-1} $(NH_4)SO_4$, 0.1 g L^{-1} KCl, 0.5 g L^{-1} K_2HPO_4, 0.5 g L^{-1} $MgSO_4.7H_2O$, and 0.01 g L^{-1} $Ca(NO_3)_2$ and 1 ml of 1000× stock of trace elements (Kolmert and Johnson, 2001) in a 1 L batch stirred tank reactor at 35 °C. The stock reactor was maintained on a basis of a weekly draw and fill in which 15 % (v/v) was replaced with fresh media and associated concentrate. The activity of the culture was routinely assessed through direct microscopic cell counts (Section 3.5.4) and measurement of the redox potential (Section 3.5.2). The planktonic microbial community in the reactor was maintained in the range of 1 - 4 × 10^9 cells ml^{-1} (Ngoma et al., 2015), Ngoma, personal communication 2018). Periodic microbial community analysis by qPCR demonstrated that *L. ferriphilum* dominated the community structure the time of the project with minor community members including *At. caldus*, *Ferroplasma acidiphilum* and *Ac. cupricumulans*.

3.3 Preparation and analysis of mineral substrates

Pyrite mineral concentrate, and metapelite high sulfur (PEL-HS) and metapelite low sulfur (PEL-LS) waste rocks were used as attachment substrates and sources of energy. The mineral concentrate (~2 kg finely milled) and waste rocks (800 g to 1 kg each) were split into a series of 30 g samples and each sample was subjected to a one-minute pulverisation process using a pulveriser supplied by the Ferguson industrial equipment group

(Johannesburg). The pulverised samples were then wet sieved to obtain a -75 µm size fraction and dried in a 37 °C walk in incubator. Thereafter, the samples were further split using a 10-Dickie & Stockler rotary splitter to obtain representative samples ranging between 100 and 200 g. The pulveriser, sieve and the rotary sample divider were cleaned using pressurized air spray after processing each sample in order to avoid cross contamination among the prepared samples. Analysis of the particle size distribution was performed using a Malvern Particle Size Analyser (Mastersizer 2000, Malven Instruments United Kingdom), based on laser light scattering by a group of particles whereby the angle of light scattering is inversely proportional to particle size (ie. the smaller the particle size, the larger the angle of light scattering).

3.3.1 Pyrite concentrates

Size analysis was performed using a Malvern Particle Size Analyser. A d_{10} of 7.3 µm, d_{50} of 39.2 µm and d_{90} of 88.8 µm were determined (Appendix C.2). The composition of the concentrate was 34.8 % sulfur and 47.45 % iron, as determined by LECO and ICP-OES, respectively. XRD analysis is shown in Table 3.1 and the XRD diffractogram can be found in Appendix C.3.

Table 3.1 Mineralogical composition (wt.%) of the pyrite concentrate as determined by XRD

Mineral concentrate	Pyrite	Chalcopyrite	Quartz	Talc
Pyrite concentrate	96.19	0.51	1.54	1.76

3.3.2 Pyrite bearing waste rocks

A bulk mineralogical analysis of two waste rock samples, namely pelitic high sulfur (PEL-HS) and pelitic low sulfur (PEL-LS) was obtained by QEMSCAN (Figure 3.1 A and B). The detailed mineralogical list is provided in Appendix C.5. The sulfur content was 28 wt.% for PEL-HS and 16.5 wt.% for PEL-LS as determined by LECO.

Acid generating minerals consist of predominately pyrite (PEL-LS: 13.99 wt.%; PEL-HS: 33.43 wt.%) and pyrrhotite (PEL-LS: 2.35 wt.%; PEL-HS: 3.9 wt.%). Based on the classification guidelines of acid neutralising capacity of minerals described by Dold (2010), acid consuming minerals within the waste samples consist predominantly of dissolving calcite (PEL-LS: 0.22 wt. %; PEL-HS: 0.03 wt.%), fast and intermediate weathering minerals represented predominantly by garnet (PEL-LS: 2.83 wt.%; PEL-HS: 4.52 wt.%) and slow weathering minerals consisting predominantly of muscovite (PEL-LS: 14.77 wt.%; PEL-HS: 12.42 wt.%). The largest component of the waste rock consisted of quartz inert minerals (PEL-LS: 36.67 wt.%; PEL-HS: 34.76 wt.%).

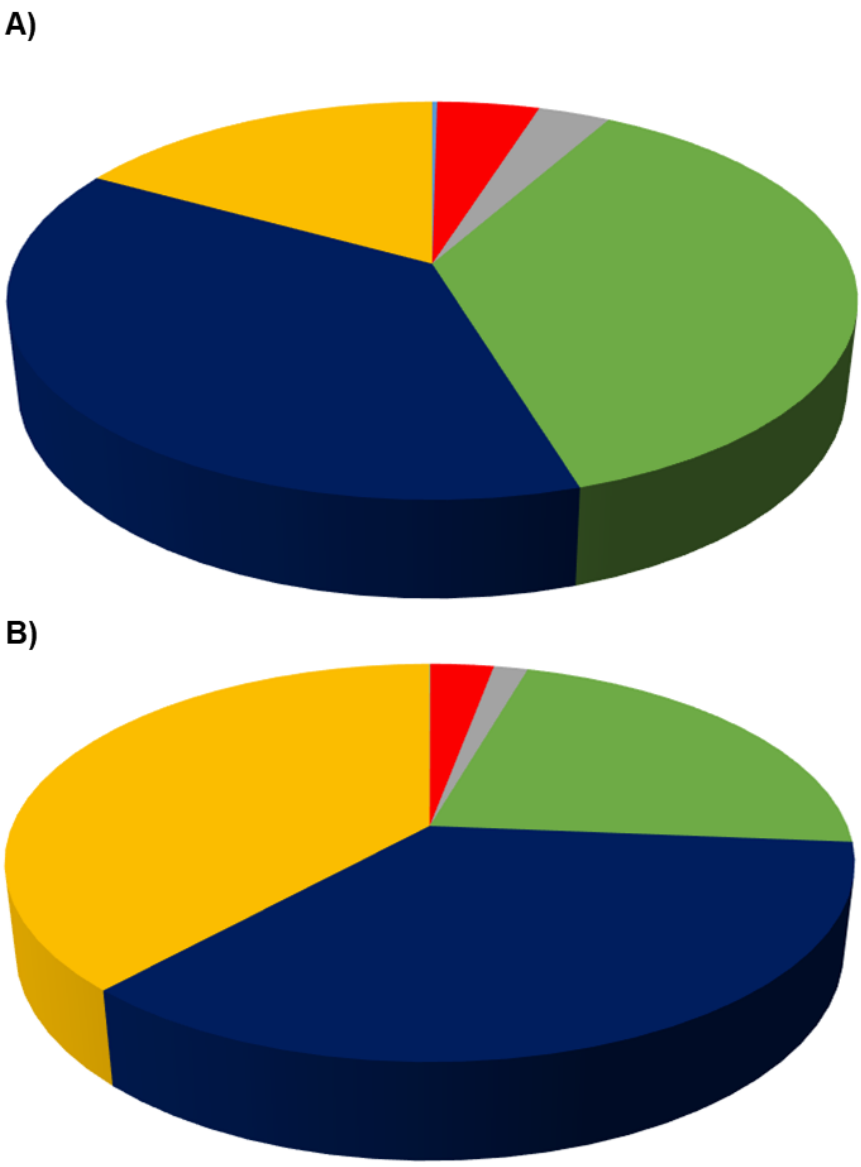

Figure 3.1: Mineralogical analysis of the two waste rock samples acquired using QEMSCAN. A (PEL-HS) and B (PEL-LS) show abundant acid forming minerals (pyrite and pyrrhotite;), dissolving mineral (calcite;), fast- (garnet;), intermediate- (Mn-Fe silicate and augite;) and slow-weathering (K-feldspar and muscovite;), respectively, and quartz as an inert mineral ( ).

3.4 Determination of a defined mineral surface area for microbial attachment

A defined surface area was established to ensure a quantifiable available mineral surface area. To establish a fixed surface area of the mineral concentrate or ore, the finely pulverised minerals were coated onto the surface of 6 mm glass beads using Bostik glue™ as shown in Figure 3.2. The coated beads were allowed to dry for a minimum of 24 hours before sterilisation (Africa, 2009). The total surface area available for microbial attachment provided by a single spherical mineral coated bead was 1.13×10^{-5} m^2. Based on a model bioleaching organism, *At. ferrooxidans*, with a surface area of 0.75 μm^2 (Ohmura et al., 1993), the theoretical maximum cell number that could attach to the available surface area provided by the mineral coated beads, assuming single layer coverage, was calculated to be 4.33×10^9

cells or 4.9×10^4 cells per bead. This translates to 1.32×10^{12} cells required to saturate 1 m^2 of a surface. Experiments were performed in batch shake flasks to assess the effect that Bostik glue™ have on microbial activity and growth, and no negative effects were observed.

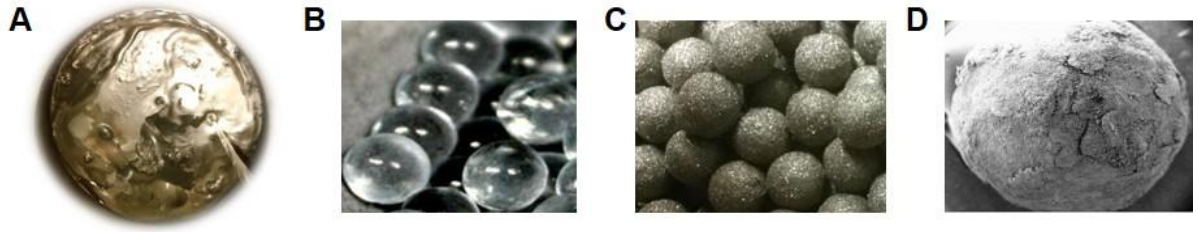

Figure 3.2: Image depicting (A) wet sieved mineral, (B) 6 mm glass beads, (C) glass beads that are coated with mineral and (D) a mineral coated bead viewed under the SEM at 1 mm scalebar.

3.4.1 Sterilisation of mineral and equipment

The mineral coated glass beads (300 for each column) were each packed into sealable bags. The samples were sterilised with a 45 kGy dose of γ-irradiation to render microorganisms that are indigenous to the mineral ores inactive (Govender et al., 2015). Tubing and column components (Figure 3.4 B) were sterilised by autoclaving them at 121 °C at a pressure of 1 atmosphere for 20 minutes. The inside of the incubator was sprayed with 70 % (v/v) ethanol.

3.5 Reactor design and operation

A reactor system was designed for this study in which a defined surface area of mineral concentrate or waste rock ore could be provided in an unsaturated flow-through system for extended bioleaching studies under defined irrigation conditions and a pre-determined operating temperature. The reactor design was informed by earlier studies performed by Bromfield et al. (2011) and Africa et al. (2013b) in which the glass columns packed with mineral coated beads (Figure 3.3) were used to investigate short term attachment (± 180 min) under saturated conditions at room temperature. The enclosed reactor-incubator (Figure 3.4) allows for a semi-sterile controlled environment, which is required when operating these extended bioleaching experiments to limit contamination. The mineral-coated beads described above allow the defined surface area while the reactor system designed and commissioned is described in the following sections.

3.5.1 Column reactors

A schematic diagram of the glass column reactors is shown on Figure 3.3 A, packed with 300 (6 mm) mineral coated glass beads. Uncoated 4 mm glass beads are layered at the top and bottom to allow for uniform media distribution (top) and drainage (bottom). The glass columns used in this study (Figure 3.3 B) were constructed by Glasschem in Stellenbosch, South Africa. Each column had a 2.5 cm diameter and a 19 cm working length (Africa et al., 2013b). The

ends of each reactor were sealed with screw-cap lids containing a rubber stopper, to prevent any leakages, to which a glass nipple was connected. Perforated polypropylene was fitted at the bottom and top, inside the screw-caps and acted as a sieve (Figure 3.3 B).

3.5.2 Incubator

A 15-channel wooden incubator with heating fans was designed and constructed for the column experiments (Figure 3.4 A and B). The size of the incubator was 40 cm height, 85 cm length and 20 cm width. Appropriate insulation was used to seal the incubator. The temperature-controlled heater with ± 0.2 °C deviation was used to maintain the temperature at 30 ± 0.2 °C. The front of the incubator was fitted with perspex, temperature resistant glass doors.

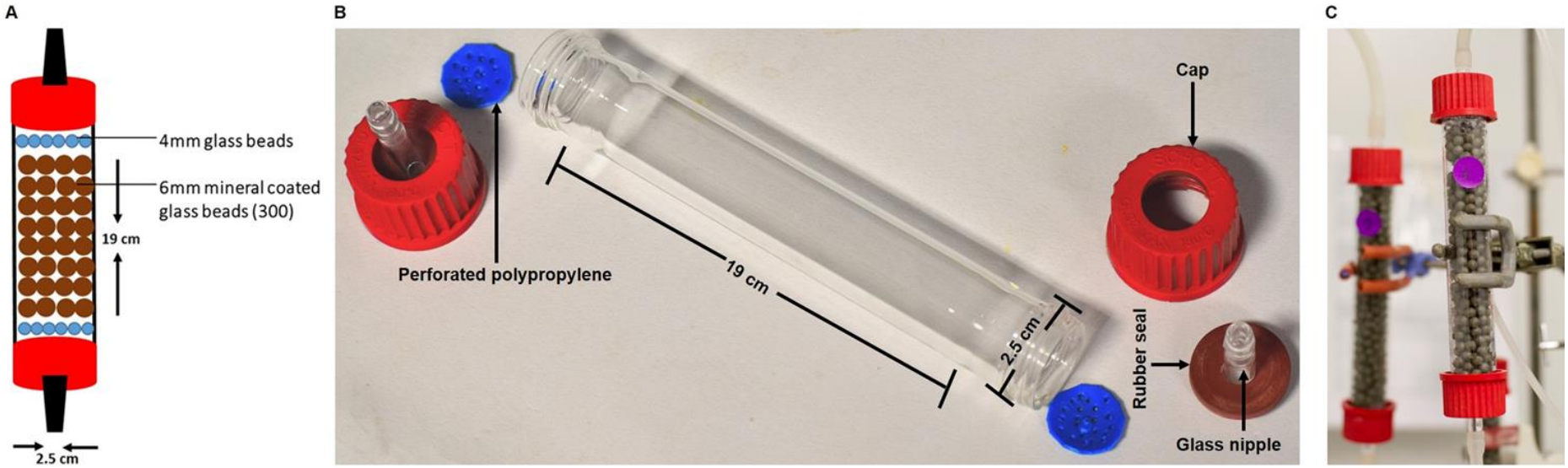

Figure 3.3: (A) Schematic diagram of the mini column, (B) Components of the mini column reactor and (C) mini column packed with 300 pyrite mineral coated glass beads

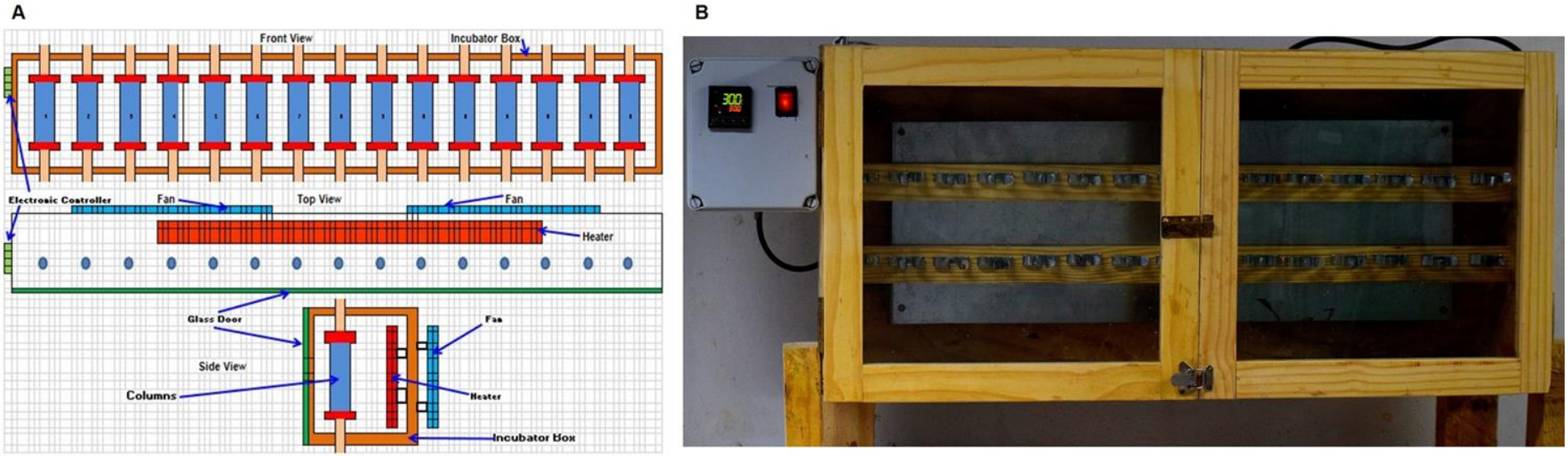

Figure 3.4: (A) Schematic design of the box incubator and (B) wooden box reactor with the capacity to fit 15 glass column reactors.

.

3.5.3 Flow-through reactor set-up and experimental run

The unsaturated flow-through reactor system was used in the experiments detailed in Chapters 5, 6 and 7. Each column was loaded with 300 mineral coated beads and operated as a continuous flow-through system. Prior to inoculation, the loaded column reactors were washed and conditioned with 0K media (pH 1.6 ; recipe found in Appendix A:) at a specified (Chapter 5, 6 and 7) flow rate for 18 hours to remove readily leachable materials and create an environment conducive for microbial attachment to the ore surface. The 0K media was sterilised by autoclaving the solution for 20 minutes at 120 °C The columns were inoculated by saturation (Tupikina et al., 2014) using upflow of 100 ml 0K media supplemented with the desired concentration of mesophilic microbial cells per kilogram of ore and 0.5 g L^{-1} of Fe^{2+} ($FeSO_4.7H_2O$) with re-circulation. The inoculum was recycled at a specified (Chapter 5, 6 and 7) flow rate in a closed circuit for 18 hours to allow microbial-mineral contacting. Thereafter, the columns were drained, and the liquid fraction collected. The solution collected was analysed for pH, redox potential, Fe^{2+} and Fe^{3+} iron concentration and the quantity of planktonic cells remaining.

Thereafter, the columns were operated as flow-through unsaturated beds in an open system at 30 °C for a specified period, with irrigant provided using a peristaltic pump. A continuous downflow of fresh sterile 0K media (pH 1.6) supplemented with 0.5 g L^{-1} Fe^{2+} ($FeSO_4.7H_2O$) was supplied. Daily samples of the effluent were taken, the volume measured and, analysed for pH, redox potential, Fe^{2+} and total iron concentration, and cell concentration.

Replicate experimental columns were run and individual columns sacrificed at regular intervals, with one sample column maintained throughout as an un-inoculated control. For each sacrificed column, the mineral coated glass beads as well as microbial cells attached to the surface were transferred into a sterile beaker and gently mixed. Individual beads were harvested, using sterile forceps, for several analyses including cell concentrations, scanning electron microscopy (SEM) and IMC. Briefly, for the determination of the cell concentrations colonising the mineral surface, beads were transferred, in duplicate, into a sterile 250 ml shake flask and subjected to the cell detachment protocol (as described in Section 3.7). For SEM, an individual bead was transferred into an Eppendorf tube and fixed with 2.5 % (v/v) glutaraldehyde at 4 °C (as described in Section 3.8). Finally, for IMC, beads were randomly selected and transferred into sterile ampoules for metabolic activity measurements using isothermal microcalorimetry (as described in Section 3.9).

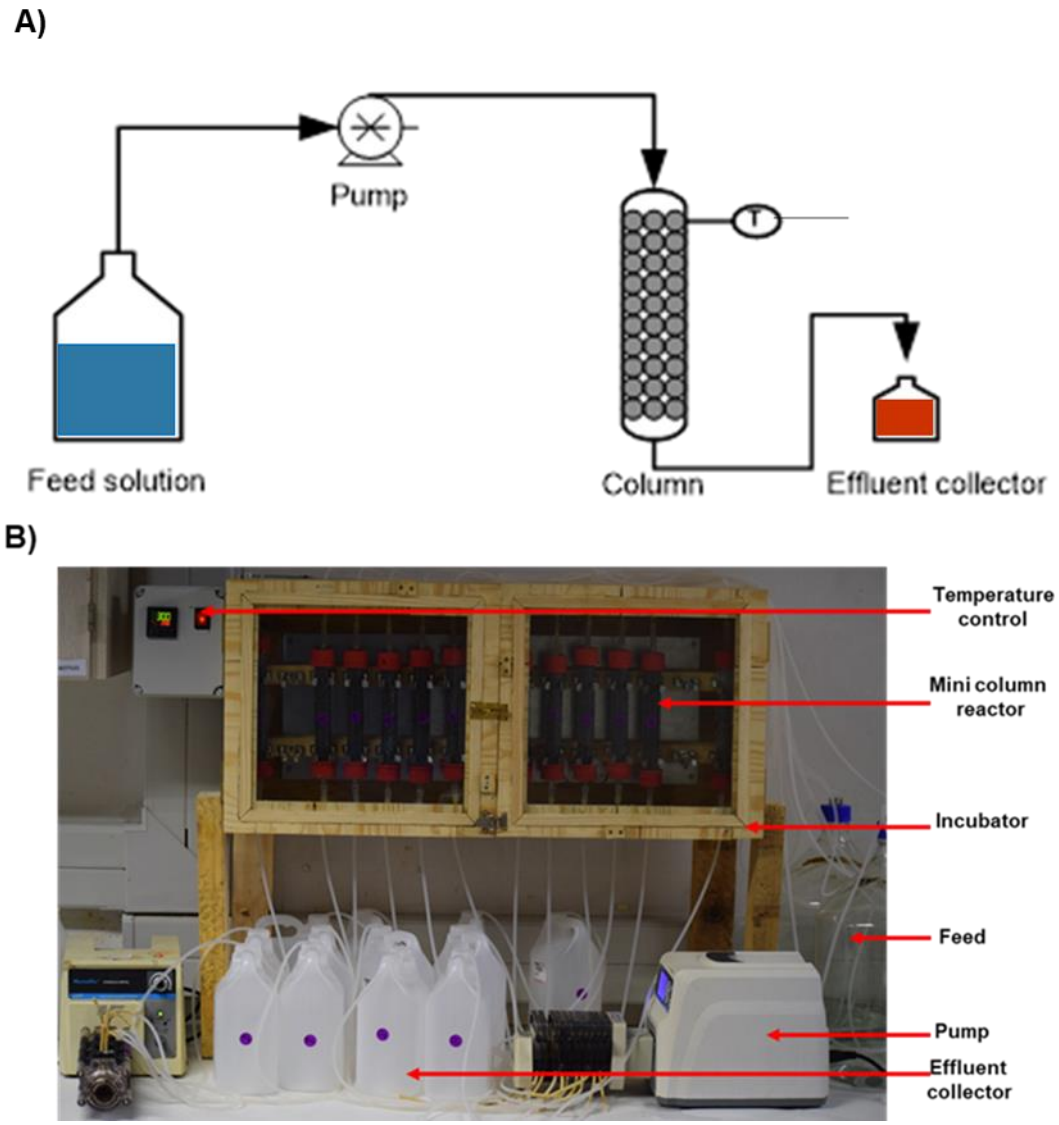

Figure 3.5: Schematic diagram (A) and the experimental setup and the flow-through column bioleaching reactor system (B).

3.6 Wet chemistry analytical techniques

3.6.1 pH

All pH measurements were performed using a Metrohm 704 pH meter and probe, calibrated at pHs 7.0, 4.0 and 1.0 before use.

3.6.2 Redox potential analysis

All redox potential readings were determined using a glass electrode with a built-in silver/silver chloride (Ag/AgCl, 3 M KCl) reference electrode, connected to a Metrohm 704 pH/Eh meter. The precision of the measurements was tested using a Crison standard redox solution having a potential of 468 mV at 25 °C.

3.6.3 Iron assay

The Fe^{2+} concentration was measured spectrophotometrically using the 1,10-phenanthroline colorimetric method described by Apha (1998) . The 1,10-phenanthroline method is based on the principle that 1-10-phenanthroline chelates with Fe^{2+}, forming an orange-red complex. To determine the total Fe concentration, following Fe^{2+} measurement, a scoop of hydroxylamine chloride was added to the same sample and blank used for the Fe^{2+} assay such that the Fe^{3+} present is reduced to Fe^{2+}. These mixtures were vortexed and left to stand for 5 minutes to allow the hydroxylamine to reduce all the Fe^{3+} to Fe^{2+}. The absorbance was measured at 510 nm using the HeλIOS α UV-visible spectrophotometer with version 7.09 software (Thermo Scientific, South Africa) and converted into Fe concentration by using a standard calibration curve (as presented in Appendix D.1). The Fe^{3+} concentration was obtained by subtracting Fe^{2+} value from Fe^{tot} value.

3.6.4 Total cell counts by microscopy

Microbial cell counts were determined using a Thoma counting chamber and an Olympus BX40 Microscope at 1500× magnification (oil phase, phase contrast optics, 15× magnification eyepiece, 100× magnification objective). The detection limit of the Thoma counting chamber was 3×10^5 cells ml^{-1}, as described by Chiume et al. (2012). Cell concentrations were determined using the following calculations:

$$Volume\ of\ one\ small\ square\ [mm^3] = depth\ \times\ area$$

$$= \frac{0.02 \times (0.05 \times 0.05)}{1000}$$

$$= 5x10^{-8} cm^3 \qquad \text{Equation 3.1}$$

$$Concentration\ total\ (cells\ mL^{-1}) =$$

$$dilution\ factor\ \times \frac{(cell\ count \times \frac{N}{n})}{volume\ one\ square\ x\ total\ number\ of\ squares} \qquad \text{Equation 3.2}$$

where N = total number of big squares (16)

n = number of squares counted (4)

3.7 Quantification of mineral-associated cells by microbial detachment and counting

Microbial detachment from the mineral surface of the mineral-coated glass beads, conducted in duplicate on approximately 100 mineral coated beads (35 g), was performed at every

column sacrifice. A modified detachment protocol, based on the protocols developed independently by the Harrison lab (CeBER, UCT) reported by Tupikina et al. (2009), Chiume et al. (2012) and Govender et al. (2013) and by the Dermergasso lab (Universidad Catolica del Norte, Antofagasta, Chile) reported by Zepeda et al. (2009), was used to detach microorganisms from the mineral surface. Briefly, the column was drained and the effluent analysed directly for microbial cell concentration. Mineral-coated beads were suspended in a volume of 0K media equivalent to half the coated bead mass (18 ml) and mixed gently by swirling the flask. The resulting cell suspension was transferred to a sterile 50 ml Falcon tube and centrifuged briefly (800 rpm at room temperature for 2 min) to remove any detached mineral matter. The supernatant, representing the microbial community loosely associated with the mineral concentrate but not firmly attached, was recovered and the cell concentration determined by direct microscopic cell counts (Section 3.5.4). The washed beads were re-suspended in the same volume of 0K media containing 0.4 % (v/v) Tween® 20 and thoroughly agitated using a bench-top vortex for 2 min, in order to detach the strongly attached microbial cells, before the solids were removed as described above. This bead washing process was repeated six times, before the cell numbers from each wash were enumerated microscopically (the refinement of the washing steps is detailed in Chapter 5). The degree of mineral surface colonisation was calculated, based on the total surface area available for microbial attachment provided by a single spherical mineral coated bead being 1.13×10^{-5} m^2. Therefore, based on a model bioleaching organism, *At*. *ferrooxidans*, with a surface area of 0.75 µm² (Ohmura et al., 1993), the theoretical maximum cell number that could attach to the available surface area provided by the mineral coated beads, assuming single layer coverage, was calculated to be 4.33×10^9 cells m^{-2} or 4.9×10^4 cells/bead. The actual count was presented as a percentage of this.

3.8 Visualisation by SEM

Scanning Electron Microscopy (SEM) was used for the visual analysis of attachment, EPS formation and colonisation of the mineral surfaces by microbial cells. Experimental samples (mineral coated beads) of microbially colonised mineral surface, as well as unleached and un-inoculated control samples of mineral, were obtained on taking columns down. These were fixed in 2.5 % (v/v) glutaraldehyde for a minimum of 24 h at 4 °C. The fixed samples were rinsed gently three times with sterile water, before being dehydrated through an alcohol series consisting of 30, 50, 70, 90, 95 and 100 % (v/v) ethanol (Merck) using 10 min contacting times. The samples were stored in 100 % (v/v) ethanol until further processing. After dehydration, the samples were mounted onto stubs and underwent critical point drying using hexamethyldisilazane (HMDS). The samples were sputter-coated with carbon before

visualisation using the SEM (FEI NOVA NANOSEM 230 with a field emission gun or Tescan MIRA3 with a Confocal Raman Imaging Extension).

3.9 Isothermal microcalorimetry

In this study, isothermal microcalorimetry (IMC) was used to quantify the metabolic activity of microbial cells colonising the mineral surface. Microcalorimetric experiments were carried out using the TAM III instrument supplied by TA Instruments, USA (Figure 3.6 A). This instrument is designed to monitor both endo- and exothermic reactions over a temperature range of 15 to 150 °C continuously. It is equipped with high-precision temperature control of the oil bath to within 0.0001 °C. A detection limit of 0.5 µW and a baseline stability (over a period of 24 h) of ± 0.2 µW characterise the instrument (Wadsö, 2002). The TAM multi-calorimeter module is fitted with six 4 ml channel micro-calorimeters (Figure 3.6 B), each holding a 4 ml ampoule containing the sample for analysis. The TAM III was operated in static ampoule mode (batch process). Batch experiments were performed with these 4 ml glass ampoules at 30 °C. For the machine control, a single ampoule was loaded aseptically with 2 ml 0K media supplemented with 0.5 g L^{-1} Fe^{2+} (pH 1.6). An abiotic control comprised of sterilised pyrite mineral coated beads, pre-wetted with 0K media, was set up in the second ampoule. The remaining 4 channels were used for experimental samples in which microbially colonised mineral-coated beads were loaded into each empty ampoule (Figure 3.6 C).

The experimental samples contained beads drawn from a representative sample of beads obtained from either the column or shake flask experiments. The bead samples were briefly and gently patted on a paper towel under a laminar flow to remove excess liquids before transferring them onto ampoules. and these were sealed. Following insertion of the ampoules into the IMC and subsequent stabilisation of the IMC system, heat-flow data were acquired for the samples. The maximum heat-flow of each ampoule was recorded for analysis. Heat output obtained from mineral-coated beads was calculated based on watt per m^2 mineral or ore surface, unless where otherwise specified.

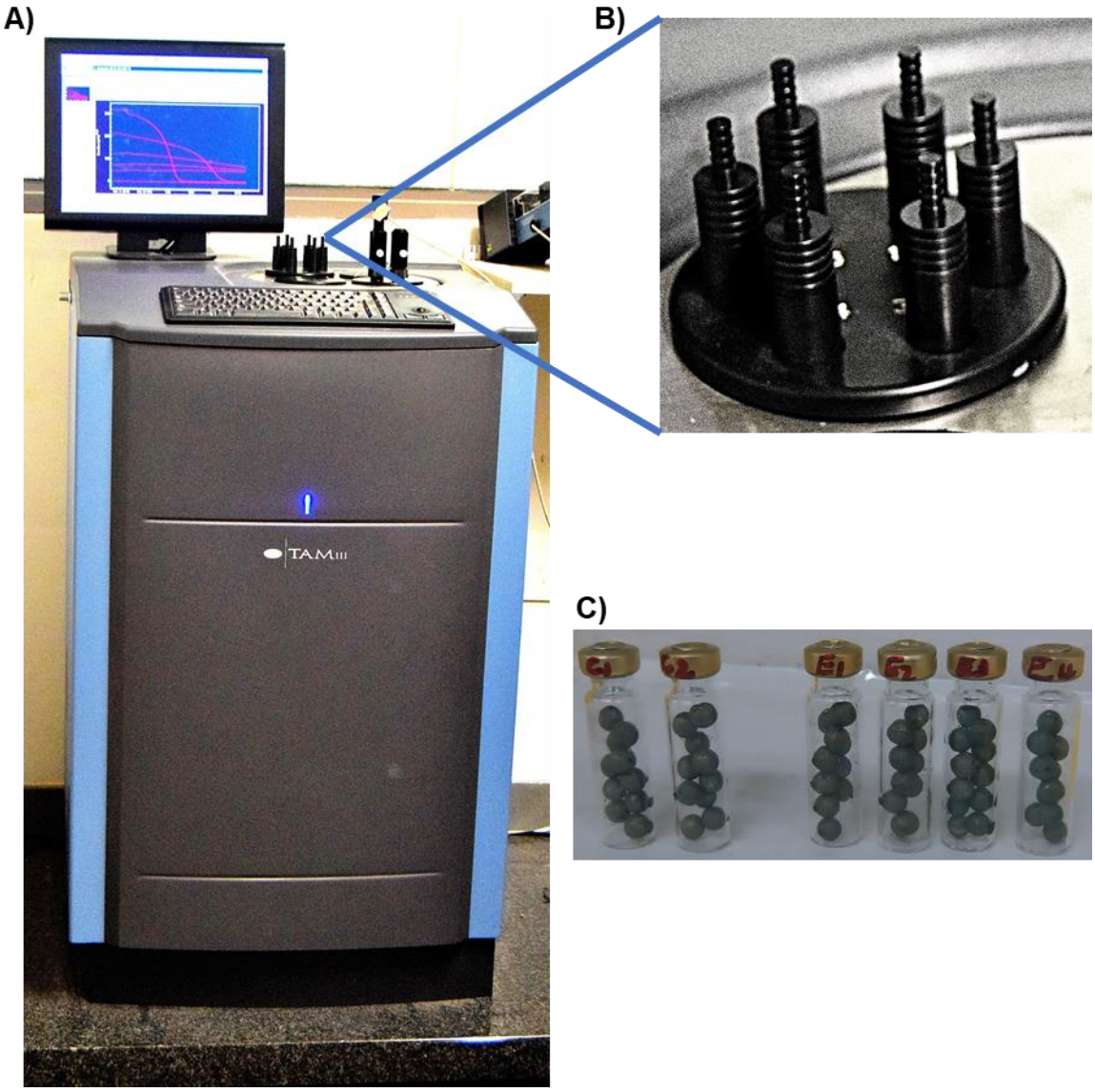

Figure 3.6: (A) The TAM III microcalorimeter used in this study was fitted with (B) a multi-calorimeter containing six channel micro-calorimeters into which (C) glass ampoules loaded with mineral coated glass beads are placed before measuring heat-flow.

3.10 EPS characterisation

EPS accumulated on the microbially colonised, PEL-HS mineral-coated glass beads packed into the glass column reactors when operated in the same way as described in Section 3.5.3. Two columns were taken down at the end of the experimental run and EPS harvesting experiments were conducted on each column as described in Section 3.10.1, alongside the other assays described above. Capsular (firmly bound) EPS recovered was analysed in terms of composition as described in Section 3.10.2. The loosely bound EPS was not of sufficient concentration to analysis.

3.10.1 EPS harvesting from the unsaturated flow-through ore bed

The colonised beads were suspended in 40 ml of 0K medium (pH 2.5) followed by settling out of the beads and centrifugation of the suspension (7,500 rpm for 20 min at 4 °C; Beckman Avanti Centrifuge). The supernatant, containing the loosely bound EPS fraction, was retained and stored at 4 °C for further processing and analysis.

The bound or capsular EPS fraction was recovered from the cell pellet using 10 ml of 30 mM dicyclohexyl-18-crown-6-ether (CE) in Tris buffer as described by Aguilera et al. (2008), followed by gentle agitation (30 rpm) for 2 hours at 4 °C to solubilise the bound EPS fraction. This was subsequently harvested (supernatant fraction) by centrifugation (7,500 rpm for 20 min at 4 °C; Beckman Avanti Centrifuge) as previously described and stored at 4 °C for further processing. A second extraction was then performed on the same sample by adding a further 10 ml of 30 mM CE, and the samples were agitated for a further 2 hours at 4 °C. As before, the supernatant fraction was harvested by centrifugation and retained for further processing.

All the samples were filtered twice through a 0.22 µm filter (Merck Millipore), before being dialysed (Pur-A-lyzer Mega 20 ml dialysis kit, Sigma Aldrich, 3.5 kDa cut-off) against sterile MilliQ water (water volume was always greater than 25 times the total sample volume to be dialysed) for 12 hours with water exchanged twice at 6 hour intervals. Samples were subsequently stored at 4 °C until quantitative EPS chemical compositional characterisation was carried out.

3.10.2 EPS biochemical characterisation

Microbial EPS is generally made up of a combination of components, including (but not limited to) polysaccharides, DNA, and lipids. Standard biochemical colorimetric assays, analytical and molecular techniques were used to measure these EPS components.

3.10.2.1 EPS sugar content analysis

The total carbohydrate content of the EPS was determined using a combination of the Dubois phenol-sulfuric assay (Dubois et al., 1956), using glucose as a standard, and an assay modified by Michel et al. (2009), which incorporated Fe^{3+} into the glucose standard to correct for any interference caused by the presence of iron in bioleaching systems. The complex carbohydrates are digested into sugar monomers, which are then detected by the creation of an orange-yellow colour. Briefly, a 200 µL sample and 200 µL of 5 % phenol were added into a test tube and mixed by vortexing. Concentrated H_2SO_4 (1 ml) was added onto the sample and immediately vortexed. Samples were allowed to stand at room temperature for 10 minutes before they were incubated at 30 ºC for a further 20 minutes. Aliquots of 250 µl were transferred to a 96 well plate and absorbance was read at 490 nm (Appendix E:-1).

This assay provides a combined quantitative indication of sugar content. In order to gain more detailed information on the composition of the extracted polysaccharide, the sugar monomers present in the polysaccharides were analysed using gas chromatography mass spectroscopy (GC-MS) at the Central Analytical Facility (CAF; Stellenbosch University). Each sample was prepared by adding 1 ml of 70 % (v/v) methanol to the samples and vortexing. Extraction was done in an oven at 60 °C for 3-4 hours and 250 µl of each of the extracted sample was transferred into a 2 ml tube and completely dried under a gentle stream of nitrogen. Subsequent to that, the samples were derivatised by adding 100 µl of 2 % methoxyamine in pyridine at 40 °C and incubated for 2 hours, followed by the addition of 50 µl N,O-Bis (trimethylsilyl) trifluoroacetamide (BSTFA) and derivatised again at 60 °C for 30 minutes. The samples were vortexed and transferred to a vial before injecting them into a GC-MS instrument for separation. Separation was performed using a gas chromatograph (6890N, Agilent technologies network) coupled to an Agilent technologies inert XL EI/CI Mass selective detector (MSD) (5975, Agilent technologies Inc., Palo Alto, CA). The GC-MS system was coupled to a CTC Analytics PAL autosampler. Separation of sugars was performed on a 30 m DB-5MS capillary column of 0.25 mm ID and 0.25 µm film thickness in which helium was used as the carrier gas at a flow rate of 1 ml min^{-1}. The injector temperature was maintained at 250 °C and 1 µl of the sample was injected in 10:1 split ratio. The oven temperature was programmed at 80 °C for 5 min; and then ramped up to 250 °C at a rate of 8 °C min^{-1} for 1 minute; followed by a ramping rate of 20 °C min^{-1} for 5 min until 320 °C and eventually to a maximum temperature of 325 °C and held for 0.25 min. The MSD was operated in a full scan mode and the source and quad temperatures were maintained at 240 °C and 150 °C, respectively. The transfer line temperature was maintained at 250 °C. The mass spectrometer was operated under electron impact mode at ionization energy of 70 eV, scanning from 40 to 650 m/z

3.10.2.2 EPS DNA content analysis

The DNA content was measured using a Nanodrop 2000 spectrophotometer (Thermo Scientific). An aliquot of 2 µL of EPS sample was placed on the Nanodrop and the concentration measured and recorded.

3.10.2.3 EPS lipid content analysis

The lipid content of the sample was measured based on Smedes and Askland (1999) method. Briefly, the samples were freeze dried overnight and, in order to solubilise complex lipids that are not soluble in methanol, 500 µl of hexane was added to freeze-dried pellet. A further 100 µl C17-TAG internal standard in hexane (1 mg ml^{-1}) and 1 ml of basic catalyst (0.5 N NaOH in methanol), were added, followed by brief vortexing and incubation at 80 ºC for 20 min, with

constant agitation at 300 rpm. The samples were allowed to cool for 5 minutes at room temperature, before 1 ml of acid catalyst (5 % (v/v) HCl in methanol) was added before repeating the vortex and incubation step. The samples were allowed to cool for another 5 minutes before the addition of 400 µl deionised H_2O to stop the reaction. Hexane (300 µl) and 100 µl C19-methyl ester internal standard in hexane (1 mg ml^{-1}) were added and vortexed well in order to extract the lipids. The samples were analysed using GC.

The GC run was conducted based on a method adapted from Griffiths et al. (2010). Fatty acid methyl esters (FAME) extracts (1 µl), containing internal standards that included glyceryl triheptadecanoate (C17-triacylglyceride) and methyl nonadecanoate (C19-methyl ester) that were added before and after transesterification respectively. Each sample was injected into a Varian 3900 GC equipped with a flame ionisation detector and SupelcoWax 10 column (30 m × 320 mm × 1.0 µm film thickness) (Supelco, USA). Standard split/splitless injection was used with a split of 100 and an injector temperature of 270 ºC. The column temperature was increased from 180 ºC to 260 ºC at 2 ºC min^{-1}. Nitrogen (2 ml min^{-1}) was used as the carrier gas and the detector temperature was 260 °C. Peaks were identified by retention time using Supelco 37 Component FAME and C14:0 to C22:0 FAME mixtures. Peak areas were used to quantify each FAME relative to the internal standards. Differences in the response factor of the detector to the range of FAMEs in the samples were negligible. The total fatty acid content was calculated by adding all the individual FAME peak areas.

Chapter 4: Refining isothermal microcalorimetry to determine metabolic activity during bioleaching

4.1 Introduction

Isothermal microcalorimetry (IMC) has been applied in a variety of biomineral studies, as detailed in Section 2.4.5, ranging from determining thermodynamics and reaction energies of microbial cultures associated with pyrite and chalcopyrite mineral particles (Rohwerder et al., 1998; Krok, 2016), to measuring activity of microorganisms that facilitate bioleaching of mine waste to determine and estimate their potential for ARD formation (Schippers et al., 1998; Schippers et al., 2000; Schippers et al., 2001; Kock and Schippers, 2006; Schwartz et al., 2006; Sand et al., 2007; Schippers et al., 2007). IMC has also been used to measure microbial activity during the leaching of copper in batch flasks and continuous stirred tank reactors (CSTR's) (Hedrich et al., 2016; Krok, 2016; Hedrich et al., 2018).

Microcalorimetry has been shown to be a suitable technique for the detection and quantification of the activity of microorganisms that facilitate leaching, due to its ability to detect and measure low metabolic activities. It has also been shown to assist in understanding various impacts that microorganisms have on both bioleaching and ARD prediction.

In this chapter, the aim is to further develop the IMC method and use it to measure the metabolic activity of mineral associated microorganisms as a function of the surface area (m^{-2}) of available mineral concentrate, with the aim of developing a method to investigate the microbial-mineral association during the colonisation of mineral surface at the onset of heap bioleaching or during uncontrolled leaching in waste rock dumps. The work includes the measurement and assessment of chemical and bio-chemical pyrite reaction rates per available surface area. Emphasis is placed on the generation of a heat-flow curve that is not prematurely truncated due to substrate limitation.

4.2 Research approach

Metabolic activity was first determined in cells that were suspended in liquid media and thereafter, a method that allowed attachment and colonisation of the fixed area mineral surface was set up and the best configuration between saturated and unsaturated surfaces was determined for the surface area study. Post the selection of the best representative configuration, reproducibility studies were performed. Correct bead loading in ampoules was assessed and these short-term experiments were conducted in concert with investigations of oxidation rates and O_2 availability or limitation. Column studies were also conducted for longer periods, and different bead loadings in microcalorimetric ampoules were also compared.

4.2.1 Heat-flow measurements from suspended microbial cells

The maximum heat-flow of microbial cells, in the absence of mineral substrate, was determined. Mixed mesophilic iron and sulfur oxidising acidophiles were obtained from the stock reactor (Section 3.2) and cell counts were performed. Cells ranging from 1×10^5 to 1×10^8 cells ml^{-1}, supplemented with 5 g L^{-1} Fe^{2+} in 0K media (making up a total volume of 2 ml) were transferred into the IMC ampoules. Cell free control ampoules contained 5 g L^{-1} Fe^{2+} in 0K media only. The ampoules were sealed and loaded into the IMC where microbial heat-flow was measured. After obtaining the maximum heat-flow, the IMC experimental run was stopped and the obtained maximum heat-flow, together with microbial cell numbers, was used to determine maximum heat-flow per cell. Iron consumed by the microbial cultures over the IMC experimental run was also measured using the spectrophotometric method detailed in Section 3.6.3.

4.2.2 Mineral colonisation

Glass beads were coated with the finely milled pyrite concentrate, as described in Sections 3.3.1 and 3.4, to provide a defined and reproducible surface area of well-liberated pyrite on which to study colonisation. These were colonised with the mixed mesophilic culture (Section 3.1) for use in IMC method development experiments. The beads were colonised in 250 ml Erlenmeyer flasks containing a working volume of 100 ml 0K basal salts medium (pH 1.6) with 0.5 g L^{-1} Fe^{2+}, 100 mineral-coated glass beads and a total cell inoculum of1×10^8 cells ml^{-1}. A control flask was not inoculated. The flasks were incubated at 30 °C for 72 hours to allow sufficient time for microbial colonisation of the mineral surface. The flasks were gently agitated at 100 rpm, to ensure adequate mixing and distribution of the media, whilst preventing coated minerals from detaching off the surface of the beads. Microbial growth and activity were assessed at 24-hour intervals over the course of the 72-hour colonisation period. Wet chemistry assessment was through planktonic microbial cell counts (Section 3.6.4), measurement of the redox potential (Section 3.6.2) and soluble iron concentrations (Section 3.6.3) at 24-hour intervals. After the 72-hour colonisation period, the colonised beads were loaded into ampoules and the maximum heat-flow was measured.

4.2.3 Isothermal microcalorimetry experiments

The microbial activity of the colonised mineral surfaces was assessed using IMC described in Section 3.9. The IMC method was scrutinised with respect to the configuration of the ampoule contents including the solid and liquid phases, availability of reactants and intra-experiment repeatability.

4.2.3.1 IMC ampoule liquid contents

In order to determine the most representative system for heat generation measurements, the degree of saturation and liquid composition in the ampoule were varied to observe the effect of the liquid phase conditions in IMC ampoules on the measured heat-flow from the colonising microbes on the pyrite coated beads (10).

In Configuration 1, the microbially-colonised pyrite-coated beads were placed in the ampoule and saturated with 0K media (pH 1.6) supplemented with 0.5 g L^{-1} of Fe^{2+}. This configuration was equivalent to the set-up for planktonic cells used in Section 4.2.1. The use of Fe^{2+} solution was informed by the frequent use of a low ferrous iron concentration during the start of shake flask or column experiments to initiate microbial activity; hence, the media was supplemented with 0.5 g L^{-1} Fe^{2+}.

Configuration 2 was set-up in the same manner as Configuration 1, except that the saturating liquid phase used was cell free leachate (obtained from colonisation studies; Section 4.2.2). Through this selection, this configuration resembles a continuation of the experimental physicochemical conditions in the colonisation studies.

In Configuration 3, unsaturated colonised pyrite-coated beads were used to more closely resemble the unsaturated environment typical heap bioleaching or waste mine dump conditions. This configuration was adapted from Krok et al. (2013).

4.2.3.2 IMC reproducibility

To assess the IMC method reproducibility, four biological repeats were loaded into the ampoules and these were run against chemical repeats (non-colonised controls). In this section, the heat-flow data produced over time was integrated, thereby generating a sigmoidal heat data curve, which shows the cumulative heat produced over time.

4.2.3.3 Pyrite oxidation rate quantification

Increasing volumetric microbially facilitated pyrite oxidation rates are expected as a function of increasing surface loadings. However, when these rates are normalised, similar specific rates are expected per unit surface area from samples treated the same way i.e. experiments conducted for the same period using the equivalent microbial culture. For pyrite oxidation rate measurements, microbially colonised mineral-coated beads were prepared in 100 ml Erlenmeyer flasks with a total working volume of 40 ml and loaded with 40 mineral coated beads; following inoculation, these were incubated at 30 °C for 24 hours. Abiotic controls were prepared in the same manner, without the inoculation. All other conditions remained the same as in Section 4.2.2. Pyrite oxidation rates (chemical and biochemical) were studied through assessing and measuring various loadings of mineral coated glass beads. This was done to correlate normalised maximum heat-flow (m^{-2}) across the different surface loadings. The

number of mineral-coated beads (using pyrite concentrate) that were loaded into the IMC ampoules, and their associated surface area, were 1 (1.13×10^{-4} m^2 total surface area), 2 (2.26×10^{-4} m^2), 3 (3.39×10^{-4} m^2) and 4 (4.52×10^{-4} m^2) beads.

The maximum heat generated in these systems was recorded and oxidation was determined according to Schippers and Bosecker (2005) and Kock and Schippers (2006). Complete oxidation of FeS_2 to Fe^{3+} and sulfate produces a reaction energy $\Delta_f H^0$ of −1546 kJ mol^{-1}. Using this value, together with molecular mass of FeS_2 (0.12 kg mol^{-1}), the measured maximum heat-flow *a*(μW) and the sample weight *w*(g), the pyrite oxidation rate *r* can be calculated using the following equation:

$$r\left(\frac{\frac{\mu g}{kg}}{s}\right) = \frac{1}{\Delta_f H°\left(\frac{kJ}{mol}\right)} \times FeS_2\left(\frac{kg}{mol}\right) \times a(\mu W) \times \frac{1}{w(g)} \qquad \text{Equation 4.1}$$

$$r\left(\frac{\frac{\mu g}{kg}}{s}\right) = \frac{1}{-1546\left(\frac{kJ}{mol}\right)} \times 0.12\left(\frac{kg}{mol}\right) \times a(\mu W) \times \frac{1}{w(g)} \qquad \text{Equation 4.2}$$

The equation was adapted to present the reaction rate as a function of surface area (A; m^2) and not mass (g) as follows:

$$r\left(\frac{\frac{\mu g}{m^2}}{s}\right) = \frac{1}{-1546\left(\frac{kJ}{mol}\right)} \times 0.12\left(\frac{kg}{mol}\right) \times a(\mu W) \times \frac{1}{A(m^2)} \qquad \text{Equation 4.3}$$

4.2.3.4 IMC ampoule gaseous reagent limitation

For the experiments on gaseous reagent limitation in the IMC ampoules, microbially colonised mineral-coated beads were prepared in 100 ml Erlenmeyer flasks with a total working volume of 40 ml, loaded with 40 mineral-coated beads and incubated at 30 °C for 24 hours. All other conditions remained the same as in Section 4.2.2. Limitation in microbial activity not due to pyrite content was observed from initial heat-flow curves. As the ampoules were sealed, it was postulated that either O_2 or CO_2 may be the limiting factor to microbial activity and thus the heat generated. Studies were performed to validate the effect of O_2 and CO_2 availability on microbial activity within the sealed vial. Two colonised mineral-coated beads were transferred into ampoules, whereafter the air was displaced from the system by introducing either N_2 or CO_2 at a rate of 0.1 or 0.5 L min^{-1} respectively for 30 seconds. The available headspace in the vials was an average of 3.77 ml. Microbially colonised, non-sparged mineral-coated beads were used as controls. After displacing the air, the ampoules were placed in the

microcalorimeter and the heat-flow output was monitored until the maximum activity was reached.

4.3 Results and discussion

4.3.1 Metabolic activity of suspended cells

Before any colonisation of mineral surfaces and measuring of metabolic activity of mineral associated microorganisms, metabolic activity of leaching microorganisms in Fe^{2+} supplemented 0K media was measured in the IMC. The graphical representation of the heat-flow curves from each of the varying concentrations are shown in Figure 4.1. The heat-flows following inoculation with 1×10^5 and 1×10^6 cells ml^{-1} were flat throughout the run. The low heat detected in these samples, however, does not equate to lack of activity by the number of cells, but to a very low number of cells coupled with low metabolic activity that is below the detection and sensitivity of the IMC technique. Heat-flows of inoculation with 5×10^7 and 1×10^8 demonstrated a semi bell curve with the initial measured points already demonstrating increased metabolic activities as demonstrated by the higher heat-flows. The higher initial heat-flows are also observed in samples inoculated with 1×10^7 cells ml^{-1}. The bell-shaped heat-flow curve represents the exponential microbial growth curve and its corresponding bell-shaped curve of specific growth rate with time in a batch cultivation system, as described by Sherwood et al. (2011) as these microbial cultures cultivated in liquid medium as a batch culture incubated in a closed vessel undergo a lag phase, increased activity to the maximum specific growth rate followed by decreasing activity on the onset of nutrient limitation or inhibition. The heat-flows of 5×10^7 and 1×10^8 inoculated samples partially demonstrated the four phases that define a microbial bell-shaped curve growth (Figure 4.1).

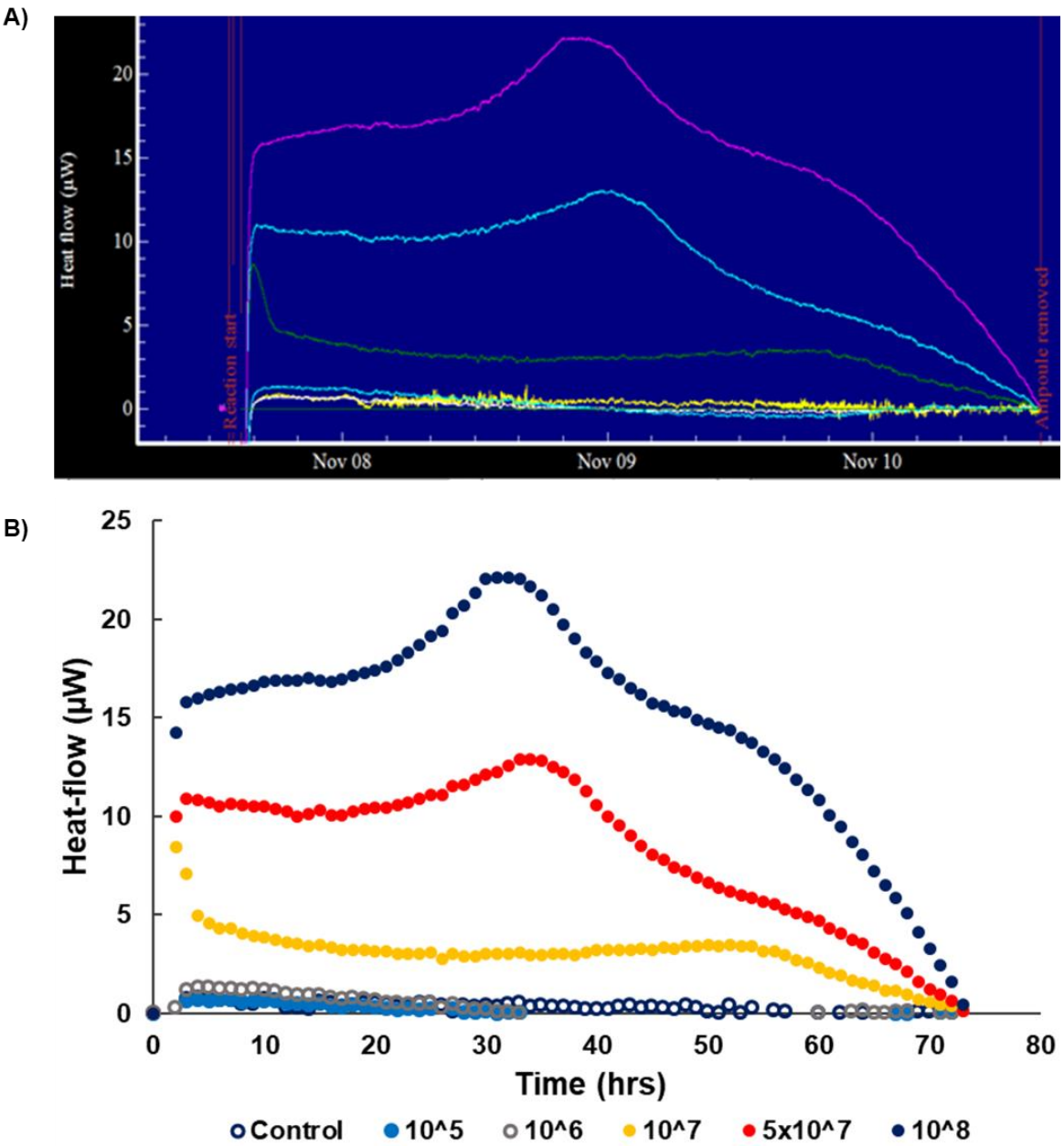

Figure 4.1: IMC measurement of varying microbial concentrations. The heat-flow profiles are presented via thermogram (A) and re-plotted for clarity (B) from the experiments ranging from 1×10^5 (●), 1×10^6 (○), 1×10^7 (●), 5×10^7 (●), 1×10^8 (●) and ○ represents the uninoculated control.

The maximum heat-flows of the above-mentioned microbial concentrations were used to determine the maximum heat-flow per cell at each concentration (Figure 4.2 ◆). It was shown that the increase in microbial concentration resulted in an increase in measured maximum heat-flow output (Figure 4.2 ●). The maximum heat-flow measured in the control sample (0K media + 5 g L^{-1} Fe^{2+}) was 0.51 µW, and the values obtained from 10^5 to 10^8 cells ml^{-1} were 0.69 µW for 10^5 and for 10^6 (1.31 µW), 10^7 (8.42 µW), 5×10^7 (12.91 µW) and 10^8 cells ml^{-1} was 22.13 µW. IMC has been reported to detect active microbial cell concentrations as low as 2.5×10^4 to10^5 cells ml^{-1} (Braissant et al., 2010a). It was also observed in the cell suspension study that when a low microbial concentration was inoculated, high heat output was measured

per cell on 1 × 10^5 cells ml^{-1} inoculation, and less heat output was measured with increasing microbial concentrations (5 × 10^7 and 1 × 10^8 cells ml^{-1}; Figure 4.2 ◆).

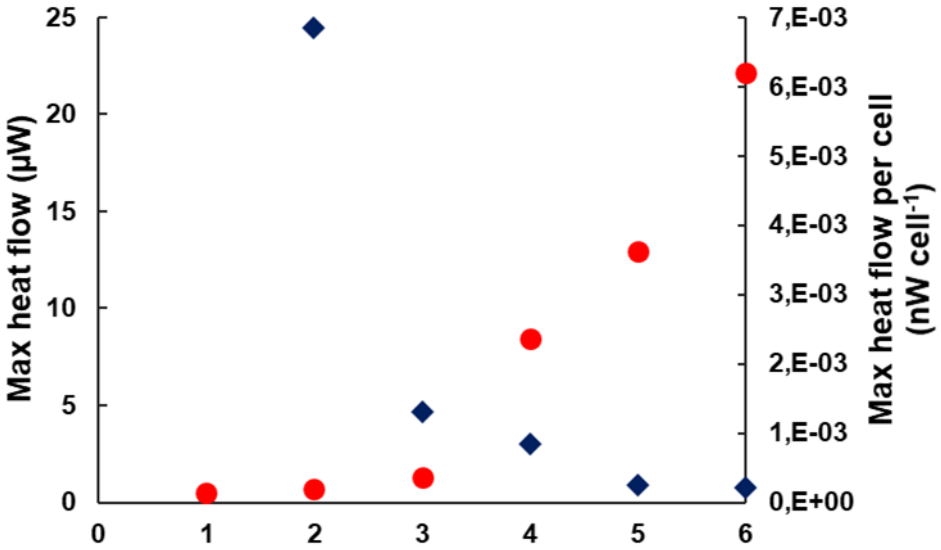

Figure 4.2: IMC measurement of maximum heat-flow (●) and maximum heat-flow per cell (◆). The various microbial concentrations (1) Control (2) 1 × 10^5 (3) 1 × 10^6 (4) 1 × 10^7 (5) 5 × 10^7 (6) 1 × 10^8 cells were loaded into the various the ampoules and their metabolic activity was measured.

After the 72-hour IMC experimental run, Fe^{2+} consumption and Fe^{3+} production was measured. The provided 5 g L^{-1} of Fe^{2+} (Figure 4.3 ■) was not depleted by the cells in any of the tested microbial concentrations. The Fe^{3+} produced ranged from 2.02 g L^{-1} for 10^5 cells ml^{-1} to 2.87 g L^{-1} for 10^8 cells ml^{-1} (Figure 4.3 ■). The inability to continue to consume Fe^{2+} (substrate) and produce Fe^{3+} (product) by the microorganisms could be attributed to a number of factors including accumulation of metabolic waste that could inhibit the microorganisms, and O_2 depletion that would limit the activity of aerobic microorganisms and oxidative reactions (Braissant et al., 2010a). A study performed in batch well plates inoculated with the same culture and supplemented with the same amount of Fe^{2+} (5 g L^{-1}) and pyrite concentrate demonstrated that the resultant Fe^{3+} from Fe^{2+} oxidation was not toxic towards microbial cultures because cell growth was evident and the supplemented Fe^{2+} was completely oxidised to Fe^{3+} after 72 hours (see Appendix D.2 ; Figure D 2-1). We have shown at this point that the IMC can detect and measure heat-flows from liquid medium suspension microbial cultures at varying concentrations, but that where the microbial concentrations are high, growth limitation may occur. It was thereafter required to measure the metabolic activity of mineral colonising microorganisms.

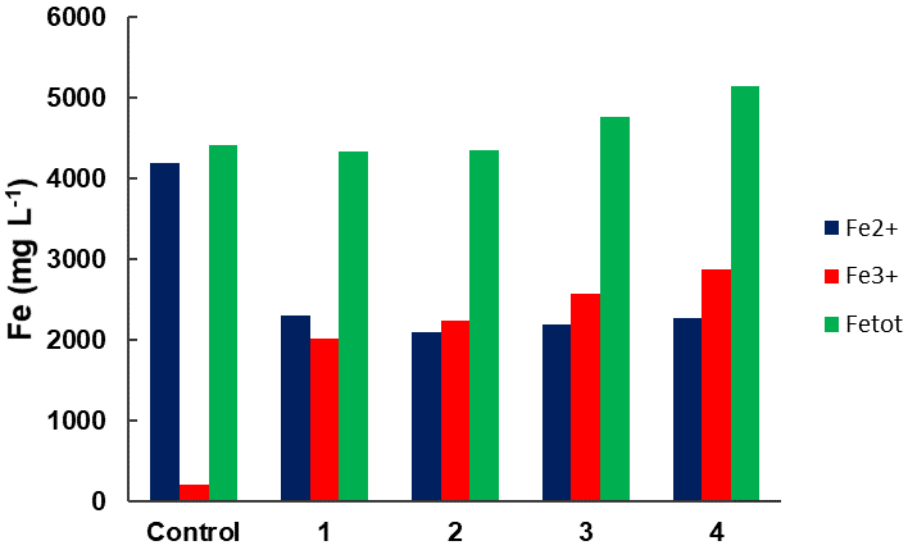

Figure 4.3: Representation of Fe^{2+} (■) oxidation to Fe^{3+} (■) by mixed mesophilic cultures during the IMC measurement of their heat-flow. (1) 1 × 10^5, (2) 1 × 10^6, (3) 5 × 10^7, (4) 1 × 10^8 cells ml^{-1}. Total iron (■) available in system at any point is also shown. *Ampoule containing 1 × 10^7 cells ml^{-1} concentration got stuck inside the machine*

4.3.2 Determining the optimal configuration for heat measurement from mineral-associated microbial populations

A study was conducted to select the most suitable and representative configuration for heat measurement. Figure 4.4 shows the maximum measured heat-flow from a defined surface area (mW m^{-2}) of the microbially colonised pyrite mineral-coated beads under the three liquid phase configurations. The ampoules loaded with microbially colonised mineral surfaces and saturated with fresh media (Configuration 1) had a maximum heat-flow of 28 ± 10 mW m^{-2} whilst the ampoules with colonised mineral surfaces saturated with cell free (filtered) leachate generated 19.9 ± 3 mW m^{-2}. The unsaturated, colonised mineral surface showed high heat-flow output (263.3 ± 2 mW m^{-2}), at least 9 times greater than the other configurations (Figure 4.4). The unsaturated mineral ore configuration has been applied in biomineral studies when measuring metabolic activity of mineral associated microorganisms using IMC (Elberling et al., 2000; Krok et al., 2013; Bararunyeretse et al., 2017; Ghadiri et al., 2018; Hedrich et al., 2018). A study from this PhD using the unsaturated mineral ore configuration is reported as Makaula et al. (2017). Hedrich et al. (2018) measured the metabolic activity of a moderately thermophilic consortium that facilitates the degradation of a copper concentrate in stirred tank bioreactors at different temperatures. In this study, an unsaturated pulp, colonised by microorganisms, was obtained from the bioreactor and activity was measured as a function of mass. Ghadiri et al. (2018) used the IMC to measure unsaturated mineral coated glass beads that were colonised by a mesophilic consortium as a function of X-ray µCT exposure. There is low solubility of O_2 into aqueous solutions and a reduced air-containing headspace, resulting in a more rapid potential oxygen limitation on studying the metabolic activities of O_2 requiring microorganisms, like bioleaching microbes, in sealed ampoules (Stumm and Morgan, 1996).

Sealed ampoules that are partly filled with static liquid medium with air in the head space would lead to aerobic respiration quickly rendering the liquid medium anoxic. This O_2 depletion can however be subverted by ensuring that microorganisms are in direct contact with air through the use of solid media such as agar or soil (Braissant et al., 2010a) and enhancing the gaseous headspace. In this thesis, the unsaturated mineral ore configuration was thus selected and used onwards as a standard method. Furthermore, the repeats of unsaturated ore beds were measured to confirm sensitivity and repeatability of IMC (Section 4.3.3).

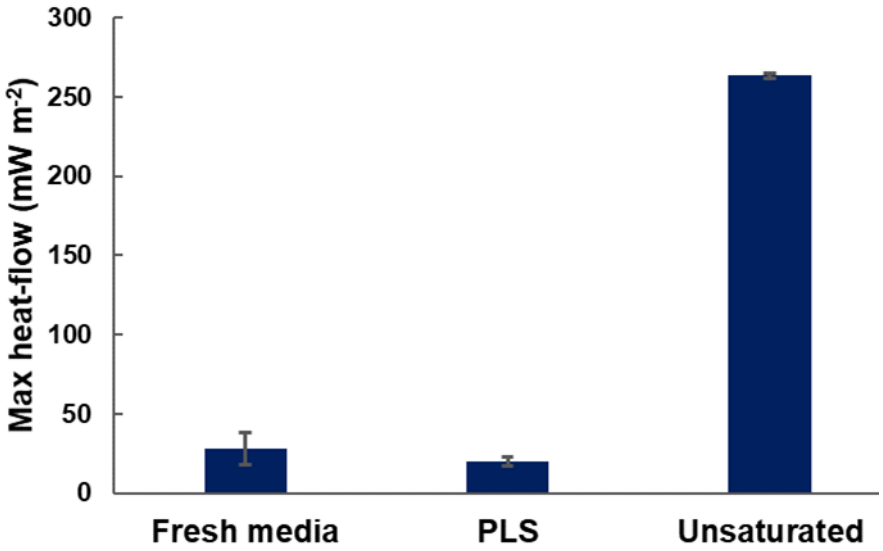

Figure 4.4: Maximum heat-flow per unit surface area of 10 colonised beads measured using the IMC for the three different saturation configurations: beads saturated with fresh media supplemented with Fe^{2+}, beads saturated with cell free leachate and unsaturated bead. Standard deviation from duplicate runs was ± 10.49 for fresh media, ± 2.98 for PLS and ± 1.63 for unsaturated.

4.3.3 Reproducibility of metabolic activity measurement by IMC

IMC is a very sensitive heat measuring instrument; thus, it was critical to demonstrate the reproducibility of the data obtained. Success in demonstrating reproducibility provides information that the heat output of mineral associated microorganisms was similar to across the mineral-coated beads. For reproducibility purposes, both the heat-flow and heat data curves were considered (Figure 4.5 A and B). The heat data curve is the integral of the heat-flow over time and is recognised as a proxy for growth. The heat-flow curve shows three (exponential, stationary and death phase) of the four typical growth phases for a batch system (Sherwood et al., 2011) i.e. lag phase is missing. This is similar to Figure 4.1 in Section 4.3.1. The heat generated in ampoules increased exponentially and corresponded with the exponential phase in the heat-flow curve. The heat-flow curve reached the maximum heat-flow and started to decline. The average maximum heat-flow was 83.7 mW m^{-2} with a standard deviation of ± 5.3 mW m^{-2} between the four repeats The exponential phase of the cumulative heat generation curve interfaced with the instantaneous heat-flow curve (Figure 4.5 C). During the decline of the heat-flow curve, the cumulative heat generation curve demonstrated entry

into a semi-stationary phase with very low heat generation. This low heat flow production could be as a result of cell death as suggested by Sherwood (2011) or due to limitation or inhibition of metabolic activity. The relationship between instantaneous heat-flow, cumulative heat generation, determined by the flow curve integration and growth is detailed in Braissant et al. (2015). The relatively good reproducibility of these curves across four biological repeats validates the postulation that the microbial cells are uniformly distributed across the mineral-coated beads colonised in a well-mixed and closed batch system, and therefore release comparable heat. To test this statistically, one way ANOVA was used and the variances of the normalised maximum heat output (mW m^{-2}), across the same experimental runs was conducted. A null hypothesis that was advanced stated that normalised heat output across the colonised surface loadings was the same and thus reproducible. For the hypothesis to be accepted, the F value had to be lower than the F-critical value. The F value was 0.46 and the F-critical value was 2.66, with p-value 0.71 and this meant that the advanced hypothesis remained and the maximum heat output (mW m^{-2}) was the same across the experimental runs. However, the mineral-associated microorganisms of interest in this thesis are cultured in unsaturated flow through system, hence reproducibility from these systems is detailed in Section 4.3.4.

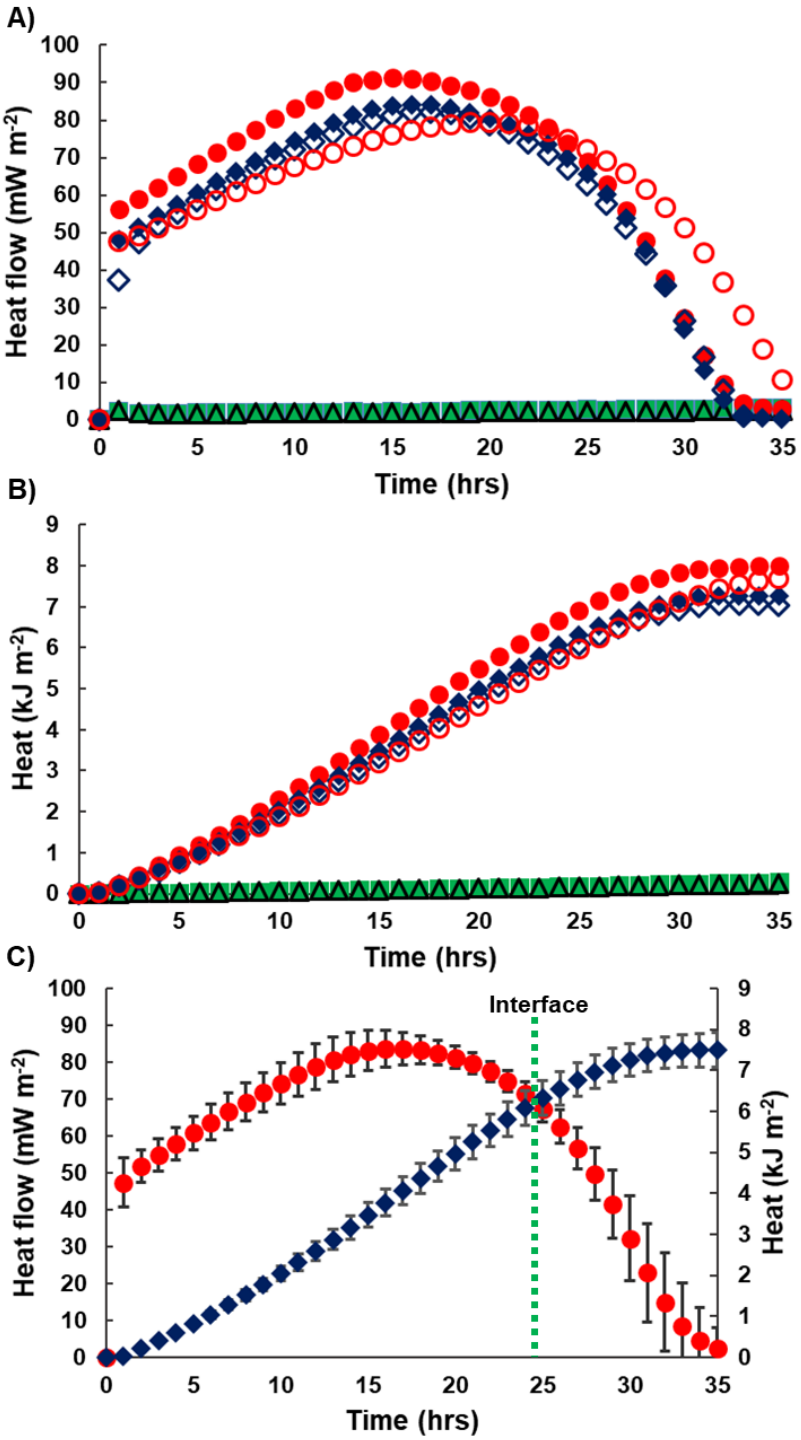

Figure 4.5: Heat-flow (A) and heat curves (B) of four biological repeats of the colonised unsaturated mineral coated glass beads (10 beads; ●,○,◆,◇ and uncolonised (chemically leached) mineral coated glass beads (10 beads) that were used as a control (■,△). (C) shows the integration of the heat-flow (●) and heat curve (◆). Error bars represent the standard deviation from the mean of four repeats.

4.3.4 IMC measurement of samples from flow-through mini column system

Data obtained from the short-term batch shake flask experiments demonstrated that microbial cells were uniformly distributed across the mineral-coated beads and showed relatively good reproducibility on measuring activity of ten beads. However, the IMC method also required

refinement, validation and assessment of reproducibility to measure microbial-mineral interactions from flow-through systems that are typically operated for longer periods and are not well mixed. For the flow-through studies (Section 3.5.3), 2 and 5 beads were selected and compared for IMC measurements. This selection of beads was informed by the fact that flow-through experiments are conducted for longer periods, hence more colonisation could be expected such that fewer beads were appropriate than the 10 beads selected for the short 24 and 72 h experiments, owing to the potential for limitation. After the 18-hour inoculation, both assays conducted with 2 (21.4 ± 1.9 mW m^{-2}) and 5 (22.5 ± 0.5 mW m^{-2}) beads gave relatively similar maximum heat-flow outputs per unit surface area. A dissimilarity in the maximum heat-flow output was observed for beads analysed by IMC after cultivation for 7 days in the flow-through system with 5 beads giving a maximum heat-flow of 287 ± 8.5 mW m^{-2}), which was almost double the maximum heat-flow produced by 2 beads of 159.1 ± 10 mW m^{-2}. The maximum heat-flow outputs measured from the 2 bead samples presented an exponential progression with time over the 20-day experimental run, whereas the 5 bead samples presented erratic maximum heat-flow output over the same period (Figure 4.6). After day 12 and 15, both 2 (330 ± 8.1 mW m^{-2} and 432 ± 31.1 mW m^{-2} respectively) and 5 (226 ± 76.6 mW m^{-2} and 475 ± 0 mW m^{-2} respectively) bead samples had similar maximum heat-flow outputs, considering the deviations in the duplicate ranges. At day 20, the maximum heat-flow produced by 2 beads was 827 ± 160 mW m^{-2}, compared with 496 ± 8.5 mW m^{-2} produced by the 5-bead sample. This suggested limitation in the 5-bead system.

It was shown that 2 beads consistently produced an exponential like maximum heat-flow output over the 20-day period whilst the data observed from 5 bead samples became inconsistent with increasing experimental run period and therefore increased cell concentrations on the mineral surface. It was shown here that microbial-mineral interaction studies that are conducted over longer periods lead to difficulties in maintaining the consistencies when measuring heat-flow at advanced stages of experimental runs. This then required an establishment of a method that would consistently be able to measure heat-flow over extended periods of time without limitation or inhibition occurring. In this study, based on the consistencies demonstrated by the 2 bead samples, this method approach was selected for further studies within this thesis. This is confirmed by statistical analysis conducted using 1, 2, 3 and 4 beads in Section 4.3.5. A full integrated data of the 2-bead experiment in a flow-through column operation is detailed in Chapter 6.

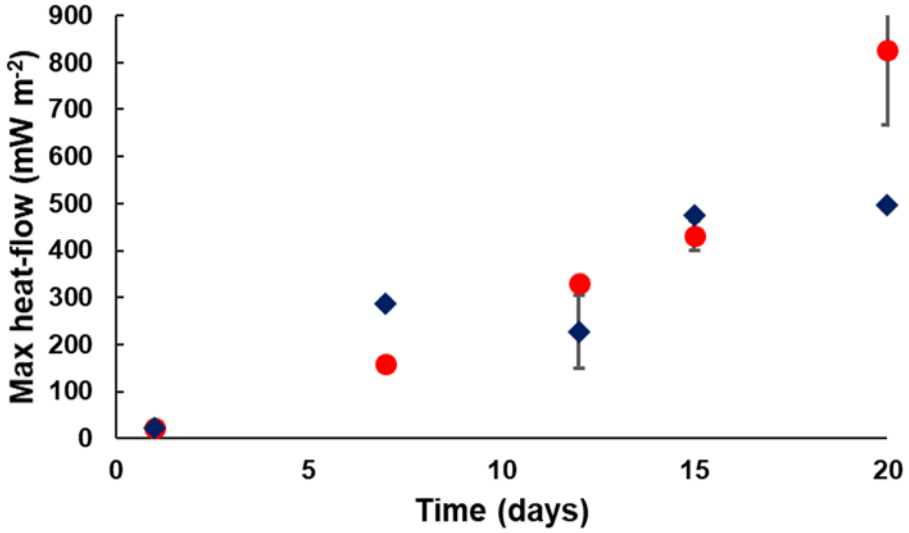

Figure 4.6: Maximum heat-flow per unit surface area of 2 (●) and 5 (◆) glass beads coated with pyrite mineral concentrate, after day 1, 7, 12, 15 and 20 measured using the IMC. Error bars represent the standard deviation from the mean of duplicates.

4.3.5 Pyrite oxidation rates

Maximum heat-flow output from the microbial colonised mineral surface increased with an increase in surface area loading (Figure 4.7 A). The measured maximum heat-flow in the biologically assisted oxidation increased from 8.3 µW when 1 bead was loaded to 26 µW when 3 beads were loaded. Thereafter, the maximum heat-flow remained relatively similar with 27 µW measured when 4 beads were loaded (Figure 4.7 A). The similar maximum heat-flow output observed for the 3 and 4 bead systems suggested that there may have been limitation in microbial activity (similar observations in Section 4.3.4). It is worth noting that these experiments were performed several days apart from each other e.g. it took a full month to complete the 1 bead experiment, including 24 hours to allow colonisation and the 700 hours to measure heat-flow in the IMC (Figure 4.8 A) . However, all the experimental parameters (e.g. cell numbers) remained the same across the studies. The normalised heat-flow curves per surface unit (m^2) of the increasing bead studies are shown in Figure 4.8 A to D. Maximum heat-flow curves of the different surface loadings was reached at different times for each loading, with 1 bead (110) 2 beads (50) 3 beads (80) and 4 beads reached maximum heat-flow curves at 50 hours. One way ANOVA was used to determine statistical variances of the normalised maximum heat output (mW m^{-2}), across the various bead loadings. A null hypothesis that was advanced stated that normalised heat output across the colonised surface loadings was the same regardless of the number of beads used. For the hypothesis to be accepted, the F value had to be lower than the F-critical value. The F value was 3.96 and the F-critical value was 4.07, with p-value 0.053 and this meant that the advanced hypothesis remained and the normalised maximum heat output (mW m^{-2}) was the same across the bead loadings of 1 to 4 beads.

The heat-flow output remained relatively constant at a low value throughout the run for all chemically oxidised surfaces (Figure 4.7 A). However, a higher output was measured when 3 beads where loaded. This result combined with the observation of a slowly increasing heat-flow value in the 3 bead run (Figure 4.8 C) suggested that there was microbial contamination in the system that facilitated the oxidation of the mineral. The pyrite mineral concentrate is subjected to sterilisation prior to every experimental run to render indigenous microorganisms inactive (Section 3.3.1). When the heat-flow values are normalised to a maximum heat-flow output per m^2 (Figure 4.7 B), the maximum heat-flow of the biologically oxidised mineral surfaces was relatively similar across the different surface loadings (taking standard deviation into consideration).

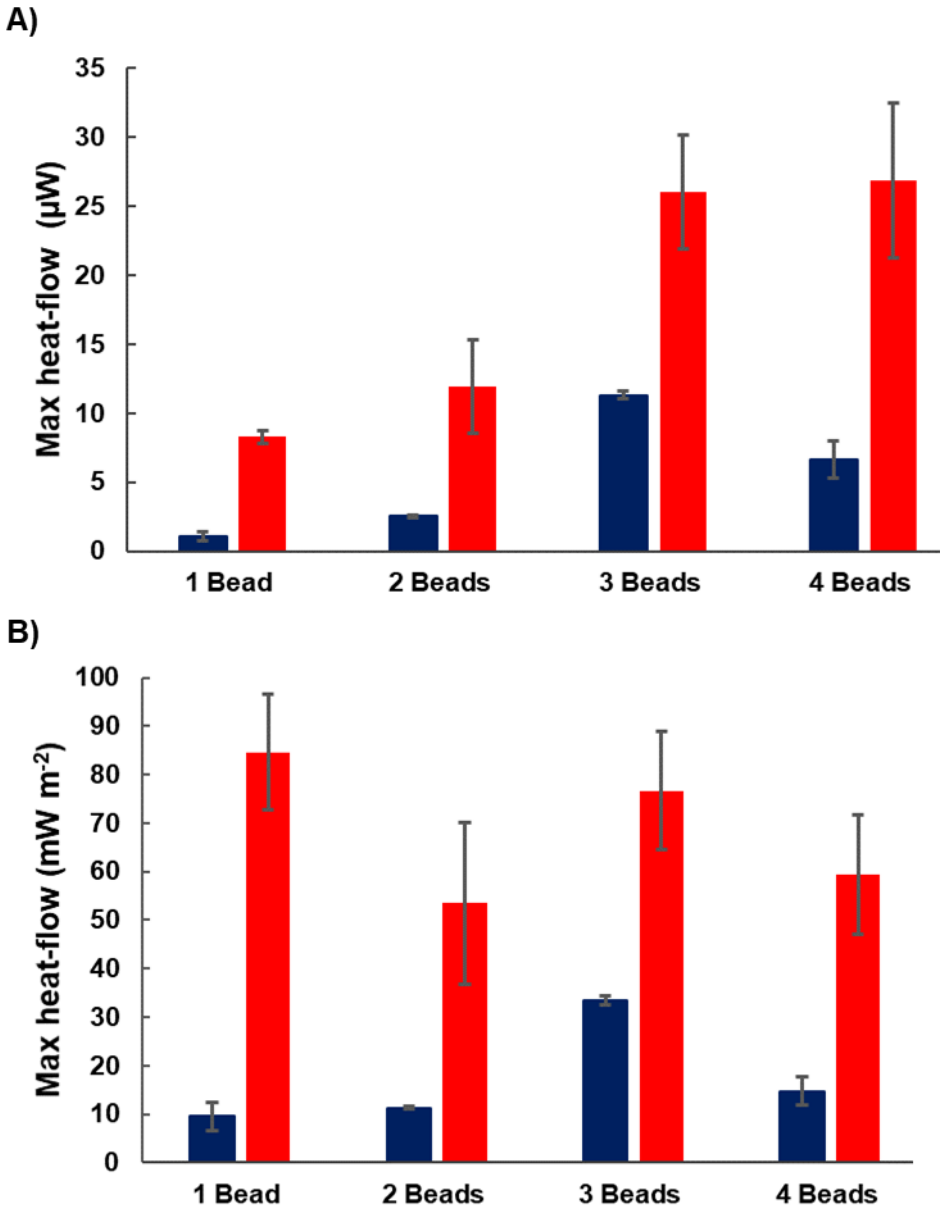

Figure 4.7: IMC measurement of maximum heat-flow from biologically (■) and chemically oxidised controls (■). (A) shows maximum heat output (µW) from the various ore surface loadings and (B) shows the normalised maximum heat output (mW m^{-2}) from the various ore surface loadings. Error bars represent the standard deviation from triplicates of biologically oxidised experiments and duplicates of chemically oxidised controls

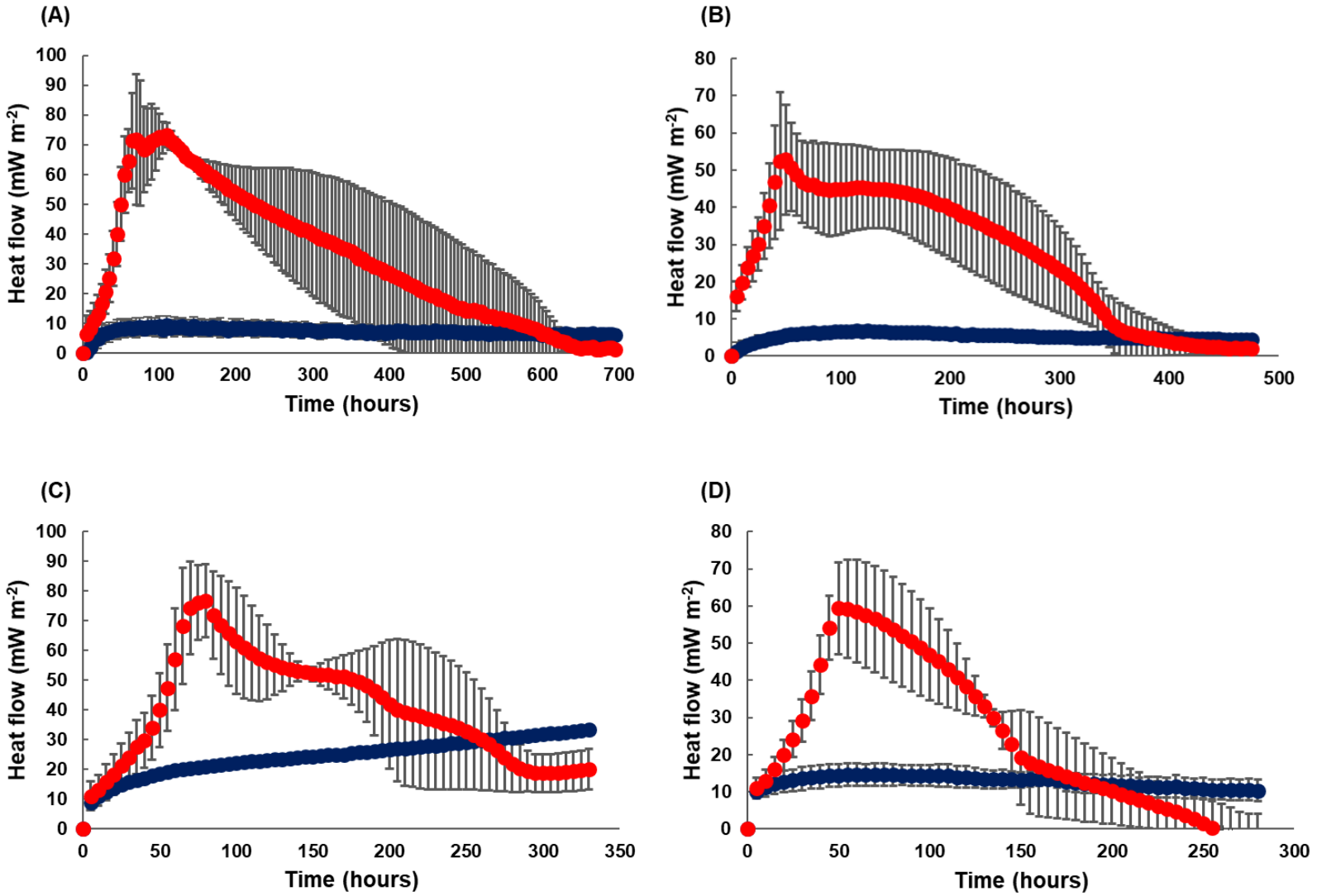

Figure 4.8: IMC measurement of the heat-flow profiles of biologically oxidised (●) and chemically oxidised (●) controls in varying colonised mineral surfaces, including 1 bead (A), 2 (B), 3 (C) and 4 beads (D). Error bars represent the standard deviation from the mean triplicates of biologically oxidised samples and duplicates of chemically oxidised controls

Biologically facilitated oxidation rates were acquired through the subtraction of the chemical oxidation rate from the combined chemical and biotic heat-flow and oxidation rates. The measured oxidation rates under abiotic conditions remained relatively unchanged despite the increasing surface area (except for the 3-bead system). The biotic oxidation rates were relatively similar across all four surface area loadings (Table 4.1).

Table 4.1: Pyrite oxidation rates calculated from both chemically and biologically facilitated degradation of pyrite

Surface area (m^2)	**Chemical oxidation rate (-µg m^{-2} s^{-1})**	**Biological oxidation rate (-µg m^{-2} s^{-1})**
1.13×10^{-4} m^{-2}	0.73 ± 0.2	5.7 ± 0.3
2.26×10^{-4} m^{-2}	0.86 ± 0.02	4.1 ± 1.1
3.39×10^{-4} m^{-2}	2.6 ± 0.07 *	5.9 ± 0.9
4.52×10^{-4} m^{-2}	1.1 ± 0.2	4.6 ± 1.0

* Suspected contamination

4.3.6 IMC ampoule gaseous reagent limitation

The time it took to reach the maximum heat-flow value decreased with the increase in surface loading (Figure 4.8). This indicates that an increase in surface area (bead numbers) and microbial cells associated with mineral surface increases metabolic activity and lead to an accelerated depletion of O_2 or CO_2. O_2 availability has been reported in previous studies as a factor that limits microbial activity in sealed ampoules (Rohwerder et al., 1998). The effect of O_2 availability on the metabolic activity of the microorganisms attached to the mineral surface was assessed through displacing the available O_2 by sparging the vials with CO_2 or N_2 gas. Two different flow rates of the gasses were used: 0.1 L min^{-1} and 0.5 L min^{-1}. The findings are represented in Figure 4.9. The normal air systems had a high maximum heat-flow of 110 mW m^{-2}. The maximum heat-flow measured was 48 mW m^{-2} for 0.1 L min^{-1} and 47 mW m^{-2} for 0.5 L min^{-1} in CO_2 enriched ampoules. For N_2 enriched ampoules, 48 mW m^{-2} was recorded for 0.1 L min^{-1} and 40 mW m^{-2} for 0.5 L min^{-1}. Sparging of ampoules with 0.1 and 0.5 L min^{-1} of both CO_2 and N_2 for 30 seconds had similar impacts when compared to one another. This confirmed that the displacement of O_2 in the system by introducing CO_2 and N_2 reduced exothermic oxidative reactions facilitated by the metabolic activity of mineral associated greatly.

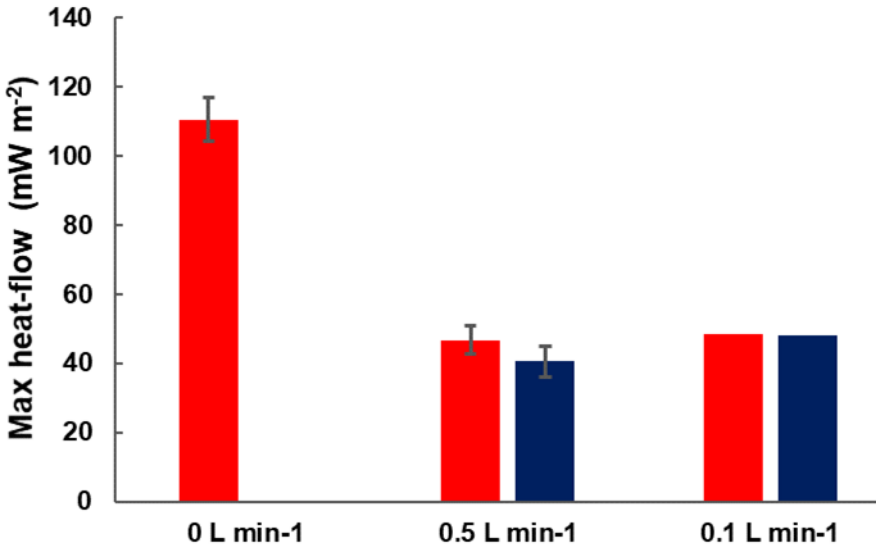

Figure 4.9: Maximum heat output for ampoules containing air only (0 L min^{-1}), and ampoules in which the air was displaced with CO_2 (■) and N_2 (■) gasses, sparged into the ampoules at rates of 0.5 and 0.1 L min^{-1}. Error bars represent the standard deviation from the duplicates of each material.

4.4 Conclusions

Previous studies have used IMC to measure mineral associated microbial populations through their metabolic activity as a function of mass using mineral slurries. In this study, a reactor set-up was designed and commissioned to allow the IMC technique to be used successfully to provide measurements of activities of mineral associated microbes as a function of mineral surface area. This is relevant because the agglomerated ores in heaps provide a surface for microorganisms to colonise.

The initial liquid culture experiments demonstrated the ability of IMC to detect and measure microbial cells of various concentrations suspended in liquid media and the oxidative abilities of the mixed mesophilic culture were also demonstrated. When both saturated and unsaturated ampoule system setups were compared, the unsaturated ore beds were shown to produce the highest maximum heat-flow and, when tested for repeatability, the system was shown to be reproducible. Based on the observed heat-flow similarities, it can be deduced that microbial communities colonising mineral surfaces, were similarly distributed across the mineral-coated beads when operated in batch systems, allowing as few as two beads to give representative data.

When the IMC was further optimised for application to measure colonisation of mineral surfaces in flow-through column reactor systems, which simulated a bioheap, microbial colonisation of pyrite surface was demonstrated to produce increasing maximum heat-flow progressively over 20 days. From the two different surface loading, 2 and 5 beads, the 2-bead loading portrayed consistent increase in maximum heat-flow production in the flow-through system. This demonstrated that the IMC could be used to measure microbial colonisation of

defined surface area, operated and colonised in a flow-through system providing defined surface area elements, in a quantitative manner. However, attention needs to be paid to the period of the experimental run in flow-through systems together with consistency in surface loading measured by IMC, in order to get consistent exponential microbial metabolic activities over the experimental run. When the maximum heat-flow was normalised to mW m^{-2} after the 24-hour experimental run, the calculated rates of reaction across the various surface loadings were similar. The oxidation rate of pyrite in the presence of active microbial cultures is considerably higher when compared to the chemical oxidation rates in the absence of microbial culture. Reagent limitation during the measurement of microbial activity was shown through O_2 displacement in ampoules loaded with colonised mineral surfaces. Both N_2 and CO_2 sparging into the vials to displace O_2 in the system were shown to be limiting to microbial activity and thus should be taken into consideration when measuring the activity of microbial populations.

These results demonstrated that IMC had the abilities to detect and measure the activity of mixed mesophilic cultures in (1) liquid cultures (2) associated with uniform mineral surface in batch shake flasks and (3) associated with uniform mineral surface in flow-through systems. It was also demonstrated that upon displacing O_2 from the vials, microbial activity was compromised. It should be recognised that the experiments were conducted for short periods, up to 30 days, and should be further tailored for studies conducted for longer periods. IMC is predominantly used in biomineral studies to measure heat output from fine mineral particles, often ran in batch shake flasks. Conducting heat output from ores with defined surface area in unsaturated ore beds, representative of a heap system, as was done in this study provides a new level of interpreting the data obtained especially for heap simulating studies.

Chapter 5: Analysis of mineral associated microorganisms by detachment and EPS

5.1 Introduction

Microbial populations in the flowing solution are typically used as an indirect indicator and representation of microbial abundance and diversity within the entire heap (Demergasso et al., 2005; Demergasso et al., 2010). However, microbial populations represented in the flowing solution in small ore beds have been shown not to accurately represent those in the ore bed as a whole (Zepeda et al., 2009; Govender et al., 2013; Tupikina et al., 2014). The flowing solution acts primarily as a method of delivery of microbial population onto the mineral surfaces. The populations are either retained and accumulate in the heap or are transported away from the ore surface, together with some of the newly formed cells, in the effluent. The retained populations are found in the largely stagnant (interstitial) zones or are associated with mineral surfaces (weakly or strongly attached), or in the bulk flowing solution (Chiume et al., 2012). To fundamentally distinguish between the interstitial, weakly-attached and strongly-attached microbial populations present within the ore bed, a detachment protocol was developed (Chiume et al., 2012; Govender et al., 2013; Cox and Bryan, 2017) and these studies are fully described in Section 2.4.1. The detachment protocol has been shown to consistently recover microbial cells that colonise various mineral surfaces in low-grade ores. This method is standardised for six washes as it was shown that after six washes, insignificant amounts of cells are recovered. However, the number of cells, and their residual activity, that remain on the ore surface post washes is yet to be fully quantified and reconciled with the detached populations.

Microbial populations associated with mineral surfaces in bioleach environments have been shown to secrete EPS (Africa et al., 2010; Zeng et al., 2010; Africa et al., 2013a). The secreted EPS matrix primarily assists mineral associated populations to associate with each other and to further strengthen their adherence onto the mineral surface (Gehrke et al., 1998). EPS and subsequent biofilm formation protect microorganisms from environmental stresses (Watnick and Kolter, 2000; Flemming and Wingender, 2010) and create permeable channels that allow un-inhibited exchange of nutrients and metabolites that are transported by solution, with the environment, thereby enhancing nutrient availability and removal of metabolites (Costerton et al., 1995). Lastly, biofilms provide a possibility of gene transfer within or between populations by conjugation (Dahlberg et al., 1997). EPS is mainly composed of polysaccharides, proteins, nucleic acids and lipids (Flemming and Wingender, 2010). Previous researchers have studied and confirmed the above-mentioned EPS biochemical components in various bioleaching microorganisms (Gehrke et al., 1998; Gehrke et al., 2001; Kinzler et al., 2003; Jiao et al., 2010;

Africa, 2017; Li et al., 2017). EPS biochemical components in leach systems have been studied over the years; however, most of the work has largely focused on single strains (Gehrke et al., 1998; Kinzler et al., 2003; Zhang, 2016; Africa, 2017). Furthermore, the determination of EPS biochemical composition from complete flow-through leach tests that resemble heap leaching or mine waste piles are yet to be studied.

In this study, glass beads coated with pyrite-bearing waste rock mineral to provide a uniformly defined surface area (Section 3.4) to allow for a quantitative assessment of microbial cells per unit surface area, were colonised in a flow-through system. A modified detachment method was developed to recover and assess microbial cells associated with pyrite-bearing mineral surface, both qualitatively and quantitatively. The assessments were made as a function of wash steps following different time periods of colonisation of a heap simulating flow-through run. SEM was used as a qualitative tool to visualise residual cells on the surface after detachment. IMC was used as a quantitative tool to measure activity of residual cells after wash steps. Finally, after the experimental runs, EPS secreted on the waste rock surface was extracted using crown ether and its biochemical composition analysed to gain more insight on the structural make-up of mixed mesophilic secreted biofilm in an unsaturated flow-through system. These tools are required to provide new insights into microbial communities colonizing mineral surfaces and the analysis of their contribution to intentional bioleaching or undesired waste rock leaching.

5.2 Research approach

The mixed mesophilic culture (Section 3.2) and PEL-HS pyrite bearing mine waste rock (Section 3.3.2) were used, the latter as an attachment substrate and source of energy. Preparation and coating of glass beads with mineral was performed (Section 3.4) and the flow-through column reactor system was set-up and operated as described in Sections 3.5.1 and 3.5.3. Solution chemistry analysis was conducted on the leachate collected from the flow-through column, including pH (Section 3.6.1) redox potential (Section 3.6.2) and Fe (Section 3.6.3) measurement. Microbial coverage analysis was determined via the detachment method (Section 3.7) and microbial distribution and growth on the mineral surface was visualised using SEM (Section 3.8). Microbial activity measurement was conducted using IMC (Section 3.9). The DNA (Section 3.10.2.2), lipid (Section 3.10.2.3), carbohydrate composition and sugar content analyses (Section 3.10.2.1) were conducted as previously described.

5.2.1 Detachment protocol wash steps

To assess and refine the standard detachment protocol, an increasing number of detachment washes, namely 3, 6 and 8 washes, were applied in this study to achieve varying levels of removal of microbial populations from mineral coated glass beads. During the establishment of the standard protocol at the Center for Bioprocess Engineering Research (CeBER), the low-grade ore colonised with microbial population was initially subjected to up to 10 washes (Harrison, personal communication 2017). However, after 6 washes, no significant further recovery of cells resulted from ore surfaces, and thus, 6 washes were selected as the standard method for removal of cells from mineral ore surfaces. The first contacting wash recovered interstitial cells, the 2nd and 3rd washes the weakly-attached cells and the final three washes including a detergent the strongly-attached microbial populations (Demergasso et al., 2010; Chiume et al., 2012; Govender et al., 2013). However, no rigorous evidence was presented that this indeed enabled all microbial activity to be recovered.

In this study, the mineral coated glass beads present a surface of finely divided ore or concentrate to represent an ore. The weakly and strongly attached populations were combined and termed “attached” to avoid excessive mineral washout from the surface in between wash steps. Due to the different nature of material and the packing, a range of detachment wash steps were assessed to determine a standard detachment method suitable for the mineral coated glass beads. Further rigorous data was collected using IMC and SEM to validate the degree of detachment achieved.

5.2.2 Summary of the extraction of EPS

EPS was cultured and extracted from a pyritic waste rock (PEL-HS) that was leached in complete flow-through system. Loosely bound EPS and capsular mineral bound EPS were extracted in a step-wise manner, as described in Section 3.10 and outlined in Figure 5.1.

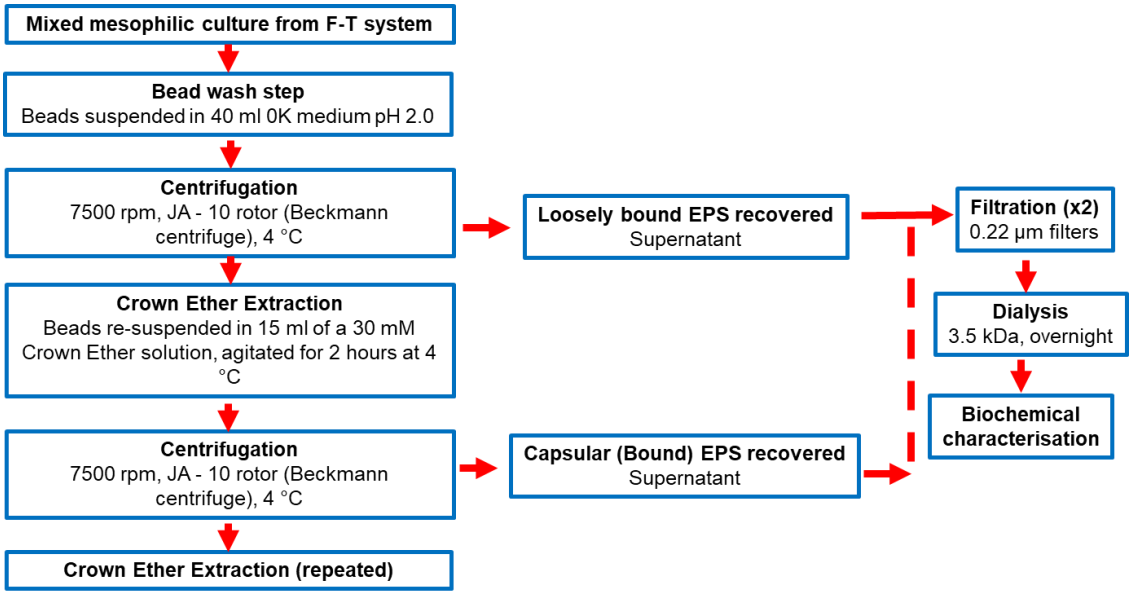

Figure 5.1: Schematic representation of the methodology used for culturing the mixed mesophilic culture on pyritic waste rock mineral operated as a complete flow-through column system, and subsequent extraction of that EPS (adapted from Aguilera et al., 2008; Africa, 2017).

5.2.3 Yield of surface associated EPS

After the extraction of EPS, duplicate 1 ml samples containing each fraction of the extracted EPS were freeze-dried to determine the dry weight. The total mass of the extracted EPS was then normalised to mg per 10^{10} cells. Standardising the extracted EPS as a mass per number of cells allowed comparisons to be drawn across the analysed compounds.

5.3 Results and Discussion

5.3.1 Leaching performance of the column system

The assessment of the flowing solution is a conventional approach to determine the performance of a heap bioleaching system. The pH, redox potential and iron composition analysis in the effluent provides an indication of microbial interaction with the mineral surface and activity. A progression of leaching within the system was observed regularly over the duration of the experimental run and is shown in Figure 5.2. The measured pH (Figure 5.2 A) increased to its highest on day 3 (pH 2.43), indicating the presence of dissolving and acid neutralising minerals in the sample. On day 7, the pH was 1.74 indicating the depletion of neutralising agents; subsequently it remained relatively constant over the duration of the experimental run, reaching a low (pH 1.44) on day 25. The redox potential (Figure 5.2 B) remained below 360 mV over the first 5 days of the experiment, indicating a dominance of Fe^{2+} over Fe^{3+}. This dominance is attributed to feed solution being supplemented with Fe^{2+} as well as low metabolic activity of the microbial population present, low cell numbers or both. Between day 5 and day 10 the redox potential increased to 678 mV and remained relatively constant thereafter. The increase in redox potential was attributed to a decrease in Fe^{2+}

concentration from 0.5 g L^{-1} that was supplemented to the feed solution, to a complete oxidation on day 10 (Figure 5.2 C) coupled with an increase in the Fe^{3+} concentration, suggesting active microbial regeneration of Fe^{3+} (Figure 5.2 D). During this period, microbial Fe^{2+} oxidation occurred at a faster rate than Fe^{3+} reduction, possibly as a result of increasing cell numbers and microbial activity in the mineral surface.

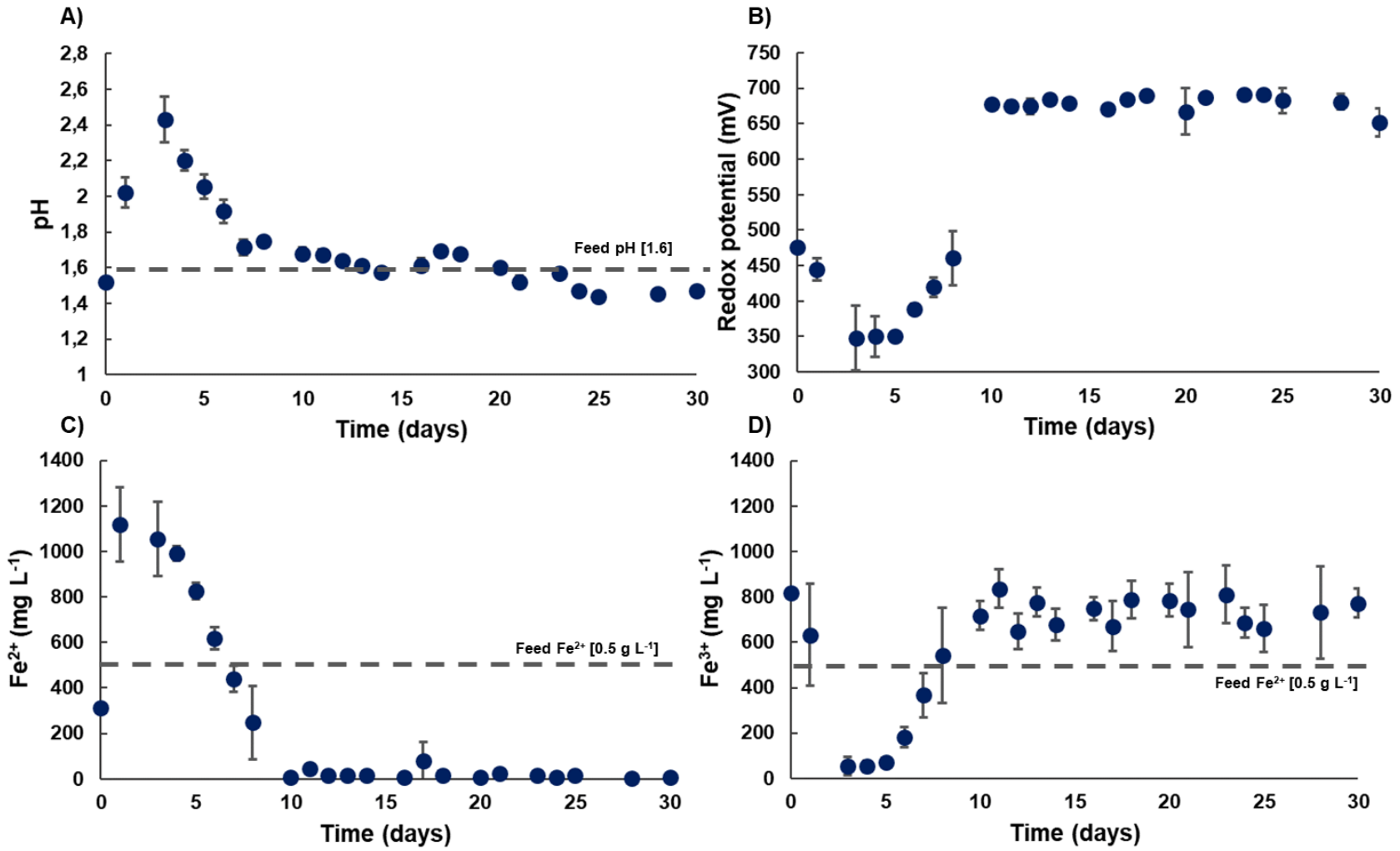

Figure 5.2: Analysis of pH (A), redox potential (B), Fe^{2+} concentration (C) and Fe^{3+} concentration (D) over 30 days at 30 °C. Error bars represent the standard deviation across samples (decreasing in number as columns were taken down).

5.3.2 Analysis of the detachment method for mineral surface colonisation

After 18 hours of inoculation, 3.49×10^9 cells (2.76×10^8 standard deviation across 5 columns) were expelled from the columns. Based on the enumerated cells in the expelled inoculum, an average of 6.51×10^9 cells was retained (attached and non-attached cells) in each column (neglecting microbial growth in the period). The columns were taken down on day 10, 20 and 30 respectively to provide samples subject to differing levels of colonisation. When each column was taken down, it was divided into three 30 g representative samples (mineral coated glass beads with attached cells). The mineral surfaces from the three representative samples were washed three, six and eight times respectively. From the 10 day column, 5.53×10^9 cells (total) were recovered from mineral surface washed three times (Figure 5.3 A), which was less than the retained number of total cells (6.51×10^9). From the mineral surface that was washed six times, 6.65×10^9 cells (2.1 % growth) were recovered (Figure 5.3 A) and 7.77×10^9 cells (16.2 %) were recovered from the mineral surface washed eight times (Figure 5.3 A).

On day 20, the cell growth from the recovered cells on the mineral surface across the various washes was 8.55×10^9 (23.9 % cell growth) for three washes, 1.12×10^{10} (41.9 %) for six washes and 1.27×10^{10} (48.7 %) for eight washes(Figure 5.3 B) when compared to the initial retained cells . When the initial retained cell numbers were compared with washes on day 30, 1.09×10^{10} (40.3 %) cell growth on the mineral surface was observed for three washes (Figure 5.3 C), 1.48×10^{10} (56 %) cell growth for six washes and 1.56×10^{10} (58.3 %) cell growth for eight washes.

Previous studies have reported that during the initial stages of a heap simulating system, rapid growth occurs in the attached phases when observed under the light microscope after detachment. However, with progression of the run, a slow microbial growth in attached phases is observed. The slow growth is attributed to several factors including, limitation of the surface area to colonise, natural detachment of the attached cells and formation of EPS that makes it difficult to dislodge cells or chunks (Govender et al., 2013) (also shown in Chapter 6) and because the ore bed was constructed with mineral-coated beads, the pockets of stagnant regions (also termed interstitial phase) that are common in agglomerated ore beds were not present. Chiume et al. (2012), Govender et al. (2013), and Cox and Bryan (2017) reported that the interstitial phase had a dominant abundance of microbial populations for the better part of the experimental runs. In this study, the loosely mineral-associated cells without firm attachment were at least one order lower than the attached cells and ranged between 2.3×10^8 and 9.4×10^8 total cells between day 10 and 30, across all washes (data not shown).

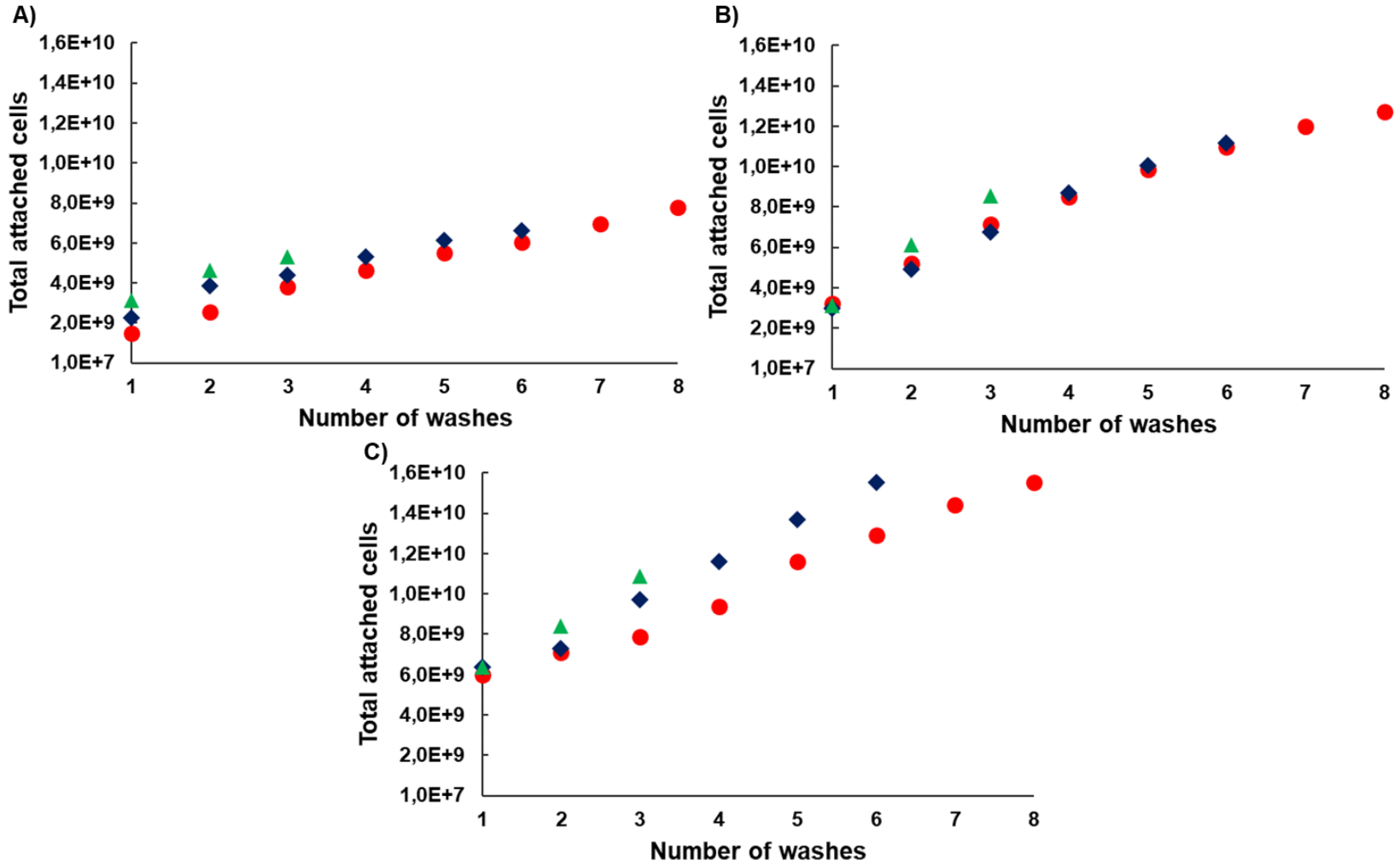

Figure 5.3: Assessment of the firmly attached cells on (A) day 10, (B) day 20 and (C) day 30. Three washes (▲), six washes (◆) and eight washes (●) are shown at each time graph.

5.3.3 SEM analysis of the mineral surface

Figure 5.4 shows SEM micrographs of the pyrite-bearing waste rock leached by a mixed mesophilic culture over 30 days. The colonised surfaces were subjected to vigorous washing steps and imaged to qualitatively assess the washing steps efficacy in detaching mineral associated microbes. Smooth surfaces, with what resembles few precipitates were observed on the surface of unleached control (Figure 5.4 A). The unwashed mineral surfaces were well colonised across the 30-day experimental run (Figure 5.4 B, F and J). The surfaces of washed samples generally appeared to be smooth compared to the non-washed colonised surfaces. At day 30, this suggested that there was substantial removal of microbial cells from the surface. These surfaces also appeared to have parts of microbial cells that were engrained in pits, R-P (Figure 5.4 K and M). This suggests that as the experimental run progressed, the mineral associated cells became entrenched to the surface. Nkulu et al. (2015) using SEM identified three stages of microbial-mineral interaction during carrollite bioleaching: (1) an initial attachment phase in the first 5 days, (2) an exponential growth phase between day 5 and 30 during which most mineral leaching occurs, and (3) a final phase normally after 30 days where microorganisms have settled on the surface and are imbedded in EPS. The formation of EPS as a function of period of experimental run explains the observation of parts of disrupted cells that are partially inside pits when surfaces were washed on day 30. Similar observations were made across the wash steps of day 10 and 20 (Figure 5.4 C, D, E, H, I and G) where substantial amounts of microbial cells were removed. On these surfaces, few residual cells were observed as well as pits. Most pit shapes were consistent with those of microbial cells, suggesting that there had been microbial cells present.

The SEM data provided understanding into the efficacy of the detachment method; however, this only provided a qualitative analysis. To obtain a quantitative analysis, the activity of residual cells was also measured with IMC (Section 5.3.4).

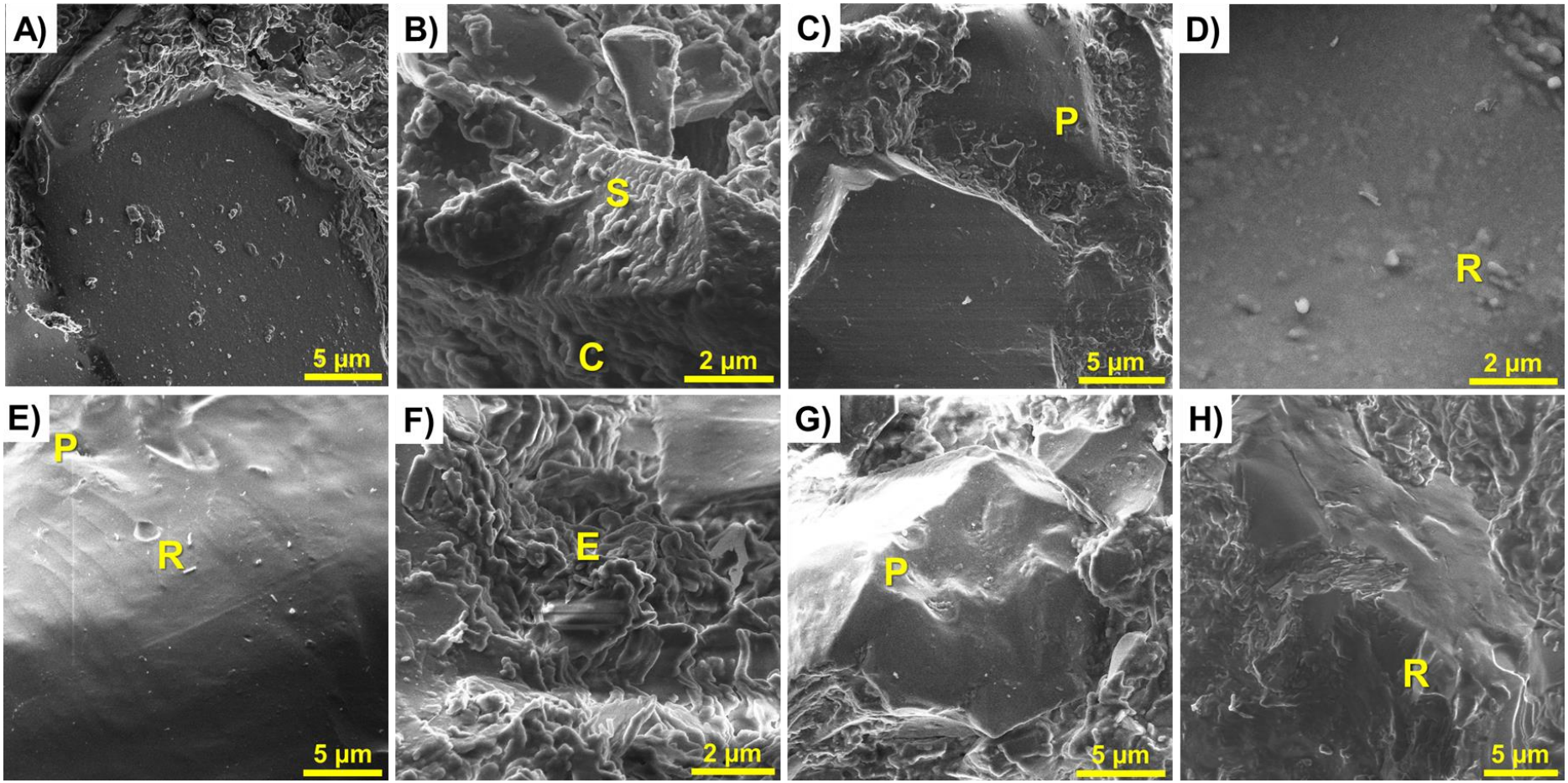
A)
5 µm
B)
S
C
2 µm
C)
P
5 µm
D)
R
2 µm
E)
P
R
5 µm
F)
E
2 µm
G)
P
5 µm
H)
R
5 µm

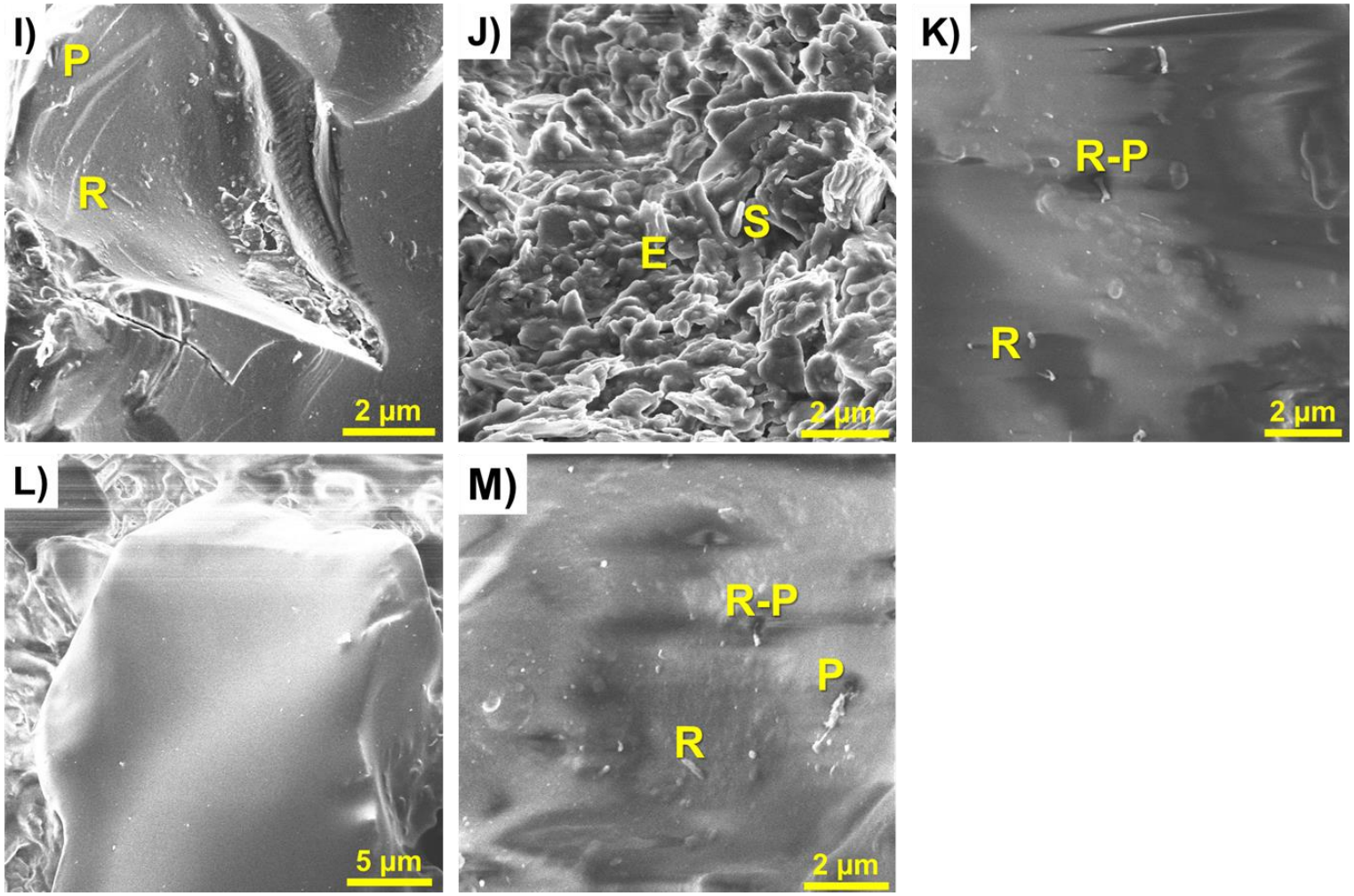

Figure 5.4: Scanning electron micrographs of PEL-HS mineral coated glass beads over 30 days before and after wash steps. Micrograph (A) shows an unleached surface abiotic control. Micrograph (B) shows a colonised surface after being in contact with microorganisms for 10 days and after, (C) three washes, (D) six washes and (E) eight washes. Micrograph (F) shows a colonised surface after being in contact with microorganisms for 20 days and after, (G) three washes, (H) six washes and (I) eight washes. Micrograph (J) shows a colonised surface after being in contact with microorganisms for 30 days and after (K) three washes, (L) six washes and (M) eight washes. Observed surface features including single cells (*S*), pits (*P*), residual cells (*R*), residual cells inside pits (*R -P*), colonies (*C*) and EPS embedded cells (*E*).

5.3.4 Measurement of the activity of mineral associated microbes

The microbial activity that was measured in this system is a combination of heat associated with microbial Fe^{2+} oxidation as well as the abiotic waste rock leaching that follows from the Fe^{3+} that is regenerated by the microbes (Rohwerder et al., 1998). Microbial activity was measured at day 10 (Figure 5.5 A) and day 30 (Figure 5.5 B), both before cell detachment and following detachment by 3, 6 and 8 washes.

The quantification of the residual, active, cells remaining on the surface after the washes was performed. On day 10, the maximum heat-flow obtained from the unwashed samples (42.5 µW) was used as reference. After three washes, 10.1 µW (23.8 %) residual heat was measured. After six washes, 5.8 µW (13.7 %) was measured and 4.0 µW (9.4 %) after eight washes. On day 30, the maximum heat-flow from the unwashed sample was 82.8 µW and 4.9 µW (6 %) heat produced by residual cells was measured after three washes and 2.1 µW (2.5 %) was measured after six washes and 1.0 µW (1.2 %) for eight washes. On day 10, 1 µW of heat was produced by 1.83×10^8 cells and 1.88×10^8 cells on day 30. The outcomes suggested that the number of microbial cells removed from mineral surfaces, at any point in time, was highly dependent on the number of washes applied. The difference in residual cells between six and eight washes were demonstrated via IMC metabolic activity studies to be insignificant. The integration of metabolic activity measurement, the detachment of microbial cells from mineral surfaces together with the visualisation of the surfaces was shown to allow for a more insightful analysis of the microbial-mineral interaction.

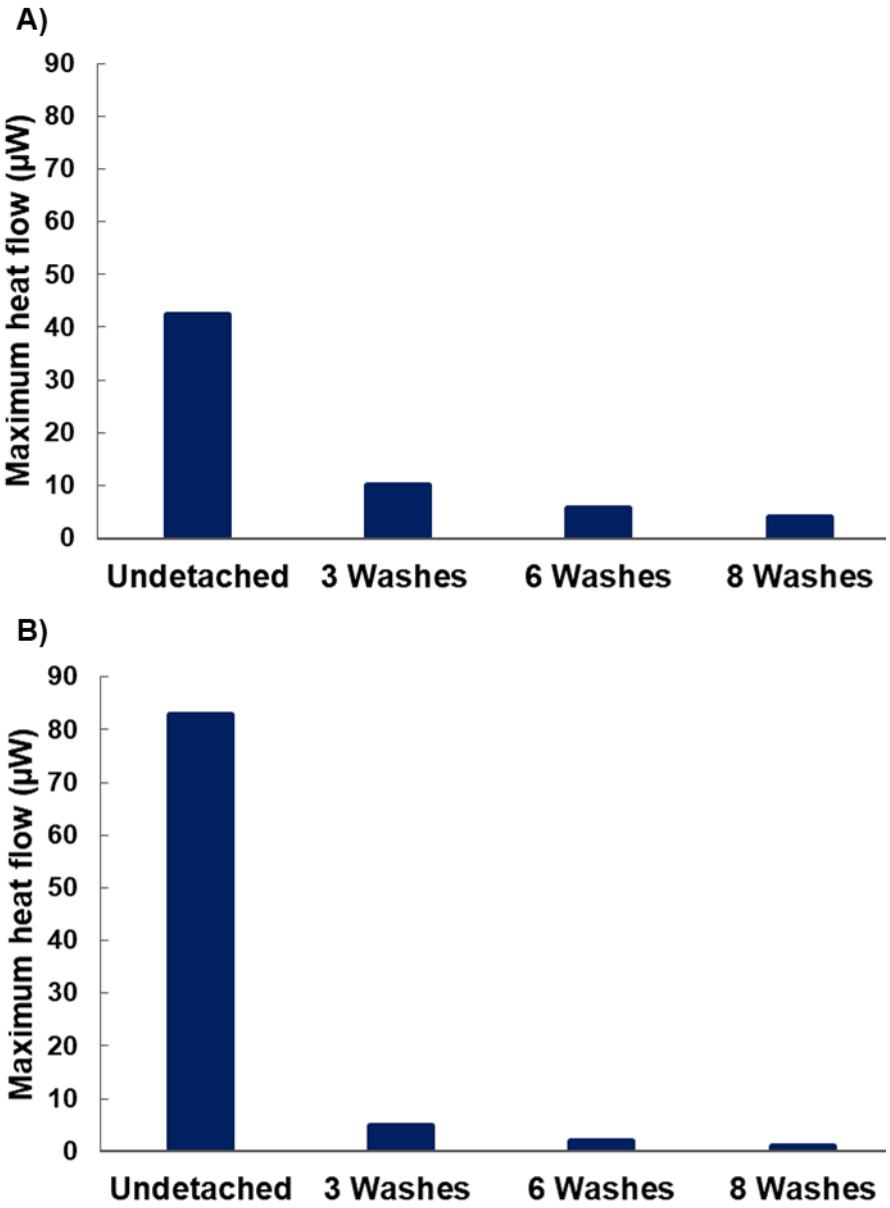

Figure 5.5: Maximum heat-flow measured from two beads colonised with mixed mesophilic culture, and two beads measured after three, six and eight washes at (A) day 10 and (B) day 30.

As shown in Figure 5.5 A and B, after washing and detaching microbial cells from the mineral surfaces, not all cells were removed. The cells remaining on the surface were expressed in maximum heat-flow and thus the actual number of cells could be determined via the following calculations:

$$\frac{\boldsymbol{No\ of\ detached\ cells\ per\ wash}}{(\boldsymbol{Max\ heat\ flow\ undetached\ cells - Max\ heat\ flow\ residual\ cells})} * \boldsymbol{Max\ heat\ flow\ residual\ cells} \qquad \text{Equation 5.1}$$

The calculations allowed for the accounting of residual cells on the surface. The more washes were performed on the mineral surfaces, the less heat-flow output was observed. Day 10 had high residual cells across the wash steps when compared to day 30. On day 10, 1.66×10^9, 1.05×10^9, and 8.07×10^8 residual cells were calculated across three, six and eight washes

respectively, whereas 6.84×10^8, 3.85×10^8 and 1.9×10^8 residual cells after the same amount of washes, were calculated in day 30 (Figure 5.6 A). Despite there having been an increase in heat-flow output and microbial cell increase on the mineral surface between day 10 and 30, the number of residual cells after each wash step on day 30 was significantly lower when compared to day 10. The metabolic activity data and the detachment data were reconciled and the total number of cells on the mineral surface (Figure 5.6 B) was determined by adding up the number of detached cells with the calculated residual cells on the surface. The calculated total number of cells, at a specific timepoint, are expected to be similar across the washes (Figure 5.6 B) and based on the variances, cell numbers were similar. On day 10, 6.98×10^9 total cells were calculated for three washes, 7.70×10^9 for six washes and 8.58×10^9 was calculated for eight washes. On day 30, 1.16×10^{10} cells were calculated for three washes, 1.52×10^{10} for six washes and 1.58×10^{10} was calculated for eight washes. On day 10, the variance between three and six washes was 5.8 %, and between six and eight washes was 7.2 %. The variance on day 30 between three and six washes was 16.9 % and between six and eight washes was 2.5 %. Using the maximum heat-flow output obtained from the undetached surfaces, an increase of 51 % (from 42.5 - 83 µW) was observed between day 10 and day 30.

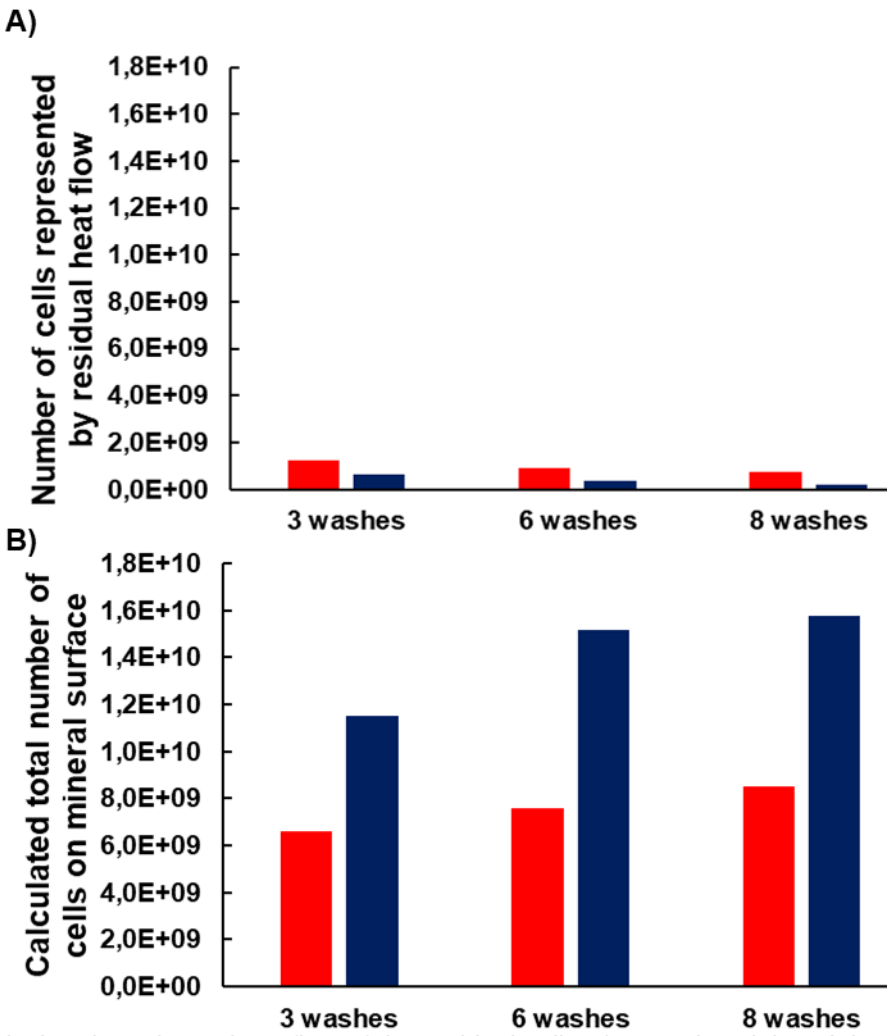

Figure 5.6: Calculated maximum heat-flow of the residual cells after washes (A) and the total number of cells (detached and residual) on the mineral surfaces across the washes (B) on day day 10 (■) and day 30 (■).

In Figure 5.7, the maximum heat-flow production per cell was calculated based on the total cells (Figure 5.6 B). On day 10, 6.1 × 10^{-3} nW $cell^{-1}$ for three washes, 5.5 × 10^{-3} nW $cell^{-1}$ for six washes and 5 × 10^{-3} nW $cell^{-1}$ was measured for eight washes. On day 30, 7.2 × 10^{-3} nW $cell^{-1}$, 5.5 × 10^{-3} nW $cell^{-1}$ and 5.3 × 10^{-3} nW $cell^{-1}$ were measured respectively for three, six and eight washes. The similar values, especially between six and eight washes, suggest that the maximum heat-flow produced by one cell was comparative and similar on both day 10 and on day 30.

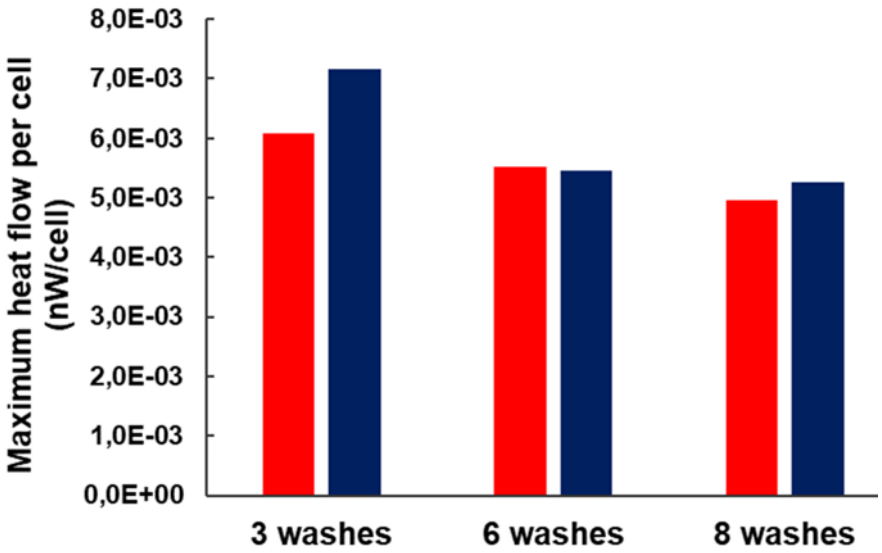

Figure 5.7: Shows the average maximum heat-flow output per cell using the calculated total detached cells as well as maximum heat-flow output from the cells at each wash on both day 10 (■)and 30 (■).

5.3.5 Yields and biochemical composition of mixed mesophilic culture EPS

5.3.5.1 Yields of loosely bound and capsular EPS

Table 5.1 shows the EPS yields recovered from the mixed mesophilic cultures grown for 32 days on the PEL-HS waste rock. The collected fractions were split into loosely bound portion that was recovered using 0K media and a capsular portion that was extracted using crown ether as described in Section 3.9.1. Amounts of EPS recovered from these fractions were 1.7 ± 0.14 mg per 10^{10} cells from the loosely bound fraction and 1.53 ± 0.54 mg from the capsular fraction.

The flow-through column leach tests, from which the EPS was extracted, was loaded with 300 glass beads that were coated with approximately 10.8 g of mineral waste rock, equating to 0.036 g per bead. In a study by Africa (2017), EPS were cultivated and extracted from 2 % wt vol^{-1} (100 g) chalcopyrite concentrate in batch 5 L Schott bottles in very short experimental runs (until cell growth entered stationary phase). These were inoculated with 10^8 cells ml^{-1}. The total amount of EPS extracted using crown ether was 2.3 ± 0.2 mg per 10^{10} cells for the loosely bound fraction and 12.1 ± 1.8 mg per 10^{10} cells for the capsular fraction, in that study. Despite the substrate being approximately 9 times greater, the loosely bound recoveries were similar in both studies and the EPS recovery in the capsular fraction were 5 times more than that recovered in this study. This (mg per 10^{10} cells) used to standardise recovered EPS mass in Africa (2017) and Gehrke et al. (1998) was adopted and applied in this study. Gehrke et al. (1998) harvested and extracted EPS and reported yields of 0.215 ± 0.03 mg per 10^{10} cells from Fe^{2+} sulfate, 2.76 ± 0.3 mg per 10^{10} cells from pyrite and 1.155 ± 0.094 mg EPS per 10^{10} cells from sulfur for colloidal EPS extracted from *At. ferrooxidans*. The magnitude of EPS recovered from pyrite in the Gehrke et al. (1998) study is similar to that recovered in this study.

Aguilera et al. (2008) demonstrated that an extraction method plays a role in the extraction capability of EPS and influences yields and composition. In that study, the crown ether extraction method was shown to have a greater recovery when compared to other extraction methods. Crown ether was also shown to result in insignificant levels of cell disruptions by (Africa, 2017) when compared to EDTA extraction method.

Table 5.1: Total EPS yields recovered from mixed mesophilic culture grown on PEL-HS. The deviation represents duplicate samples

Fraction	Dry EPS weight (mg per 10^{10} cells)	% of total dry weight EPS
Loosely bound	1.70 ± 0.141	53
Capsular	1.53 ± 0.54	47
Total	3.23	100

5.3.5.2 Biochemical composition of loosely bound and capsular EPS

Microbial EPS in acidic environments typically consist of a mixture of macromolecules, including proteins, polysaccharides, lipids, nucleic acids as well as uronic acids, humic substances and heavy metals (Michel et al., 2009; Yu et al., 2018). Each analysed biochemical fraction in this study contained varying proportions of the measured compounds (Table 5.2). Amounts of DNA measured in the loosely bound fraction (3.88 ± 0.68 mg) was 9 times higher than that measured in capsular fraction (0.41 ± 0.14 mg). The method of collecting loosely bound fraction described in Section 3.9 makes eDNA naturally vulnerable to contaminants including iron precipitates. We postulate that contaminants interfered with the nanodrop reading and provided a false positive and high DNA amount. This is supported by a small peak observed on the nanodrop that was out of range (data not shown). However, when the capsular DNA was measured with nanodrop, it peaked at 260nm. Both the loosely bound and capsular DNA did not appear when run on an electrophoresis gel (suspected degradation for capsular DNA). Furthermore, the high DNA amounts resulted in the EPS mass balance not closing. DNA contributed 27 % (0.41 mg) of the capsular mass in this study. Aguilera et al. (2008) demonstrated the presence of DNA in low amounts compared to other components. For the three eukaryotic biofilm samples recovered from the bottom surface of a river, the NaCl extraction method produced five times more DNA when compared to other extraction methods applied in the same study. Africa (2017) recovered relatively low concentrations of nucleic matter (2 %) from colonised chalcopyrite using crown ether and 0 % using EDTA. Very little is known about the role of eDNA in the successful production of biofilm and its constituent cells in biofilms associated with mineral leaching. Lorenz and Wackernagel (1994) proposed that extracellular nucleic material within EPS may contribute some means of protection for biofilm-associated cells against DNases. Lebaron et al. (1997) suggested that the EPS interface within a biofilm concentrates cells and allows for a greater probability of cell-to-cell contact and DNA or plasmid exchange, leading to enhanced horizontal gene transfer. Yu et

al. (2018) demonstrated that eDNA formation plays an important role in the adsorption process on the mineral surface and is critical for the substantive formation of other EPS components such as polysaccharides and proteins. Furthermore, eDNA has also implicated in the formation and stabilisation of the biofilm matrix (Montanaro et al., 2011).

Excessive amounts of iron (4.98 ± 1.54 mg) were detected in the loosely bound fraction and could be a consequence of the flow-through experimental operating conditions. The system is continuously fed with 500 mg L^{-1} of Fe^{2+} and upon draining the columns, the residual iron (mostly oxidised to Fe^{3+}), which was washed along with the recovered loosely bound fraction, was still present and thus the remnants of it were reflected in the loosely bound EPS fraction. Amount of iron detected in the capsular EPS was 0.25 ± 0.06 mg and contributed 16.4 %. The presence of iron has previously been demonstrated in capsular bound EPS (Africa, 2017). EDTA extracted mineral bound EPS in Africa (2017) contained a significant amount of iron, which contributed 31 % of the total mass recovered, whereas the crown ether extracted EPS contained 10 % of the total recovered mass. Zeng et al. (2010) reported very low distributive amounts of iron (0.45 %) in their study. Kinzler et al. (2003) demonstrated elevated concentrations of Fe^{3+} within the EPS of various *At. ferrooxidans* strains. The increase was attributed to Fe^{3+} being complexed within the EPS reaction space. The study also reported that strains with high iron content in the EPS possessed higher oxidation activity than those, which contained less or no iron. Holmes et al. (1999) and Fowler et al. (2001) showed that Fe^{3+} complexed within the reaction space were the oxidants that enhanced the rate of leaching.

Both fractions contained very low amounts of lipids with the loosely bound fraction containing 0.09 ± 0.012 mg, while 0.063 ± 0.026 mg (4.2 %) was contained in the capsular fraction. The presence of lipids in the EPS has been postulated in previous studies to contribute to the interaction between colonising microorganisms and the surface, as well as acting as biosurfactants (Sand and Gehrke, 1999; Flemming and Wingender, 2010). Sand and Gehrke (1999) isolated EPS from *At. ferrooxidans* that was grown on various sources. Substantial amounts of lipids were measured, ranging from 36,9 % (iron sulfate substrate), 39.4 % (pyrite substrate) and 53.8 % for (sulfur substrate) (Kinzler et al., 2003; Harneit et al., 2006). Zeng et al. (2010) measured 41.6 % of lipids from EPS of a mixed culture of moderately thermophilic microorganisms grown on chalcopyrite.

Higher amounts of total carbohydrates were evident in the capsular fraction (0.43 ± 0.09 mg; 28.5 %) than in the loosely bound fraction (0.25 ± 0.09 mg). Previous studies have shown carbohydrates to be a major component of EPS alongside proteins (Sutherland, 2001; Aguilera et al., 2008; Vu et al., 2009; Xu et al., 2009; Sheng et al., 2010; Ozturk et al., 2014).

In our study, carbohydrates (28.5 %) were the most prevalent compounds compared to the other measured components in this study. Li and Sand (2017) reported 24 % presence of carbohydrates in planktonic cells and 18 % in biofilms of *Sulfobacillus thermosulfidooxidans* that was grown on pyrite grains. The shift in prevalence of carbohydrates in the two states was attributed to the change of microbial lifestyle triggered by microbial adhesion to mineral surfaces. Zeng et al. (2010) measured 58.6 % of carbohydrates in their study. Govender and Gericke (2011) measured high amounts of carbohydrates from EPS extracted from various microorganisms that were grown on various minerals across varying temperatures. The amounts of carbohydrates measured from EPS of *At. caldus*, *Leptosprillium spp*, and *Sulfobacillus spp* grown on pyrite (35 °C) and sphalerite (37 °C) were 81 % and 85 % respectively. For EPS of *At. caldus*, *Leptosprillium spp*, *Sulfobacillus spp*, and *Ferroplasma spp* grown on chalcopyrite and sphalerite at 45 °C, carbohydrates accounted for 69 % and 87 % of the mass respectively. EPS extracted from *Acidianus spp*, *Metallosphaera spp*, and *Sulfolobus spp* grown on chalcopyrite at 70 °C contained 62 % carbohydrates. The capsular carbohydrates (29 %) measured in our study were further processed and sugar monomers were measured (Section 5.3.5.3).

Table 5.2: Biochemical compositional analysis of EPS extracted from mixed mesophilic culture grown on PEL-HS. Results presented and analysed per recovered EPS fraction. The deviation represents duplicate samples

Fraction	Total carbohydrates (mg)	DNA (mg)	Lipids (mg)	Iron (mg)
Loosely bound	0.25 ± 0.09	3.88 ± 0.68	0.09 ± 0.012	4.98 ± 1.54
Capsular	0.43 ± 0.09	0.41 ± 0.14	0.063 ± 0.026	0.25 ± 0.06

Table 5.3 shows the recovery of measurable components from the capsular EPS extracted with crown ether. Formation of capsular EPS is critical during sulfidic mineral degradation processes as it offers the oxidation facilitating microorganisms with more protection in harsh microenvironments and allow for bioleach oxidative reactions to take place in close proximity to the cell as described by the indirect contact mechanism (Schippers and Sand, 1999; Crundwell, 2003). Approximately 76 % of measurable EPS was recovered, leaving 24 % unaccounted EPS mass (Table 5.3). EPS has been reported to constitute between 50 – 90 % of the total biofilm mass (Christensen and Characklis, 1990; Wingender et al., 1999). Zeng et al. (2010) recovered 66 mg g^{-1} of measurable EPS in a mixed moderately thermophilic culture containing *At. caldus*, *L. ferriphilum* cultured in a CSTR with a 6 – 8 % chalcopyrite mineral loading at 48 °C after 24 days. In a study by Govender and Gericke (2011) EPS was grown on various mineral substrates and 75 % of measured EPS was recovered from pyrite grown mesophilic consortia at 35 °C. Africa (2017) recovered 89 % (using crown ether) and 57 % (using EDTA) of the measurable EPS mass of *M. hakonensis* grown on chalcopyrite at 65 °C. The unaccounted mass is typically attributed to the non-measured compounds as well as

heavy metals. Govender and Gericke (2011) attributed the unaccounted mass to lipids, DNA and metal ions, which were not measured.

Table 5.3: Mass balancing of mineral bound EPS, recovered from mixed mesophilic culture grown on PEL-HS. The deviation represents duplicate samples

Mineral bound EPS	Mass (mg)	% total mineral bound EPS
Total recovered mass	1.53 ± 0.54	100
Mass of measurable components	1.16	75.8
Unaccounted mass	0.37	24.2

5.3.5.3 Sugar monomers present in capsular EPS carbohydrates

Both carbohydrate samples of loosely bound and capsular EPS were analysed for sugar monomers. In loosely bound EPS, some sugar monomers were not detected (galactose, frucose, lactose, maltose, trehalose, sucrose and myo-inositol) whilst others were present, but were below the detection limit (mannose, mannitol, sorbitol and glucose). Of the sugar monomers measured using the GC-MS, three sugars were detected in the capsular bound fraction (Figure 5.9): D-galactose (37.3 %), D-fructose (36.5 %) and trehalose (26.2 %).

Table 5.4 shows the various sugar monomers that are reported in bioleach environments. In a study by Sand and Gehrke (1999), rhamnose (10.8 %), fucose (17.1 %), xylose (0.8 %), mannose (0.7 %), glucose (15.2 %) and glucuronic acid (3.3 %) sugars were detected from EPS extracted from *At. ferrooxidans* grown on pyrite. Africa (2017) reported that *M. hakonensis* EPS extracted from the chalcopyrite system contained rhamnose (0.5 %), fucose (0.7 %), mannose (11.5 %), galactose (7 %) and glucose (80.3 %). Jiao et al. (2010) report the presence of glucose (20.1 and 17.2 %), galactose (12.1 and 5.6 %), rhamnose (13.0 and 17.7 %), mannose (11.8 and 21.9 %), hexose (25.5 and 12.0 %), heptose (28.4 and 19.5 %) and arabinose (1.0-4.2%) for EPS extracted from two pellicle biofilms predominantly comprised of *Leptospirillum* group II (43 %) and III (28 %) as well as archaea (29 %). Zhang et al. (2017) reported that a 78.4 % carbohydrate content was measured from capsular EPS of *Ferroplasma acidiphilum* grown on pyrite. Monosaccharides like glucose, fucose, arabinose, galactose, mannose, and sialic acid were detected when carbohydrates were further processed. In a study by Zeng et al. (2010), rhamnose (18.1 %), fucose (31.1 %), xylose (5.7 %), mannose (5.2 %), glucose and (31.6 %) were reported on mixed moderate thermophiles that were dominated by *At. caldus* and *L. ferriphilum* and grown on chalcopyrite concentrate.

The sugar monomers from EPS of bioleach microorganisms reported in the literature varied and these variations were informed by the microbial spiecie(s) type, growth substrates, extraction method as well as the type of instrument used to measure them (Africa, 2017; Zeng

et al., 2010; Sand and Gehrke, 1999). The sugar monomers that were detected in this study only carried two common sugars with other studies (galactose and fructose) and one other uncommon sugar (trehalose). It did not contain the other common sugars across differing EPS extractions: rhamnose, fucose, mannose and glucose. In other words, the EPS in this study varied from the common sugars that were previously reported in EPS from bioleach environments, with galactose and fructose being the common sugar monomers. The other sugar, trehalose detected in this study are yet to be reported in EPS isolated from bioleach environments. The sugar monomers measured for in this study were the same suite measured by Africa (2017), which included galactose, frucose, lactose, maltose, trehalose, sucrose, myo-inositol, mannose, mannitol, sorbitol and glucose. However, only galactose was the common sugar detected in both studies. All other sugars were found to be below the detection limit.

Table 5.4: Summary of sugar monomers reported in bioleach environments

	This study	Africa (2017)	Zhang et al. (2017)	Sand and Gehrke (1999)	Jiao et al. (2010)	Zeng et al. (2010)
Sugar monomers	Mixed mesophiles	*M. hakhonensis*	*F. acidiphilum*	*At. ferroxidans*	Mixed mesophiles	Mixed moderate thermophiles
Galactose	37.3	7	√		12.1 and 5.6	
Fructose	36.5					
Trehalose	26.2					
Rhamnose		0.5		10.8	13.0 and 17.7	18.1
Mannose		11.5	√	0.7	11.8 and 21.9	5.2
Fucose		0.7	√	17.1		31.1
Xylose				0.8		5.7
Glucose		80.3	√	15.2	20.1 and 17.2	31.6
Heptose					28.4 and 19.5	
Glucuronic acids				3.3		
Arabinose			√		1.0-4.2	
Hexose					25.5 and 12.0	
Sialic acid			√			

√**:** Detected monomers but values not provided in the study

Trehalose is described by Elbein et al. (2003) as a non-reducing disaccharide that links two glucose units in an α,α-1,1-glycosidic linkage. This sugar is found in microorganisms, fungi, plants, and invertebrates. Trehalose acts both as a main reserve of carbohydrates and as a cellular protector against a variety of nutritional and environmental stress challenges including oxidative stress, heat shock, osmotic and/or saline stress, and xenobiotics, thus increasing

cell resistance to such challenges (Elbein et al., 2003; Yoshida and Sakamoto, 2009; Sakamoto et al., 2011). Zhu et al. (2013) reported an upregulation of trehalose at 24 hours, in the biofilm of fungal pathogen *Candida albicans*. It was shown in the same study that the lack of trehalose resulted in defective hyphae formation, thus compromising the development of biofilm and drug resistance efficiency of *Candida albicans*. The monosaccharide molecule, D-fructose (36.5 %) detected in this study, is a less common polysaccharide constituent and thus has not been reported on extensively (D'Ayala et al., 2008). In a study by Dogan et al. (2015) where sugar monomers extracted from the EPS of a thermal *Bacillus licheniformis* strain were measured, 27.1 µg ml^{-1} of fructose was reported. The authors showed that the two techniques namely HPLC and LC-MS that were used to measure the same sample, produced varying results, with glucose being the common sugar monomer. In a more recent and relevant study, Markosyan et al. (2019) used HPLC to measure EPS that was extracted from a *L. ferriphilum* strain. The authors reported a presence of fructose in the EPS, together with glucose and mannose. EPS components like lipids have been reported to mediate the initial attachment of cells whilst sugars like glucose, mannose and fucose are important for colonization and construction of a mature biofilm architecture of acidophiles (Zhang et al., 2019b).

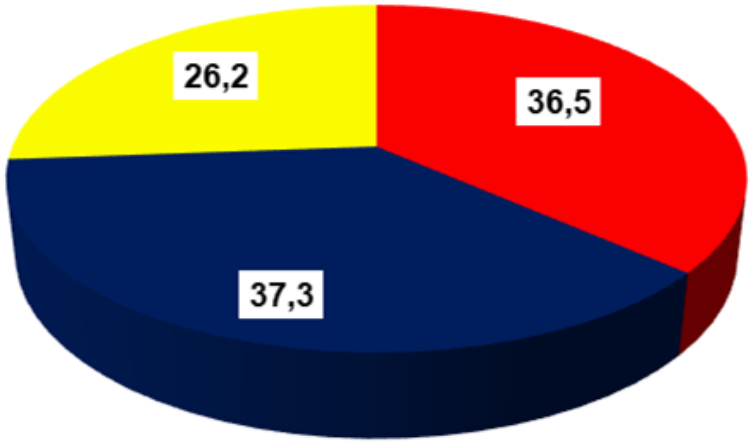

Figure 5.9: Distribution of sugar monomers present in the capsular EPS extracted from mixed mesophilic culture grown on PEL-HS waste rock substrate. Three sugar monomers were detected including: D-Galactose ■, D-Fructose ■ and Trehalose ■.

5.4 Conclusions

The detachment method was successfully carried out in this study on mineral coated glass beads as representative of ore while providing a uniform surface area. Although six washes were normalised in previous studies for the detachment of ore mineral-associated cells, the confidence in those studies was mainly based on the low number of cells enumerated under a light microscope between six and eight washes. The novel approach applied in this study whereby detachment wash steps, the visualisation of mineral associated microorganisms as a function of wash steps, and the quantitative determination of mineral interacting

microorganisms as a function of wash steps was shown to be complementary to each other. The microbial cells that remained interacting with mineral surface after the detachment washes were successfully accounted for using IMC and reconciled with the detached cells to provide a full description of the attached population. This provided a new level of confidence on the detachment method and that six washes provided a reliable estimation of the mineral associated cells. The employment of the detachment method has the potential to allow for a further direct microscopic enumeration of microbial populations associated with the mineral surfaces over a period of time during heap simulating bioleaching processes and potentially during the characterisation of waste materials for ARD potential.

Secondly, the cultivation, extraction and analysis the biochemical components of EPS in a complete flow-through column system was successfully demonstrated. The components were highly dependent on the fraction type, with the capsular fraction presenting with more detectable and reliable components when compared to the loosely bound fraction. Carbohydrates (neutral sugars) were the dominant component and this was consistent with EPS isolated from mesophilic leaching microbes in batch studies. The components of the extracted capsular EPS included carbohydrates, DNA, iron and lipids and the sugar monomers identified by GC-MS, including galactose, fructose and trehalose. The sugars monomers reported in this study have been reported previously in various EPS studies in bioleach environments albeit different microorganisms and mineral substrates were used, however, trehalose was not consistent with sugars isolated from EPS of other bioleach microorganisms reported in the literature and requires further interrogation in futures studies. These findings allow us to study and understand the formation and development of EPS and its biochemical components in a complete flow-through system and this knowledge is key for both mineral degradation for commercial purposes (value recovery) and for environmental purposes (ARD prevention).

Chapter 6: Using isothermal microcalorimetry and resultant metabolic activity to assess microbial colonisation in bioleaching of a pyrite concentrate

6.1 Introduction

Oxidative mineral bioleaching exploits the metabolic activity of a consortium of iron and sulfur oxidising microorganisms to extract valuable metals from mineral ore to enable their recovery. The role of microorganisms in the mineral dissolution process is generally described by the indirect contact mechanism (Sand et al., 2001). Effective attachment and growth of acidophilic microorganisms on the mineral surface is a key factor in enhanced mineral dissolution (Sand and Gehrke, 2006).

A number of studies have investigated microbial attachment on to mineral surfaces and their subsequent colonisation. EPS formation as well as factors influencing attachment, colonisation and EPS formed on the mineral surface has been reported. Africa et al. (2013b) and Bromfield et al. (2011) quantified attachment to mineral surfaces in both submerged batch systems and in a flow-through system as a function of microbial species and mineral surface. Bromfield et al. (2011) showed that there was a link between the extent of attachment in sulfide minerals for *M. hakonensis* after growth on sulfur, ferrous sulfate, chalcopyrite mineral concentrate and pyrite mineral concentrate, and the highest extents of attachment were observed for attachment to chalcopyrite after growth on sulfur. Africa et al. (2013b) reported greater attachment levels to sulfide minerals over low-grade ores in the continuous flow-through column reactor for mesophilic microorganisms, with the extents of attachment being less than that observed in the shake flask systems reported in literature. Chiume et al. (2012) investigated the role of irrigation rates on colonisation of crushed and agglomerated sulfidic ores and observed that lower irrigation rates lead to enhanced surface colonisation. Govender et al. (2013) and Tupikina et al. (2014) investigated colonisation and cell growth on crushed, low-grade sulfidic ores. Govender et al. worked on a pure culture (*At. ferrooxidans*) with a focus on colonisation and growth rates while Tupikina et al. (2014) focused on community dynamics in the whole ore system in response to culture conditions, leading to calculation of growth rates of individual species. Echeverría-Vega and Demergasso (2015) used microscopy to demonstrate cell growth of attached bacteria using without detachment. Govender et al. (2015) extended this study to account for the impact of physiological conditions on colonisation. All these studies relied on detachment of microbial cells from the mineral ore surfaces, and their subsequent counting, to quantify them. Using the detachment method, the extent of detachment corresponding to maximum attachment could not be determined quantitatively. Further, while a measure of population size was

obtained, the activity of this population across the zones of free-flowing liquid, interstitial zone and mineral attached cells could not be determined quantitatively. Isothermal microcalorimetry (IMC) provides a direct, complementary method applicable for use in measurement of metabolic activity of microorganisms colonising mineral surfaces *in situ* i.e. without requiring their detachment.

In this study, IMC was used to measure quantitatively the metabolic activity of a mixed mesophilic culture colonising the surface of pyrite mineral concentrate-coated beads at a feed flow rate of 60 ml h^{-1}. IMC was used in conjunction with traditional methods to study the progression of microbial-mineral interaction. Both mineral leaching performance and the quantification of microbial community by cell detachment and counting were used in combination with IMC. This integration of IMC with traditional analytical methods allows for a relationship to be established between (1) metabolic activity on the ore surface and number of colonising cells; (2) metabolic activity and the mineral surface coverage by colonising cells i.e. on the basis of mineral surface area; and (3) metabolic activity and leaching performance in the flow-through mini column leaching in which a defined mineral surface area can be provided by the use of mineral-coated beads. This performance, metabolic activity and colonisation can be represented on the basis of surface area.

6.2 Experimental approach

The mixed mesophilic culture (Section 3.2) was used in this study. A pyrite concentrate (Section 3.3.1) was used as an attachment substrate and source of energy, coated onto glass beads (Section 3.4). The flow-through column reactor system was set-up and operated at a flow rate of 60 ml h^{-1} as described in Section 3.5.1 and 3.5.3. Solution chemistry analysis was conducted, including measurement of pH, redox potential and ferrous and total iron (Section 3.6). Microbial coverage analysis via the detachment method and total cell counts using light microscopy was conducted (Section 3.7), microbial distribution and growth on the mineral surface was analysed using SEM visualization (Section 3.8) and the activity of mineral surface associated microorganisms was conducted using IMC (Section 3.9).

6.2.1 Determination of pyrite oxidation rates

For the determination of pyrite oxidation rates, two colonised beads (2.26×10^{-4} m^{-2}) from every column sacrifice were transferred to IMC ampoules and the combined microbial and chemical maximum heat output was measured. The oxidation rates of pyrite were determined using heat output values obtained from IMC as described in Section 4.2.3.

6.3 Result and discussion

6.3.1 Leaching performance in column reactor system

Each column was inoculated with 2×10^9 cells per kilogram of ore, which was equivalent to approximately 7.8×10^6 cells per column of 300 beads. The inoculation process was carried out by saturating the columns with 100 ml of the inoculum and circulating the fluid at a 60 ml h^{-1} flow rate with up-flow recycle, to allow maximum microbe-mineral contacting. After 18 hours of microbe-mineral contacting, the average number of cells recorded in the effluent across the columns was approximately $4.81 \times 10^6 \pm 9.8$ % cells while 3.27×10^6 cells were associated with or attached to the mineral surface (as determined by sacrifice of the first column). Therefore, approximately 40 % of cells were associated with or firmly attached to the mineral surface at 18 h and an increase in total cell number of 3.5 % had resulted from cell growth over the 18-hour contacting period.

The performance of a heap bioleaching system is typically assessed through the analysis of the effluent. The pH, redox potential and Fe^{2+}/Fe^{3+} composition analysis provides an indication of microbial interaction with the mineral surface and activity. The changes in the effluent cell concentration for the flow-through column are shown in Figure 6.1, the effluent pH redox potential and iron speciation are shown in Figure 6.2, Figure 6.3 and Figure 6.4 respectively.

The pH in the effluent remained between pH 1.53 and 1.61 throughout the experimental run after changing the feed (pH 1.6) to flow-through operation. The redox potential increased rapidly between days 10 and 15, reaching the highest recorded redox potential of 672 mV after 19 days, after which a slight decrease was observed. The un-inoculated abiotic control column remained cell free with negligible change in redox potential over the experimental period. Within the inoculated experimental columns, no visually detectable cells were observed in the eluted effluent over the first 6 days of leaching under flow-through conditions, detection limit of the microscopic cell counting technique of 3.12×10^5 cells ml^{-1}. The slow growth of cells attached to the mineral surface could be attributed to the microorganisms adapting to the new surface environment. Cells were microscopically detected in the effluent, across all the columns, on day 7, at an average of $7.03 \times 10^5 \pm 3.93 \times 10^5$ cells ml^{-1}. This was followed by a steady increase in the cumulative cell numbers emanating from the columns for the remainder of the experimental period. The cumulative exponential increase in cell numbers between 10 -15 days corresponded with an increase in the measured redox potential over the same period.

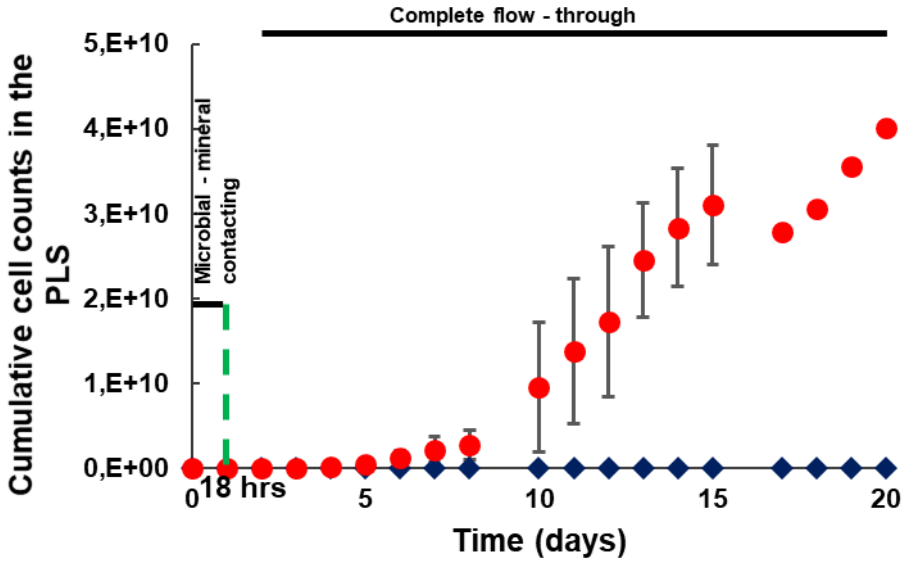

Figure 6.1: The cumulative cell numbers present in the experimental (●) and abiotic control (◆) column effluent over the course of the experimental period. The phases of the experimental period are indicated, showing the initial inoculation and microbe-mineral contacting time of 18 hrs, as well as the period of continuous operation. Error bars represent the standard deviation from the mean cell count across the 6 columns initially (decreasing as columns were sacrificed on 18 hours, day 7, 12, 15 and 20).

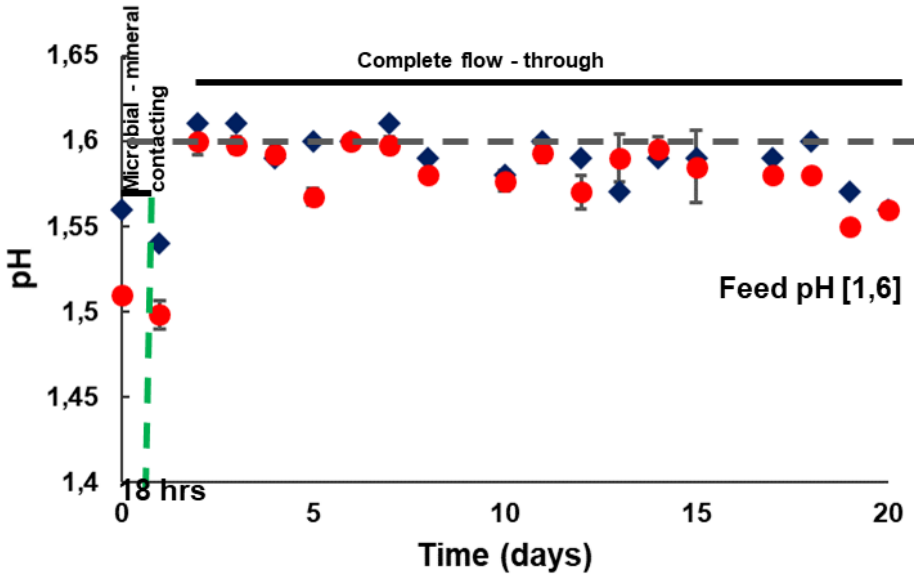

Figure 6.2: Measured pH of the experimental (●) and abiotic control (◆) column effluent over the course of the experimental period. The phases of the experimental period are indicated, showing the initial inoculation and microbe-mineral contacting time of 18 hrs, as well as the period of continuous operation. Error bars represent the standard deviation from the mean pH across the 6 experimental columns at the same time point (decreasing as columns were sacrificed on 18 hours, day 7, 12, 15 and 20).

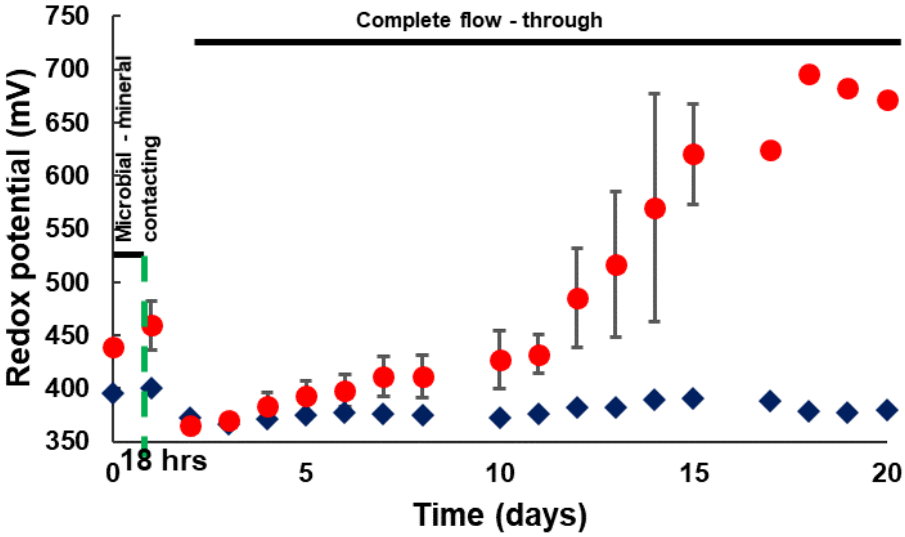

Figure 6.3: Measured redox potential of the experimental (●) and abiotic control (◆) column effluent over the course of the experimental period. The phases of the experimental period are indicated, showing the initial inoculation and microbe-mineral contacting time of 18 hrs, as well as the period of continuous operation. Error bars represent the standard deviation from the mean redox potential across the 6 experimental columns at the same time point (decreasing as columns were sacrificed on 18 hours, day 7, 12, 15 and 20).

The increase in microbial cell number in the effluent coupled with an increase in the redox potential suggest an increase in microbial numbers on the mineral surface as well as an increase in the metabolic activity of the microorganisms, indicative of the establishment of an active leaching system. The increase in redox potential in the effluent corresponded to a decreased Fe^{2+} concentration in solution (Figure 6.4 A) coupled with an increase in the Fe^{3+} concentration (Figure 6.4 B), suggesting active microbially facilitated regeneration of Fe^{3+}. The Fe^{2+} decreased steadily from 0.61 g L^{-1} on day 7, in concert with redox potential and Fe^{3+}, and was largely oxidised by day 15 (0.014,7 g L^{-1}), whereas the un-inoculated control remained relatively similar to the fed 0.5 g L^{-1}. In the same period, Fe^{3+} increased from 0.25 to 0.68 g L^{-1}.

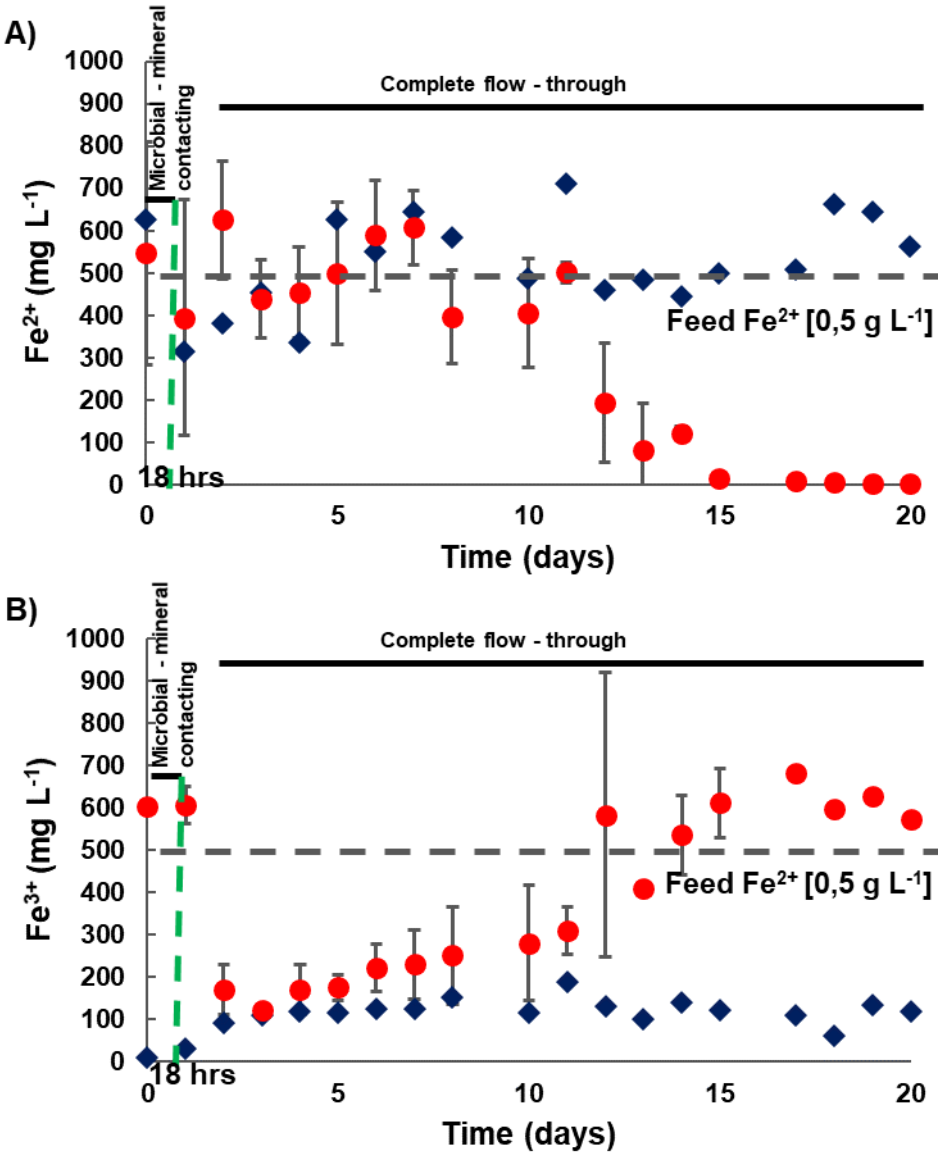

Figure 6.4: Iron (Fe) assay of the experimental (●) and abiotic control (◆) column effluent over the course of the experimental period. A is Fe^{2+} and B is Fe^{3+}. The phases of the experimental period are indicated, showing the initial inoculation and microbe-mineral contacting time of 18 hrs, as well as the period of continuous operation. Error bars represent the standard deviation from the mean Fe^{2+} and Fe^{3+} across the 6 experimental columns at the same time point (decreasing as columns were sacrificed on 18 hours, day 7, 12, 15 and 20).

6.3.2 Mineral associated microbial community and its coverage

Figure 6.5 shows the number of microbial cells mechanically detached from the mineral surface, classified as either loosely associated or firmly attached cells, as well as the percentage of mineral surface covered by the microorganisms (Section 3.4). After the 18-hour inoculation period, a total of 1.04×10^{11} cells m^{-2} was found associated with and attached to the mineral surface. This is equivalent to approximately 7.9 % coverage of the available surface area (assuming a monolayer of cells is formed and a uniform mineral surface area). For the purposes of this investigation, the mineral-associated cells are defined as being representative of the total of the weakly and strongly attached cells (firmly attached) as well

as loosely associated microbial cells removed by the initial liquid wash. Minor changes in the loosely mineral-associated phase were observed, increasing from 2.63 × 10^9 cells m^{-2} after day 1 to 4.75 × 10^9 cells m^{-2} after day 20 (~2-fold increase). The firmly attached microorganisms grew in number for the majority of the experiment and after 15 days there were approximately 3.22 × 10^{11} cells m^{-2} (>3-fold increase) covering approximately 24.4 % of the available surface area. A decline in the firmly attached cell numbers was observed between days 15 and 20 to yield approximately 1.42 × 10^{11} cells m^{-2} covering 10.7 % of the available surface area at day 20. The observed increases in microbial numbers associated with the mineral are in line with the increases in the effluent cell numbers, which reached 4.01 × 10^{10} total cells after 20 days (Figure 6.1).

Govender et al. (2013) observed similar attachment trend, whereby a decline in strongly attached cells (quantified by detachment) was recorded from approximately 15 days. The authors postulated that this was possibly due to migration of cells from the strongly to the weakly attached phase or a decrease in the efficacy of the detaching method due to integration of mineral associated cells with EPS or both. In Chapter 5 we show even at advanced stages (30 days) that the microbial cells on the mineral surface were dislodged successfully. The measured concentration of loosely associated cells remained low at approximately 1 % of firmly attached cells over the experimental period, peaking at approximately 2.69 × 10^{10} cells m^{-2} after 20 days of continuous operation. The low concentration of loosely associated cells in this study differed from the interstitial cell concentrations reported by Chiume et al. (2012) and Govender et al. (2013) that were ± 10 fold higher than the cells reported in this study, owing to the absence of agglomeration with fines in this study, thereby limiting the interstitial liquid volumes, through the use of a uniform bead size, leading to consistent voidage across the bed packing.

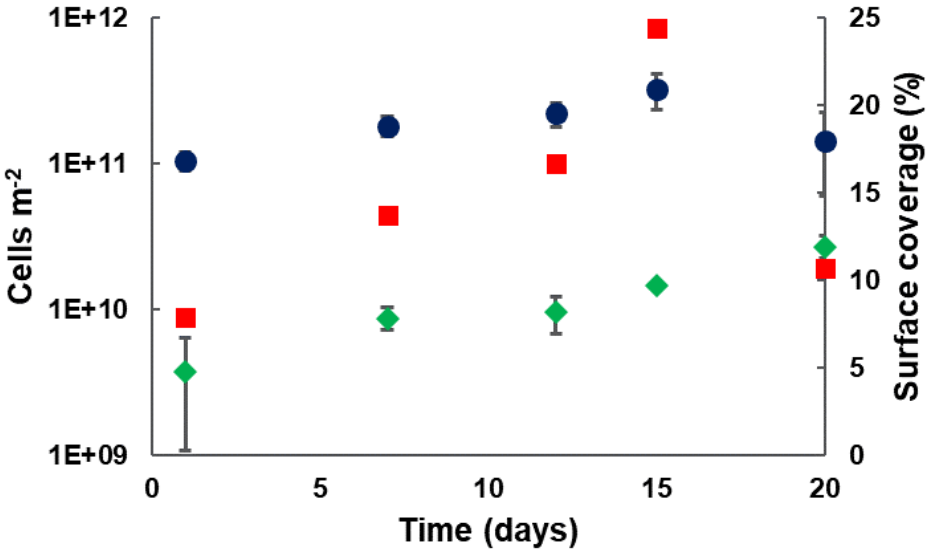

Figure 6.5: Assessment of the loosely mineral-associated cells without firm attachment (◆), microorganisms firmly attached to the mineral surface (●) at each time point, as well as the calculated percentage of surface microbial coverage (■). The degree of surface coverage was determined from the number of cells firmly attached to the mineral. Error bars represent the standard deviation from the mean of the mineral-associated and firmly attached cells across the wash repeats.

6.3.3 Visualization of mineral surface colonisation

The mineral surfaces of the pyrite-coated glass beads were visualised using SEM following colonisation with microorganisms to assess the extent of microbial attachment and colonisation of the mineral surface through the formation of micro-colonies and secretion of EPS (Figure 6.6). The SEM micrographs show a progression in the microbial and mineral interaction over the experimental period. In particular, the micrographs show single celled microorganisms and pits on the mineral surface as well as EPS bound microorganisms covering the surface. The single cells observed on the mineral surface at 1, 7, 12 and 15 days may represent initial attachment of cells. The mineral surface observation suggests that intense microbial growth occurred on the mineral surface between 15 and 20 days. A layer of a polymeric substance over the mineral surface containing a significant proportion of microbial cells, relative to the surrounding mineral surface, was observed on the SEM images of mineral coated beads from the column sacrificed at day 20.

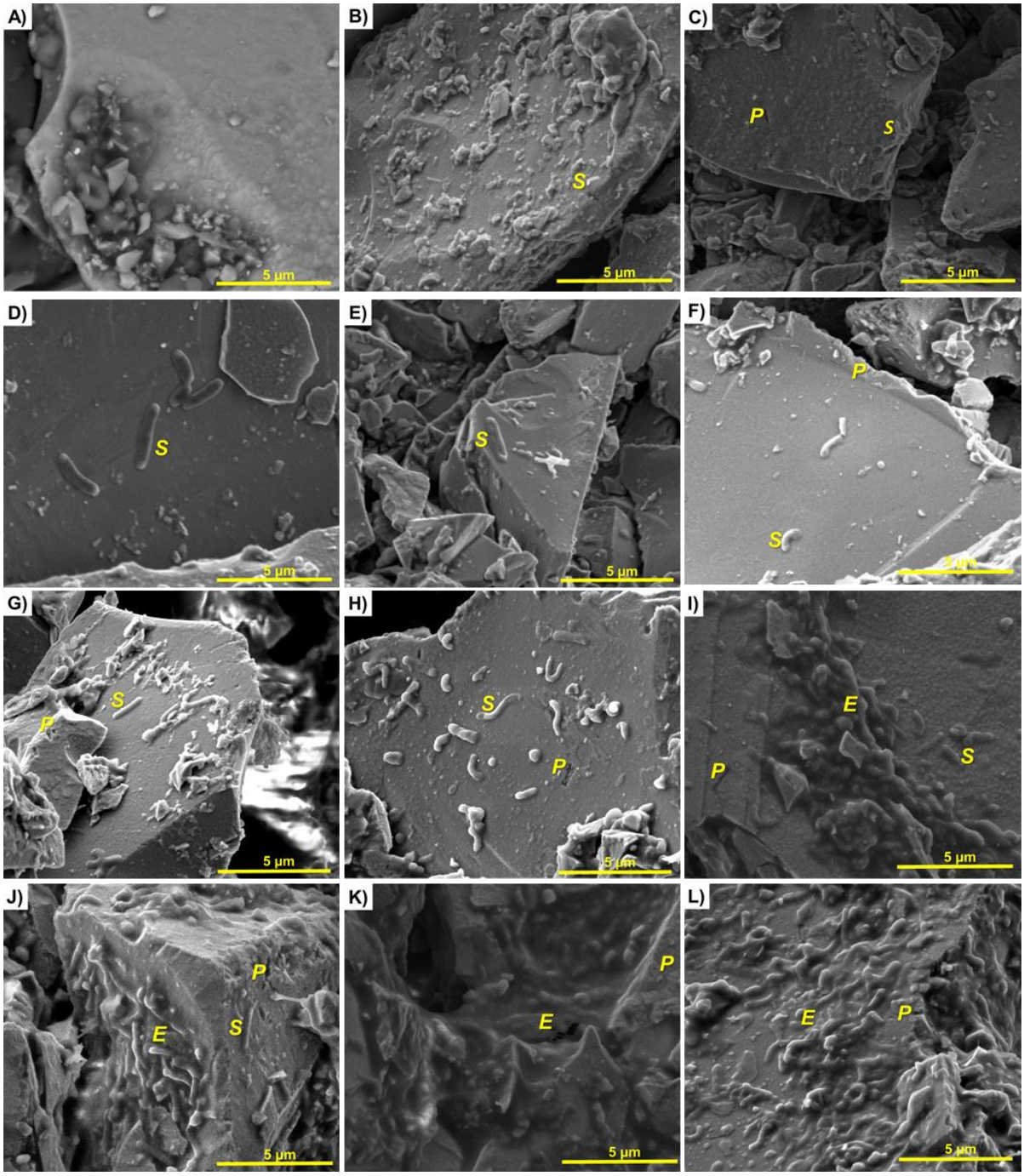

Figure 6.6: Scanning electron micrographs of pyrite mineral concentrate coated glass beads over 20 days. Micrograph A shows an unleached surface as an abiotic control, B, shows a pyrite surface after being in contact with microorganisms for 1 day, C, 7 days, D and E, 12 days, F, G and H 15 days, and I, J, K and L show bioleached mineral surface after 20 days. Observed surface features including single cells (*S*), pits (*P*) and EPS embedded cells (*E*), are labelled. A scale bar (5 µm) is shown on each image.

The mineral surface was also observed after the detachment of microbial cells. This was done to assess visually the efficacy of the detachment of individual and EPS bound cells attached to the mineral surface (Figure 6.7). Two undetached mineral surfaces on day 15 and 20 (Figure 6.7 A and B) are shown to have EPS that are in various developmental phases. Figure 6.7 (A) portrays single cells and cells that are adhering to each other seemingly at the

early stage of developing EPS whereas Figure 6.7 (B) portrays microbial cells that are largely embedded in EPS matrix. Figure 6.7 (C and D) show detached mineral surfaces on day 15 whereas E and F show detached surfaces on day 20. The detached surfaces indicated that the attached single and EPS bound cells were removed from the mineral surface. The pits indicated by the yellow arrows are similar to the shape of *At. ferrooxidans* that was reported by Edwards et al. (2001) on a pyrite surface. However, it was observed when the detached cells were enumerated under a light microscope that the detachment method employed did not result in the disassociation of all cells from within the EPS bound micro-colonies. This was due to the large clumps that represented masses of cells that were embedded in EPS. This was also supported by the decrease in microbial cells detached from the mineral surface, determined by microscopic cell counts on day 20 compared with day 15.

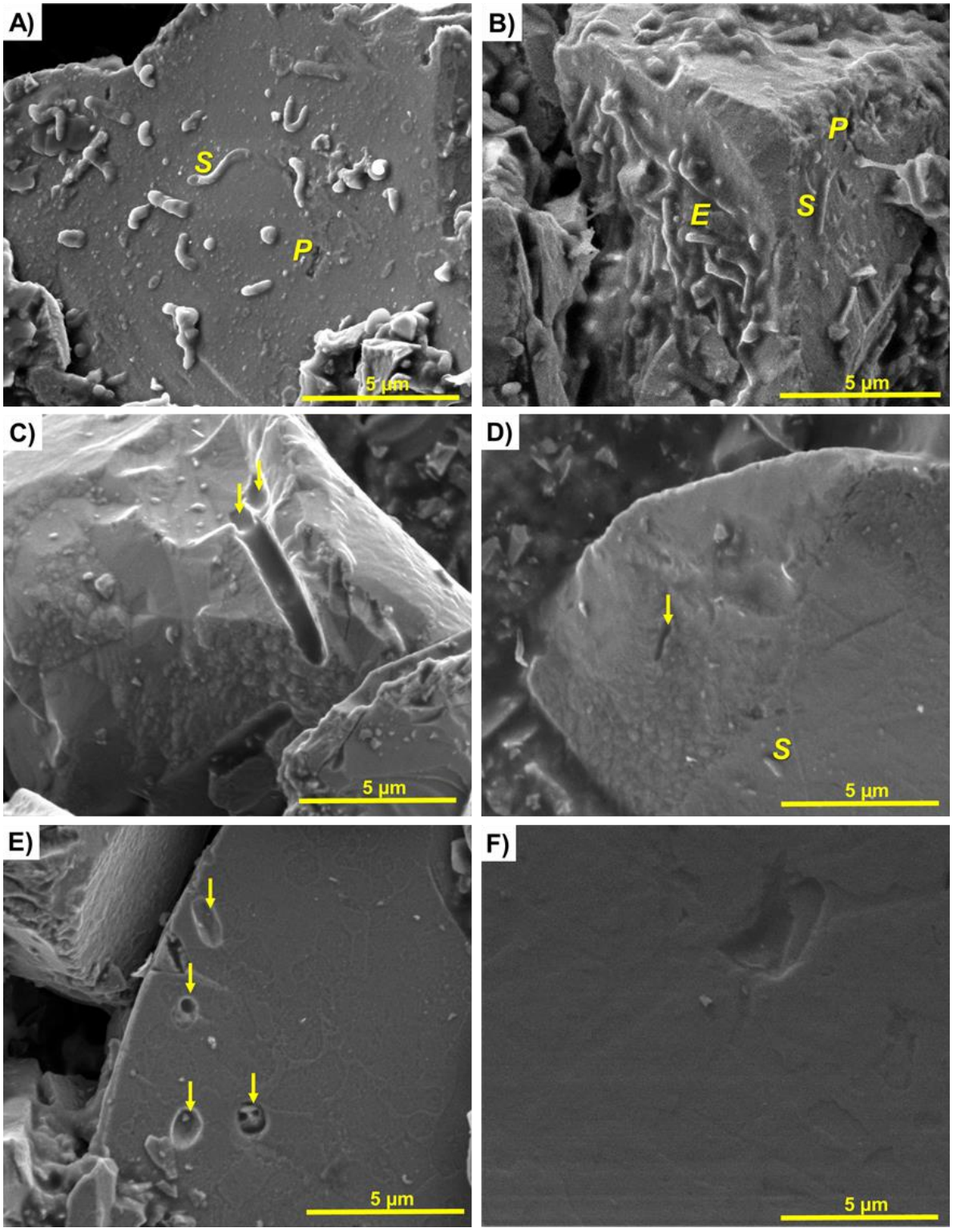

Figure 6.7: Scanning electron micrographs of pyrite mineral concentrate coated glass beads before and after the detachment of microbial cells. Micrograph A shows pyrite surface after being in contact with microorganisms for 15 days and B, 20 days. Micrographs C and D show the pyrite mineral concentrate coated glass beads after detachment on day 15 and E and F after detachment on day 20. Observed surface features including single cells (*S*), pits (*P*) and EPS embedded cells (*E*), are labelled. Arrows show pits that resemble microbial cell shapes. A scale bar (5 µm) is shown on each image.

6.3.4 Microbial activity on the mineral surface

Isothermal microcalorimetry (IMC) was employed to assess the metabolic activity of microbial cells colonising the mineral surface. This activity is a combination of the heat associated with microbial respiration (Fe^{2+} oxidation) as well as the abiotic pyrite leaching that follows from the Fe^{3+} regeneration by the microbes (Rohwerder et al., 1998). Microorganisms associated with the mineral surface showed a pattern of increasing maximum heat output under defined conditions in the IMC over the course of the 20 day experimental period, corresponding to the bioleaching activity of the columns (Figure 6.8). An upward trend was observed when the microbial activity of mineral associated cells was measured over 20 days. The maximum heat produced per unit surface area increased from 21.4 mW m^{-2} after 1 day to 827 mW m^{-2} on day 20. The average heat-flow as a function of each microbial cell associated with the mineral surface was also assessed (Figure 6.9).

Microbial attachment and growth on the mineral surface progressed with time and followed a typical microbial growth curve. Attachment provides localised high concentrations of metabolites responsible for energy metabolism of microorganisms and consequent metal leaching. This also resulted in firm attachment to the mineral substratum, preventing wash out with the medium during metabolism, cell growth and biofilm formation on the mineral surface (Singh et al., 2013) and formation of EPS based biofilm in which tailored bioleach conditions can develop. The average maximum heat produced per cell associated with the mineral surface also increased from day 1 (1.2×10^{-4} nW $cell^{-1}$) to day 12 (15×10^{-4} nW $cell^{-1}$), stabilising on day 15 (13.4×10^{-4} nW $cell^{-1}$). The heat per cell measured on day 20 was 58.4×10^{-4} nW $cell^{-1}$ (not shown). However, due to the EPS formed on the surface on day 20 (Figure 6.6 *E*), it was apparent that the cells detached from the mineral surface under-represented the firmly attached microbial cells present when quantified under the light microscope. Assuming the heat generation per cell was unchanged from the stabilized value at 15 days, a total cell number of 5.5×10^{11} cells m^{-2} is predicted. This requires further investigation for confirmation.

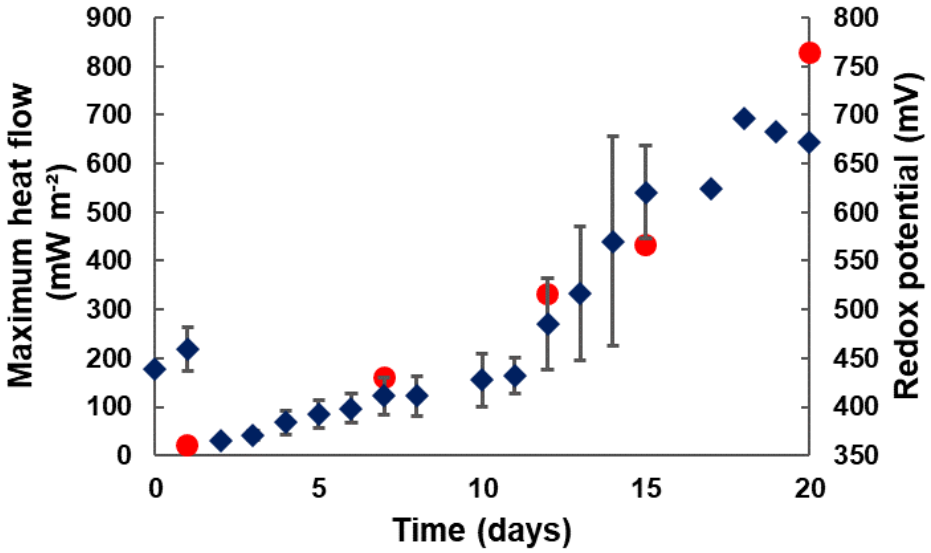

Figure 6.8: Maximum heat-flow per unit surface area (●) after day 1, 7, 12, 15 and 20 measured using the IMC, as well as recorded redox potential (◆) of columns at time of sacrifice. Error bars represent the standard deviation from the mean redox potential across the 6 experimental columns at the same time point (decreasing as columns were sacrificed).

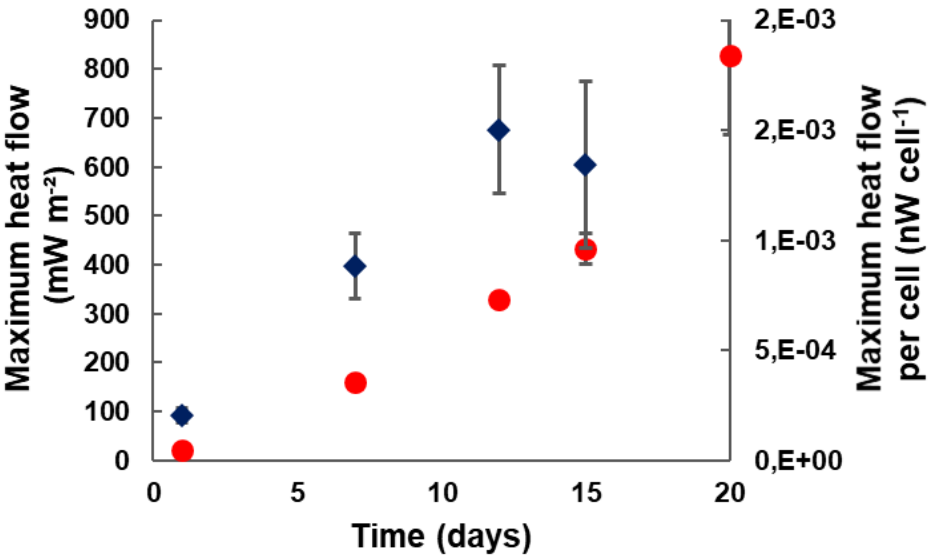

Figure 6.9: Maximum heat-flow per unit surface (●) area after day 1, 7, 12, 15 and 20 measured using the IMC, as well as the average maximum heat produced as a function of the microbial cells attached to the pyrite surface (◆). Error bars represent the standard deviation from duplicates.

Pyrite oxidation rates are reported in Figure 6.10. The determined oxidation rates increased from -1.7 µg m^{-2} s^{-1} on day 1 to -64.5 µg m^{-2} s^{-1} on day 20 with the rate almost doubling between day 15 (-33.7 µg m^{-2} s^{-1}) and day 20. The rapid increase in the latter period coincided with the formation of EPS (Figure 6.6 F and G), which has been reported in the literature to provide favorable conditions for the acceleration in the facilitation of Fe^{3+} regeneration and thus accelerate rates of oxidation (Gehrke et al., 1998; Zhang et al., 2016). Furthermore, it is postulated through the modelling of the mineral associated microbial populations including those in interstitial zones that an accumulation in Fe^{3+} concentration is achieved in the EPS

reaction space (Govender et al., 2014). When the biotic and abiotic IMC heat output emanating from the mineral associated microorganisms was used to calculate oxidation rates of the same pyrite concentrate similar rates were reported across the different surface area loadings when they were normalised (Section 4.3.5).

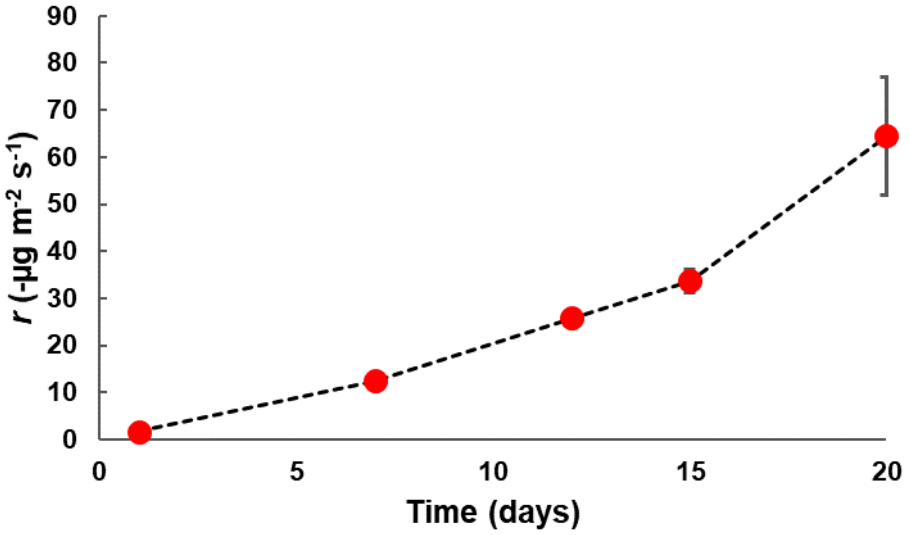

Figure 6.10: The progressive pyrite oxidation rates of combined biological and chemical oxidation of pyrite concentrates over a 20 day experimental period. Error bars represent the standard deviation from duplicates.

6.4 Conclusions

In Chapter 4, IMC was shown to be able to measure and assess the activity of microbial cells in a state of association with pyrite mineral surface quantitatively. In this current investigation an integration of wet chemistry analysis, qualitative SEM visualization and quantitative IMC measurement and the detachment method demonstrated that the activity of mineral associated microorganisms as well as microbial growth on the mineral surface and the resulting oxidation rates progressed with time. The more microbial cells were associated with the mineral surface, the more heat was produced as a result of the interfacial microbial-mineral activity. This was demonstrated through the accelerated heat output that was complemented by the formation of EPS on the later stages of the run. The cells that attached to, and colonized the mineral surfaces only covered a fraction of the available surface area. In the presence of EPS, the apparent metabolic activity of cells associated with the mineral surface increased significantly. This is because the EPS-bound microbial cells were not readily disassociated from the EPS matrix such that the overall mineral-associated cells were under-represented, though further work to verify this with quantitative measurement of the EPS should still be undertaken. This presents a way forward to measure quantitatively the progress and performance of microorganisms that facilitate leaching during the early stages

of a bioheap process, which is very critical and potentially sets the tone for the rest of the process.

Chapter 7: Exploring microbial colonisation across mineral ore grade: A case study to develop a flow-through biokinetic test for characterizing acid rock drainage (ARD) potential

7.1 Introduction

Colonisation of mineral surfaces is a process that is encouraged in bioleaching for metal recovery for commercial value. However, the same process is unwanted in mine wastes where it presents the potential to cause environmental harm through acidification, salinisation and metal deportment. Initial attachment, subsequent colonisation and EPS formation strongly depend on the nature of the microbial species as well as their pre-cultivation conditions, grade of mineral substrates and flow rate of irrigant (refer to Section 2.4.1 for detailed description on colonisation of mineral surfaces). Most colonisation studies are carried out in the context of understanding the role of colonisation with regards to bioleaching for value recovery. Investigation of colonisation in the context of ARD characterisation and utilising waste rock minerals that resonate with those stockpiled in mine dumps is necessary. The aim of this chapter is to establish a flow-through biokinetic system that accounts for leach solution chemistry, microbial-mineral interactions (including colonisation) and acid neutralising and acid forming reactions and relates the refined system to the standard static and batch biokinetic tests. The potential to develop an unsaturated, flow-through biokinetic test is explored using two pyrite-bearing, low grade waste rock samples, with the aim to better represent the open system of a waste rock dump. The results obtained are compared to the static tests and to the shake flask-based batch biokinetic tests using both mineral suspension and mineral-coated beads. An understanding of the impact of ore grade on colonisation and metabolic activity is key to optimising the intentional leach process, while minimising the unintentional leaching of waste deposits. Furthermore, the microbial-mineral interfaces and associated microbial activity are investigated in the flow-through biokinetic system at various flow rates to provide improved understanding of the operating environment and these are related back to the colonisation of pyrite concentrate (presented in Chapter 6).

7.2 Introduction to ARD characterisation

A global, standard practice for the characterisation of ARD generation potential, known as the “wheel approach” (Morin and Hutt, 1998), caters for laboratory, field based and whole rock geochemical assessments. The common laboratory test used as first indicator of ARD potential is the static test suite. These tests are fast, inexpensive and can be used easily to test multiple samples (White III et al., 1999; Smart et al., 2002; Verburg et al., 2009). This

approach uses extreme oxidants, providing worst case data, but also is carried out in batch, allowing overall neutralisation of acid formed based on neutralising capacity present in the rock in a manner independent of their relative rates. The latter may hide acid forming capacity in the long term (Lapakko, 2002; Hesketh et al., 2010). By providing 'snapshot' data rather than a time course, no relative rates of acid consumption and production are indicated.

The kinetic leach test provides an advantage when compared to static tests since these account for relative rates and are more representative of the actual field conditions (Bradham and Caruccio, 1990). Commonly used kinetic tests include laboratory-based column tests, humidity cells and field-based test pads (Sapsford et al., 2009). These kinetic tests require longer periods to generate meaningful data (several months to years), making them costly to run, often ~US$ 700-1000s (Broadhurst et al., 2013; Parbhakar-Fox and Lottermoser, 2015) with a delay in data availability to inform appropriate disposal approaches. Furthermore, these tests do not consider the microbial-mineral interaction between the sulfide-bearing waste material and the indigenous iron- and sulfur-oxidising microorganisms that catalyse ARD formation.

To address these shortcomings and complement the existing static and kinetic characterisation tests, a batch biokinetic test was developed by researchers at the University of Cape Town (Hesketh et al., 2010; Broadhurst et al., 2013). The biokinetic test holds several advantages over conventional kinetic tests for measuring the ARD potential, including the delivery of meaningful data regarding the long term ARD generating potential and its kinetics in a relatively short space of time (± 3 months) and being relatively inexpensive to operate (Broadhurst et al., 2013). The configuration of the batch biokinetic test does not, however, represent the typical fluid contacting mechanism in the waste rock dump nor does it consider the washout of neutralising capacity in a flow-through system, such as a waste rock dump, where the kinetics of acid neutralisation and acid generation may differ.

Refinement of the batch biokinetic test to develop a flow-through lab-scale ARD characterisation test is desired to remove the limitations encountered in batch conditions and allow assessment of the mineral-microbe interactions within the waste rock. Microbial activity and the association and colonisation of the mineral surface by the microorganisms plays a key role in the generation of ARD from waste rock dumps.

7.3 Research approach

The mixed mesophilic culture (Section 3.2) was used in this study. Two pyrite bearing waste rock samples were used in this study: PEL-HS and PEL-LS (Section 3.3.2), coated onto glass beads (Section 3.3). The flow-through column reactor system was set-up and operated as

described in Section 3.5.2 and 3.5.3 Solution chemistry analysis was conducted, including measurement of pH, redox potential and Fe (Section 3.6). Microbial coverage analysis via the detachment method was conducted (Section 3.7), microbial distribution and growth on the mineral surface was analysed using SEM visualization (Section 3.8) and microbial activity measurement was conducted using IMC (Section 3.9).

7.3.1 Static tests

The static tests were conducted on both pyrite-bearing waste rocks using acid-base accounting (ABA) and net acid generation (NAG) tests. The ABA test, conducted according to Smart et al. (2002), measures the net acid producing potential (NAPP), which represents the balance between maximum potential acidity (MPA) and the acid neutralising capacity (ANC). The measured values were expressed as kg H_2SO_4 tonne^{-1} of solid waste rock. A negative NAPP indicates that the sample had sufficient ANC to counterbalance acid production. Similarly, when the MPA is greater than the ANC value and the NAPP was positive, this means that the sample is acid generating. The NAG test was determined according to Stewart et al. (2006) and allows both acid forming and neutralising reactions to occur simultaneously. These tests were performed in triplicate.

7.3.1.1 Acid neutralising capacity (ANC) test

ANC was determined by adding a known volume of hydrochloric acid (HCl) to a 250 ml shake flask containing 2 g of -75 µm pulverised sample. Each sample was allowed to react at 90 °C for a maximum of 2 hours. The mixture was cooled and back-titrated with a standardised solution of sodium hydroxide (NaOH) to determine the quantity of HCl reacted, according to Smart et al. (2002). A detailed procedure is found in Appendix G.

7.3.1.2 Maximum potential acidity (MPA) test

MPA, given by (Equation 7.1), quantifies the total potential for acid generation from the total sulfur content of the sample (in wt %), with the assumption that all sulfur exists as pyrite and that sulfides completely oxidize to form sulfuric acid, hence requiring a conversion factor of 30.6 (Weber et al., 2005).

$$MPA\ kg\ H_2SO_4\ t^{-1} = (\text{total S}\ \%)\ \times 30.6 \qquad \text{Equation 7.1}$$

7.3.1.3 Net acid generation (NAG) test

In the NAG test, hydrogen peroxide was reacted with each waste rock sample to promote the oxidation of sulfide constituents present. Unlike the ANC test, the NAG test involves

simultaneous acid generation and neutralisation, with outcomes being the net acid generated by the sample (Stewart et al., 2006).

A 2.5 g aliquot of each milled waste rock sample was weighed and transferred into a 500 ml shake flask. To this, 250 ml 15 % H_2O_2 solution was added. This solution was corrected to a pH between 4.5 and 5.0 using a 2 M NaOH solution. The mass of the flask was recorded and allowed to react overnight. After 24 hours, the flasks were boiled for two hours where minimal effervescence was observed. Thereafter, dH_2O was used to correct the mass of the flask to its original weight, accounting for evaporation. The sample was cooled and allowed to settle for one hour. Prior to filtering, the mass of the filter paper was recorded. Both the filtrate and the filter cake were recovered. The filtrate was titrated against a 0.1 M NaOH solution to a pH of, firstly, 4.5 and, secondly, 7.0, with the volumes of NaOH used being recorded. The filter cake was recovered and once again reacted with a 15 % H_2O_2 solution, with the mass of sample lost, i.e. as unrecoverable from the filter paper, being recorded. This was repeated until the filtrate pH was pH 4.5 or more. The NAG values for each titration were calculated.

$$NAG = \frac{49 \times \mathrm{VNaOH} \times \mathrm{M}}{\mathrm{W}} \qquad \text{Equation 7.2}$$

where *V* is the total volume of 0.1 M NaOH used in each titration step (ml), *M* is the molarity of the NaOH solution used and W is the mass (g) of ore samples used in each reaction step.

7.3.2 Biokinetic tests

7.3.2.1 Batch biokinetic tests

Biokinetic experiments were conducted in shake flasks containing 0K media (pH 1.6) supplemented with 0.5 g L^{-1} Fe^{2+}, as $FeSO_4$ $7H_2O$, and incubated at 30°C. The biotic conditions were inoculated with 10^8 cells ml^{-1}. Two approaches were used for the flask biokinetic experiments: (i) mineral slurry and (ii) mineral coated glass beads. For the slurry, 7.5 g milled mineral was added to each flask containing a total working volume of 150 ml (0.05 g ml^{-1}). For the mineral coated beads, 100 beads of 6 mm diameter were coated with the respective mineral waste rock (3.6 g; Section 3.3) and added to each flask with a total working volume of 100 mL (~0.036 g ml^{-1}). Prior to inoculation, both slurry and waste rock coated beads were washed and conditioned with 0K media (pH 1.6) for 24 hours to initiate neutralising reactions. After 24 hours, the pH in the respective shake flasks was re-adjusted to pH 1.6 using concentrated H_2SO_4.

7.3.2.2 Flow-through biokinetic test

The columns were inoculated under saturation conditions using an upward flow of 100 ml 0 K media supplemented with 10^{10} mixed mesophilic microbial cells kg^{-1} of ore and 0.5 g L^{-1} Fe^{2+}

as $FeSO_4$ $7H_2O$ in a closed circuit. The inoculum suspension was recycled for 18 h to allow microbe-mineral contacting. Thereafter, the columns were drained, and the liquid fraction collected. A continuous downward flow of sterile fresh 0 K media (pH 1.6) supplemented with 0.5 g L^{-1} Fe^{2+} ($FeSO_4$ $7H_2O$) was introduced and operated until the end of the experimental run.

7.4 Results and Discussion: Part 1 – ARD characterisation studies

In this first part of results and discussion, the focus is mainly on the development of the flow through biokinetic test and considers, in particular, the wet chemistry analysis between the batch biokinetic tests and the flow-through biokinetic configuration operated at two different flow rates, including a discussion on static test.

7.4.1 Static test results

The static test results are presented in Table 7.1 and indicate that both the PEL-LS and PEL-HS samples were acid generating. The sulfur content of the feed samples, determined by LECO analysis (Section 3.2.2), were 21.04 wt.% for PEL-HS and 10.0 wt.% for PEL-LS, consistent with a combined pyrite and pyrrhotite content of 37.5 wt.% for PEL-HS and 16.5 wt.% for PEL-LS. MPA was determined from the sulfur content as 643 kg $H_2SO_4^{-1}$ for PEL-HS and 305 kg $H_2SO_4^{-1}$ for PEL-LS. The ANC values of PEL - HS and PEL-LS were 48.1 and 32.0 kg $H_2SO_4^{-1}$, respectively. The resultant NAPP values were 599 and 273 kg $H_2SO_4^{-1}$ for PEL - HS and PEL-LS, respectively.

Table 7.1: Static ARD test results for PEL-LS and PEL-HS pyrite bearing waste rocks

Feed sample	Sulfur grade wt.%	MPA kg $H_2SO_4^{-1}$	ANC kg $H_2SO_4^{-1}$	NAPP kg $H_2SO_4^{-1}$	NAG_{pH}	ARD classification
PEL-HS	21.04	643	48.1	599	2.24	PAF
PEL-LS	10.0	305	32.0	273	2.20	PAF

The high sulfur content consistent with high proportionality of acid forming (AF) minerals in both samples, coupled with relatively low presence of acid neutralising (AN) minerals resulted in both samples being classified as potentially acid forming (PAF). The measured NAG_{pH} for PEL-HS and PEL-LS of 2.24 and 2.2 confirm their classification as PAF (Figure 7.1). The samples were further assessed through comparing batch biokinetic test results and the flow-through biokinetic test configuration.

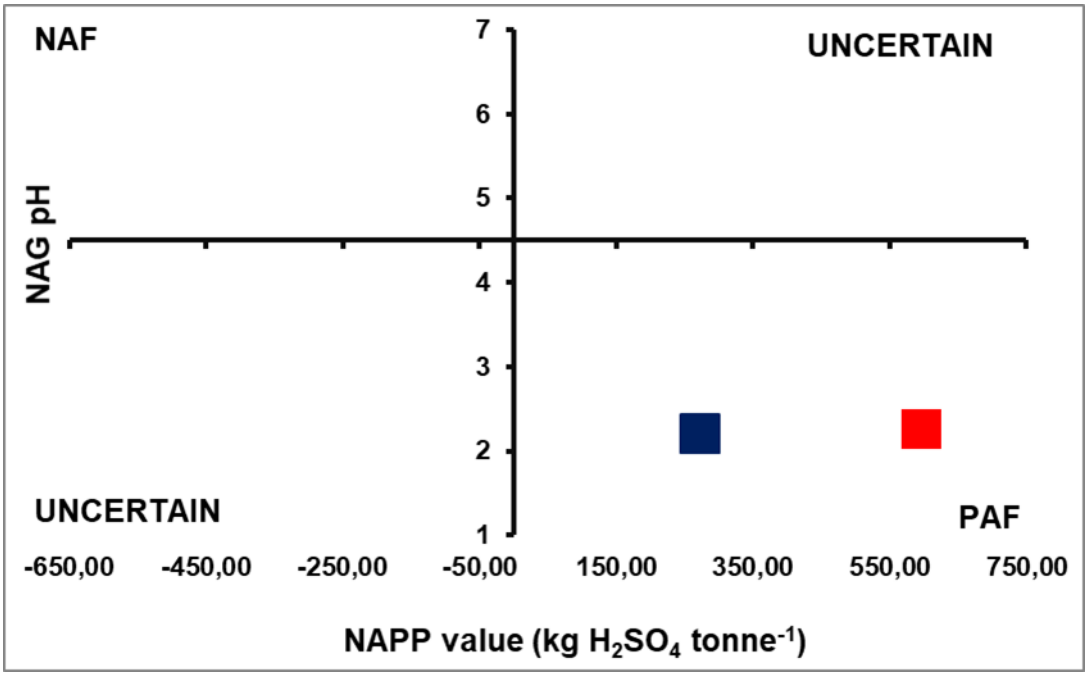

Figure 7.1: Static ARD classification plot for PEL-LS (■)and PEL-HS (■)waste rock samples.

7.4.2 Performance across the biokinetic systems

The waste rock was pre-washed for 24 hours prior to being inoculated to remove acid soluble material. Following inoculation, the pH of the un-inoculated PEL-LS control in the suspended mineral batch biokinetic test (BT) increased to pH 2.77 on day 4 (Figure 7.2 A), whereafter it remained constant till day 13, before declining to reach pH 2.1 on day 23. The un-inoculated PEL-HS reached a maximum pH of 3.48 on day 6, before it declined to pH 1.97 on day 23 (Figure 7.2 A). Despite these samples being not inoculated, the decline in pH could be attributed to the action of indigenous iron- and sulfur oxidising microorganisms inherent to the waste material as this material had not been sterilised. The pH of the inoculated PEL-LS sample increased to pH 2.18 on day 4 and declined to pH 1.51 by day 12 (Figure 7.2 A), whereafter it remained relatively constant. The pH of inoculated PEL-HS sample also reached a maximum of pH 2.2 on day 4, then declined to 1.51 by day 11 (Figure 7.2 A). The decline in pH is attributed to activity of the inoculated microbial culture and the indigenous microbes facilitating the degradation of the waste rock surface.

In the batch biokinetic test using coated beads (BT-CB), the waste rock mineral coated beads were sterilised prior to the experimental run. The pH of un-inoculated PEL-LS increased to pH 2.97 on day 17 (Figure 7.2 B) and the un-inoculated PEL-HS increased gradually to maximum pH of 3.48 on day 21 (Figure 7.2 B), before decreasing slightly. The extended acid neutralisation resulted from the absence of onset of acidification owing to the absence of iron- and sulfur-oxidising microorganisms. The pH of inoculated PEL-LS test declined from a maximum of pH 1.75 on day 3 to pH 1.45 on day 30 (Figure 7.2 B) and the pH of PEL-HS test

declined from pH 1.78 on day 3, to 1.28 on day 18 (Figure 7.2 B). Waste rock mineral-coated beads packed into the column reactors (FT-CB) and irrigated at 60 ml h^{-1} flow rate, were also sterilised prior to experimental run, and unlike the batch shake flasks, were operated continuously in an open circuit with a feed containing 0.5 g L^{-1} Fe^{2+} as $FeSO_4$ $7H_2O$, at pH 1.6 (Figure 7.2 C). Following inoculation during which pH decreased, the pH of the samples increased from pH 1.38 to 1.77 for PEL-HS (Figure 7.2 C) and 1.6 for PEL-LS (Figure 7.2 C). The pH in the un-inoculated samples increased from pH1.6 to 2.01 for PEL-HS (Figure 7.2 C) and 1.69 for PEL-LS (Figure 7.2 C). The pH increase in the effluent suggests an initial dissolution of acid neutralising minerals such as calcite. During the complete flow-through operation phase, the average pH for the experimental PEL-HS and PEL-LS samples were 1.61 (± 0.035) and 1.59 (± 0.011) respectively and the average pH for control samples was 1.63 (± 0.024) for PEL-HS and 1.61 (± 0.022) for PEL-LS. These remained relatively stable and similar to the pH 1.6 media fed to the column reactors continuously in flow-through operation. This suggests that the residence time in the column was too low to liberate these compounds significantly to be detected by solution measuring techniques. The relatively constant pH also suggests a lack of detectable activity in the leaching of the available sulfidic mineral in both waste rocks. It was shown in Chapter 6 that despite having a lack of detection of leaching activity in solution chemistry at 60 ml h^{-1}, there was evidence of leaching activity when mineral colonising microbial populations were measured directly.

In the waste rock mineral-coated beads packed into the column reactors (FT-CB) at 4 ml h^{-1} flow rate, the pH of un-inoculated column containing PEL-LS increased to pH 2.83 on day 2 due to acid neutralising capacity being solubilised, before declining to pH 1.6 by day 12 and a lowest point of pH 1.44 on day 20 (Figure 7.2 D) due to acidification and the wash out of acid neutralisation. In the PEL-HS column, the pH increased to pH 3.2 on day 2, before declining to pH 1.65 by day 12 and a minimum of pH 1.54 on day 21 (Figure 7.2 D). The decline in pH could attributed to the depletion of neutralising minerals, removed by the flow-through nature of the column. The pH in the inoculated PEL-LS increased only to pH 2.27 on day 4 owing to the early onset of microbially-mediated acidification, thereafter decreasing to pH 1.45 by day 11 and to pH 1.37 on day 20 (Figure 7.2 D). In the PEL-HS column, the pH increased to pH 2.25 on day 4, before declining through pH 1.5 on day 8 and pH 1.25 on day 20 (Figure 7.2 D). The pH profiles of the inoculated tests across the three biokinetic tests (Figure 7.2 A, B and D) showed that microbial activity facilitated leaching of the sulfidic waste rock and that the rates of acidification and neutralisation were not equivalent. The pH profiles of the flow-through system at 60 ml h^{-1} flow rate showed a lack of significant detectable change between media fed pH and effluent pH, thus suggesting a lack of sensitivity on the techniques to

effectively detect activity in the solution during leaching of the available sulfidic mineral in both waste rocks.

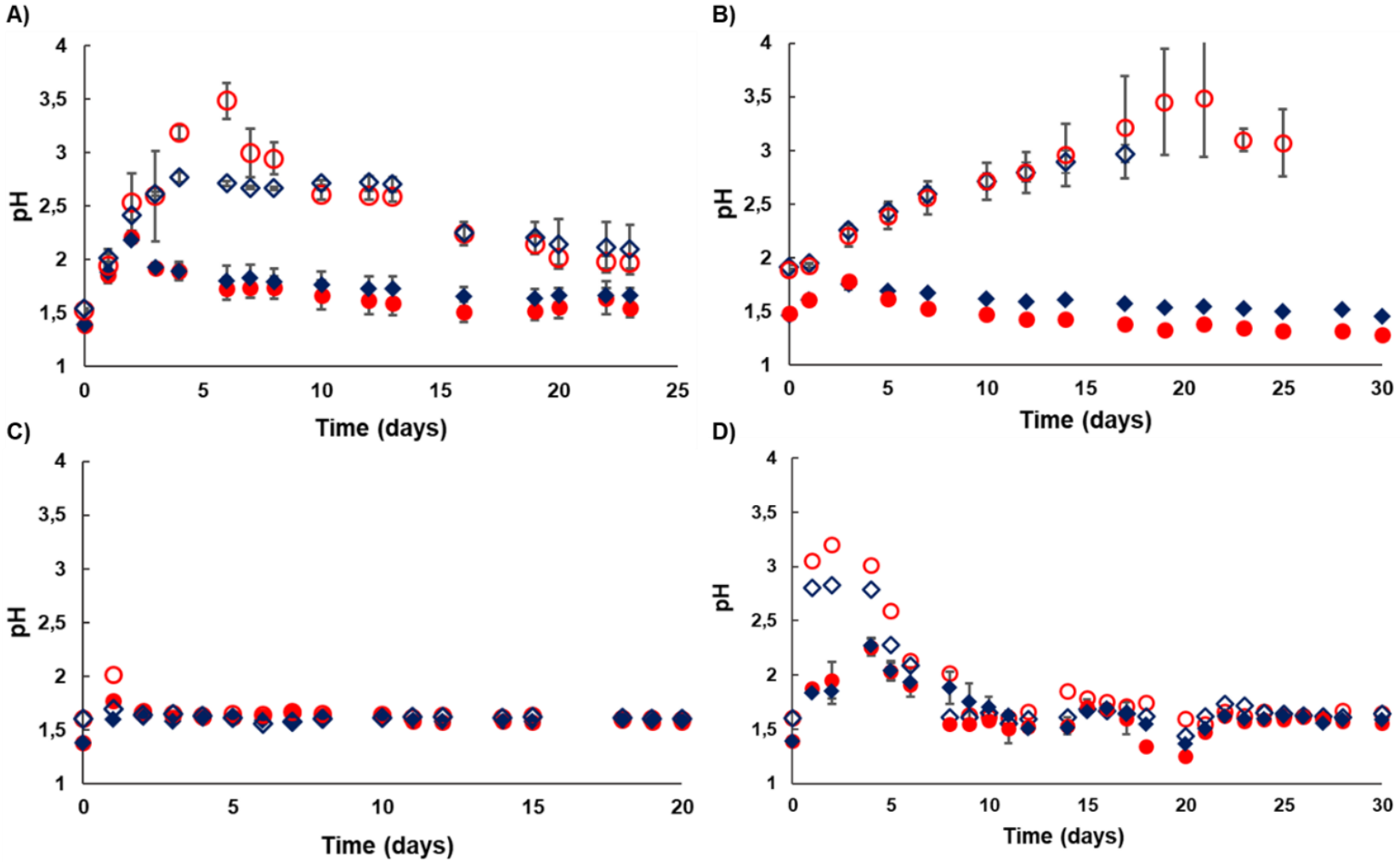

Figure 7.2: Analysis of pH across the biokinetic test approaches, (A) batch slurry (BT), (B) batch waste rock coated glass beads (BT-CB), (C) waste rock coated glass beads in a flow-through column (FT-CB; 60 ml h^{-1}) and (D) waste rock coated glass beads in a flow-through column (FT-CB; 4 ml h^{-1}). All experiments were conducted at 30 °C. The samples include PEL-LS un-inoculated (◇), PEL-HS un-inoculated (○), PEL-LS inoculated (◆) and PEL-HS inoculated (●). Error bars represent the standard deviation from the mean pH across the three experimental shake flasks and five columns at the same time point.

In the batch biokinetic test with un-sterilised suspended mineral, the redox potential of both the un-inoculated PEL-LS and PEL-HS remained in the range ~250 mV to 300 mV until day 10. Thereafter, it increased gradually to a maximum of 666 mV and 649 mV by day 22 in the PEL-LS (Figure 7.3 A) and PEL-HS tests (Figure 7.3 A) respectively. The redox potential in the inoculated PEL-LS increased from 480 mV at the start of the run to 712 mV on day 4 and remained relatively stable thereafter (Figure 7.3 A); similarly, the PEL-HS test redox potential increased from 468 mV to 696 mV in the same period and then stabilised (Figure 7.3 A). In the BT-CB using sterilised mineral, the redox potential of un-inoculated PEL-LS (Figure 7.3 B) and PEL-HS (Figure 7.3 B) tests remained in the range 250 to 300 mV over the 17 and 25 day duration of the runs respectively. This can be attributed to the absence of indigenous microbial populations due to sterilisation.

In the inoculated BT-CB tests, the redox potential of PEL-LS increased from 498 mV on day 1 to 683 mV on day 7 (Figure 7.3 B) and that of PEL-HS from 488 mV on day 1 to 710 mV on day 10 (Figure 7.3 B) and remained relatively stable throughout the experimental run. In the flow-through tests using sterile mineral (FT-CB) at 60 ml h^{-1} flow rate, the redox potential of the inoculated samples decreased from 499 to 401 mV for PEL-HS (Figure 7.3 C) and from 504 to 430 mV for PEL-LS during the 18-hour inoculation period. The redox potential of the un-inoculated samples remained the same at 301 mV for PEL-HS (Figure 7.3 C) and increased from 301 to 335 mV for PEL-LS. The redox potential of both PEL-HS and PEL-LS inoculated samples remained relatively low, circa 300 to 500 mV, throughout the continuous flow-through operation (Figure 7.3 C). This suggests either a lack of effective and detectable iron-oxidizing microbial activity that would result in the catalysed regeneration of Fe^{3+} and associated increased redox potential, or that the microbial activity generating Fe^{3+} is insignificant with respect to the Fe^{3+} leaching of the mineral and the flow rate of the solution. When this is related back to the pyrite concentrate study (Chapter 6) that was operated at the same flow rate (60 ml h^{-1}), a high redox potential was recorded reaching a maximum of 696 mV (Figure 6.3). This suggests that the mineral grade plays a role in determining microbial-mineral interaction and thus the facilitation of leaching.

In the un-inoculated PEL-LS and PEL-HS flow-through tests using sterile mineral (FT-CB) at 4 ml h^{-1} flow rate, the redox potential remained low throughout the 30 day experimental run, increasing gradually from 300 to 400 mV (Figure 7.3 D). An increase in redox potential of the inoculated PEL-LS test was evident from day 10 (391 mV) to day 21 (700 mV; Figure 7.3 D), whereafter it remained relatively stable. The redox potential of inoculated PEL-HS test increased from 416 mV to 689 mV in the same period (Figure 7.3 D). Based on solution chemistry, both waste rock minerals are acid forming across three biokinetic systems (Figure 7.3 A, B and D), supporting the metabolism of iron- and sulfur-oxidising microorganisms. At

60 ml h^{-1} flow rate, not enough evidence is provided in the solution chemistry, both pH and redox potential, to suggest that in the inoculated samples there is active degradation of both waste rocks facilitated by microbial populations (Figure 7.3 C)

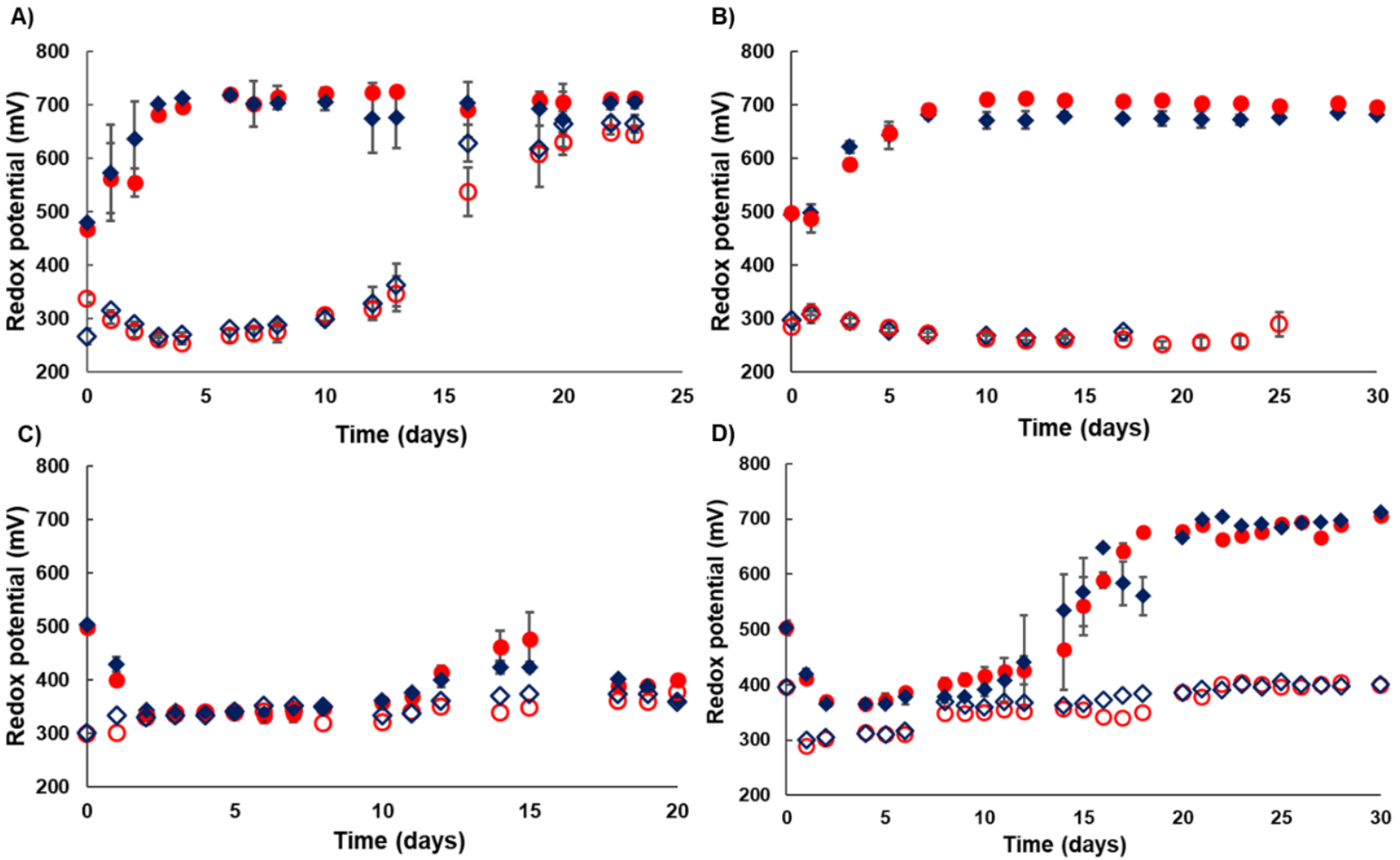

Figure 7.3: Measured redox potential across the biokinetic test approaches, (A) batch slurry (BT), (B) batch waste rock coated glass beads (BT-CB), (C) waste rock coated glass beads in a flow-through column (FT-CB; 60 ml h^{-1}) and (D) waste rock coated glass beads in a flow-through column (FT-CB; 4 ml h^{-1}). All experiments were conducted at 30 °C. The samples include PEL-LS un-inoculated (◇), PEL-HS un-inoculated (○), PEL-LS inoculated (◆) and PEL-HS inoculated (●). Error bars represent the standard deviation from the mean redox potential across the three experimental shake flasks and five columns at the same time point

In the flow-through biokinetic system at 4 ml h^{-1} flow rate, it has been shown through both solution pH and redox potential profiles that the inoculated microbial populations facilitated the degradation of the two waste rock minerals, albeit requiring longer to establish the leaching environment. Moreover, acid neutralising capacity was washed out of the columns during the early onset of acidification, negating its role in neutralisation. The 0.5 g L^{-1} Fe^{2+} supplemented at the beginning of the experimental run, as well as that generated through mineral leaching in the batch biokinetic tests (Figure 7.4 A and B) , and the 0.5 g L^{-1} Fe^{2+} that was continuously fed in flow-through biokinetic system at 4 ml h^{-1} (Figure 7.4 D), was dominantly oxidised across three inoculated waste rock samples. The same amount of Fe^{2+} supplemented in the flow-through biokinetic system at 60 ml h^{-1}, remained relatively the same throughout when measured in the effluent. By day two, the Fe^{2+} was completely depleted by the microbial populations present in both inoculated PEL- LS and PEL-HS respectively (Figure 7.4 A) and this was maintained throughout the experimental run. In the absence of oxidising microbial populations, the 0.5 g L^{-1} Fe^{2+} supplemented in the un-inoculated increased gradually and reached a cumulative maximum of 1.36 g L^{-1} for PEL-LS on day 10 (Figure 7.4 A) and 1.53 g L^{-1} for PEL-HS on day 12 (Figure 7.4 A), thereafter oxidation was evident, suggesting the presence of indigenous oxidising microbial populations. In the BT-CB test, depletion of Fe^{2+} was achieved by day 5 for both PEL-LS and PEL-HS respectively (Figure 7.4 B). In the sterilised and un-inoculated samples, the Fe^{2+} increased gradually and reached a cumulative maximum of 1.21 g L^{-1} on day 12 for PEL-LS (Figure 7.4 B) and 1.31 g L^{-1} on day 19 for PEL-HS (Figure 7.4 B).

In the FT-CB system at 60 ml h^{-1} flow rate, the Fe^{2+} decreased from 0.841 at day 0 to 0.382 g L^{-1} at day for PEL-LS (Figure 7.4 C) and 0.831 at day 0 to 0.495 g L^{-1} at day 2 for PEL-HS (Figure 7.4 C). The measured Fe^{2+} remained relatively similar to the fed 0.5 g L^{-1} throughout the experimental run. The measured effluent of Fe^{2+} in the inoculated PEL-LS (Figure 7.4 C) and PEL-HS (Figure 7.4 C) samples also remained relatively similar to the fed Fe^{2+}. Fe^{2+} was largely oxidised into Fe^{3+} under the same flow rate on a pyrite concentrate (Figure 6.4; Chapter 6). At a lower flow rate of 4 ml h^{-1} (Figure 7.4 D), the Fe^{2+} of the sterile and un-inoculated increased from 0.5 at day 0 to 1.11 g L^{-1} at day 1 for PEL-LS (Figure 7.4 D) and increased from 0.5 at day 0 to 1.14 g L^{-1} at day 1 for PEL-HS (Figure 7.4 D). The initial increase in Fe^{2+} in both samples suggested that there was a washout of readily leachable Fe^{2+} on the waste rock surfaces and was also due to the absence of oxidising microbial populations. The Fe^{2+} decreased gradually until a concentration similar to the feed was achieved and then it remained relatively stable throughout the experimental run. In the inoculated samples, the Fe^{2+} reached a maximum of 1.87 g L^{-1} for PEL-LS (Figure 7.4 D) and 1.67 g L^{-1} for PEL-HS (Figure 7.4 D).

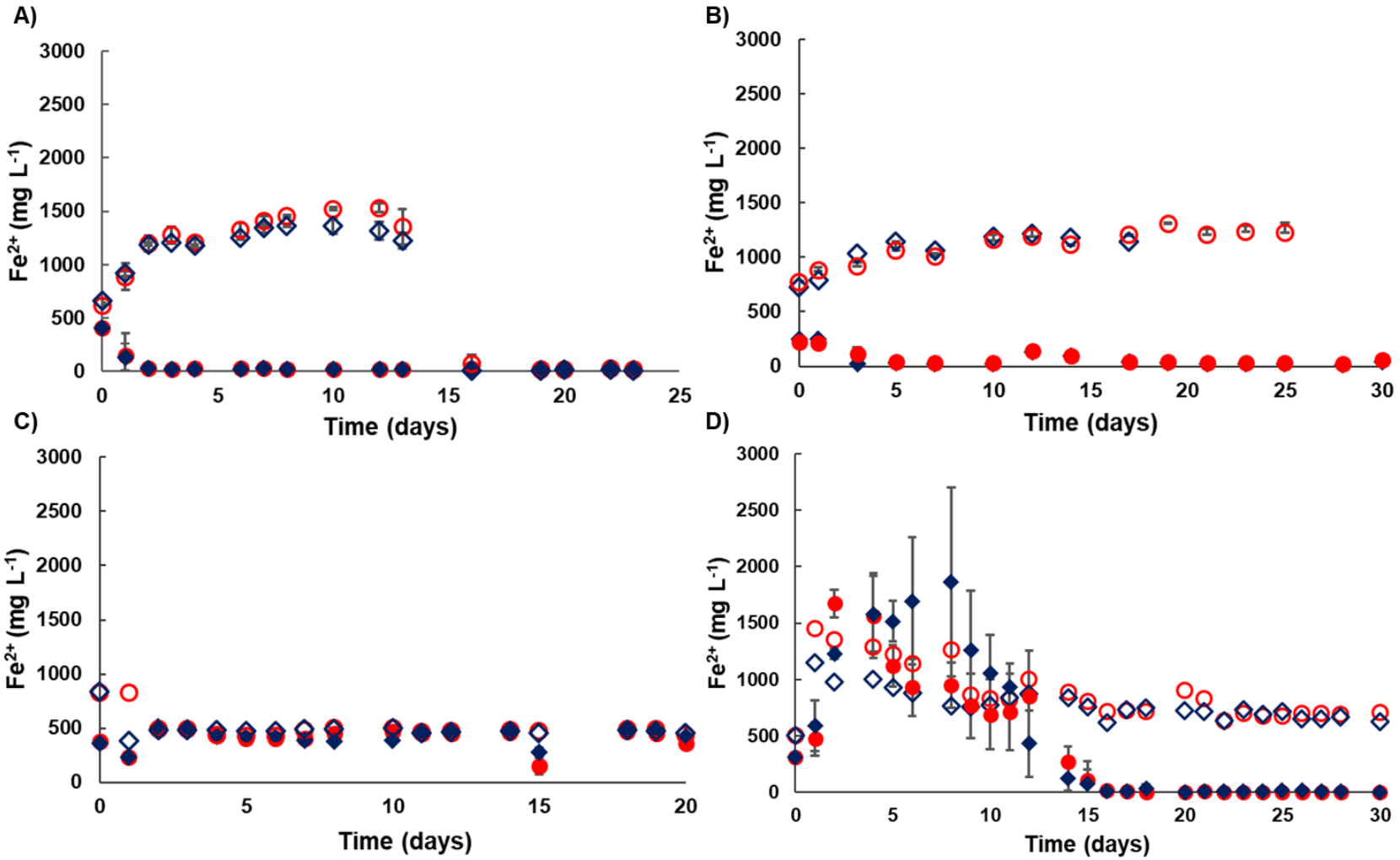

Figure 7.4: Measured Fe^{2+} across the three biokinetic test approaches, (A) batch slurry (BT), (B) batch waste rock coated glass beads (BT-CB), (C) waste rock coated glass beads in a flow-through column (FT-CB; 60 ml h^{-1}) and (D) waste rock coated glass beads in a flow-through column (FT-CB; 4 ml h^{-1}). All experiments were conducted at 30 °C. The samples include PEL-LS un-inoculated (◇), PEL-HS un-inoculated (○), PEL-LS inoculated (◆) and PEL-HS inoculated (●). Error bars represent the standard deviation from the mean Fe^{2+} across the three experimental shake flasks and five columns at the same time point.

The Fe^{2+} decreased and was depleted by day 15 in both waste rock samples due to microbial activity facilitating its oxidation and Fe^{2+} remained oxidised throughout rest of the experimental run. The Fe^{3+} trend across the biokinetic tests (Figure 7.5 A, B, C, and D) corresponded with the trends of Fe^{2+} (Figure 7.4) and redox potential (Figure 7.3) counterparts. The Fe^{3+} of the un-inoculated waste rock samples increased from 0.06 on day 13 to 1.31 g L^{-1} on day 23 (Figure 7.5 A) and from 0.19 on day 13 to 1.53 g L^{-1} on day 23 (Figure 7.5 A). The increase suggested that there was a presence of oxidising microbial populations that facilitated the regeneration of Fe^{3+} and this corresponded with the decline in Fe^{2+} (Figure 7.4 A and B) and an increase in redox potential (Figure 7.3 A and B). The Fe^{3+} in the un-inoculated and sterilised samples for both PEL-LS and PEL-HS remained relatively low with now indication of any accelerated oxidation (Figure 7.5 B, C and D). The Fe^{3+} of the inoculated increased gradually from 2.29 to 3.6 g L^{-1} for PEL-LS and from 2.34 to 4.1 g L^{-1} for PEL-HS over 23 days (Figure 7.5 A). The Fe^{3+} increased from 1.25 to 4.58 g L^{-1} for PEL-LS and from 1.33 to 7.4 g L^{-1} for PEL-HS over 30 days (Figure 7.5 B). The Fe^{3+} remained relatively unchanged for both PEL-LS and PEL-HS throughout the continuous flow-through experimental run at 60 ml h^{-1} flow rate (Figure 7.6 C). Conversely, at 4 ml h^{-1} flow rate, an increase in Fe^{3+} between day 14 and 16 was observed in both inoculated PEL-LS and PEL-HS and thereafter the measured effluent Fe^{3+} was in excess of the fed and oxidised Fe^{2+}, suggesting that there was active degradation of the sulfidic waste rock surface facilitated by oxidising microbial populations (Figure 7.5 D).

Solution chemistry analysis between the two waste rocks at the two different flow rates generally showed completely different outcomes. At high flow rates, changes in solution chemistry were not detectable in the effluent, whereas at lower flow rates performance of the system (both pyrite sulfidic waste rocks) was detected and noticeable. It is also worth noting that in Chapter 6, when the same high flow rates were applied in a pyrite concentrate system, the changes in solution chemistry were detectable. This suggests that the grade of a mineral had a significant impact on microbial behaviour and performance

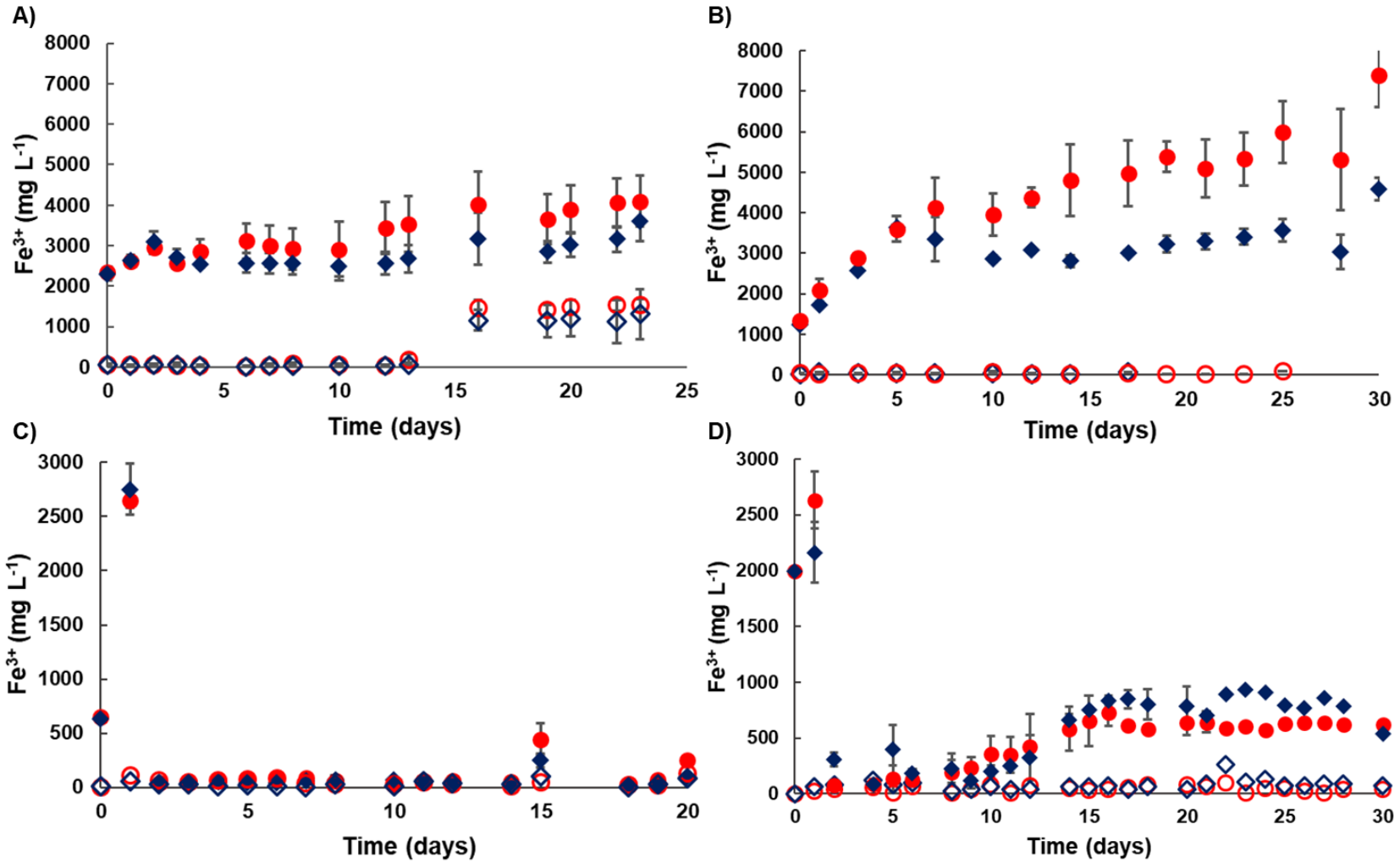

Figure 7.5: Measured Fe^{3+} across the three biokinetic test approaches, (A) batch slurry (BT), (B) batch waste rock coated glass beads (BT-CB), (C) waste rock coated glass beads in a flow-through column (FT-CB; 60 ml h^{-1}) and (D) waste rock coated glass beads in a flow-through column (FT-CB; 4 ml h^{-1}). All experiments were conducted at 30 °C. The samples include PEL-LS un-inoculated (◇), PEL-HS un-inoculated (○), PEL-LS inoculated (◆) and PEL-HS inoculated (●). Error bars represent the standard deviation from the mean redox Fe^{3+} across the three experimental shake flasks and five columns at the same time point

7.5 Results and Discussion: Part 2 – Mineral-microbe interaction studies

In this part, the microbial-mineral interfacial activities observed with the waste rock samples are presented at the two irrigation rates. Further these are compared to the interactions with the pyrite concentrate, allowing microbial colonisation of and activity on sulfidic ores to be considered as a function of mineral grade and flow rates.

7.5.1 SEM surface visualisation

Colonisation of the mineral surfaces from the flow-through systems at 60 ml h^{-1} and 4 ml h^{-1} flow rates were analysed by SEM. The SEM micrographs in Figure 7.6 show leached waste rock surfaces sampled at day 1 and 20. The micrographs in Figure 7.7 show leached waste rock surfaces sampled at day 10, 20 and 30. Single microbial cells (S) on the surface, colonies (C), microbial cells embedded in EPS (E), pits (P) as well as associated precipitates (*p*) are notable. Rod-shaped bacilli are easily distinguishable from the spirilli. Single cells are observed on the surface on both mineral samples at day 10 and day 20 (A-D) as well as at day 30 of LS (E). Colonies are visible from day 20 to day 30 on both mineral samples (C-F). On day 30, cells embedded in EPS are distinctively visible on the HS mineral surface (F).

The cells attached to the mineral surface were mostly observed in, but not limited, to the regions containing surface defects. These observations are supported by Harneit et al. (2006), Africa et al. (2010) and Ghorbani et al. (2012). Harneit et al. (2006) visualised the attachment and biofilm formation of *At. ferrooxidans* cells on pyrite coupons using AFM and fluorescent microscopy and revealed preferential attachment of cells to visible surface defects, attributed to improved availability of sulfide and Fe^{2+} in these areas. Africa et al. (2010) applied DAPI fluorescent staining to show that a mixed microbial culture of *At. ferrooxidans* and *L. ferriphilum* attached preferentially to the defects on pyrite and chalcopyrite surfaces of mineralogically characterised thin sections exposed to thin film flow, representative of the heap leaching environment. Rojas-Chapana et al. (1998) proposed that nutrient concentration gradients were generated at pyrite fragmentation sites, which attracted the settlement of microbes at these specific sites, i.e. defects over others. Progressive abundance of microbial colonisation of the mineral surface was observed over the 30-day experimental run. The pits observed in Figure 7.6 C on the mineral surface subjected to high flow rates (60 ml h^{-1}) were similar to those observed on deliberately washed mineral surface in Chapter 6 (Figure 6.7), as well as those of a thermophilic archaea *Acidianus spp* on sulfur prills reported by (Zhang et al., 2019b). These pits suggest that there is an involuntary detachment of the cells due to the high flow rates fed into the system. On the undetached pyrite concentrate mineral surfaces on Figure 6.6 in Chapter 6, the observed EPS were more pronounced and visible (day 20)

compared to the EPS observed on waste rock surfaces here. This is despite the samples (Figure 6.6 and Figure 7.6) being operated at the same flow rates (60 ml h^{-1}).

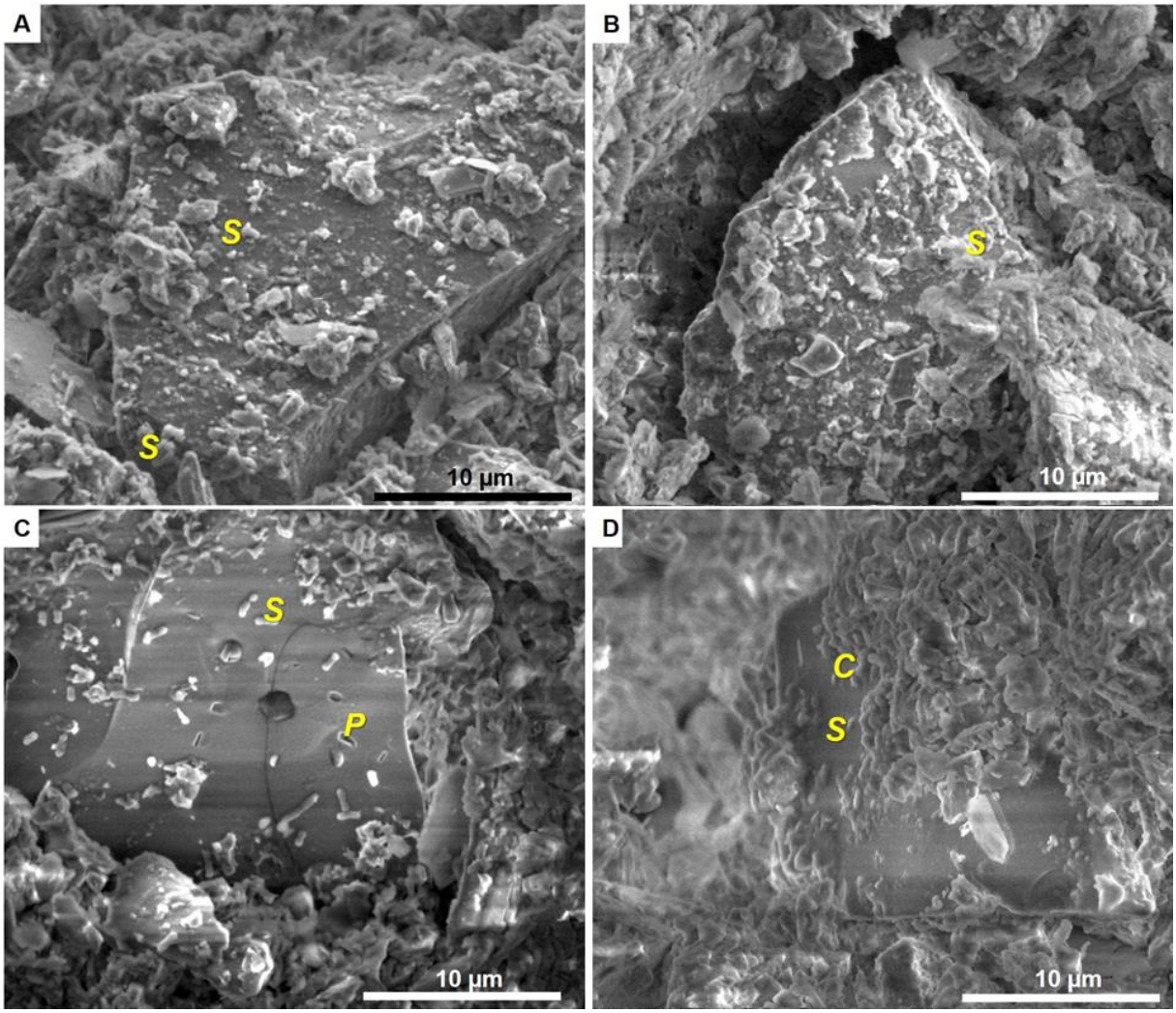

Figure 7.6: SEM images of colonised pyrite bearing waste rocks coated onto glass beads over 20 days. Microbial-mineral interactions on PEL-LS surfaces are shown in micrograph A, day 1 and C, day 20 and interactions on PEL-HS surfaces are shown in micrograph B, day 1, and D, day 20. Observed surface features including single cells (S), pits (P), and colonies (C), are labelled. A scale bar (10 µm) is shown on each image.

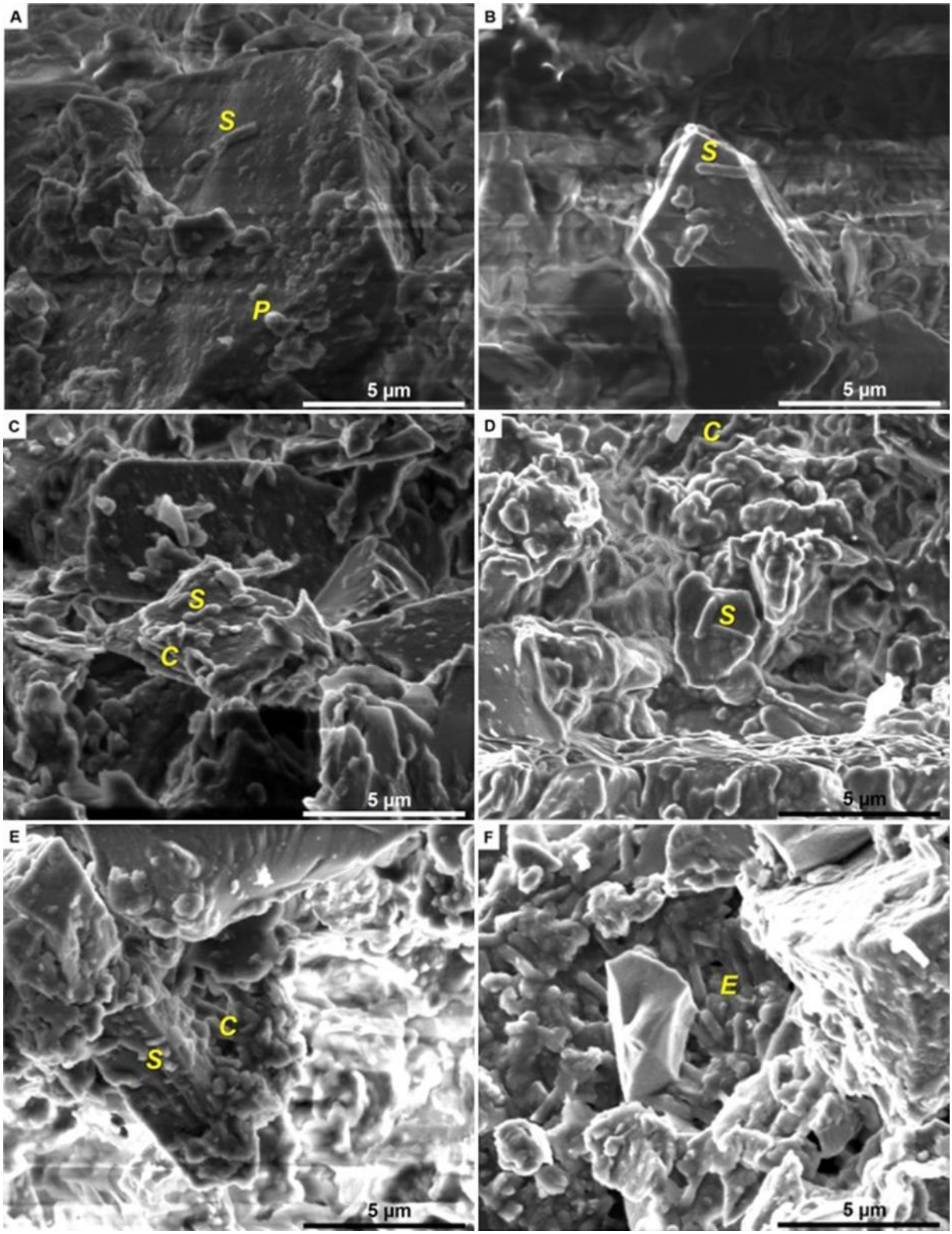

Figure 7.7: SEM images of colonised pyrite bearing waste rocks coated onto glass beads over 30 days. Microbial-mineral interactions on PEL-LS surfaces are shown in micrograph A, day 10, C, day 20 and E, day 30 and interactions on PEL-HS surfaces are shown in micrograph B, day 10, D, day 20 and F, day 30. Observed surface features including single cells (S), precipitates (P), colonies (C) and EPS embedded cells (E), are labelled. A scale bar (5 µm) is shown on each image.

7.5.2 Microbial coverage of waste rocks

Cells on the waste rock mineral surfaces were mechanically detached and microscopically counted. Firmly attached cell numbers, as well as the percentage of mineral surface that is covered by these microorganisms in a monolayer are presented in Figure 7.8 A. Assuming a monolayer, the approximate number of cells required to saturate the surface is calculated at 1.32×10^{12} cells m^{-2}. At a flow rate of 60 ml h^{-1}, after the 18-hour inoculation period, 9.21×10^{10} cells m^{-2} or approximately 7 % coverage for PEL-LS and 1.08×10^{11} cells m^{-2} or 8.2 % coverage for PEL-HS was achieved. The surface coverage on pyrite concentrate at the same time (18 hrs) on was 7.9 % (Figure 6.5), despite having a lower inoculum of 2×10^{7} cells ml^{-1}. This suggests that a higher number of cells initially attached to a surface with higher sulfide content. Microbial growth was observed on the mineral surface and a total of 2.36×10^{11} cells m^{-2} (17.9 % coverage) on PEL-LS and 2.85×10^{11} cells m^{-2} (21.6 % coverage) on PEL-HS were observed on day 20 (Figure 7.8 A) compared to a low surface coverage on the pyrite concentrate surface (10.7 %) that was caused by the difficulty in enumerating cells entrapped in EPS clumps after detachment. Although EPS was also observed on the mineral surface of both waste rocks, no EPS clumps were observed under the light microscope after detachment. At 4 ml h^{-1}, the firmly attached cells after the 18-hour inoculation period there were 9.21×10^{10} cells m^{-2} or approximately 7 % coverage for PEL-LS and 1.08×10^{11} cells m^{-2} or approximately 8.2 % coverage for PEL-HS was achieved. At day 30, microbial populations observed on the mineral surface were 4.61×10^{11} cells m^{-2} (34.9 % coverage) on PEL-LS and 3.3×10^{11} cells m^{-2} (35.4 % coverage) on PEL-HS (Figure 7.8 B). A growth in microbial populations was observed throughout both the experimental runs at 60 ml h^{-1} and 4 ml h^{-1} and the metabolic activity of surface associated populations was measured with IMC.

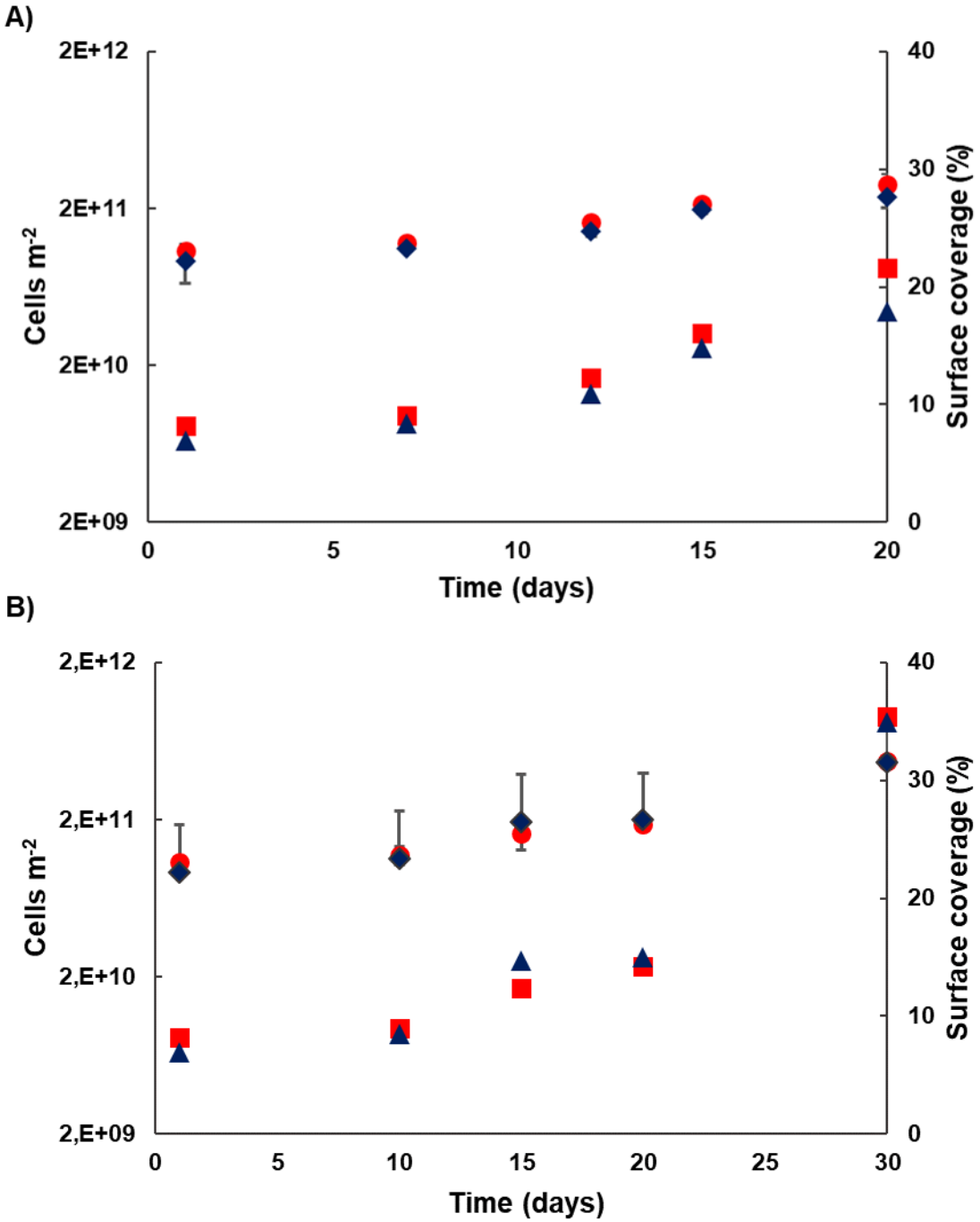

Figure 7.8: Assessment of firmly attached cells to the mineral surface of PEL-LS (◆) and PEL-HS (●) at each time point, as well as the calculated percentage of surface microbial coverage of PEL-LS (▲) and PEL-HS (■) in the flow-through biokinetic system at 60 ml h^{-1} (A) and 4 ml h^{-1} (B) flow rates. The degree of surface coverage was determined from the number of cells firmly attached to the mineral. Error bars represent the standard deviation from the mean of the mineral-associated and firmly attached cells across the three wash repeats.

7.5.3 Microbial-mineral activity measurement

Microbial communities attach to solid surfaces and produce EPS for the development of a biofilm (Watnick and Kolter, 2000). Using IMC, the activity of mineral associated microbial community was quantified at different stages of the experimental run, using the maximum heat produced per unit surface (mW m^{-2}). This activity is a combination of the heat associated with

microbial Fe^{2+} oxidation as well as the Fe^{3+} leaching of pyrite on the waste rock mineral surfaces that follows from the Fe^{3+} regeneration by microbial oxidation. The observations of microbial growth on waste rock surfaces in terms of cell number was complemented by measurement of metabolic activity resulting from the oxidative processes, facilitated by the colonised cells (Figure 7.9 A). After 18 hours (day 1), the measured maximum heat output of samples operated at 60 ml h^{-1} was 63 mW m^{-2} for PEL-LS and 123 mW m^{-2} for PEL-HS. At day 20 this increased to 157 mW m^{-2} for PEL-LS and 293 mW m^{-2} PEL-HS. This increase in metabolic activity corresponds with an increase in the active microbial communities associated with the waste rock surfaces. The measured heat output of the microorganisms, however attached to pyrite concentrate was 21.4 mW m^{-2} after the inoculation period (day 1) and 827 mW m^{-2} at day 20. This shows again the importance and impact of the mineral substrate.

After inoculation, two beads of each waste rock sample were analysed, showing heat generation of 104 mW m^{-2} for PEL-LS and 130 mW m^{-2} for PEL-HS. Between the 18 hours (day 1) post inoculum and day 20, the maximum heat output of both waste rock samples remained in the range 120 to 150 mW m^{-2}. On day 30, the measured maximum heat output was 326 mW m^{-2} for PEL- LS and 289 mW m^{-2} for PEL-HS, indicating substantial growth and increase in metabolic activity. The microbial activity of PEL-LS and PEL-HS on day 30 was 3.1 times and 2.2-fold higher than on day 1, respectively. A previous study conducted on these waste materials using the same microbial consortium in batch shake flasks for 15 days presented a maximum heat output of 237 mW m^{-2} for PEL-LS and 373 mW m^{-2} for PEL-HS.

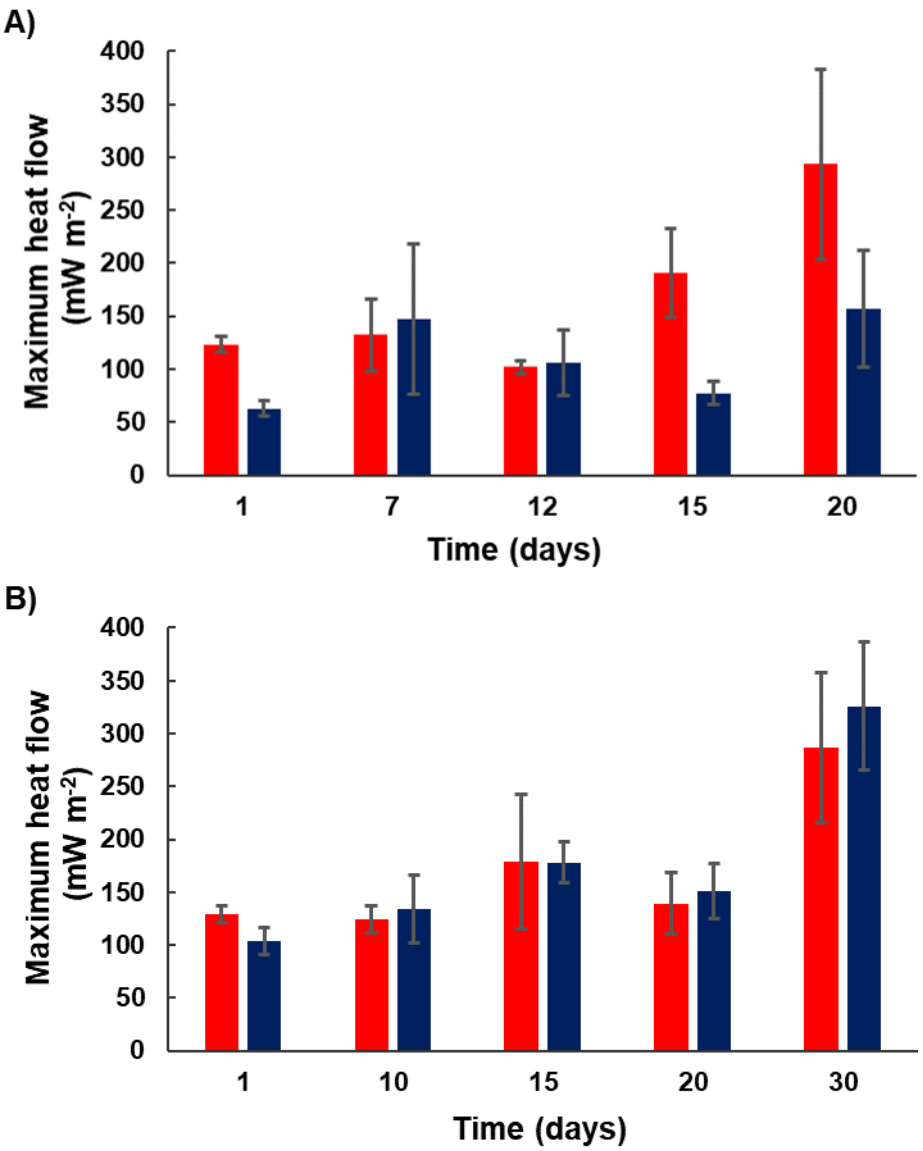

Figure 7.9: Maximum heat-flow per unit surface area for PEL-HS (■) and PEL-LS (■) after day 1, 10, 15 and 20 at 60 ml h^{-1} (A) and after day 1, 10, 15, 20 and 30 at 4 ml h^{-1} (B) were measured using the IMC. Error bars represent the standard deviation from the duplicates of each material.

Upon showing the microbial activities on the mineral surfaces of the varying mineral grades it is shown that microbial adherence to mineral surfaces and their activity on the mineral surface is dependent on the grade of the mineral as well as the solution flow rate passing through the columns (Table 7.2). More cells were detached from mineral surfaces that were operated at higher flow rates and Chiume et al. (2012) showed instances where higher flow rates portrayed higher cell attachments. However, the authors showed that lower flow rates had overall higher degree of microbial attachment. With more information presented in this study including SEM information, the subtle differences witnessed across the different mineral grades and flow rates could be attributed to the formation of EPS during experimental runs.

Table 7.2: A comparison of microbial-mineral interactivities across the different mineral grades on day 20.

Mineral type	Flow rate (ml h^{-1})	Incoculum (cells kg^{-1})	Detached cells (Total)	Detached cells (cells m^{-2})	Cell coverage (%)	Max heat-flow (mW m^{-2})
Pyrite concentrate	60	2×10^9	1.62×10^9	1.42×10^{11}	10.7	827
PEL-HS	60	1×10^{10}	3.26×10^9	2.85×10^{11}	21.6	157
PEL-LS	60	1×10^{10}	2.70×10^9	2.36×10^{11}	17.9	293
PEL-HS	4	1×10^{10}	2.15×10^9	1.88×10^{11}	14.2	146
PEL-LS	4	1×10^{10}	2.27×10^9	1.99×10^{11}	15.0	153

7.5.4 Sulfur content of feed and leachate sample

Post the flow-through experimental run for the 4 ml h^{-1} flow rate, the leached residual waste rock samples were recovered and their sulfur content analysed using LECO, as described in Section 3.3.2, and compared to the feed sulfur content to determine the extent of their leach (Table 7.2). The sulfur leached out of the waste rock samples after the 30-day flow-through experimental run was 2.14 % for PEL-HS (10.2 % of that available) and 4.22 % for PEL-LS (42.3 % of that available). A considerable amount of sulfur was still available for continued acid generation in both samples after 30 days, indicating that an extended leach time would be required for complete acidification. Assuming that leaching conditions remain constant in the system, it would take a further 264 and 41 days to completely leach sulfur out of PEL-HS and PEL-LS respectively.

Table 7.3 Sulfur content of the feed samples and residual leached sample at 4 ml h^{-1} flow rate

Sample	Feed Sulfur wt.%	Residual Sulfur wt.%
PEL-HS	21.04	18.90
PEL-LS	10.00	5.75

7.6 Integrated summary and conclusions

The unsaturated, flow-through biokinetic column test offers advantage over the batch biokinetic test through showing depletion of readily acid neutralising minerals early in the experimental run. Solution chemistry analysis showed minimal changes in solution regarding the performance of the system at 60 ml h^{-1}, however, at a flow rate of 4 ml h^{-1} the changes in solution chemistry were more pronounced. This is attributed to the high feed rate resulting in a very low residence time in the column reactor, thus lessening the contacting time of solution and microbial associated surfaces. Secondly, the mineral grade was also shown to play an important role at these high flow rates. In the pyrite concentrate study (Chapter 6), changes in solution chemistry were more pronounced and detectable at 60 ml h^{-1}. The establishment of a well colonised mineral surface of both PEL-LS and PEL-HS was observed with the progression of the column test experimental run, with increasing microbial numbers and activity associated

with increasing mineral colonisation, demonstrated by IMC and SEM respectively, within 20 days at 60 ml h^{-1} flow rate and 30 days at 4 ml h^{-1} flow rate. The microbial cells associated with pyrite concentrate however, demonstrated high activity despite being inoculated with lesser microbial numbers. This showed that the grade of the mineral plays an important role in determining the oxidation rate. The presence of EPS was more pronounced on the surface of the pyrite concentrate. The flow-through configuration has been shown in this study as a suitable system complementary to the available suite of tests that characterise the potential of acid forming in sulfide rich waste material through provision of relative kinetic data on neutralisation and acidification, their potential washout with time and the role of microbial colonisation. Further studies on waste material with lower sulfide content and extended run periods are recommended to solidify the establishment of the system from which a defined method for the flow-through test can be recommended.

Chapter 8: Concluding remarks and recommendations

8.1 Concluding remarks

The aim of this thesis was to study colonisation of pyrite mineral surfaces by mixed mesophilic cultures in an integrated qualitative and quantitative manner. This understanding is important to both heap bioleaching for metal extraction and safe disposal of waste rock to prevent ARD generation, and thus in the case of ARD characterisation. To study colonisation, methods were established to enable experimental studies to inform a thorough understanding of how microbial populations progressively associate with mineral surfaces of varying grade at different irrigation rates over the colonising period. This mineral association was further correlated with efficiency of pyrite dissolution. The literature emphasises the importance of microbial-mineral association and presents this process as being critical for the acceleration of metal dissolution. Effective mineral surface colonisation by active mesophilic cultures during the early stages of heap bioleaching is important for facilitating mineral leaching for base metal recovery, thereby increasing the oxidative reaction of the process. Oxidative reactions are exothermic and because the leaching of recalcitrant chalcopyrite happens effectively at temperatures above 65 °C, it is important to achieve maximum colonisation of the mineral surfaces through mesophilic cultures at the beginning of the process, thereby making it possible to ramp up the temperatures through generation of metabolic heat and heat from oxidation reactions, thereby reaching the higher temperatures required for chalcopyrite mineral leaching, through microbial succession, quickly. Similarly, effective colonisation and microbial activity is key to regeneration of lixiviants Fe^{3+} and H^{+} for the leaching of other base metals such as chalcocite, covellite, pentlandite and enargite.

Methods that allowed for the integrative determination of microbial association with the mineral surface, including IMC for the measurement of heat output as a function of surface unit and the detachment method for the reliable estimation of mineral associated microbial communities, were successfully refined in this study. Once these were established, the growth and activity of mineral associated microorganisms over time was successfully tracked and measured as a function of mineral surface area, allowing its extent and time course to be determined as well as key variables such as ore grade and irrigation rate to be assessed. During the advanced stages of the experimental run, the formation of EPS was observed through SEM visualisation and its presence contributed significantly to the oxidation rate of mineral associated cells. As a result of this, it was important to understand the EPS and for the first time in a complete flow-through system, the EPS was successfully extracted, and its biochemical components were characterised. Microbial growth, activity and performance on the mineral surface were shown to be dictated by operating conditions such as feed solution

flow rate and sulfide content of the mineral substrate. This level of understanding of microbial colonisation and activity informs the development of both a small scale, flow through feasibility test for determination of metal recovery, its kinetics and its acid requirement from a fully liberated mineral as well as a small scale, flow through characterisation test to assess the environmental impact of waste rock and tailings deposits where leaching it not precluded. The development of the sulfidic waste feasibility and characterisation tests by extension of the biokinetic test for characterising ARD potential to a flow-through system was investigated, using detachment and activity to fully map to the performance data.

The establishment of the mineral-coated glass bead bed provided a defined surface area that allowed for determination of microbial adherence to the surface in a quantitative manner. The relatively even distribution of microbial presence across the mineral surface from bead to bead was demonstrated in this thesis through reproducibility studies across increasing numbers of beads using IMC. The calorimetric method, that was refined to measure microbial-mineral interactions per unit surface (Chapter 4), demonstrated the ability to measure metabolic activities of mixed mesophilic cultures that were suspended in liquid solution as well as microbial communities associated with mineral surfaces in both batch and flow-through systems. Upon comparing different incubation conditions in the IMC vials for the determination of a reproducible experimental set up to provide optimum heat output from mineral-associated microbial communities without introducing experimental limitations, the unsaturated bed produced the highest heat output (263.3 mW m^{-2} ± 2) when compared to the bed saturated with fresh media (28 mW m^{-2} ± 10) and those saturated with cell free leachate (19.9 mW m^{-2} ± 3). The unsaturated ore bed condition provided a standard method for measuring activities of mineral associated microbial communities through minimising oxygen limitation. When the surface area loadings were increased, it was also shown through the measured heat flow that activity of mineral associated communities increased with the increasing loadings and that limitation in activity was also quickly reached. It was further shown that O_2 presence in the batch ampoules plays a critical role in the activity of mineral associated communities and therefore cognisance of the availability of O_2 or its limitation and its impact when measuring activities should be taken into account. On integrating the metabolic activity results from the IMC analysis with solution chemistry-based assays such as redox potential, Fe^{2+} oxidation and the detachment method, an increase in microbial activity, performance and population per unit mineral surface area with experimental run time was investigated. During the early stages of the experimental run (between day 1 and 12) increasing growth of microbial cells associated with pyrite concentrate surface (measured by detachment) was observed. This was complemented by an increase in the metabolic activity of associated cells. However, after a period of time (15-20 days), the microbial growth measured by detachment and counting did

not parallel the metabolic activity on the pyrite concentrate surface measured by IMC. This was attributed to the formation of EPS that embedded cells making it difficult to distinguish single cells under a light microscope and resulting in an underestimate of cell number on detachment.

The traditional detachment method that is used to remove cells from low-grade mineral ores currently applies six wash steps. These include (1) gentle rinsing of the surface to remove non-attached cells, (2) removal of the weakly attached cells through vortexing and (3) removal of strongly attached cells by adding surfactant and vortexing. In this study, the weakly and strongly attached cells were combined and termed “attached”. In validating and refining the method, three, six and eight wash steps were assessed for their ability to remove cells from the mineral surface. These wash steps were applied across the sampling point at 30 days in the experimental run. The wash steps (3, 6 and 8) were shown to not dislodge all the mineral associated cells as there were still residual cells on the mineral surface when observed using SEM. The microbial cells were each detached from a 30 g sample (glass beads coated with mineral) and the number of cells detached on day 10 were 5.53×10^9 cells after three washes, 6.65×10^9 after six washes and 7.77×10^9 after eight washes. On day 20, 8.55×10^9 cells were detached after three washes, 1.12×10^{10} cells after six washes and 1.27×10^{10} after eight washes, whereas on day 30 1.27×10^{10}. On day 30 1.09×10^{10} total cells were recovered after three washes, 1.48×10^{10} after six washes and 1.56×10^{10} after eight washes. The number of cells recovered increased as a function of both the detachment wash steps as well as the progression of the experimental run. Using both the number of detached cells and the activity of residual cells determined by IMC, the total cells (both recovered via detachment and the residual mineral associated cells) present on the mineral surface were determined. Based on the total cell concentration determined, the residual cell fraction on day 30 accounted for 6 % after three washes, 2.5 % after six washes and 1.2 % after eight washes. Based on the 2.5 % variance between six and eight washes on day 30, six washes were demonstrated to be a reliable number of washes to provide a satisfactory estimation of detached cells. The integrative use of the detachment method and IMC assisted with elucidating the detachment (microbial numbers) and the microbial activity phenomenon. Activity of residual cells post wash steps was used together with detached cells in order to determine the total number of mineral associated cells at any point in time. The total number of cells was similar across the wash steps at any point in time when IMC and detachment were integrated. The successful integration of IMC and detachment method is not only applicable to mineral surfaces with defined surface area as shown in this study but also has the potential to be successfully applied in tracking colonisation on agglomerated ore surfaces. Applying the detachment

method together with the IMC, it is possible to measure the metabolic activity of mineral associated communities as a function of the surface area of the mineral.

It was shown in this study that the mineral associated cells progressed both in terms of growth in microbial cell numbers and their activity across the three pyrite-containing mineral ores of varying grade. Mineral grade influenced microbial cell growth, performance and activity over time. Rapid microbial activity and performance was observed on the pyrite concentrate reaching a heat flow of 827 mW m^{-2}. On the same time point (day 20), the microbial culture associated with PEL-LS reached a heat flow rate of 293 mW m^{-2} and that associated with PEL-HS reached 157 mW m^{-2}. This demonstrated that the higher the sulfide content of the mineral, with low to no presence of instant neutralising minerals, the higher the chances of microbial attachment and subsequent colonisation that result in an accelerated facilitation of the leaching process. The impact of flow rate towards microbial adherence and colonisation of mineral surfaces was shown to vary with the sulfide content of the minerals. Firstly, at high flow rates (60 ml h^{-1}) changes in solution chemistry were insignificant in pyritic waste rocks with lower sulfide content. However, on pyrite concentrate, the change in solution chemistry was more pronounced at the same rate. Significant change in the solution chemistry was observed in the sulfide pyritic waste rocks (PEL-HS and PEL-LS) only when low flow rates of 4 ml h^{-1} were applied. This showed that microbial communities adhered more to minerals with higher sulfide content and that was evident through the accelerated facilitation of regeneration of Fe^{3+} observed in solution chemistry (redox potential and iron). On the mineral surface, the number of cells associated with the mineral surface increased with the activity up until day 12 were 2.2 × 10^{11} cells m^{-2} accounting for 16.7 % surface coverage and with a measured heat flow of 330.6 mW m^{-2}. However, on day 20, the number of enumerated attached cells was 1.42 10^{11} cells m^{-2} accounting for 10.7 % surface coverage. The marked decline in mineral associated cell numbers was complemented by the significant increase in metabolic activity (827 mW m^{-2}). The deviation between the number of cells and the associated activity was attributed to the formation of EPS that embedded cells within a matrix. When the same flow rate was applied on minerals with a lower sulfide content, no significant difference was observed. The measured microbial activity on the mineral surface of the two low sulfidic waste rocks was observed on day 30 as 157 mW m^{-2} measured on the PEL-HS and 293 mW m^{-2} on the PEL-LS. At lower flow rates of 4 ml h^{-1}, on day 30, 146 mW m^{-2} was measured for PEL-HS and 153 mW m^{-2} was measured for PEL-LS. The PEL-LS waste rock material had a lower neutralisation capacity than PEL-HS, thus more microbial activity was measured on PEL-LS. This showed that microbial colonisation of mineral surfaces and activity is dictated by the sulfide content, the gangue materials present and the flow rate of the irrigant.

Through microscopic visualisation studies, it was shown that mineral associated microbial communities become embedded in EPS as the flow-through experimental run progressed. Stemming from this, extraction and characterisation of EPS from mixed mesophilic cultures was carried out. For the first time in a complete flow-through, unsaturated system, EPS of mixed mesophilic cultures was successfully extracted, and its biochemical contents characterised. Capsular EPS fraction had a yield of 1.53 mg per 10^{10} cells with a closing mass balance; conversely, loosely bound EPS components extracted were erratic and the mss balance across these did not close. Similar to the EPS investigations reported in other mesophilic leaching systems, total carbohydrates (28.5 %) were the dominant component of the capsular EPS. DNA (27 %), iron (16.4 %) and lipids (4.2 %) were also present in the EPS. Sugar monomers identified in the extracted capsular EPS by GC-MS included galactose, fructose and trehalose. Galactose and fructose were consistent with EPS sugar monomers reported in batch bioleach environments. Sugar monomers from loosely bound were below the detection limit. Although trehalose have been reported elsewhere as an EPS component, it is yet to be reported in bioleach conditions. The successful identification and characterisation of EPS constituents in a flow-through system creates a potential of studying and understanding architectural and structural make-up of EPS during bioleach processes characterised by open, flow through systems and is recommended for further study.

The development of the flow-through experimental set-up using liberated mineral under defined surface area conditions provides a basis for the development of a feasibility test for optimum metal recovery from specific ores. Similarly, this set-up can be used to characterise waste rock for its acid generation capacity and metal mobilisation as the flow-through system allows the relative kinetics of acidification and neutralisation to be taken into account. This was demonstrated in the thesis through the development of the flow-through biokinetic test for ARD characterisation.

The further refinement of the UCT developed batch and semi batch biokinetic test for ARD characterisation into a flow-through biokinetic system that resembles a waste dump was demonstrated. The washout of neutralising agents at the early stages of the experimental run was demonstrated in the flow-through system and this allowed for a conducive environment for further microbial mineral interactions and thus leaching of the waste rock material. This is contrary to the batch biokinetic systems that retain the neutralising agents thus affecting the activity. Microbial-mineral interaction and subsequent colonisation, which is reported to play a significant role in the degradation of mineral surface and proliferation toxic metal(s) laden effluents, was shown in this study to proliferate with the progression of the test. Microbial growth and progression were demonstrated on PEL-HS and PEL-LS waste rock using irrigant flow rates of 60 ml h^{-1} and 4 ml h^{-1}. At a higher flow rate of 60 ml h^{-1} no significant changes

were observed in the solution chemistry of both waste rock effluents. However, at a lower flow rate of 4 ml h^{-1} there were more pronounced changes in the solution chemistry of the waste rock effluent. Despite this contrast, microbial association with the mineral surface and growth was evident under both conditions. This further demonstrated the importance of considering microbial mineral interactions in addition to effluent solution chemistry. The flow-through test together with the batch test and static test characterised both waste rock minerals as potentially acid forming material. Because mine waste rock stockpiles are in a form of a heap, the flow-through biokinetic better emulates the typical nature of a mine waste pile.

This study provided further insights into colonisation coupled with microbial growth, performance and activity in a heap bioleaching simulating environment. The refined IMC method was an appropriate tool to measure the activity of colonising microorganisms and that IMC could be applied in concert with traditional measuring techniques and detachment method to provide consolidated and more informed information on microbial-mineral interactions and colonisation over a period.

8.2 Recommendations

Adapting and furthering the information gathered from this thesis, which focused on studying microbial-mineral interaction and colonisation of mixed mesophilic cultures in flow-through conditions, future studies that would add value should include the decoupling of the contributions (activity, growth and performance) of iron oxidisers such as *L. ferriphillum* and sulfur oxidisers such as *At. caldus* to further understand their contributions as single strains as well in mixed cultures. Understanding how single strains interact and cooperate with one another in mixed microbial environments would allow for a clearer understanding of their functions and interactions with various mineral surfaces and thus assist in furthering the understanding of heap bioleaching.

The temperature of a typical bioheap progresses from ambient temperatures to an excess of 80 °C and during this period a succession in microbial dominance and performance is observed. With the demonstration in this study that EPS is secreted in open flow-through systems that resemble a bioheap and with the prevention of microbial cells from environmental harsh conditions such heat, being among the function of EPS, it would be beneficial to investigate the activity and growth of mesophilic strains across the temperature ranges as well as potential community shifts toward heterotrophs that can grow utilising EPS and/or dead cells. This will help understand if the contributions of mesophilic culture strains on increasing temperature as well as their behaviour in succession of microbial communities.

Ore samples in the form of fully liberated mineral particles that were coated onto glass spherical beads were packed in this study. This was done to provide a defined surface area and enable the study of colonisation and metabolic activity per surface area. Future studies should integrate related studies on whole ore with these studies, investigating microbial-mineral interactions in flow-through systems using crushed rock thus allowing both the kinetics of microbial growth activity and mineral sulfide dissolution as well as the impact of liberation of mineral grains to be studied. Further, focus on microbial-mineral interactions across various mineral types is proposed.

Microbial-mineral interactions were assessed in this study over a short period (30 days max). It would be beneficial to further refine the measuring of interactions in long term experimental runs. This could be done through measuring the activity of mineral associated microbial communities at various stages including single cells, colonies embedded in EPS, early developmental stages of a biofilm and a matured biofilm.

Post the 30 day experimental run in Chapter 7 significant amounts of sulfur content (Table 7.3) still remained unleached and this motivates for longer experimental runs to be conducted..

At the end of the experimental run (Chapter 5) during leaching of PEL-HS, EPS was extracted with its biochemical components analysed, in the flow-through system. Biochemical components have been shown to contribute to the structural and mechanical formation of the EPS and thus biofilm. The extension of the flow-through unsaturated runs with intermittent extraction of EPS is needed in order to gain insight on EPS formation as well as its biochemical components. The application of lectin screening is necessary to reconcile and consolidate the sugar monomer data obtained in this study. In a broader sense, it would be necessary to study EPS formation, structure and architecture as a function of temperature in succession studies. This is expected to shed light on the influence of EPS on creating a tailored leach environment.

The flow-through biokinetic system was demonstrated in this study as a possible tool to characterise mine waste material for their potential to form acid. Because this study was a first of its kind, waste rock minerals with higher sulfide mineral that were prewashed initially to initiate the neutralising reactions in order to provide a conducive environment for microorganisms to attach and colonise mineral surfaces. Future investigations should use waste rock material or coal waste with lower sulfide content and incorporate indigenous microorganisms to further refine the flow-through biokinetic system and explore its potential further.

References

Acosta, M., Galleguillos, P., Ghorbani, Y., Tapia, P., Contador, Y., Velásquez, A., Espoz, C., Pinilla, C., Demergasso, C., Variation in microbial community from predominantly mesophilic to thermotolerant and moderately thermophilic species in an industrial copper heap bioleaching operation. Hydrometallurgy, 2014, **150**, 281-289.

Africa, C.-J., 2009. Microbial attachment to sulfide minerals in a bioleach environment. University of Cape Town.

Africa, C.-J., 2017. Investigation of microbial metal-sulfide interfacial environments under mineral bioleach simulated conditions. University of Cape Town.

Africa, C.-J., Harrison, S.T.L., Becker, M., Hille, R.P.v., In situ investigation and visualisation of microbial attachment and colonisation in a heap bioleach environment: The novel biofilm reactor. Minerals Engineering, 2010, **23(6)**, 486-491.

Africa, C.-J., van Hille, R.P., Sand, W., Harrison, S.T.L., Investigation and in situ visualisation of interfacial interactions of thermophilic microorganisms with metal-sulphides in a simulated heap environment. Minerals Engineering, 2013a, **48**, 100-107.

Africa, C.J., van Hille, R.P., Harrison, S.T., Attachment of *Acidithiobacillus ferrooxidans* and *Leptospirillum ferriphilum* cultured under varying conditions to pyrite, chalcopyrite, low-grade ore and quartz in a packed column reactor. Applied Microbiology and Biotechnology, 2013b, **97(3)**, 1317-1324.

Aguilera, A., Souza-Egipsy, V., San Martin-Uriz, P., Amils, R., Extraction of extracellular polymeric substances from extreme acidic microbial biofilms. Applied Microbiology and Biotechnology, 2008, **78(6)**, 1079-1088.

Akcil, A., Koldas, S., Acid Mine Drainage (AMD): causes, treatment and case studies. Journal of Cleaner Production, 2006, **14(12-13)**, 1139-1145.

Apha, A., Standard methods for the examination of water and wastewater. 1998, **21**, 1378.

Bararunyeretse, P., Ji, H., Yao, J., Toxicity of nickel to soil microbial community with and without the presence of its mineral collectors-a calorimetric approach. Environmental Science and Pollution Research, 2017, **24(17)**, 15134-15147.

Barnes, H.L., Romberger, S.B., Chemical aspects of acid mine drainage. Journal of the Water Pollution Control Federation, 1968, **40(3)**, 371-384.

Bartlett, R.W., Simulation of ore heap leaching using deterministic models. Hydrometallurgy, 1992, **29(1-3)**, 231-260.

Bartlett, R.W., Metal extraction from ores by heap leaching. Metallurgical Materials Transactions B, 1997, **28(4)**, 529-545.

Becker, M., Dyantyi, N., Broadhurst, J.L., Harrison, S.T.L., Franzidis, J.P., A mineralogical approach to evaluating laboratory scale acid rock drainage characterisation tests. Minerals Engineering, 2015, **80**, 33-36.

Beech, I.B., Smith, J.R., Steele, A.A., Penegar, I., Campbell, S.A., The use of atomic force microscopy for studying interactions of bacterial biofilms with surfaces. Colloids surfaces B: Biointerfaces, 2002, **23(2-3)**, 231-247.

Bellenberg, S., Barthen, R., Boretska, M., Zhang, R., Sand, W., Vera, M., Manipulation of pyrite colonization and leaching by iron-oxidizing *Acidithiobacillus* species. Applied Microbiology and Biotechnology, 2015, **99(3)**, 1435-1449.

Bellenberg, S., Diaz, M., Noel, N., Sand, W., Poetsch, A., Guiliani, N., Vera, M., Biofilm formation, communication and interactions of leaching bacteria during colonization of pyrite and sulfur surfaces. Research in Microbiology, 2014, **165(9)**, 773-781.

Bellenberg, S., Leon-Morales, C.-F., Sand, W., Vera, M., Visualization of capsular polysaccharide induction in *Acidithiobacillus ferrooxidans*. Hydrometallurgy, 2012, **129-130**, 82-89.

Bhappu, R.B., Johnson, P.H., Brierley, J.A., Reynolds, D.H., Theoretical and practical studies on dump leaching. Transactions of the Metallurgical Society of AIME, 1969, **244**, 307-320.

Binning, G., Quate, C.F., Gerber, C., Atomic force microscope. Physical Review Letters, 1986.

Blight, K., Ralph, D., Effect of ionic strength on iron oxidation with batch cultures of chemolithotrophic bacteria. Hydrometallurgy, 2004, **73(3-4)**, 325-334.

Bond, P.L., Druschel, G.K., Banfield, J.F., Comparison of acid mine drainage microbial communities in physically and geochemically distinct ecosystems. Applied Environmental Microbiology, 2000, **66(11)**, 4962-4971.

Bradham, W.S., Caruccio, F.T., 1990. A comparative study of tailings analyses using acid/base accounting, cells, columns and soxhlets, In *Proceedings of the Mining and Reclamation Conference and Exhibition.* West Virginia University Publications Service, pp. 19-25.

Braissant, O., Keiser, J., Meister, I., Bachmann, A., Wirz, D., Gopfert, B., Bonkat, G., Wadso, I., Isothermal microcalorimetry accurately detects bacteria, tumorous microtissues, and parasitic worms in a label-free well-plate assay. Biotechnology Journal, 2015, **10(3)**, 460-468.

Braissant, O., Wirz, D., Gopfert, B., Daniels, A.U., Use of isothermal microcalorimetry to monitor microbial activities. FEMS Microbiology Letters, 2010, **303(1)**, 1-8.

Brandl, H., Microbial leaching of metals. Biotechnology 2001, **10**, 191-224.

Brantley, S.L., 2008. Kinetics of mineral dissolution, In *Kinetics of water-rock interaction*. Springer, pp. 151-210.

Brierley, C.L., How will biomining be applied in future? Trans Nonferrous Metals Society of China, 2008a, **18(6)**, 1302-1310.

Brierley, C.L., Brierley, J.A., Progress in bioleaching: part B: applications of microbial processes by the minerals industries. Applied Microbiology Biotechnology, 2013, **97(17)**, 7543-7552.

Brierley, J.A., A perspective on developments in biohydrometallurgy. Hydrometallurgy, 2008b, **94(1-4)**, 2-7.

Brierley, J.A., Brierley, C.L., Present and future commercial applications of biohydrometallurgy. Hydrometallurgy, 2001, **59(2-3)**, 233-239.

Brissova, M., Fowler, M.J., Nicholson, W.E., Chu, A., Hirshberg, B., Harlan, D.M., Powers, A.C., Assessment of human pancreatic islet architecture and composition by laser scanning confocal microscopy. Journal of Histochemistry and Cytochemistry, 2005, **53(9)**, 1087-1097.

Broadhurst, J.L., Bryan, C.G., Becker, M., Franzidis, J., Harrison, S., 2013. Characterising the acid generating potential of mine wastes by means of laboratory-scale static and biokinetic tests, In *International Mine Water Association*, ed. Brown, A., Figueroa, L. Wolkersdorfer. Reliable Mine Water Technology, Colorado, USA, pp. 275-281.

Bromfield, L., Africa, C.J., Harrison, S.T.L., van Hille, R.P., The effect of temperature and culture history on the attachment of *Metallosphaera hakonensis* to mineral sulfides with application to heap bioleaching. Minerals Engineering, 2011, **24(11)**, 1157-1165.

Bruynesteyn, A., Hackl, R.P., Evaluation of acid production potential of mining waste materials. Minerals and the Environment, 1982, **4(1)**, 5-8.

Bryan, C.G., Hallberg, K.B., Johnson, D.B., Mobilisation of metals in mineral tailings at the abandoned São Domingos copper mine (Portugal) by indigenous acidophilic bacteria. Hydrometallurgy, 2006, **83(1-4)**, 184-194.

Bryner, L.C., Walker, R.B., Palmer, R., Some factors influencing the biological and non-biological oxidation of sulfide minerals. Trans. Soc. Min. Eng. AIME, 1967, **238**, 56-65.

Buchholz, F., Harms, H., Maskow, T., Biofilm research using calorimetry--a marriage made in heaven? Biotechnology Journal, 2010, **5(12)**, 1339-1350.

Bustos, S., Castro, S., Montealegre, R., The Sociedad Minera Pudahuel bacterial thin-layer leaching process at Lo Aguirre. FEMS Microbiology Reviews, 1993, **11(1-3)**, 231-235.

Castro, C., Zhang, R., Liu, J., Bellenberg, S., Neu, T.R., Donati, E., Sand, W., Vera, M., Biofilm formation and interspecies interactions in mixed cultures of thermo-acidophilic archaea *Acidianus spp*. and *Sulfolobus metallicus*. Research in Microbiology, 2016, **167(7)**, 604-612.

Chen, B.W., Wen, J.K., Feasibility study on heap bioleaching of chalcopyrite. Rare Metals, 2013, **32(5)**, 524-531.

Chiume, R., Minnaar, S.H., Ngoma, I.E., Bryan, C.G., Harrison, S.T.L., Microbial colonisation in heaps for mineral bioleaching and the influence of irrigation rate. Minerals Engineering, 2012, **39**, 156-164.

Christensen, B.E., Characklis, W.G., Physical and chemical properties of biofilms. Biofilms, 1990, **93**, 130.

Clark, M.E., Batty, J.D., Van Buuren, C.B., Dew, D.W., Eamon, M.A., Biotechnology in minerals processing: Technological breakthroughs creating value. Hydrometallurgy, 2006, **83(1-4)**, 3-9.

Colmer, A.R., Hinkle, M.E., The role of microorganisms in acid mine drainage: A preliminary report. Science, 1947, **106(2751)**, 253-256.

Coram-Uliana, N.J., van Hille, R.P., Kohr, W.J., Harrison, S.T.L., Development of a method to assay the microbial population in heap bioleaching operations. Hydrometallurgy, 2006, **83(1-4)**, 237-244.

Córdoba, E.M., Muñoz, J.A., Blázquez, M.L., González, F., Ballester, A., Leaching of chalcopyrite with ferric ion. Part I: General aspects. Hydrometallurgy, 2008, **93(3-4)**, 81-87.

Córdoba, E.M., Muñoz, J.A., Blázquez, M.L., González, F., Ballester, A., Passivation of chalcopyrite during its chemical leaching with ferric ion at 68 °C. Minerals Engineering, 2009, **22(3)**, 229-235.

Costerton, J.W., Irvin, R.T., Cheng, K.J., The bacterial glycocalyx in nature and disease. Annual Reviews in Microbiology, 1981, **35(1)**, 299-324.

Costerton, J.W., Lewandowski, Z., Caldwell, D.E., Korber, D.R., Lappin-Scott, H.M., Micriobial Biofilms. 1995, **49(1)**, 711-745.

Coupland, K., Johnson, D.B., Geochemistry and microbiology of an impounded subterranean acidic water body at Mynydd Parys, Anglesey, Wales. Geobiology, 2004, **2(2)**, 77-86.

Cox, A., Bryan, C.G., 2017. Insights into heap bioleaching at the agglomerate-scale, In *Solid State Phenomena*. Trans Tech Publ, pp. 185-188.

Crundwell, F.K., How do bacteria interact with minerals? Hydrometallurgy, 2003, **71(1-2)**, 75-81.

Cuevas, C.H., Valenzuela, P.D.T., Strategies to capture biotechnology opportunities in Chile. Electronic Journal of Biotechnology, 2004, **7(2)**, 189-205.

D'Ayala, G., Malinconico, M., Laurienzo, P., marine derived polysaccharides for biomedical applications: Chemical modification approaches. Molecules, 2008, **13(9)**, 2069-2106.

Dahlberg, C., Linberg, C., Torsvik, V.L., Hermansson, M., Conjugative plasmids isolated from bacteria in marine environments show various degrees of homology to each other and are not closely related to well-characterized plasmids. Applied Environmental Microbiology, 1997, **63(12)**, 4692-4697.

de Andrade Lima, L.R.P., Liquid axial dispersion and holdup in column leaching. Minerals Engineering, 2006, **19(1)**, 37-47.

Delgado, M., Jerez, C., Toledo, H., 1995. In vitro expression of a *Leptospirillum ferroxidans* gene homologous to the tar Chemotactic receptor gene from *Escherichia coli*, In *Proceedings of the International Biohydrometallurgy symposium IBS-95*. Universidad de Chile, pp. 119-128.

Demergasso, C., Galleguillos, F., Soto, P., Serón, M., Iturriaga, V., Microbial succession during a heap bioleaching cycle of low grade copper sulfides. Hydrometallurgy, 2010, **104(3-4)**, 382-390.

Demergasso, C.S., Galleguillos P, P.A., Escudero G, L.V., Zepeda A, V.J., Castillo, D., Casamayor, E.O., Molecular characterization of microbial populations in a low-grade copper ore bioleaching test heap. Hydrometallurgy, 2005, **80(4)**, 241-253.

Devasia, P., Natarajan, K.A., Sathyanarayana, D.N., Rao, G.R., Surface chemistry of *Thiobacillus ferrooxidans* relevant to adhesion on mineral surfaces. Applied Environmental Microbiology, 1993, **59(12)**, 4051-4055.

Dew, D.W., Lawson, E.N., Broadhurst, J.L., 1997. The BIOX® process for biooxidation of gold-bearing ores or concentrates, In *Biomining*. Springer, pp. 45-80.

Dew, D.W., Rautenbach, G.F., Van Hille, R.P., Davis-Belmar, C.S., Harvey, I.J., Truelove, J.S., 2011. High temperature heap leaching of chalcopyrite: method of evaluation and process model validation, In *Proceedings of international conference on percolation leaching: The status globally and in Southern Africa*, pp. 201-218.

Dignac, M.-F., Urbain, V., Rybacki, D., Bruchet, A., Snidaro, D., Scribe, P., Chemical description of extracellular polymers: implication on activated sludge floc structure. Water Science Technology, 1998, **38(8-9)**, 45-53.

Dimitrijević, M., Kostov, A., Tasić, V., Milosević, N., Influence of pyrometallurgical copper production on the environment. Journal of Hazardous Materials, 2009, **164(2-3)**, 892-899.

Dixon, D.G., Analysis of heat conservation during copper sulphide heap leaching. Hydrometallurgy, 2000, **58(1)**, 27-41.

Dixon, S., Definition of economic optimum for the leaching of high acid-consuming copper ores. Mining, Metallurgy Exploration, 2004, **21(4)**, 198-201.

Dogan, N.M., Doganli, G.A., Dogan, G., Bozkaya, O., Characterization of Extracellular Polysaccharides (EPS) Produced by Thermal Bacillus and Determination of Environmental Conditions Affecting Exopolysaccharide Production International Journal of Environmental Research, 2015, **9(3)**, 1107-1116.

Dold, B., 2010. Basic concepts in environmental geochemistry of sulfidic mine-waste management, In *Waste management*. IntechOpen.

Dold, B., Acid rock drainage prediction: A critical review. Journal of Geochemical Exploration, 2017, **172**, 120-132.

Dold, B., Wade, C., Fontboté, L., Water management for acid mine drainage control at the polymetallic Zn–Pb–(Ag–Bi–Cu) deposit Cerro de Pasco, Peru. Journal of Geochemical Exploration, 2009, **100(2-3)**, 133-141.

Domic, E.M., 2007. A review of the development and current status of copper bioleaching operations in Chile: 25 years of successful commercial implementation, In *Biomining*. Springer, pp. 81-95.

Drake, B., Prater, C.B., Weisenhorn, A.L., Gould, S.A.C., Albrecht, T.R., Quate, C.F., Cannell, D.S., Hansma, H.G., Hansma, P.K., Imaging crystals, polymers, and processes in water with the atomic force microscope. Science, 1989, **243(4898)**, 1586-1589.

Druschel, G.K., Baker, B.J., Gihring, T.M., Banfield, J.F., Acid mine drainage biogeochemistry at Iron Mountain, California. Geochemical Transactions, 2004, **5(2)**, 13.

du Plessis, C.A., Batty, J.D., Dew, D.W., 2007. Commercial applications of thermophile bioleaching, In *Biomining*. Springer, pp. 57-80.

Dubois, M., Gilles, K.A., Hamilton, J.K., Rebers, P.A., Smith, F., Colorimetric method for determination of sugars and related substances. Analytical chemistry, 1956, **28(3)**, 350-356.

Dyantyi, N., 2014. Application of mineralogy in the interpretation of laboratory scale acid rock drainage (ARD) prediction tests: A Gold Case Study. University of Cape Town.

Echeverría-Vega, A., Demergasso, C.J.H., Copper resistance, motility and the mineral dissolution behavior were assessed as novel factors involved in bacterial adhesion in bioleaching. Hydrometallurgy, 2015, **157**, 107-115.

Edwards, K.J., Hu, B., Hamers, R.J., Banfield, J.F., A new look at microbial leaching patterns on sulfide minerals. FEMS microbiology ecology, 2001, **34(3)**, 197-206.

Egiebor, N.O., Oni, B., Acid rock drainage formation and treatment: a review. Asia-Pacific Journal of Chemical Engineering, 2007, **2(1)**, 47-62.

Elbein, A.D., Pan, Y.T., Pastuszak, I., Carroll, D., New insights on trehalose: a multifunctional molecule. Glycobiology, 2003, **13(4)**, 17R-27R.

Elberling, B., Schippers, A., Sand, W., Bacterial and chemical oxidation of pyritic mine tailings at low temperatures. Journal of Contaminant Hydrology, 2000, **41(3-4)**, 225-238.

Fagan, M.A., Ngoma, I.E., Chiume, R.A., Minnaar, S., Sederman, A.J., Johns, M.L., Harrison, S.T.L., MRI and gravimetric studies of hydrology in drip irrigated heaps and its effect on the propagation of bioleaching micro-organisms. Hydrometallurgy, 2014, **150**, 210-221.

Flemming, H.-C., Biofilms and environmental protection. Water Science Technology, 1993, **27(7-8)**, 1-10.

Flemming, H.-C., Wingender, J., The biofilm matrix. Nature Reviews Microbiology, 2010, **8(9)**, 623.

Flemming, H.-C., Wingender, J., Mayer, C., Korstgens, V., Borchard, W., 2000. Cohesiveness in biofilm matrix polymers, In *Symposia-Society for General Microbiology*. Cambridge; Cambridge University Press; 1999, pp. 87-106.

Florian, B., Noël, N., Thyssen, C., Felschau, I., Sand, W., Some quantitative data on bacterial attachment to pyrite. Minerals Engineering, 2011, **24(11)**, 1132-1138.

Fowler, T., Crundwell, F., Leaching of zinc sulfide by *Thiobacillus ferrooxidans*: bacterial oxidation of the sulfur product layer increases the rate of zinc sulfide dissolution at high concentrations of ferrous ions. Applied Environmental Microbiology, 1999, **65(12)**, 5285-5292.

Fowler, T.A., Holmes, P.R., Crundwell, F.K., Physiology and biotechnology-mechanism of pyrite dissolution in the presence of *Thiobacillus ferrooxidans*. Applied Environmental Microbiology, 1999, **65(7)**, 2987-2993.

Fowler, T.A., Holmes, P.R., Crundwell, F.K., On the kinetics and mechanism of the dissolution of pyrite in the presence of *Thiobacillus ferrooxidans*. Hydrometallurgy, 2001, **59(2-3)**, 257-270.

Franzmann, P.D., Haddad, C.M., Hawkes, R.B., Robertson, W.J., Plumb, J.J., Effects of temperature on the rates of iron and sulfur oxidation by selected bioleaching Bacteria and Archaea: application of the Ratkowsky equation. Minerals Engineering, 2005, **18(13-14)**, 1304-1314.

Gahan, C.S., Srichandan, H., Kim, D.-J., Akcil, A., Biohydrometallurgy and biomineral processing technology: A review on its past, present and future. Research Journal of Recent Sciences 2012, **2277**, 2502.

Gehrke, T., Hallmann, R., Kinzler, K., Sand, W., The EPS of *Acidithiobacillus ferrooxidans*-a model for structure-function relationships of attached bacteria and their physiology. Water Science Technology, 2001, **43(6)**, 159-167.

Gehrke, T., Hallmann, R., Sand, W., Importance of exopolymers from *Thiobacillus ferrooxidans* and *Leptospirillum ferrooxidans* for bioleaching. Biohydrometallurgical Processing, 1995, **1**, 1-11.

Gehrke, T., Telegdi, J., Thierry, D., Sand, W., Importance of extracellular polymeric substances from *Thiobacillus ferrooxidans* for bioleaching. Applied Environmental Microbiology, 1998, **64(7)**, 2743-2747.

Gericke, M., Review of the role of microbiology in the design and operation of heap bioleaching processes. Journal of the Southern African Institute of Mining Metallurgy, 2012, **112(12)**, 1005-1012.

Gericke, M., Muller, H.H., Neale, J.W., Norton, A.E., Crundwell, F.K., 2005. Inoculation of heap-leaching operations, In *Proceedings of the 16th international biohydrometallurgy symposium*. Cape Town, Compress, pp. 255-264.

Gericke, M., Neale, J.W., Van Staden, P.J., A Mintek perspective of the past 25 years in minerals bioleaching. Journal of the Southern African Institute of Mining Metallurgy, 2009, **109(10)**, 567-585.

Ghadiri, M., Harrison, S.T., Fagan-Endres, M.A., Influence of X-ray μ-Computed Tomography on the microbial activity of a mixed thermophilic and mesophilic bioleaching culture colonising a mineral surface. Biochemical Engineering Journal, 2018, **139**, 123-131.

Ghauri, A.M., Okibe, N., J.D., B., Attachment of acidophilic bacteria to solid surfaces: The significance of species and strain variations. Hydrometallurgy, 2007, **85(2-4)**, 72-80.

Ghorbani, Y., Franzidis, J.-P., Petersen, J., Heap leaching technology – current state, innovations and future directions: A review. Mineral Processing and Extractive Metallurgy Review, 2015.

Ghorbani, Y., Petersen, J., Harrison, S.T.L., Tupikina, O.V., Becker, M., Mainza, A.N., Franzidis, J.-P., An experimental study of the long-term bioleaching of large sphalerite ore particles in a circulating fluid fixed-bed reactor. Hydrometallurgy, 2012, **129-130**, 161-171.

Golela, M.T., 2018. Effect of microbial consortium on the biokinetic test for assessing acid rock drainage potential. Cape Peninsula University of Technology.

Golyshina, O.V., Yakimov, M.M., Lünsdorf, H., Ferrer, M., Nimtz, M., Timmis, K.N., Wray, V., Tindall, B.J., Golyshin, P.N., *Acidiplasma aeolicum* gen. nov., sp. nov., a euryarchaeon of the family *Ferroplasmaceae* isolated from a hydrothermal pool, and transfer of *Ferroplasma cupricumulans* to *Acidiplasma cupricumulans* comb. nov. International journal of systematic and evolutionary microbiology, 2009, **59(11)**, 2815-2823.

Gómez, E., Blazquez, M.L., Ballester, A., Gonzalez, F., Study by SEM and EDS of chalcopyrite bioleaching using a new thermophilic bacteria. Minerals Engineering, 1996, **9(9)**, 985-999.

González-Toril, E., Llobet-Brossa, E., Casamayor, E., Amann, R., Amils, R., Microbial ecology of an extreme acidic environment, the Tinto River. Applied and Environmental Microbiology, 2003, **69(8)**, 4853-4865.

González, D.M., Lara, R.H., Alvarado, K.N., Valdez-Pérez, D., Navarro-Contreras, H.R., Cruz, R., García-Meza, J.V., Evolution of biofilms during the colonization process of pyrite by *Acidithiobacillus thiooxidans*. Applied Microbiology Biotechnology, 2012, **93(2)**, 763-775.

Goodman, A., Ralph, B., 1980. A microcalorimetric study of the metabolic activity of two *Thiobacillus* species, In *Biogeochemistry of Ancient and Modern Environments*. Springer, pp. 477-483.

Govender, E., Bryan, C.G., Harrison, S.T.L., Quantification of growth and colonisation of low grade sulphidic ores by acidophilic chemoautotrophs using a novel experimental system. Minerals Engineering, 2013, **48**, 108-115.

Govender, E., Bryan, C.G., Harrison, S.T.L., Effect of physico-chemical and operating conditions on the growth and activity of *Acidithiobacillus ferrooxidans* in a simulated heap bioleaching environment. Minerals Engineering, 2015, **75**, 14-25.

Govender, E., Kotsiopoulos, A., Bryan, C.G., Harrison, S.T.L., Modelling microbial transport in simulated low-grade heap bioleaching systems: The biomass transport model. Hydrometallurgy, 2014, **150**, 299-307.

Govender, Y., Gericke, M., Extracellular polymeric substances (EPS) from bioleaching systems and its application in bioflotation. Minerals Engineering, 2011, **24(11)**, 1122-1127.

Gray, N.F., Field assessment of acid mine drainage contamination in surface and ground water. Environmental Geology, 1996, **27(4)**, 358-361.

Griffiths, M., Van Hille, R., Harrison, S., Selection of direct transesterification as the preferred method for assay of fatty acid content of microalgae. Lipids, 2010, **45(11)**, 1053-1060.

Harneit, K., Göksel, A., Kock, D., Klock, J.H., Gehrke, T., Sand, W., Adhesion to metal sulfide surfaces by cells of *Acidithiobacillus ferrooxidans*, *Acidithiobacillus thiooxidans* and *Leptospirillum ferrooxidans*. Hydrometallurgy, 2006, **83(1-4)**, 245-254.

Harrison, S.T., Franzidis, J., van Hille, R.P., Mokone, T., Broadhurst, J.L., Mbamba, C.K., Opitz, A., Chiume, R., Vries, E., Stander, H.-M., 2013. Evaluating approaches to and benefits of minimising the

formation of acid rock drainage through management of the disposal of sulphidic waste rock and tailings, ed. Commission, W.R., Pretoria.

Harvey, T.J., Bath, M., 2007. The GeoBiotics GEOCOAT® Technology–progress and challenges, In *Biomining*. Springer, pp. 97-112.

Hawkes, R.B., Franzmann, P.D., O'hara, G., Plumb, J.J., *Ferroplasma cupricumulans* sp. nov., a novel moderately thermophilic, acidophilic archaeon isolated from an industrial-scale chalcocite bioleach heap. Extremophiles, 2006, **10(6)**, 525-530.

Hedrich, S., Guezennec, A.G., Charron, M., Schippers, A., Joulian, C., Quantitative monitoring of microbial species during bioleaching of a copper concentrate. Frontiers in Microbiology, 2016, **7**, 2044.

Hedrich, S., Joulian, C., Graupner, T., Schippers, A., Guézennec, A.-G., Enhanced chalcopyrite dissolution in stirred tank reactors by temperature increase during bioleaching. Hydrometallurgy, 2018, **179**, 125-131.

Hesketh, A.H., Broadhurst, J.L., Bryan, C.G., van Hille, R.P., Harrison, S.T.L., Biokinetic test for the characterisation of AMD generation potential of sulfide mineral wastes. Hydrometallurgy, 2010, **104(3-4)**, 459-464.

Hlongwane, P., 2015. The influence of solid loading and particle size on the characterisation of sulphide containing ores using the Biokinetic test. University of Cape Town.

Holmes, P., Fowler, T., Crundwell, F., The mechanism of bacterial action in the leaching of pyrite by *Thiobacillus ferrooxidans*. An electrochemical study. Journal of the Electrochemical Society, 1999, **146(8)**, 2906-2912.

Jerez, C.A., Chemotactic transduction in biomining microorganisms. Hydrometallurgy, 2001, **59(2-3)**, 347-356.

Jiao, Y., Cody, G.D., Harding, A.K., Wilmes, P., Schrenk, M., Wheeler, K.E., Banfield, J.F., Thelen, M.P., Characterization of extracellular polymeric substances from acidophilic microbial biofilms. Applied and Environmental Microbiology, 2010, **76(9)**, 2916-2922.

Johnson, D., 2009. Extremophiles: acidic environments, In *The Desk Encyclopedia of Microbiology*. Academic Press of Elsevier Oxford, pp. 463-482.

Johnson, D.B., Biodiversity and interactions of acidophiles: Key to understanding and optimizing microbial processing of ores and concentrates. Transactions of Nonferrous Metals Society of China, 2008, **18(6)**, 1367-1373.

Johnson, D.B., Okibe, N., Hallberg, K.B., Differentiation and identification of iron-oxidizing acidophilic bacteria using cultivation techniques and amplified ribosomal DNA restriction enzyme analysis. Journal of Microbiological Methods, 2005, **60(3)**, 299-313.

Jones, G.C., van Hille, R.P., Harrison, S.T., Reactive oxygen species generated in the presence of fine pyrite particles and its implication in thermophilic mineral bioleaching. Applied Microbiology and Biotechnology, 2013, **97(6)**, 2735-2742.

Jordan, M.A., 1993. The oxidation of base metal sulphides and pyritic gold concentrates with particular reference to mechanism and preferential release of ferrous iron. University of Exeter.

Kalinkin, A., Kalinkina, E., Vasil'eva, T., Effect of mechanical activation on sphene reactivity. Colloid Journal, 2004, **66(2)**, 160-167.

Kappes, D.W., 2002. Precious metal heap leach design and practice, In *Proceedings of the Mineral Processing Plant Design, Practice, Control*, pp. 1606-1630.

Kawabe, Y., Inoue, C., Suto, K., Chida, T., Inhibitory effect of high concentrations of ferric ions on the activity of *Acidithiobacillus ferrooxidans*. Journal of Bioscience Bioengineering 2003, **96(4)**, 375-379.

Kelly, D.P., Wood, A.P., Reclassification of some species of *Thiobacillus* to the newly designated genera *Acidithiobacillus* gen. nov., *Halothiobacillus* gen. nov. and *Thermithiobacillus* gen. nov. International Journal of Systematic and Evolutionary Microbiology, 2000, **50(2)**, 511-516.

Kinzler, K., Gehrke, T., Telegdi, J., Sand, W., Bioleaching—a result of interfacial processes caused by extracellular polymeric substances (EPS). Hydrometallurgy, 2003, **71(1-2)**, 83-88.

Kock, D., Schippers, A., Geomicrobiological investigation of two different mine waste tailings generating acid mine drainage. Hydrometallurgy, 2006, **83(1-4)**, 167-175.

Koerdt, A., Gödeke, J., Berger, J., Thormann, K.M., Albers, S.-V., Crenarchaeal biofilm formation under extreme conditions. PloS One, 2010, **5(11)**, e14104.

Koleini, S.J., Aghazadeh, V., Sandström, Å., Acidic sulphate leaching of chalcopyrite concentrates in presence of pyrite. Minerals Engineering, 2011, **24(5)**, 381-386.

Kolmert, s., Johnson, D.B., Remediation of acidic waste waters using immobilised, acidophilic sulfate-reducing bacteria. Journal of Chemical Technology & Biotechnology, 2001, **76(8)**, 836-843.

König, R., Winkler, G., C. Plinius secundus d. Ä. Naturkunde, 1989, **37**, 1990-2004.

Krok, B., Schippers, A., Sand, W., 2013. Copper recovery by bioleaching of chalcopyrite: A microcalorimetric approach for the fast determination of bioleaching activity, In *Advanced Materials Research*. Trans Tech Publ, pp. 322-325.

Krok, B.A., 2016. Microcalorimetric Investigations on Copper Sulfide Bioleaching.

Langmuir, D., Aqueous environmental. Geochemistry Prentice Hall: Upper Saddle River, NJ, 1997.

Lapakko, K., Metal mine rock and waste characterization tools: an overview. Mining, Minerals Sustainable Development, 2002, **67**, 1-30.

Lawrence, R., Wang, Y., Determination of neutralization potential for acid rock drainage prediction. MEND project, 1996, **1(3)**, 38.

Lebaron, P., Bauda, P., Frank, N., Lett, M., Roux, B., Hubert, J., Duval-Iflah, Y., Simonet, P., Faurie, G., Normand, P., Recombinant plasmid mobilization between *E. coli* strains in seven sterile microcosms. Canadian Journal of Microbiology, 1997, **43(6)**, 534-540.

Lei, J., Huaiyang, Z., Xiaotong, P., Zhonghao, D., The use of microscopy techniques to analyze microbial biofilm of the bio-oxidized chalcopyrite surface. Minerals Engineering, 2009, **22(1)**, 37-42.

Li, Q., Becker, T., Sand, W., Quantification of cell-substratum interactions by atomic force microscopy. Colloids and Surfaces B: Biointerfaces, 2017, **159**, 639-643.

Li, Q., Becker, T., Zhang, R., Xiao, T., Sand, W., Investigation on adhesion of *Sulfobacillus thermosulfidooxidans* via atomic force microscopy equipped with mineral probes. Colloids Surf B Biointerfaces, 2019, **173**, 639-646.

Li, Q., Sand, W., Mechanical and chemical studies on EPS from *Sulfobacillus thermosulfidooxidans:* from planktonic to biofilm cells. Colloids Surf B Biointerfaces, 2017, **153**, 34-40.

Li, Q., Sand, W., Zhang, R., Enhancement of biofilm formation on pyrite by *Sulfobacillus thermosulfidooxidans*. Minerals, 2016, **6(3)**.

Liu, H., Gu, G., Xu, Y., Surface properties of pyrite in the course of bioleaching by pure culture of *Acidithiobacillus ferrooxidans* and a mixed culture of *Acidithiobacillus ferrooxidan*s and *Acidithiobacillus thiooxidans*. Hydrometallurgy, 2011, **108(1-2)**, 143-148.

Liu, H.L., Chen, B.Y., Lan, Y.W., Cheng, Y.C., SEM and AFM images of pyrite surfaces after bioleaching by the indigenous *Thiobacillus thiooxidans*. Applied Microbiology and Biotechnology, 2003, **62(4)**, 414-420.

Liu, R., Chen, J., Zhou, W., Cheng, H., Zhou, H., Insight to the early-stage adsorption mechanism of moderately thermophilic consortia and intensified bioleaching of chalcopyrite. Biochemical Engineering Journal, 2019, **144**, 40-47.

Lizama, H.M., Copper bioleaching behaviour in an aerated heap. International Journal of Mineral Processing, 2001, **62(1-4)**, 257-269.

Lorenz, M.G., Wackernagel, W., Bacterial gene transfer by natural genetic transformation in the environment. Microbiology and Molecular Biology Reviews, 1994, **58(3)**, 563-602.

Ma, S., Banfield, J.F., Micron-scale Fe^{2+}/Fe^{3+}, intermediate sulfur species and O_2 gradients across the biofilm–solution–sediment interface control biofilm organization. Geochimica et Cosmochimica Acta, 2011, **75(12)**, 3568-3580.

Makaula, D.X., Huddy, R.J., Fagan-Endres, M.A., Harrison, S.T.L., Using isothermal microcalorimetry to measure the metabolic activity of the mineral-associated microbial community in bioleaching. 2017, **106**, 33-38.

Mangold, S., Harneit, K., Rohwerder, T., Claus, G., Sand, W., Novel combination of atomic force microscopy and epifluorescence microscopy for visualization of leaching bacteria on pyrite. Applied and Environmental Microbiology, 2008a, **74(2)**, 410-415.

Mangold, S., Laxander, M., Harneit, K., Rohwerder, T., Claus, G., Sand, W., Visualization of *Acidithiobacillus ferrooxidans* biofilms on pyrite by atomic force and epifluorescence microscopy under various experimental conditions. Hydrometallurgy, 2008b, **94(1-4)**, 127-132.

Marín, S., Acosta, M., Galleguillos, P., Chibwana, C., Strauss, H., Demergasso, C.J.H., Is the growth of microorganisms limited by carbon availability during chalcopyrite bioleaching? , 2017, **168**, 13-20.

Markosyan, L., Badalyan, H., Vardanyan, N., Vardanyan, A., Study of colloidal polysaccharides produced by iron oxidizing bacteria *Leptospirillum ferriphilum* CC. Geomicrobiology Journal, 2019, **36(2)**, 188-193.

Michel, C., Beny, C., Delorme, F., Poirier, L., Spolaore, P., Morin, D., d'Hugues, P., New protocol for the rapid quantification of exopolysaccharides in continuous culture systems of acidophilic bioleaching bacteria. Applied Microbiology and Biotechnology, 2009, **82(2)**, 371-378.

Miller, J.D., Lin, C.L., Garcia, C., Arias, H., Ultimate recovery in heap leaching operations as established from mineral exposure analysis by X-ray microtomography. International Journal of Mineral Processing, 2003, **72(1-4)**, 331-340.

Montanaro, L., Poggi, A., Visai, L., Ravaioli, S., Campoccia, D., Speziale, P., Arciola, C.R.J.T.I.j.o.a.o., Extracellular DNA in biofilms. 2011, **34(9)**, 824-831.

Morin, K.A., Hutt, N.M., 1998. Kinetic tests and risk assessment for ARD, In *Fifth Annual British Columbia Metal Leaching and ARD Workshop*, pp. 9-10.

Müller, D., Schabert, F.A., Büldt, G., Engel, A., Imaging purple membranes in aqueous solutions at sub-nanometer resolution by atomic force microscopy. Biophysical Journal, 1995, **68(5)**, 1681-1686.

Munoz, J., Gonzalez, F., Blazquez, M., Ballester, A., A study of the bioleaching of a Spanish uranium ore. Part I: A review of the bacterial leaching in the treatment of uranium ores. Hydrometallurgy, 1995, **38(1)**, 39-57.

Murr, L., Brierley, J.A., 1978. The use of large-scale test facilities in studies of the role of microorganisms in commercial leaching operations, In *Metallurgical applications of bacterial leaching and related microbiological phenomena*. Elsevier, pp. 491-520.

Mutch, L.A., Watling, H.R., Watkin, E.L.J., Microbial population dynamics of inoculated low-grade chalcopyrite bioleaching columns. Hydrometallurgy, 2010, **104(3-4)**, 391-398.

Neu, T.R., Lawrence, J.R., Development and structure of microbial biofilms in river water studied by confocal laser scanning microscopy. FEMS Microbiology Ecology, 1997, **24(1)**, 11-25.

Neu, T.R., Lawrence, J.R., 1999. [10] Lectin-binding analysis in biofilm systems, In *Methods in enzymology*. Elsevier, pp. 145-152.

Neu, T.R., Swerhone, G.D., Lawrence, J.R., Assessment of lectin-binding analysis for in situ detection of glycoconjugates in biofilm systems. Microbiology, 2001, **147(2)**, 299-313.

Ngoma, E.I., Ojumu, T.V., Harrison, S.T.L., Investigating the effect of acid stress on selected mesophilic micro-organisms implicated in bioleaching. Minerals Engineering, 2015, **75**, 6-13.

Ngulube, Q., 2013. Growth of mixed culture of moderate thermophiles for commercial heap bioleaching of low-grade copper sulphide ores. University of Cape Town.

Nielsen, P.H., Jahn, A., 1999. Extraction of EPS, In *Microbial extracellular polymeric substances*. Springer, pp. 49-72.

Nkulu, G., Gaydardzhiev, S., Mwema, E., Compere, P., SEM and EDS observations of carrollite bioleaching with a mixed culture of acidophilic bacteria. Minerals Engineering, 2015, **75**, 70-76.

Noël, N., Florian, B., Sand, W., AFM & EFM study on attachment of acidophilic leaching organisms. Hydrometallurgy, 2010, **104(3-4)**, 370-375.

Norris, P.R., 2007. Acidophile diversity in mineral sulfide oxidation, In *Biomining*. Springer, pp. 199-216.

Novo, M.T.M., De Souza, A.P., Garcia Jr, O., Ottoboni, L.M., RAPD genomic fingerprinting differentiates *Thiobacillus ferrooxidans* strains. Systematic Applied Microbiology and Biotechnology, 1996, **19(1)**, 91-95.

O'Kane, M., Barbour, S., Haug, M., 1999. A framework for improving the ability to understand and predict the performance of heap leach piles, In *Copper*, pp. 10-13.

Ohmura, N., Kitamura, K., Saiki, H., Selective adhesion of *Thiobacillus ferrooxidans* to pyrite. Applied and Environmental Microbiology, 1993, **59(12)**, 4044-4050.

Okibe, N., Gericke, M., Hallberg, K.B., Johnson, D.B., Enumeration and characterization of acidophilic microorganisms isolated from a pilot plant stirred-tank bioleaching operation. Applied and Environmental Microbiology, 2003, **69(4)**, 1936-1943.

Okibe, N., Johnson, D.B., Biooxidation of pyrite by defined mixed cultures of moderately thermophilic acidophiles in pH-controlled bioreactors: Significance of microbial interactions. Biotechnology bioengineering, 2004, **87(5)**, 574-583.

Olson, G.J., Brierley, J.A., Brierley, C.L., Bioleaching review part B. Applied Microbiology and Biotechnology, 2003, **63(3)**, 249-257.

Opitz, A.K.B., 2013. An investigation into accelerated leaching for the purpose of ARD mitigation. University of Cape Town.

Opitz, A.K.B., Becker, M., Broadhurst, J.L., Bradshaw, D.J., Harrison, S.T.L., 2016. The biokinetic test as a geometallurgical indicator for acid rock drainage potentials., In *The third ausimm international geometallurgy conference, Perth, WA*, p. 16.

Opitz, A.K.B., Harrison, S.T.L., 2016. Effect of Inoculum concentration on the Biokinetic tests for characterising ARD. , In *Biohydrometallurgy '16*, Falmouth, United Kingdom.

Orell, A., Navarro, C.A., Arancibia, R., Mobarec, J.C., Jerez, C.A., Life in blue: copper resistance mechanisms of bacteria and archaea used in industrial biomining of minerals. Biotechnology Advances, 2010, **28(6)**, 839-848.

Ozturk, S., Aslim, B., Suludere, Z., Tan, S., Metal removal of cyanobacterial exopolysaccharides by uronic acid content and monosaccharide composition. Carbohydrate Polymers, 2014, **101**, 265-271.

Panda, S., Akcil, A., Pradhan, N., Deveci, H., Current scenario of chalcopyrite bioleaching: a review on the recent advances to its heap-leach technology. Bioresource Technology, 2015, **196**, 694-706.

Panda, S., Sanjay, K., Sukla, L., Pradhan, N., Subbaiah, T., Mishra, B., Prasad, M., Ray, S., Insights into heap bioleaching of low grade chalcopyrite ores—A pilot scale study. Hydrometallurgy, 2012, **125**, 157-165.

Parbhakar-Fox, A., 2012. Establishing the value of an integrated geochemistry-mineralogy-texture approach for acid rock drainage prediction. University of Tasmania.

Parbhakar-Fox, A., Lottermoser, B.G., A critical review of acid rock drainage prediction methods and practices. Minerals Engineering, 2015, **82**, 107-124.

Petersen, J., Dixon, D., Thermophilic heap leaching of a chalcopyrite concentrate. Minerals Engineering, 2002, **15(11)**, 777-785.

Petersen, J., Dixon, D.G., Competitive bioleaching of pyrite and chalcopyrite. Hydrometallurgy, 2006, **83(1-4)**, 40-49.

Petersen, J., Dixon, D.G., 2007a. Modeling and optimization of heap bioleach processes, In *Biomining*. Springer, pp. 153-176.

Petersen, J., Dixon, D.G., 2007b. Principles, mechanisms and dynamics of chalcocite heap bioleaching, In *Microbial Processing of Metal Sulfides*, pp. 193-218.

Petersen, J., Minnaar, S., du Plessis, C., Carbon dioxide and oxygen consumption during the bioleaching of a copper ore in a large isothermal column. Hydrometallurgy, 2010, **104(3-4)**, 356-362.

Plumb, J.J., Hawkes, R.B., Franzmann, P.D., 2007. The microbiology of moderately thermophilic and transiently thermophilic ore heaps, In *Biomining*. Springer, pp. 217-235.

Pradhan, N., Nathsarma, K.C., Srinivasa Rao, K., Sukla, L.B., Mishra, B.K., Heap bioleaching of chalcopyrite: A review. Minerals Engineering, 2008, **21(5)**, 355-365.

Purevdorj-Gage, L., Stoodley, P., Hydrodynamic considerations of biofilm structure and behavior. Microbial Biofilms, 2004.

Quatrini, R., Valdés, J., Jedlicki, E., Holmes, D.S., 2007. The use of bioinformatics and genome biology to advance our understanding of bioleaching microorganisms, In *Microbial Processing of Metal Sulfides*. Springer, pp. 221-239.

Ramirez-Aldaba, H., Vazquez-Arenas, J., Sosa-Rodriguez, F.S., Valdez-Perez, D., Ruiz-Baca, E., Garcia-Meza, J.V., Trejo-Cordova, G., Lara, R.H., Assessment of biofilm changes and concentration-depth profiles during arsenopyrite oxidation by *Acidithiobacillus thiooxidans*. Environmental Science and Pollution Research, 2017, **24(24)**, 20082-20092.

Ratner, B.D., Hoffman, A.S., Schoen, F.J., Lemons, J.E., *Biomaterials science: an introduction to materials in medicine*. 2004, Elsevier.

Rawlings, D., Tributsch, H., Hansford, G., Reasons why '*Leptospirillum*'-like species rather than *Thiobacillus ferrooxidans* are the dominant iron-oxidizing bacteria in many commercial processes for the biooxidation of pyrite and related ores. Microbiology, 1999, **145(1)**, 5-13.

Rawlings, D.E., Heavy metal mining using microbes. Annual Review of Microbiology, 2002, **56**, 65-91.

Rawlings, D.E., Characteristics and adaptability of iron- and sulfur-oxidizing microorganisms used for the recovery of metals from minerals and their concentrates. Microbial Cell Factories, 2005, **4(1)**, 13.

Rawlings, D.E., Dew, D., du Plessis, C., Biomineralization of metal-containing ores and concentrates. Trends in Biotechnology, 2003, **21(1)**, 38-44.

Rawlings, D.E., Johnson, D.B., The microbiology of biomining: development and optimization of mineral-oxidizing microbial consortia. Microbiology, 2007, **153(Pt 2)**, 315-324.

Remonsellez, F., Galleguillos, F., Moreno-Paz, M., Parro, V., Acosta, M., Demergasso, C., Dynamic of active microorganisms inhabiting a bioleaching industrial heap of low-grade copper sulfide ore monitored by real-time PCR and oligonucleotide prokaryotic acidophile microarray. Microbial biotechnology, 2009, **2(6)**, 613-624.

Renman, R., Jiankang, W., Jinghe, C., Bacterial heap-leaching: Practice in Zijinshan copper mine. Hydrometallurgy, 2006, **83(1-4)**, 77-82.

Ritchie, A., Sulfide oxidation mechanisms: controls and rates of oxygen transport. The Environmental Geochemistry of Sulfide Mine Wastes, 1994, 201-245.

Roberto, F.F., 16S-rRNA gene-targeted amplicon sequence analysis of an enargite-dominant bioleach demonstration in Peru. Hydrometallurgy, 2018, **180**, 271-276.

Robertson, S., Van Staden, P., Vercuil, A., Glover, G., Shaidaee, B., 2007. Heap bioleaching of low-grade chalcopyrite ore from the Darehzare deposit, In *ALTA*.

Rodríguez, Y., Ballester, A., Blázquez, M.L., González, F., Muñoz, J.A., Study of Bacterial Attachment During the Bioleaching of Pyrite, Chalcopyrite, and Sphalerite. Geomicrobiology Journal, 2003, **20(2)**, 131-141.

Rodríguez, Y., Ballester, A., Blázquez, M.L., González, F., Muñoz, J.A., New information on the chalcopyrite bioleaching mechanism at low and high temperature. Hydrometallurgy, 2003, **71(1-2)**, 47-56.

Rohwerder, T., 1995. Entwicklung eines kalorimetrischen Aktivitätstestes zur Quantifizierung der Schwermetallmobilisierung durch acidophile Bakterien.

Rohwerder, T., Gehrke, T., Kinzler, K., Sand, W., Bioleaching review part A: progress in bioleaching: fundamentals and mechanisms of bacterial metal sulfide oxidation. Applied Microbiology and Biotechnology, 2003, **63(3)**, 239-248.

Rohwerder, T., Sand, W., 2007. Mechanisms and biochemical fundamentals of bacterial metal sulfide oxidation, In *Microbial processing of metal sulfides*. Springer, pp. 35-58.

Rohwerder, T., Schippers, A., Sand, W., Determination of reaction energy values for biological pyrite oxidation by calorimetry. Thermochimica acta, 1998, **309(1-2)**, 79-85.

Rojas-Chapana, J., Bärtels, C., Pohlmann, L., Tributsch, H., Co-operative leaching and chemotaxis of *thiobacilli* studied with spherical sulphur/sulphide substrates. Process Biochemistry, 1998, **33(3)**, 239-248.

Romero, J., Yañez, C., Vásquez, M., Moore, E.R., Espejo, R.T., Characterization and identification of an iron-oxidizing, *Leptospirillum*-like bacterium, present in the high sulfate leaching solution of a commercial bioleaching plant. Research in microbiology, 2003, **154(5)**, 353-359.

Ruan, R., Liu, X., Zou, G., Chen, J., Wen, J., Wang, D., Industrial practice of a distinct bioleaching system operated at low pH, high ferric concentration, elevated temperature and low redox potential for secondary copper sulfide. Hydrometallurgy, 2011, **108(1-2)**, 130-135.

Ruan, R., Zou, G., Zhong, S., Wu, Z., Chan, B., Wang, D., Why Zijinshan copper bioheapleaching plant works efficiently at low microbial activity–Study on leaching kinetics of copper sulfides and its implications. Minerals Engineering, 2013, **48**, 36-43.

Ruihua, L., Lin, Z., Tao, T., Bo, L., Phosphorus removal performance of acid mine drainage from wastewater. Journal of hazardous materials, 2011, **190(1-3)**, 669-676.

Russel, M., Yao, J., Chen, H., Wang, F., Zhou, Y., Choi, M.M., Zaray, G., Trebse, P., Different technique of microcalorimetry and their applications to environmental sciences: A review. Journal of American Science, 2009, **5**, 194-208.

Sakamoto, T., Kumihashi, K., Kunita, S., Masaura, T., Inoue-Sakamoto, K., Yamaguchi, M., The extracellular-matrix-retaining cyanobacterium Nostoc verrucosum accumulates trehalose, but is sensitive to desiccation. FEMS Microbiology Ecology, 2011, **77(2)**, 385-394.

Sampson, M., Phillips, C., Blake II, R., Influence of the attachment of acidophilic bacteria during the oxidation of mineral sulfides. Minerals Engineering, 2000, **13(4)**, 373-389.

Sand, W., Gehrke, T., 1999. Analysis and Function of the EPS from the Strong Acidophile *Thiobacillus ferrooxidans*, In *Microbial Extracellular Polymeric Substances: Characterization, Structure and Function*, eds. Wingender, J., Neu, T.R., Flemming, H.-C. Springer Berlin Heidelberg, Berlin, Heidelberg, pp. 127-141.

Sand, W., Gehrke, T., Extracellular polymeric substances mediate bioleaching/biocorrosion via interfacial processes involving iron(III) ions and acidophilic bacteria. Research in Microbiology, 2006, **157(1)**, 49-56.

Sand, W., Gehrke, T., Jozsa, P.-G., Schippers, A., (Bio) chemistry of bacterial leaching—direct vs. indirect bioleaching. Hydrometallurgy, 2001, **59(2-3)**, 159-175.

Sand, W., Gerke, T., Hallmann, R., Schippers, A., Sulfur chemistry, biofilm, and the (in) direct attack mechanism—a critical evaluation of bacterial leaching. Applied Microbiology and Biotechnology, 1995, **43(6)**, 961-966.

Sand, W., Jozsa, P.-G., Kovacs, Z.-M., Săsăran, N., Schippers, A., Long-term evaluation of acid rock drainage mitigation measures in large lysimeters. Journal of Geochemical Exploration, 2007, **92(2-3)**, 205-211.

Sanhueza, A., Ferrer, I., Vargas, T., Amils, R., Sánchez, C., Attachment of *Thiobacillus ferrooxidans* on synthetic pyrite of varying structural and electronic properties. Hydrometallurgy, 1999, **51(1)**, 115-129.

Sapsford, D.J., Bowell, R., Dey, M., Williams, K.P., Humidity cell tests for the prediction of acid rock drainage. Minerals Engineering, 2009, **22(1)**, 25-36.

Schabert, F.A., Henn, C., Engel, A., Native *Escherichia coli* OmpF porin surfaces probed by atomic force microscopy. Science, 1995, **268(5207)**, 92-94.

Schippers, A., *Untersuchungen zur Schwefelchemie der biologischen Laugung von Metallsulfiden*. 1998, Shaker.

Schippers, A., 2007. Microorganisms involved in bioleaching and nucleic acid-based molecular methods for their identification and quantification, In *Microbial processing of metal sulfides*. Springer, pp. 3-33.

Schippers, A., Bosecker, K., 2005. Bioleaching, In *Microbial Processes and Products*. Springer, pp. 405-412.

Schippers, A., Hedrich, S., Vasters, J., Drobe, M., Sand, W., Willscher, S., 2014. biomining: metal recovery from ores with microorganisms, In *Geobiotechnology I: Metal-related Issues*, eds. Schippers, A., Glombitza, F., Sand, W. Springer Berlin Heidelberg, Berlin, Heidelberg, pp. 1-47.

Schippers, A., Jozsa, P.-G., Kovacs, Z.M., Jelea, M., Sand, W., Large-scale experiments for microbiological evaluation of measures for safeguarding sulfidic mine waste. Waste Management, 2001, **21(2)**, 139-146.

Schippers, A., Jozsa, P.-G., Sand, W., Evaluation of the efficiency of measures for sulphidic mine waste mitigation. Applied Microbiology Biotechnology, 1998, **49(6)**, 698-701.

Schippers, A., Jozsa, P.-G., Sand, W., Kovacs, Z.M., Jelea, M., Microbiological pyrite oxidation in a mine tailings heap and its relevance to the death of vegetation. Geomicrobiology Journal, 2000, **17(2)**, 151-162.

Schippers, A., Kock, D., Schwartz, M., Böttcher, M.E., Vogel, H., Hagger, M., Geomicrobiological and geochemical investigation of a pyrrhotite-containing mine waste tailings dam near Selebi-Phikwe in Botswana. Journal of Geochemical Exploration, 2007, **92(2-3)**, 151-158.

Schippers, A., Rohwerder, T., Sand, W., Intermediary sulfur compounds in pyrite oxidation: implications for bioleaching and biodepyritization of coal. Applied Microbiology Biotechnology, 1999, **52(1)**, 104-110.

Schippers, A., Sand, W., Bacterial leaching of metal sulfides proceeds by two indirect mechanisms via thiosulfate or via polysulfides and sulfur. Applied and Environmental Microbiology, 1999, **65(1)**, 319-321.

Schlesinger, M.E., King, M.J., Sole, K.C., Davenport, W.G., *Extractive metallurgy of copper*. 2011, Elsevier.

Schroeter, A.W., Sand, W., Estimations on the degradability of ores and bacterial leaching activity using short-time microcalorimetric tests. FEMS Microbiology Reviews, 1993, **11(1-3)**, 79-86.

Schröter, A., Sand, W., Microcalorimetry-- a modern technique for microbiology and biohydrometallurgy. 1988.

Schröter, A., Sand, W., Salley, J., McCready, R., Wichlacz, P., Investigations on leaching bacteria by microcalorimetry. Biohydrometallurgy, 1989, 427-438.

Schwartz, M., Schippers, A., Hahn, L., Hydrochemical models of the sulphidic tailings dumps at Matchless (Namibia) and Selebi-Phikwe (Botswana). Environmental Geology, 2006, **49(4)**, 504-510.

Sheng, G.P., Yu, H.Q., Li, X.Y., Extracellular polymeric substances (EPS) of microbial aggregates in biological wastewater treatment systems: a review. Biotechnology Advances, 2010, **28(6)**, 882-894.

Sherwood, L., Willey, J.M., Woolverton, C., *Prescott's microbiology*. 2011, McGraw-Hill.

Shiers, D., Blight, K., Ralph, D., Sodium sulphate and sodium chloride effects on batch culture of iron oxidising bacteria. Hydrometallurgy, 2005, **80(1-2)**, 75-82.

Shiers, D., Ralph, D., Bryan, C., Watling, H., Substrate utilisation by *Acidianus brierleyi*, *Metallosphaera hakonensis* and *Sulfolobus metallicus* in mixed ferrous ion and tetrathionate growth media. Minerals Engineering, 2013, **48**, 86-93.

Shiers, D.W., Collinson, D.M., Watling, H.R., Life in heaps: a review of microbial responses to variable acidity in sulfide mineral bioleaching heaps for metal extraction. Research in Microbiology, 2016, **167(7)**, 576-586.

Singer, P.C., Stumm, W., Acidic mine drainage: the rate-determining step. Science, 1970, **167(3921)**, 1121-1123.

Singh, G., Mine water quality deterioration due to acid mine drainage. International journal of mine water, 1987, **6(1)**, 49-61.

Singh, S., Panda, S., Mishra, S., Pradhan, N., Mohanty, R., Sukla, L., Evaluation of microbial population and attachment study during bio-heap leaching at Malanjkhand copper project. International Journal of Environment Waste Management, 2013, **11(1)**, 75-86.

Smart, M., Huddy, R.J., Edward, C.J., Fourie, C., Shumba, T., Iron, J., Harrison, S.T.L., 2017. Linking microbial community dynamics in biox® leaching tanks to process conditions: Integrating lab and commercial experience, In *Solid State Phenomena*, pp. 38-42.

Smart, R., Skinner, W., Levay, G., Gerson, A., Thomas, J., Sobieraj, H., Schumann, R., Weisener, C., Weber, P., Miller, S., ARD test handbook: project P387A, prediction and kinetic control of acid mine drainage. AMIRA, International Ltd, Ian Wark Research Institute, Melbourne, Australia, 2002.

Smedes, F., Askland, T., Revisiting the development of the Bligh and Dyer total lipid determination method. Marine Pollution Bulletin, 1999, **38(3)**, 193-201.

Starkey, M., Parsek, M.R., Gray, K.A., Chang, S.I., 2004. A sticky business: the extracellular polymeric substance matrix of bacterial biofilms, In *Microbial biofilms*. American Society of Microbiology, pp. 174-191.

Stewart, W.A., Miller, S.D., Smart, R., 2006. Advances in acid rock drainage (ARD) characterisation of mine wastes. Asmr.

Stumm, W., Morgan, J., 1996. Aquatic Chemistry–chemical equilibria and rates in natural waters 3rd edition. Wiley-Interscience, New York.

Surette, M.G., Stock, J.B., 1994. Transmembrane signal transducing proteins, In *New Comprehensive Biochemistry*. Elsevier, pp. 465-483.

Sutherland, I.W., Biofilm exopolysaccharides: a strong and sticky framework. 2001, **147(1)**, 3-9.

Suzuki, I., Microbial leaching of metals from sulfide minerals. Biotechnology Advances, 2001, **19(2)**, 119-132.

Sverdrup, H.U., Ragnarsdottir, K.V., Koca, D., On modelling the global copper mining rates, market supply, copper price and the end of copper reserves. Resources, Conservation Recycling, 2014, **87**, 158-174.

Tapia, J., Munoz, J., Gonzalez, F., Blázquez, M., Malki, M., Ballester, A., Extraction of extracellular polymeric substances from the acidophilic bacterium *Acidiphilium*. Water Science Technology, 2009, **59(10)**, 1959-1967.

Tempel, K., 2003. Commercial biooxidation challenges at Newmont's Nevada operations, In *2003 SME annual meeting*, pp. 03-067.

Temple, K.L., Colmer, A.R., The autotrophic oxidation of iron by a new bacterium: *Thiobacillus ferrooxidans*. Journal of Bacteriology, 1951, **62(5)**, 605.

Tributsch, H., Bennett, J.C., Semiconductor-electrochemical aspects of bacterial leaching. I. Oxidation of metal sulphides with large energy gaps. Journal of Chemical Technology Biotechnology, 1981, **31(1)**, 565-577.

Tupikina, O.V., Minnaar, S.H., Rautenbach, G.F., Dew, D.W., Harrison, S.T.L., Effect of inoculum size on the rates of whole ore colonisation of mesophilic, moderate thermophilic and thermophilic acidophiles. Hydrometallurgy, 2014, **149**, 244-251.

Tupikina, O.V., Minnaar, S.H., van Hille, R.P., van Wyk, N., Rautenbach, G.F., Dew, D., Harrison, S.T.L., Determining the effect of acid stress on the persistence and growth of thermophilic microbial species after mesophilic colonisation of low grade ore in a heap leach environment. Minerals Engineering, 2013, **53**, 152-159.

Tupikina, O.V., Ngoma, I.E., Minnaar, S., Harrison, S.T.L., Some aspects of the effect of pH and acid stress in heap bioleaching. Minerals Engineering, 2011, **24(11)**, 1209-1214.

Tyson, G.W., Chapman, J., Hugenholtz, P., Allen, E.E., Ram, R.J., Richardson, P.M., Solovyev, V.V., Rubin, E.M., Rokhsar, D.S., Banfield, J.F., Community structure and metabolism through reconstruction of microbial genomes from the environment. Nature 2004, **428(6978)**, 37.

Van Aswegen, P.C., Van Niekerk, J., Olivier, W., 2007. The BIOX™ process for the treatment of refractory gold concentrates, In *Biomining*. Springer, pp. 1-33.

van Hille, R.P., van Wyk, N., Froneman, T., Harrison, S.T., 2013. Dynamic evolution of the microbial community in BIOX leaching tanks, In *Advanced Materials Research*. Trans Tech Publ, pp. 331-334.

van Loosdrecht, M.C., Lyklema, J., Norde, W., Zehnder, A., Influence of interfaces on microbial activity. Microbiology Molecular Biology Reviews, 1990, **54(1)**, 75-87.

Van Staden, P., Gericke, M., Craven, P., Minerals biotechnology: trends, opportunities and challenges. Hydrometallurgy, 2008, 6-13.

Van Staden, P., Shaidaee, B., Yazdani, M., 2005. A collaborative plan towards the heap bioleaching of low grade chalcopyritic ore from a new Iranian mine, In *Proceedings of the 16th international biohydrometallurgy symposium*. Cape Town, Compress, pp. 115-123.

Verburg, R., Bezuidenhout, N., Chatwin, T., Ferguson, K., The Global Acid Rock Drainage Guide (GARD Guide). Mine Water and the Environment, 2009, **28(4)**, 305-310.

Vu, B., Chen, M., Crawford, R.J., Ivanova, E.P., Bacterial extracellular polysaccharides involved in biofilm formation. Molecules, 2009, **14(7)**, 2535-2554.

Wadsö, I., Isothermal microcalorimetry in applied biology. Thermochimica acta, 2002, **394(1-2)**, 305-311.

Wadsö, I., Goldberg, R.N., Standards in isothermal microcalorimetry Pure applied chemistry, 2001, **73(10)**, 1625-1639.

Waksman, S.A., Joffe, J., Microorganisms concerned in the oxidation of sulfur in the soil ll. *Thiobacillus thiooxidans*, a new sulfur-oxidising organism isolated from the soil Journal of Bacteriology, 1922, **7(2)**, 239-256.

Wang, Y., Su, L., Zeng, W., Wan, L., Chen, Z., Zhang, L., Qiu, G., Chen, X., Zhou, H., Effect of pulp density on planktonic and attached community dynamics during bioleaching of chalcopyrite by a moderately thermophilic microbial culture under uncontrolled conditions. Minerals Engineering, 2014, **61**, 66-72.

Ward, N., Fraser, C.M., How genomics has affected the concept of microbiology. Current Opinion in Microbiology, 2005, **8(5)**, 564-571.

Watling, H., Microbiological Advances in Biohydrometallurgy. Minerals, 2016, **6(2)**.

Watling, H., Elliot, A., Maley, M., Van Bronswijk, W., Hunter, C., Leaching of a low-grade, copper–nickel sulfide ore. 1. Key parameters impacting on Cu recovery during column bioleaching. Hydrometallurgy, 2009, **97(3-4)**, 204-212.

Watling, H., Watkin, E., Ralph, D., The resilience and versatility of acidophiles that contribute to the bio-assisted extraction of metals from mineral sulphides. Environmental Technology, 2010, **31(8-9)**, 915-933.

Watling, H.R., The bioleaching of sulphide minerals with emphasis on copper sulphides — A review. Hydrometallurgy, 2006, **84(1-2)**, 81-108.

Watling, H.R., Johnson, J.J., Shiers, D.W., Gibson, J.A.E., Nichols, P.D., Franzmann, P.D., Plumb, J.J., Effect of temperature and inoculation strategy on Cu recovery and microbial activity in column bioleaching. Hydrometallurgy, 2016, **164**, 189-201.

Watnick, P., Kolter, R., Biofilm, city of microbes. Journal of Bacteriology, 2000, **182(10)**, 2675-2679.

Weber, P.A., Thomas, J.E., Skinner, W.M., Smart, R.S.C., A methodology to determine the acid-neutralization capacity of rock samples. The Canadian Mineralogist, 2005, **43(4)**, 1183-1192.

White III, W., Lapakko, K., Cox, R., Static-test methods most commonly used to predict acid-mine drainage: practical guidelines for use and interpretation. The environmental geochemistry of mineral deposits. Part A: Processes, techniques, health issues. Reviews in Economic Geology A, 1999, **6**, 325-338.

Wingender, J., Neu, T.R., Flemming, H.-C., 1999. What are bacterial extracellular polymeric substances?, In *Microbial extracellular polymeric substances*. Springer, pp. 1-19.

Woldringh, C., De Jong, M., Van den Berg, W., Koppes, L., Morphological analysis of the division cycle of two *Escherichia coli* substrains during slow growth. Journal of Bacteriology, 1977, **131(1)**, 270-279.

Wolfaardt, G.M., Lawrence, J.R., Korber, D.R., 1999. Function of EPS, In *Microbial extracellular polymeric substances*. Springer, pp. 171-200.

Wu, A., Yin, S., Wang, H., Qin, W., Qiu, G., Technological assessment of a mining-waste dump at the Dexing copper mine, China, for possible conversion to an in situ bioleaching operation. Bioresource Technology, 2009, **100(6)**, 1931-1936.

Xu, C., Santschi, P.H., Schwehr, K.A., Hung, C.-C., Optimized isolation procedure for obtaining strongly actinide binding exopolymeric substances (EPS) from two bacteria (*Sagittula stellata* and *Pseudomonas fluorescens Biovar II*). Bioresource Technology, 2009, **100(23)**, 6010-6021.

Yager, T.R., Bermúdez-Lugo, O., Mobbs, P.M., THE MINERAL INDUSTRIES OF AFRICA. Minerals Yearbook: Area Reports: International Review Africa the Middle East, 2015, **3**.

Yin, S., Wang, L., Kabwe, E., Chen, X., Yan, R., An, K., Zhang, L., Wu, A., Copper Bioleaching in China: Review and Prospect. Minerals, 2018, **8(2)**.

Yoshida, T., Sakamoto, T., Water-stress induced trehalose accumulation and control of trehalase in the *cyanobacterium* <I>*Nostoc punctiforme* </I>IAM M-15. The Journal of General and Applied Microbiology, 2009, **55(2)**, 135-145.

Yu, R., Hou, C., Liu, A., Peng, T., Xia, M., Wu, X., Shen, L., Liu, Y., Li, J., Yang, F., Qiu, G., Chen, M., Zeng, W., Extracellular DNA enhances the adsorption of *Sulfobacillus thermosulfidooxidans* strain ST on chalcopyrite surface. Hydrometallurgy, 2018, **176**, 97-103.

Yu, R., Shi, L., Gu, G., Zhou, D., You, L., Chen, M., Qiu, G., Zeng, W., The shift of microbial community under the adjustment of initial and processing pH during bioleaching of chalcopyrite concentrate by moderate thermophiles. Bioresource Technology, 2014, **162**, 300-307.

Yuan, R., Wen, J., Che, X., Bioleaching study for Zijinshan Copper Mine. Non-ferrous Metal, 2000, **52(4)**, 159-161.

Zeng, W., Qiu, G., Zhou, H., Liu, X., Chen, M., Chao, W., Zhang, C., Peng, J., Characterization of extracellular polymeric substances extracted during the bioleaching of chalcopyrite concentrate. Hydrometallurgy, 2010, **100(3-4)**, 177-180.

Zepeda, V., Galleguillos, F., Urtuvia, V., Molina, J., Demergasso, C., 2009. Comparison between the bacterial populations from solutions and minerals in 1 m test columns and the industrial low grade copper sulphide bioleaching process in the Escondida Mine, Chile, In *Advanced Materials Research*. Trans Tech Publ, pp. 63-66.

Zhang, F., Yan, C., Teng, H.H., Roden, E.E., Xu, H., In situ AFM observations of Ca–Mg carbonate crystallization catalyzed by dissolved sulfide: Implications for sedimentary dolomite formation. Geochimica et Cosmochimica Acta, 2013, **105**, 44-55.

Zhang, R., 2016. Biofilm formation and extracellular polymeric substances of acidophilic metal/sulfur-oxidizing archaea. Universitätsbibliothek Duisburg-Essen.

Zhang, R., Bellenberg, S., Castro, L., Neu, T.R., Sand, W., Vera, M., Colonization and biofilm formation of the extremely acidophilic archaeon *Ferroplasma acidiphilum*. Hydrometallurgy, 2014, **150**, 245-252.

Zhang, R., Bellenberg, S., Neu, T.R., Sand, W., Vera, M., 2016. The biofilm lifestyle of acidophilic metal/sulfur-oxidizing microorganisms, In *Biotechnology of Extremophiles:*. Springer, pp. 177-213.

Zhang, R., Neu, T.R., Blanchard, V., Vera, M., Sand, W., Biofilm dynamics and EPS production of a thermoacidophilic bioleaching archaeon. New Biotechnology, 2019a, **51**, 21-30.

Zhang, R., Neu, T.R., Li, Q., Blanchard, V., Zhang, Y., Sand, W., Insight into interactions of thermoacidophilic archaea with elemental sulfur: biofilm dynamics and EPS analysis. Frontiers in Microbiology, 2019b, **10**, 896.

Zhang, R.Y., Blanchard, V., Vera Véliz, M., Sand, W., EPS characterization of a cell wall-lacking archaeon *Ferroplasma acidiphilum*. Solid State Phenomena, 2017, **262**, 434-438.

Zhu, Z., Wang, H., Shang, Q., Jiang, Y., Cao, Y., Chai, Y., Time course analysis of *Candida albicans* metabolites during biofilm development. Journal of Proteome Research, 2013, **12(6)**, 2375-2385.

Zobell, C., Bacterial adhesion model. Journal of Bacteriology, 1943, **46**, 39-52.

Appendix A: Media composition and stock culture maintenance

0 K Basal salts medium

Chemical	Mass (g)
$(NH_4)_2SO_4$	3
KCl	0.1
$MgSO_4.7H_2O$	0.5
K_2HPO_4	0.5
$Ca(NO_3)_2.4H_2O$	1.45

The chemical ingredients were dissolved in 1 L distilled water, the pH of the medium adjusted to 1.6 using concentrated H_2SO_4 and then autoclaved for 20 minutes at 120° C.

Stock culture and maintenance

A mixed mesophilic culture was used (UCT stock) containing *At. ferrooxidans*, *A. cupricumulans, Archaea*, *Fe. acidiphilum*, and predominantly *L. ferriphilum,* confirmed by qPCR and grown on pyrite concentrate in a 1 litre batch stirred tank reactor at 35 °C and solid loading of 3 % wt/vol. The reactor was sub-cultured once weekly to ensure activity, by removing approximately 150 ml slurry and re-filling the volume up to the 1 L mark with fresh Norris media (0.4 g L^{-1} $(NH_4)_2SO_4$, 0.2 g L^{-1} K_2HPO_4, 0.5 g L^{-1} $MgSO_4.7H_2O$ and 0.1 g L^{-1} KCl) and 3.5 g of pyrite concentrate.

Appendix B: Quantification of maximum attachment per unit surface area

Quantification of the maximum attachment per available surface area provides information on whether or not the column had been saturated by the inoculum. Saturation of the surface available for attachment by the inoculum may influence the final attachment and colonisation efficiencies observed. Thus, the calculations below allowed the impact of inoculum concentration on the initial attachment to be analysed and allowed more adequate comparison of extent of attachment and colonisation across experiments.

Calculation of the maximum attachment per unit surface area was carried out and the following assumptions were made:

- Repulsive forces between cells and minerals were ignored
- Attachment was monolayered with cells orientated such that the major axis was parallel to the surface of the mineral coated bead as depicted below

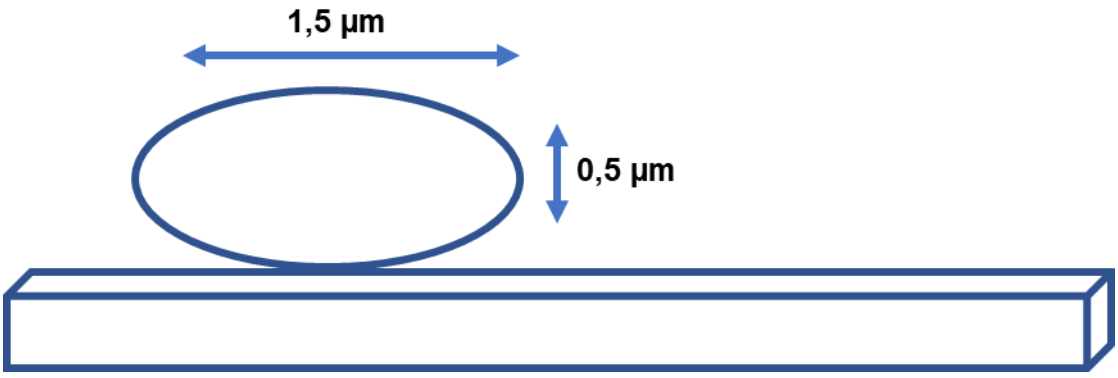

- Dimensions of the mesophilic microorganisms used: 1.5 × 0.5 µm

Surface area of microbial cell is therefore: 0.75 μm^2

Dimensions used were based on the findings of Ohmura et al. (1993) for *At. ferrooxidans*.

- For column experiments the surface area available for attachment was calculated by quantifying the total surface area of the spherical glass beads housed in the reactor

Average diameter of spherical glass bead: 6×10^{-3} m

Number of beads used: 300

Total surface area made available by spherical, mineral coated, glass beads

$$= 300 *(4* \pi * r^{2})$$

$$= 3.4 \times 10^{-2}\ m^2$$

- The maximum number of *At. ferrooxidans* cells that could be accommodated by the available surface area in the packed column reactor was calculated. This number will be referred to as the saturation cell number.

Saturation cell number calculation:

$$= \frac{Total\ surface\ area\ made\ available\ for\ attachment\ by\ coated\ glass\ beads\ [m^2]}{Surface\ area\ per\ microbial\ cell\ \left[\frac{m^2}{cell}\right]}$$

$$= \frac{3.4 \times 10^{-2}}{7.5\ \times\ 10^{-13}}$$

$$= 4.5\ \times 10^{10}$$

Appendix C: Mineralogical information of substrates used

C.1 ICP-OES (Fe) and LECO (S) analysis for Pyrite concentrate

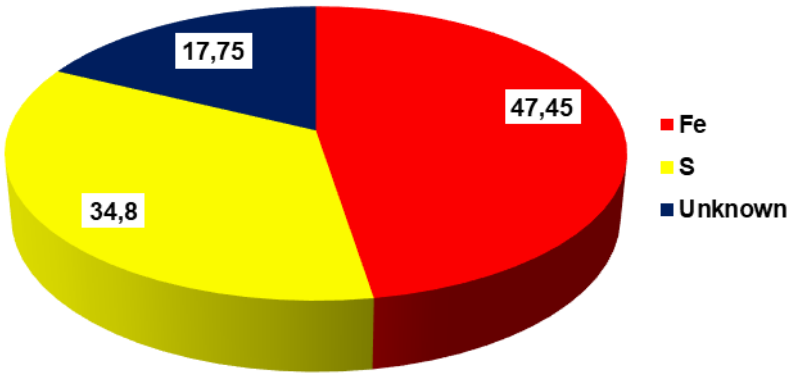

Figure: C.1-1 ICP-OES analysis for Fe and LECO analysis for sulfur of the pyrite concentrate mineral

C.2 Particle size distribution of pyrite concentrate mineral

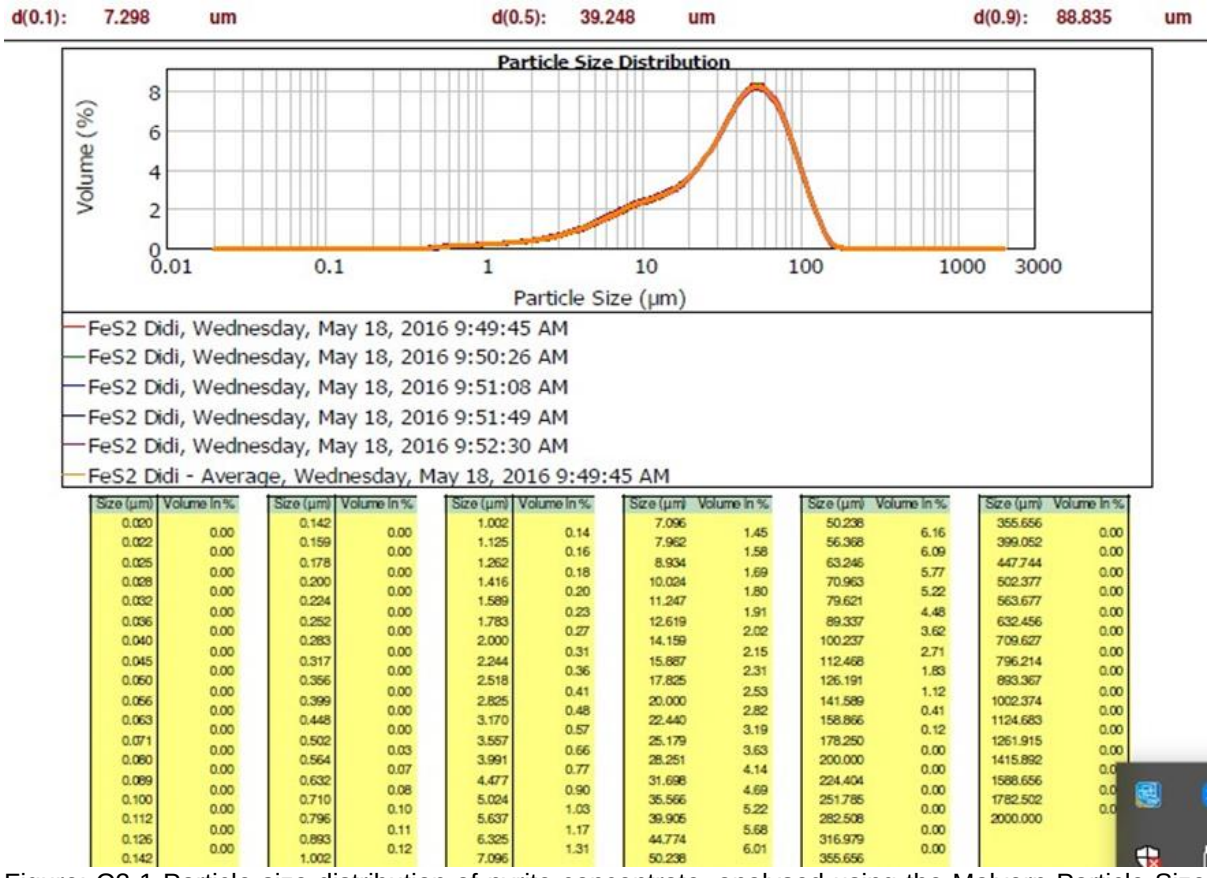

Figure: C2-1 Particle size distribution of pyrite concentrate, analysed using the Malvern Particle Size Analyser

C.3 XRD diffractogram

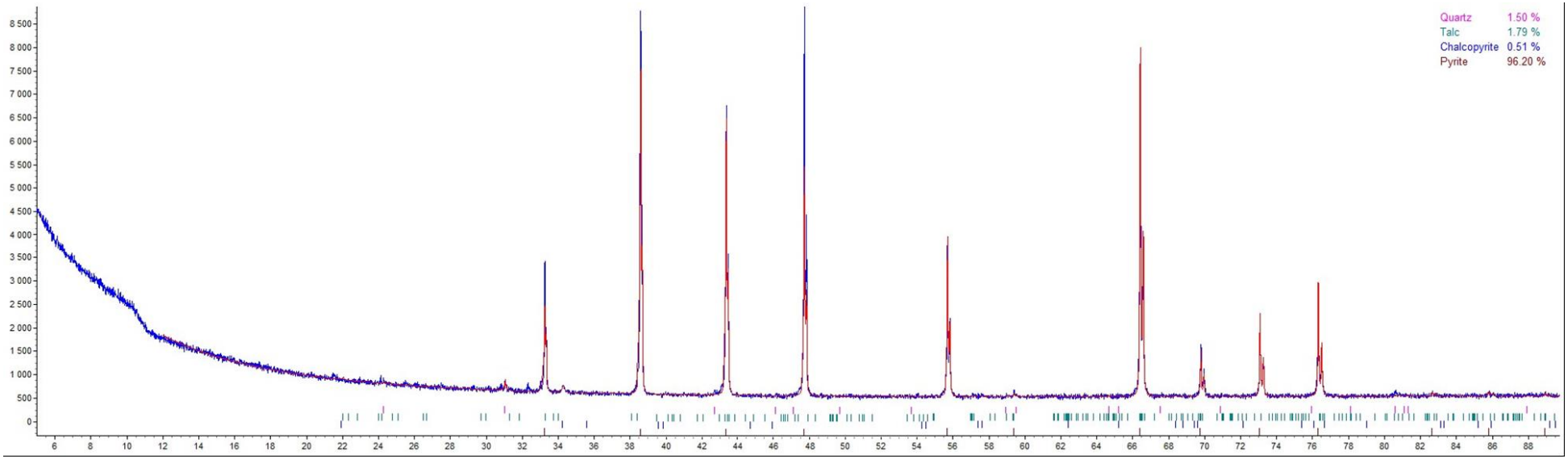

Figure: C3-1 Depiction of XRD diffractogram of the pyrite concentrate mineral

C.4 QEMSCAN images of waste rock samples

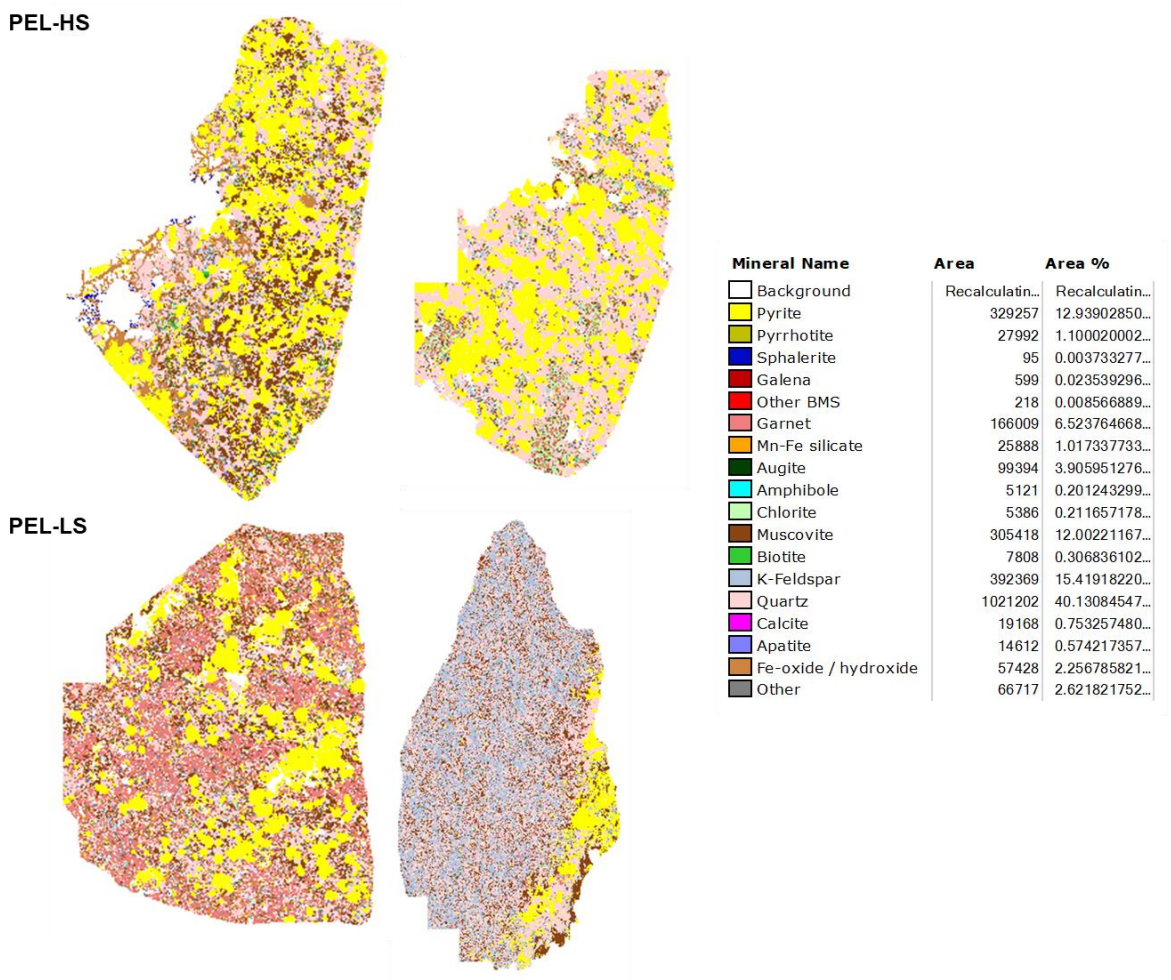

Figure: C3-1 QEMSCAN images of PEL-LS and PEL-HS of the waste samples.

C.5 Waste rock mineral mass determined by QEMSCAN

Mineral type	PEL-HS (%)	PEL-LS (%)
Pyrite	33,43	13,99
Pyrrhotite	3,90	2,35
Sphalerite	0,06	0,02
Galena	0,07	0,09
Other BMS	0,02	0,02
Garnet	2,83	4,52
Mn-Fe silicate	0,12	0,30
Augite	0,47	0,92
Amphibole	0,15	0,55
Chlorite	0,38	0,91
Muscovite	12,42	14,77
Biotite	0,74	1,64
K-Feldspar	3,52	13,25
Quartz	34,76	36,67
Calcite	0,22	0,03
Apatite	0,40	0,51
Fe-oxide / hydroxide	5,45	8,06
Other	1,06	1,39
SUM	100,00	100,00

Appendix D: Analytical methods

D.1 Ferrous iron and total iron concentration

The protocol presented here was obtained from the CeBER manual of analytical laboratory methods. The Fe^{2+} and total iron concentrations of the collected samples were determined colormetrically using the 1-10 phenanthroline method developed by Komadel and Stucki (1988). The reagents were prepared as follows:

- A fresh stock of Fe^{2+} solution at 1000 mg L^{-1} was used as the standard.
- An ammonium acetate buffer solution is made by dissolving 250 g of ammonium acetate ($NH_4C_2H_3O_2$) in 150 ml of distilled water, followed by the addition of 700 ml of concentrated glacial acetic acid.
- To make the 1-10 phenanthroline indicator solution, 2127.7 mg of 1-10 phenanthroline ($C_{12}H_8N_2.H_2O$) was dissolved in 100 ml of distilled water in a 1000 ml. volumetric flask. The solution was diluted with distilled water to 1000 ml, providing a concentration in excess of the stoichiometric requirements.
- To obtain the total iron concentration, a spatula tip of hydroxylamine was added to each sample to convert all iron present to the Fe^{2+} form, after the Fe^{2+} assay was performed.

Standard curves of the relationship between Fe^{2+} concentration and absorbance were constructed by adding 2 ml aliquot of acetate buffer, followed by 2 ml of 1-10 phenanthroline solution into test tubes. The standard Fe^{2+} stock solution was diluted to provide samples of 0, 6.25, 12.5, 25 and 50 ppm. From these, 1 ml was pipetted into the respective test-tubes. On addition of samples containing Fe^{2+}, solution reacted to form an orange-red colour. The concentration of 0 ppm was made up of pure Millipore water, and was required to zero the spectrophotometer. The absorbance maximum was determined through a scan of a Fe^{2+} sample and confirmed to be 510 nm. The standard curves generated are presented in Figure D2-1.

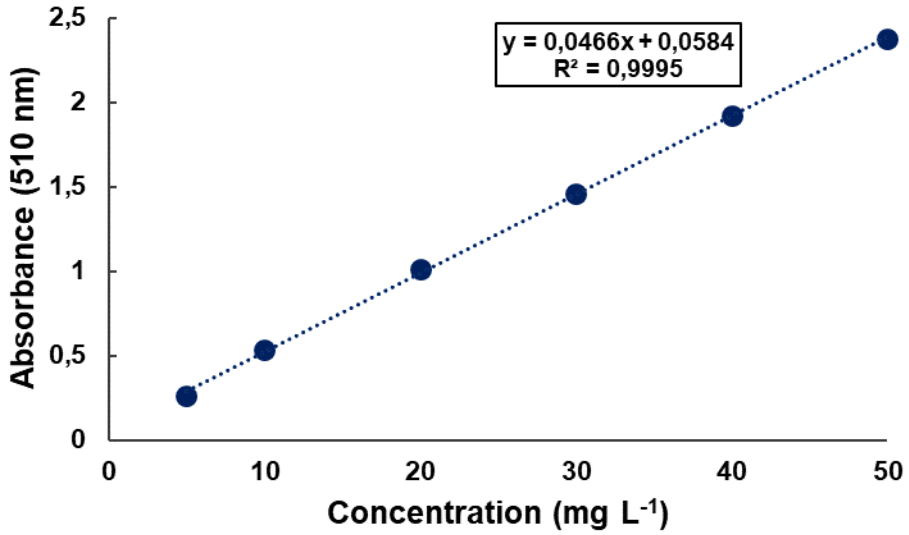

Figure: D1-1 Fe^{2+} standard curve that was used to obtain the Fe^{2+} and Fe^{tot} concentrations. Error bars represent the standard deviation from triplicates.

D.2 Fe^{2+} oxidation

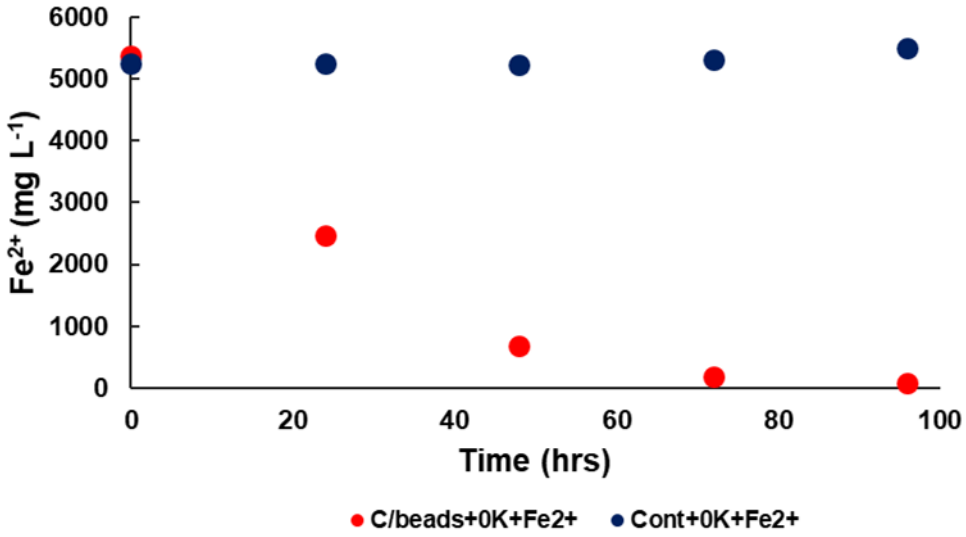

Figure: D2-1 Demonstration of the complete oxidation of Fe^{2+} after 72 hours, (●) is the experimental sample with microbial presence and (●) is the control in the absence of microorganisms.

Appendix E: Carbohydrates analysis by phenol-sulfuric acid method

The phenol-sulfuric acid method measures total carbohydrates in a variety of samples, including whole cells. The protocol digests complex carbohydrates into sugar monomers, which are then detected by the creation of an orange-yellow colour (Dubois et al., 1956). It is very sensitive, fairly easy and reliable, but it uses toxic and dangerous reagents and the standard curve is different for different sugars (e.g. glucose vs mannose or sucrose). If the composition of the carbohydrates to be tested is known, it is recommended that a relevant mixture of sugars be used to generate the standard curve. If not, pure glucose is generally used.

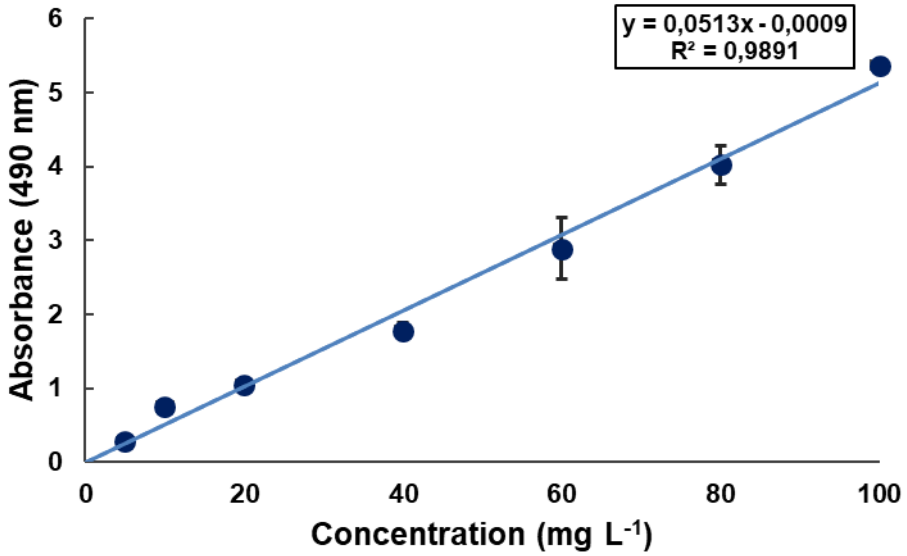

Figure: E-1 Standard curve to obtain carbohydrates concentration. Error bars represent the standard deviation from the mean of five repeats

For the standard curve, make up a solution of 0.2 mg ml^{-1} glucose in deionised H_2O. This will give a sample of 40 µg glucose in 200 µl, which will have an absorbance of approximately 1. Make 4-5 dilutions between 4 and 40 µg glucose per sample.

Procedure

1. Add 200 µl of sample and 200 µl of 5 % phenol into a test tube and mix by vortexing

2. Carefully add 1 ml of concentrated sulfuric acid in a direct stream straight onto the sample and mix immediately by vortexing

3. Stand at room temperature for 10 min

4. Incubate in a 30 ºC water bath for 20 min

5. Read absorbance at 490 nm

Appendix F: GC-MS results

F.1 Chromatograms of loosely bound (LB) EPS samples

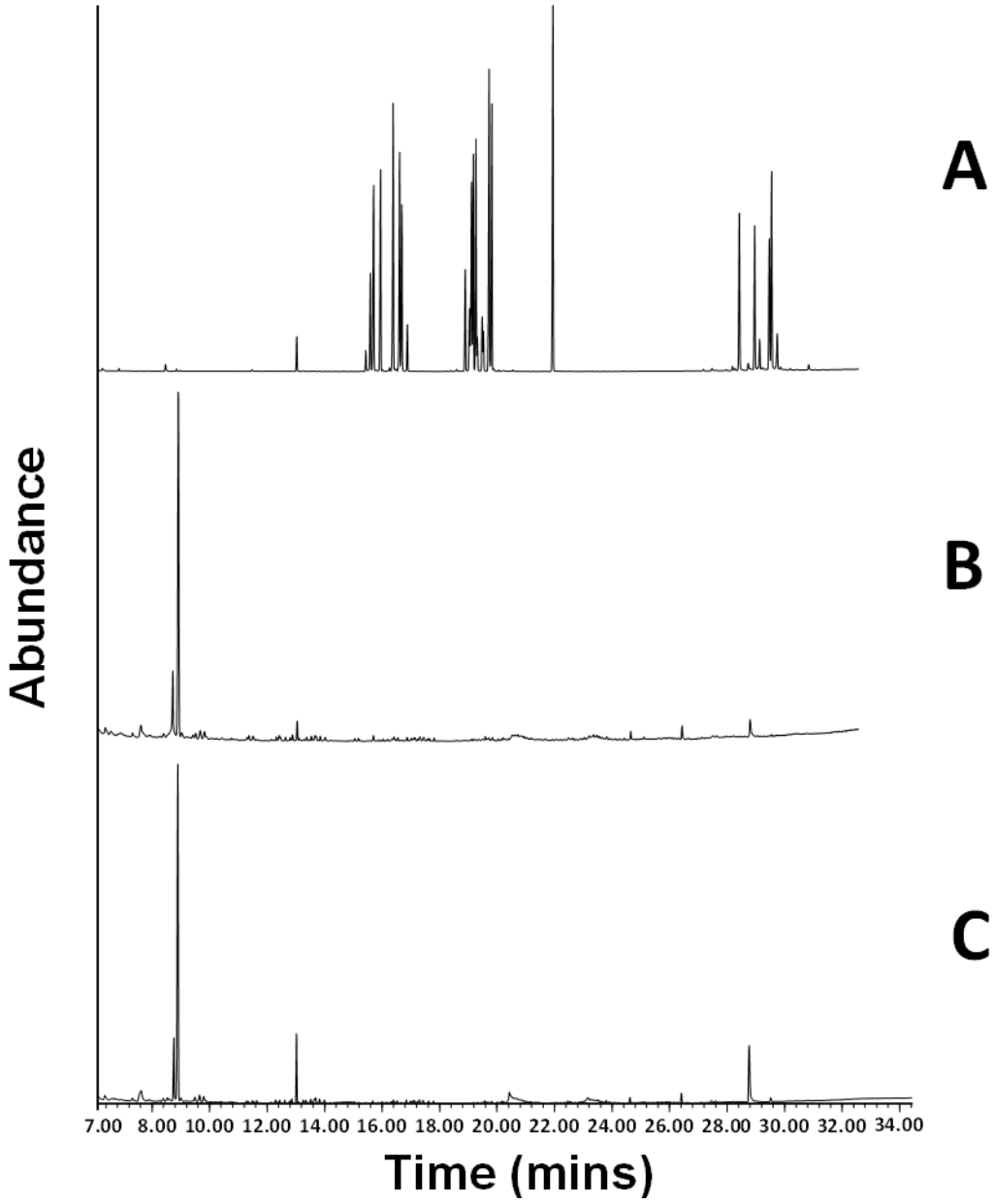

Figure: E1-1 Overlayed chromatograms of a mixed sugar standard (50 g L^{-1}) (A), sample LBA (B) and sample LBB (C).

F.2 Overlayed chromatograms of capsular (CAPS) EPS samples

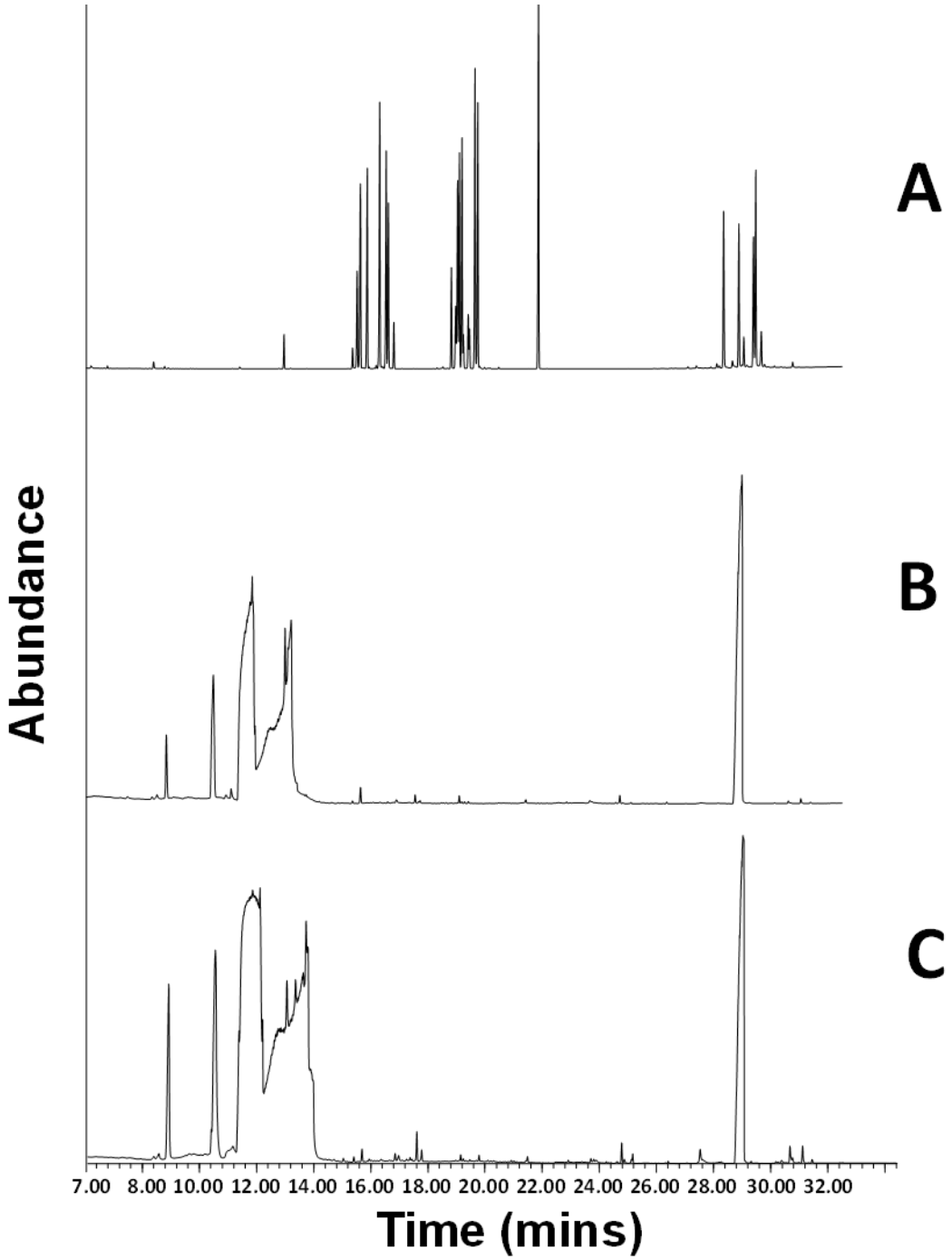

Figure: E2-1 Overlayed chromatograms of a sugar mix standard (50 g L^{-1}) (A), sample $CAPS_A$ (B) and sample $CAPS_{A1}$ (C).

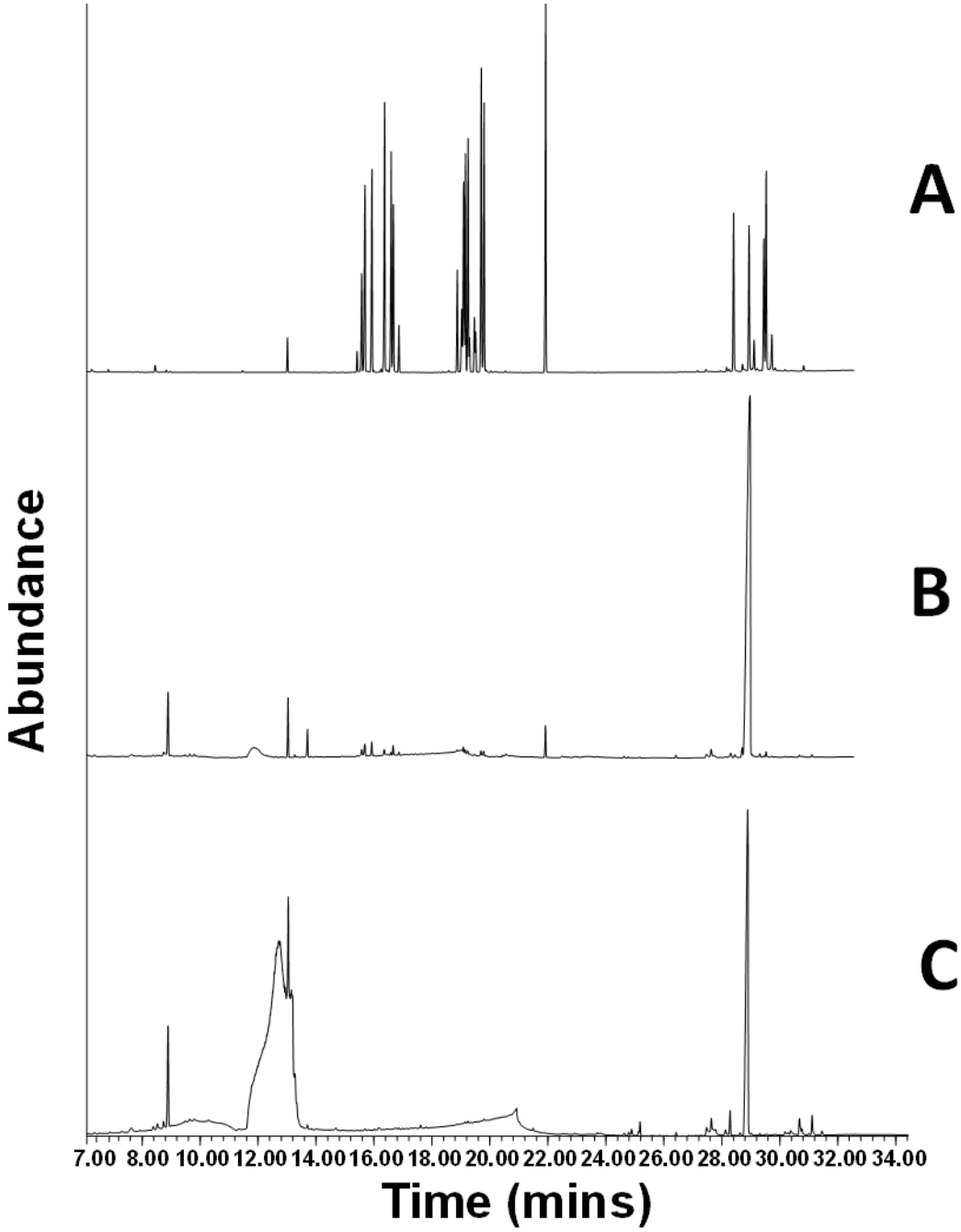

Figure: E2-2 Overlayed chromatograms of a sugar mix standard (50 g L^{-1}) (A), sample $CAPS_B$ (B) and sample $CAPS_{B1}$ (C).

Table: E2-1 Concentration (mg L^{-1}) of sugars detected in the 6 samples

		Compound Identification										
Sample name (CAF)	**Sample name (Client)**	**D-Fructose**	**D-Galactose**	**D-Mannose**	**D-Glucose**	**Mannitol**	**Sorbitol**	**Myo-Inositol**	**Sucrose**	**alpha-Lactose**	**D-Maltose**	**Trehalose**
		Concentration ppm (mg L^{-1})										
UCT_02	**LB_A**	Nd	Nd	< 10	< 10	< 10	< 10	Nd	Nd	Nd	Nd	Nd
UCT_04	**LB_B**	Nd	Nd	< 10	< 10	< 10	< 10	Nd	Nd	Nd	Nd	Nd
UCT_06	**CAPS_A**	15.55	15.86	< 10	< 10	< 10	< 10	Nd	Nd	Nd	Nd	10.77
UCT_05	**CAPS_A1**	15.59	15.87	< 10	< 10	< 10	< 10	Nd	Nd	Nd	Nd	10.96
UCT_03	**CAPS_B**	15.85	16.35	< 10	< 10	< 10	< 10	Nd	22.87	17.92	14.55	12.30
UCT_01	**CAPS_B1**	15.60	15.84	< 10	< 10	< 10	< 10	Nd	Nd	Nd	Nd	10.86

Nd = not detected, <10 = sample concentration is below the GC-MS detection limit

Appendix G: ARD characterisation static tests

G.1 Acid neutralisation capacity tests (ANC)

Fizz ratings and associated acid quantities and concentrations to be used in the ANC determination

		HCl		
Reaction	**Fizz rating**	**Molarity (M)**	**Volume (ml)**	**NaOH molarity (M)**
No reaction	0	0.5	4	0.1
Slight reaction	1	0.5	8	0.1
Moderate reaction	2	0.5	20	0.5
Strong reaction	3	0.5	40	0.5
Very strong rxn	4	1	40	0.5
	5*	1	60	0.5

*5 is used for very high ANC material (> 400 kgH_2SO_4/t) e.g. limestone

The standard ANC test was modified from the methodology developed by Sobek *et. al* (1978).

1. 2 grams of -75 µm fraction dry sample was accurately weighed and transferred into clean 250 ml dry Erlenmeyer flasks.
2. A certain amount of hydrochloric acid was added into the sample based on fizz rating.
3. 20 ml of deionized water was also added constantly in each sample using measuring cylinder.
4. Flasks were weighed in an electronic balance and the mass was recorded. Four blank flasks containing deionized water and appropriate amount of HCl were prepared for each fizz rating.
5. The flasks were heated in a hot plate at 90°C for a maximum of two hours until reaction stops.
6. This was indicated by non-evolution of gas bubbles and particles settled evenly at the bottom of the flask.
7. During heating deionised water was added occasionally to avoid dryness of the sample.
8. Upon the completion of the reaction, flasks were cooled at room temperature and deionised water was added to make up to their original weighs before heating.
9. The pH of the ANC solution was measured to determine if sample was correctly fizz rated and this was confirmed by pH between 0.8 to 1.5.

10. Those samples that had pH above 1.5 were fizz rated low and were changed into the next higher fizz, and samples that had pH were 0.8 were repeated on lower fizz because too much acid was added.
11. Samples were filtered to avoid any oxidation that could result from pyrite on solid residue.
12. The clear liquid was then back titrated into two end points of pH 5 and 7 using 0.5 molar concentration of NaOH.
13. Two drops of 30 % H_2O_2 were added at pH 5 to precipitate Fe^{2+} into Fe^{3+}.
14. Samples were further titrated to pH 7 and the amount of NaOH used was recorded.
15. The amount of HCl consumed was converted into Kg H_2SO_4/t using formula below.

Calculation of ANC

ANC = [Y x MHCl / wt] x C.

Where:

Y = (Vol. of HCl added) - (Vol. of NaOH titrated x B)

B = (Vol. of HCl in blank) / (Vol. of NaOH titrated in blank)

MHCl = Molarity of HCls

wt = Sample weight in grams

C = Conversion factor

C = 49.0 (to calculate kg H2SO4/t)

C = 5.0 (to calculate % CaCO3 equivalent)

G.2 Net Acid Generation test

1. The net acid Generation (NAG) is a static test that was used to provides direct empirical estimate of the overall sample reactivity.
2. This method was also employed in this study to determine the semi-soluble acid minerals such as sulfate and other potential acid generating sulfur bearing minerals.
3. NAG testing was carried out in accordance with the method described in Sobek et al., 1978).

4. 250 ml of 15 % H_2O_2 was added into an Erlenmeyer flask containing 2.5g of pulverised sample less than -75 µm fraction.
5. The H_2O_2 was allowed to react with the sample overnight, and the following day the NAG solution was gently heated in a hot plate to 90°C for a maximum of 2 hours.
6. Deionised water was added continuously to avoid dryness of the flasks.
7. The heating was done to remove excess H_2O_2 and also to facilitate the release of inherent neutralizing capacity such as carbonate buffering.
8. The solution was then allowed to cool at room temperature for a maximum of two hours.
9. Evaporation was accounted by addition of deionised water to make up the flasks into their pre-weighed volumes and this was followed by measuring and recording the NAG pH. The test also reports the NAG value, measured in equivalent kilograms of sulfuric acid (H_2SO_4) per tonne.
10. The above method was adapted for the test samples in order to track the pH change through the latter portion of the test

List of publications and conference presentations

Publications

1. Didi X. Makaula, Robert J. Huddy, Marijke A. Fagan-Endres, Susan T.L. Harrison. Using isothermal microcalorimetry to measure the metabolic activity of the mineral-associated microbial community in bioleaching. Minerals Engineering, 106, (2017) 33 – 38
2. Didi X. Makaula, Robert J. Huddy, Marijke A. Fagan-Endres, Susan T.L. Harrison. Investigating the microbial metabolic activity on mineral surfaces of pyrite rich waste rocks in an unsaturated heap-simulating column system. Solid State Phenomena, 262, (2017) 228-232
3. Didi X. Makaula, Robert J. Huddy, Marijke A. Fagan-Endres, Susan T.L. Harrison. Developing a flow-through biokinetic test to characterize ARD potential: investigating the microbial metabolic activity on pyrite-bearing waste rock surfaces in an unsaturated ore bed. Proceedings 11th ICARD | IMWA, Wolkersdorfer, Ch.; Sartz, L.; Weber, A.; Burgess, J.; Tremblay, G. (eds. 2018) | MWD Conference – “Risk to Opportunity”
4. Didi X. Makaula, Susan T.L. Harrison. Establishing the flow-through biokinetic test to characterise sulfidic waste rock mineral for its potential to form ARD. Minerals Engineering (under revision)

Conference presentations

1. Didi X. Makaula, Robert J. Huddy, Susan T.L. Harrison. Assessment of microbial attachment during bioleaching of mineral ores using A “flow-through” column-based method. *SAIMM Mineral processing 2014*, Lord Charles Hotel, Somerset West, 7-8 August 2014. Short oral presentation and poster.
2. Didi X. Makaula, Robert J. Huddy, Susan T.L. Harrison. Use of microcalorimetry to measure microbial activity on pyrite concentrate surface. *SAIMM Mineral processing 2015*, Vineyard Hotel, Newlands, Cape Town, 6-7 August 2015. Poster presentation.
3. Didi X. Makaula, Robert J. Huddy, Marijke A. Fagan-Endres, Susan T.L. Harrison. Assessing microbial activity on pyrite concentrate mineral surface during bioleaching. *South African society for microbiology (SASM) 2016 Biennial Congress*, Coastlands, Umhlanga, Durban, 17-20 January 2016. Oral presentation.

4. Didi X. Makaula, Robert J. Huddy, Marijke A. Fagan-Endres, Susan T.L. Harrison. Using isothermal microcalorimetry to measure the metabolic activity of the mineral-associated microbial community in bioleaching. *Biohydrometallurgy 2016*, Falmouth, Cornwall, UK. 20-22 June 2016. Oral presentation.
5. Didi X. Makaula, Robert J. Huddy, Marijke A. Fagan-Endres, Susan T.L. Harrison. Investigating microbial metabolic activity on the surfaces of pyrite bearing waste rocks in an unsaturated ore bed. *SAIMM Minerals Research Showcase 2017*, Philippi Village, Cape Town, 3-4 August 2017. Oral presentation.
6. Didi X. Makaula, Robert J. Huddy, Marijke A. Fagan-Endres, Susan T.L. Harrison. Investigating the microbial metabolic activity on mineral surfaces of pyrite-rich waste rocks in an unsaturated heap-simulating column system. *22nd International Biohydrometallurgy Symposium 2017*, TU Bergakademie Freiberg, Germany, 24-27 September 2017. Poster presentation.
7. Didi X. Makaula, Robert J. Huddy, Marijke A. Fagan-Endres, Susan T.L. Harrison. Quantitative and qualitative analysis of the detachment of mineral associated microorganisms from particulate mineral coated onto glass beads for flow-through leaching tests. *Biohydrometallurgy 2018*, Windhoek, Namibia, 12-13, June 2018. Poster presentation.
8. Didi X. Makaula, Susan T.L. Harrison. Establishing the flow through biokinetic system as a viable test for the characterisation of sulfidic waste rock mineral for ARD potential. *Biohydrometallurgy 2018*, Windhoek, Namibia, 12-13, June 2018. Oral presentation.
9. Didi X. Makaula, Robert J. Huddy, Marijke A. Fagan-Endres, Susan T.L. Harrison. Developing a Flow-Through Biokinetic Test to Characterize ARD Potential: Investigating the Microbial Metabolic Activity on Pyrite-bearing Waste Rock Surfaces in an Unsaturated Ore Bed. *11th ICARD | IMWA 2018*, Pretoria, South Africa, 10-14 September 2018. Oral presentation.